MycoKeys 61: 1–26 (2019)
doi: 10.3897/mycokeys.61.46446
http://mycokeys.pensoft.net

RESEARCH ARTICLE

A peer-reviewed open-access journal
MycoKeys
Launched to accelerate biodiversity research

Descriptions of five new species in *Entoloma* subgenus *Claudopus* from China, with molecular phylogeny of *Entoloma* s.l.

Xiao-Lan He[1], Egon Horak[2], Di Wang[1], Tai-Hui Li[3], Wei-Hong Peng[1], Bing-Cheng Gan[1]

1 *Soil and Fertilizer Institute, Sichuan Academy of Agricultural Sciences, Chengdu 610066, China* **2** *Schlossfeld 17, A-6020 Innsbruck, Austria* **3** *State Key Laboratory of Applied Microbiology Southern China, Guangdong Provincial Key Laboratory of Microbial Culture Collection and Application, Guangdong Institute of Microbiology, Guangdong Academy of Sciences, Guangzhou 510070, China*

Corresponding author: *Wei-Hong Peng* (pwh424@163.com)

Academic editor: *M.P. Martín* | Received 11 September 2019 | Accepted 21 October 2019 | Published 5 December 2019

Citation: He X-L, Horak E, Wang D, Li T-H, Peng W-H, Gan B-C (2019) Descriptions of five new species in *Entoloma* subgenus *Claudopus* from China, with molecular phylogeny of *Entoloma* s.l. MycoKeys 61: 1–26. https://doi.org/10.3897/mycokeys.61.46446

Abstract

Entoloma subgenus *Claudopus* is widely distributed, yet the taxonomy and systematics of its species are still poorly documented. In the present study, more than forty collections of *Claudopus* were gathered in China and subsequently analysed, based on morphological and molecular data. The results revealed first a high level of species diversity of *Claudopus* in China and second, there is a wide ecological range regarding the substrates and the habitats ranging from temperate, tropical to subalpine locations. Based on morphological and molecular evidence, five novel species from China are proposed, viz. *E. conchatum*, *E. flabellatum*, *E. gregarium*, *E. pleurotoides* and *E. reductum*. Molecular phylogeny of *Entoloma* s.l. was also reconstructed, based on 187 representatives of *Entoloma* s.l. by employing the combined ITS, LSU, mtSSU and RPB2 sequences. Ten monophyletic clades (*Claudopus*, *Leptonia*, *Nolanea*, Cuboid-spored *Inocephalus*, "*Alboleptonia*", *Cyanula*, *Pouzarella*, *Rhodopolia*, *Prunuloides* and *Rusticoides*) were recovered, while 13 taxa could not be placed in any defined clades. The results confirmed that *Claudopus* in a traditional morphological sense is not monophyletic and the *Rusticoides*-group, previously considered within *Claudopus*, formed a separate clade; but section *Claudopus* and relatives of *E. undatum* belong to a distinctive monophyletic group. Despite some monophyletic groups in *Entoloma* s.l. being distinctive in both morphology and molecular phylogeny, they were still treated as subgenera of *Entoloma* s.l. temporarily, because accepting them as genera will make *Entoloma* s.l. paraphyletic.

Keywords
Entolomataceae, systematics, taxonomy, multi-gene analyses, ecology

Introduction

Entoloma P. Kumm. is a large agaric genus and more than 1000 species have been reported worldwide. Subgenus *Claudopus* is one of the most distinctive groups in this genus. By comparison, the pleurotoid or omphalinoid basidiomes of all described species of *Claudopus* are small and, accordingly, are often overlooked and thus neglected during field work. Macromorphologically, members of *Claudopus* are characterised by the fibrillose, non-gelatinised pileipellis and the eccentric, lateral or absent stipe. Macroscopically, fresh basidiomes of *Claudopus* are readily confused with species belonging to genera *Clitopilus* (Fr. ex Rabenh.) P. Kumm., *Crepidotus* (Fr.) Staude, *Hohenbuehelia* Schulzer, *Marasmiellus* Murrill or *Pleurotellus* Fayod but, under the microscope, the identification of *Claudopus* is immediately confirmed by the typical angular basidiospores.

To date, the taxonomic position of *Claudopus* (and of other entolomatoid taxa) is still controversial and unresolved. Horak (1980, 2008) accommodated pleurotoid *Claudopus* at generic level. Largent (1994) proposed 13 entolomatoid genera, including *Claudopus* as a recognised genus. Noordeloos (1992, 2004) proposed that *Claudopus* should be included in the genus *Entoloma*. All these proposals were based on morphological characters. However, molecular analysis has substantially altered traditional concepts in many fungal groups, showing that the taxonomic delimitation, based on morphological characters alone, is in fact artificial and speculative (Li et al. 2011; Chen et al. 2016; Han et al. 2016). In recent years, molecular markers have also been employed in phylogenetic studies on entolomatoid groups. In a paper by Co-David et al. (2009), three *Claudopus* species are nested in the monophyletic *Nolanea-Claudopus* Clade. As a consequence, the authors concluded that the traditional concept of *Claudopus* is polyphyletic. However, it was obvious that the number of samples was too limited to support the placement of *Claudopus* within *Nolanea*. Two subsequent molecular phylogenetic studies have also demonstrated that *Claudopus* (only pleurotoid species and relatives of *E. undatum* (Gillet) M.M. Moser were included) was grouped with *Nolanea* and *Leptonia* members, but no significant support was received (Baroni and Matheny 2011; Kinoshita et al. 2012). However, it is noteworthy that, in these studies, *Claudopus* species were actually nested in a monophyletic subclade (Baroni and Matheny 2011; Kinoshita et al. 2012). In two more recent studies (Vila et al. 2014; He et al. 2015), the results suggested that section *Claudopus* and *E. undatum* complex species could belong to a monophyletic group. Additionally, *E. rusticoides* (Gillet) Noordel. and associated taxa in sect. *Undatum* (Noordeloos 2004) are rather distant from the monophyletic *Claudopus* lineage (Vila et al. 2014). However, in all the previous studies, limited

taxa of *Claudopus* were included to support these conclusions and we expect that the topologies of the phylogenetic trees will probably significantly change with the increase in samples taken into account.

Based on Index of Fungi, the reference for about 70 species of "*Claudopus*" (both at subgeneric or generic level, including the *rusticoides*-group) were found in the pertinent literature. Substantial contributions were published, for example, by Dennis (1970), Esteve-Raventos and De La Cruz (1998), Horak (1980, 2008), Largent (1976, 1994), Largent et al. (2011), Manimohan et al. (2002, 2006), Noordeloos (1981, 1992, 2004), and Pegler (1983). Recently, two Chinese *Claudopus* species were added to the list (Deng et al. 2015; He et al. 2015). However, *Claudopus* worldwide still remains poorly understood and, for many species, no additional records have been added since the first publication.

There are several reasons why the taxonomy of *Claudopus* worldwide is not well understood yet. For many species, the original descriptive documentation is inadequate and/or type material is either not extant or in poor condition (Horak, unpubl. data). In addition, the knowledge of macroscopic and microscopic characters of nearly all described species is limited, at least by comparison with taxa of *Entoloma* s.l. The colour of the young basidiomes ranges from white, grey to pale brown. Bluish colours are the exception and are observed only in a few species (Horak 1980; Manimohan et al. 2002; Morozova et al. 2012). As a rule, the majority of the original descriptions are relying on macromorphological features which have led to persisting confusion regarding the circumscription of taxa. Furthermore, the number of reliable microscopical characters (basidiospores, pileipellis structure) is restricted. Distinctive cheilocystidia are not found in most species of *Claudopus*. Presence or absence of clamp connections (in particular at the basal septum of basidia) have not been given adequate attention in many of the earlier descriptions. Only recently, few species of *Claudopus* have been described by combining both morphologic and molecular data (Largent et al. 2011; Vila et al. 2014; Deng et al. 2015; He et al. 2015). Accordingly, identification of *Claudopus*, based on both morphological characters and molecular markers, will be helpful to fill a gap in our knowledge of *Claudopus* and bring clarifications regarding taxonomic relationships in this group.

To better understand the phylogeny of the genus *Entoloma* s.l. and the placement of *Claudopus* in this genus, a more comprehensive molecular phylogeny of *Entoloma* s.l. was carried out by employing the combined ITS, LSU, mtSSU and RPB2 sequences in the present paper. On the other hand, both descriptive and molecular information about 5 new taxa in subgenus *Claudopus* recently discovered at various localities in China is provided and the first record of *Entoloma byssisedum* var. *microsporum* Esteve-Rav. & Noordel. (originally reported from Spain) is listed for the Chinese mycota. Key and descriptions also take the recently described Chinese *Claudopus* species into consideration, viz. *E. crepidotoides* W.Q. Deng & T.H. Li and *E. alpinum* Xiao L. He, W.H. Peng & B.C. Gan (Deng et al. 2015; He et al. 2015). It can be assumed that the number of Chinese representatives of *Claudopus* will significantly increase with further fieldwork.

Material and methods

Morphological descriptions

Photographs of fresh specimens are taken *in situ* and all relevant ecological data are recorded at the actual habitat. All macromorphologic descriptions are also based on fresh material. Colour notations follow Kornerup and Wanscher (1978). Micromorphologic data are sketched with the help of a drawing tube attached to a Wild M 20 microscope. Basidiospores, basidia and pileipellis were mounted and measured in 5% potassium hydroxide (KOH) and/or 1% Congo Red. Measurements of the basidiospores exclude hilar appendix (apiculus). Q is used to mean "length/width ratio" of a basidiospore in profile view; ± means sample standard deviation; ***Q*** means average Q of all basidiospores; *x* means of basidiospore length and width. All holotype collections are kept in the Mycological Herbarium of Soil and Fertilizer Institute, Sichuan Academy of Agricultural Sciences (**SAAS**); isotypes and duplicates are preserved in Herbarium ZT, ETH, Zurich, Switzerland.

DNA extraction, PCR amplification and sequencing

Procedures of Genomic DNA extraction, PCR amplification, PCR products purification and sequencing were the same as in previous studies (He et al. 2013). The primers for RPB2 amplification were rpb2-6f and rpb2-7r, rpb2-i6f and rpb2-i7r (Co-David et al. 2009). The ITS regions were amplified with primer pairs ITS5 and ITS4 (White et al. 1990). The nLSU regions were amplified with primer pairs LR0R and LR5 (http://www.biology.duke.edu/fungi/mycolab/primers.htm). The mtSSU regions were amplified with primer pairs MS1 and MS2 (White et al. 1990).

Sequence alignment and phylogenetic analyses

Phylogenetic analyses were carried out, based on the ITS dataset and the combined dataset of ITS, nLSU, RPB2 and mtSSU. Sequences used in analysis are listed in table 1 and aligned in muscle 3.6 (Edgar 2004). If necessary, the aligned sequences were manually modified employing BioEdit 7.0.9.0 (Hall 1999). Representative sequences, published in previous studies, focused on entolomatoid fungi and new sequences, generated in this study, were selected for the present molecular analyses (Co-David et al. 2009; Baroni et al. 2011; Baroni and Matheny 2011; Largent et al. 2011; Kinoshita et al. 2012; Morgado et al. 2013; Morozova et al. 2014; Vila et al. 2014; He et al. 2015; Kokkonen 2015). The quality of these sequences was further accessed and those sequences in low quality were excluded in the present study. Almost all representative species in these studies were included. No conflicts between the ITS, nLSU, RPB2 and mtSSU datasets were observed by comparing the topologies resulting from the phylogenetic analysis of the single gene and therefore they were combined in the analysis.

Maximum Likehood (ML), Maximum Parsimony (MP) and Bayesian analyses were performed on the combined dataset, respectively. ML analyses were carried out by the web RAxML Version 8 (http://www.phylo.org/sub_sections/portal/) under the GTR+G+T model with 1000 bootstrap replicates (Stamatakis 2014). "Find best tree using maximum likelihood search" option was selected when analysing. MP analyses was performed using PAUP* version 4.0b10 (Swofford 2003). All characters were treated as unordered and of equal weight. Gaps were treated as missing data. Bootstrap values (BS) were calculated from 1000 replicates. Bayesian analyses were performed using MrBayes 3.2.6 (Ronquist and Huelsenbeck 2003). The best substitution models for each marker were selected by using Akaike Information Criterion (AIC) in jModelTest 2.1.7 (Darriba et al. 2012). GTR+I+G model was employed for nLSU, mtSSU and ITS, SYM+G for RPB2. Six Markov chains were run for 2 runs from random starting trees for 15 million generations and sampled every 100 generations. Average standard deviation of split frequencies below 0.05 is an indication of convergence. Bayesian Posterior Probabilities (BPP) were determined after calculating a 75% majority rule consensus tree.

Results

Taxonomy

1. *Entoloma conchatum* Xiao L. He & E. Horak, sp. nov.
MycoBank No: 817515
Figures 1a, b, 2

Type. China. Sichuan Prov., Miyi County, Huangqiao reservoirs, ca. 1500 m elev., 26°42'–27°10'N, 101°41'–102°15'E, on soil, 13 September 2015, X.L. He (*SAAS 1712*, holotype; *ZT 13628*, isotype).

Sequences ex holotype. KU312111 (ITS), KU534220 (nLSU), KU534459 (RPB2), KU534432 (mtSSU).

Etymology. *conchatum* (Lat.), referring to the conchate shape of the basidiomes.

Diagnosis. *Entoloma conchatum* closely resembles *Entoloma parasiticum* (Quél.) Kreisel, described from Europe and N-America but differs by smaller basidiospores. The Australian *C. viscosus* is separated from *E. conchatum* by its sticky pileus and the absence of rhizoids at the base of the rudimentary stipe.

Pileus 7–15 mm, conchate, broadly convex, at first white, becoming orange-white, yellowish-white and finally pale pinkish in age, entirely matted-tomentose to matted-depressed fibrillose, opaque, dry, not hygrophanous, margin not transparent-striate. Lamellae with 2–4 tiers of lamellulae, adnexed, up to 2 mm wide, subventricose, subdistant, white at first, becoming pinkish in age, entire margin concolorous. Stipe 1–3 × 0.5–1 mm, lateral, strongly reduced, covered with minute, white fibrils, base with white mycelium. Rhizoids absent. Context white, thin, unchanging. Odour and taste not distinctive.

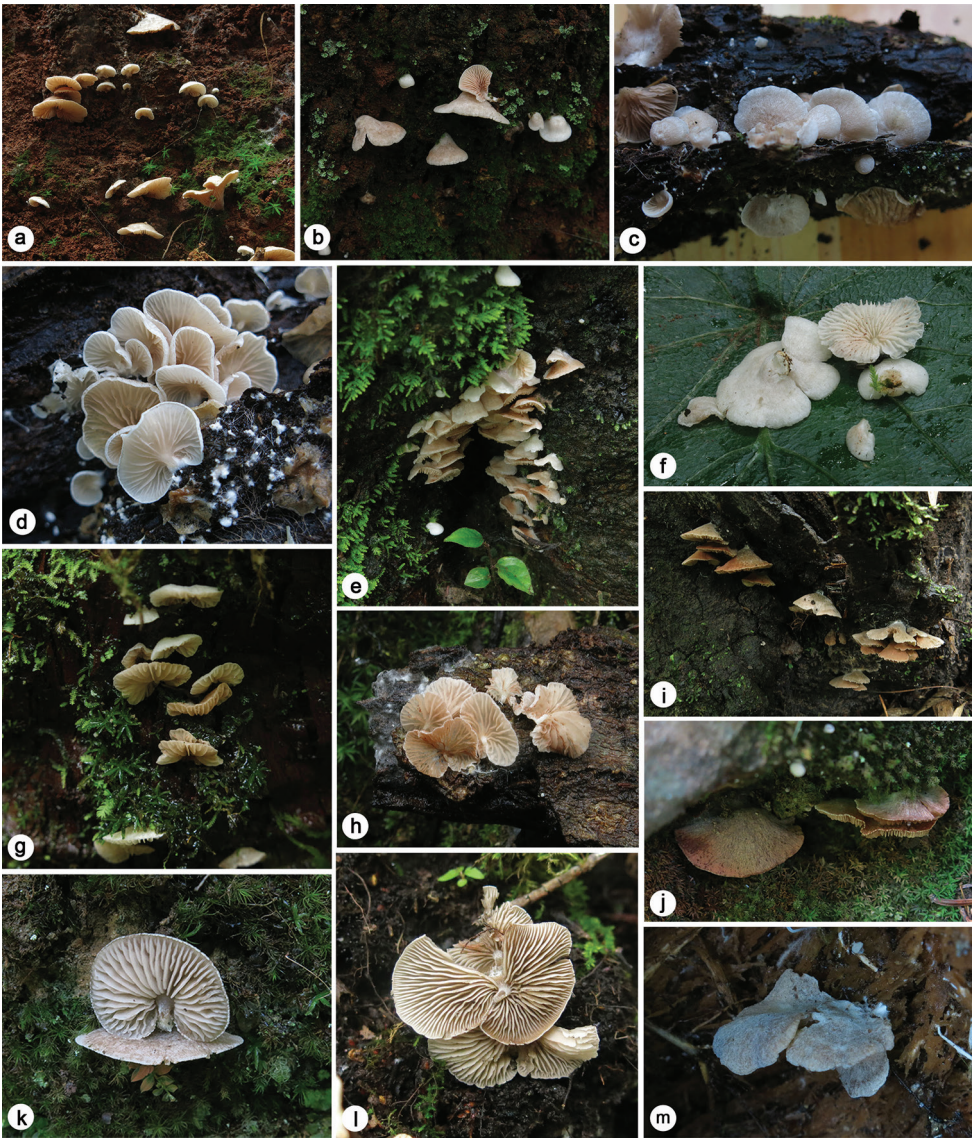

Figure 1. Basidiomes of *Claudopus* species **a** Basidiomes of *E. conchatum* on soil (SAAS 1712) **b** Basidiomes of *E. conchatum* on stem of live *Pinus* (SAAS 1014) **c** Pileus of *E. flabellatum* (SAAS 1501) **d** Lamellae of *E. flabellatum* (SAAS 1080) **e** Basidiomes of *C. gregarious* on bark-wood of live *Castanopsis* (SAAS 1220) **f** Red droplets on the lamellar edges of *E. gregarium* (SAAS 1493) **g** Basidiomes of *E. pleurotoides* on decaying bark-wood of *Castanopsis* (SAAS 1215) **h** Basidiomes of *E. pleurotoides* on bark-wood of live *Castanopsis* (SAAS 1252) **i** Basidiomes of *E. reductum* on decaying stump of *Castanopsis* (holotype, SAAS 1091) **j** Mature basidiomes of *E. reductum* on rock (SAAS 2068) **k** Young basidiomes of *E. reductum* on soil (SAAS 1016) **l** Lamellae of *E. byssisedum* var. *microsporum* (SAAS 1828) **m** Basidiomes of *E. byssisedum* var. *microsporum* on decaying stump of *Betula* (SAAS 1160).

Basidiospores 8–10 (10.5) × (6) 6.5–8 μm (x = 9.0 ± 0.3 × 7.3 ± 0.3 μm), Q = 1.2–1.4, ***Q*** = 1.28 ± 0.03, 5–6-angled, heterodiametric in profile view. Basidia 28–34 × 9–12 μm, subclavate, 4-spored (also often 2-spored). Lamellar edge fertile. Cheilocystidia, pleurocystidia and caulocystidia absent. Pileipellis a cutis composed of cylindrical hyphae, terminal cells (25–)35–50 × 4–7 μm, cylindrical (or slender subclavate, weakly gelatinised wall thin, smooth or minutely encrusted with pale yellow pigment. Oleiferous hyphae numerous in pileipellis. Clamp-connections present in all tissues.

Habitat. Amongst moss on stem base of living conifers and fallen branches of conifers (*Pinus* sp., *Picea* sp.), or on roadside in conifers forest or broadleaf forest.

Additional materials examined. China. Sichuan Prov., Miyi County, Huangqiao Reservoirs, ca. 1500 m elev., 26°42'N, 101°41'E, on soil, 13 September 2015, *X.L. He* (*SAAS 1415*); on fallen branches of conifers, 13 September 2015, *X.L. He* (*SAAS 1117*); X.L. He (*SAAS 1378*); amongst moss on stem base of living conifers, 13 September 2015, *X.L. He* (*SAAS 1470*); on soil, 13 September 2015, *X.L. He* (*SAAS 1014*; *ZT 13609*; *SAAS 1364*; *ZT 13615*). Yunnan Prov., Jinghong County, Dadugang, ca. 1200 m elev., 22°30'N, 101°45'E, on soil, 27 August 2011, *X.L. He and M. Zhang* (*GDGM 28817*).

Remarks. *Entoloma conchatum* is characterised by basidiomes gradually changing colour from white to pinkish, matted-fibrillose pileus, 5–6-angled basidiospores and presence of clamp connections.

Macromorphologically (white fibrillose basidiomes), the following taxa resemble *E. conchatum* viz. *E. crepidotoides* W.Q. Deng & T.H. Li, recently described from tropical China, *E. indocarneum* Manim., Leelav. & Noordel. from India, *E. exiguum* Esteve-Rav. & M. de la Cruz, *E. jahnii* Wölfel & Winterh. and *E. parasiticum* from Europe, *Claudopus minutoincanus* Largent & Abell-Davis, *E. pitereka* Noordel. & G.M. Gates, *C. rupestris* Largent & Abell-Davis and *C. viscosus* Largent & Abell-Davis from Australia and, finally, *C. pandanicola* E. Horak from Papua New Guinea. However, *E. jahnii*, *E. exiguum* and *E. parasiticum* are readily distinguished by the much larger basidiospores (9.4–12 × 6.4–8.3 μm, 9.5–12.5 × 8–10.5 μm, 9.7–12.9 × 7.6–10.2 μm, respectively; Esteve-Raventos & De La Cruz 1998; Noordeloos 1992, 2004). *Entoloma pitereka* differs in the prominent basal rhizomorphs and larger basidiospores (8–12 × 6–8 μm, Noordeloos and Gates 2012); *C. pandanicola* is separated by the translucent striate pileus and smaller basidiospores (7–8 × 6.5–7.5 μm, Horak 1980). *C. minutoincanus* is different from *E. conchatum* in the sticky pileus and absence of clamp connections; *C. rupestris* is separated by the 4–5-angled and smaller basidiospores (6.5–9.2 × 6–8 μm) and absence of clamp connections; *C. viscosus* is distinctive by the presence of rhizoids and absence of clamp connections (Largent et al. 2011). The only white *Claudopus* species recently described from tropical China, *E. crepidotoides*, is recognised by the smaller basidiospores (8–9 × 6–7 μm, Deng et al. 2015). *E. indocarneum* (as *E. carneum* Manim., Leelav. & Noordel. in Manimohan et al. 2002) is readily distinguished from *E. conchatum* by its smooth pileus, presence of mycelial rhizoids and narrower basidiospores (7.5–10 × 5–7 μm, Manimohan et al. 2002).

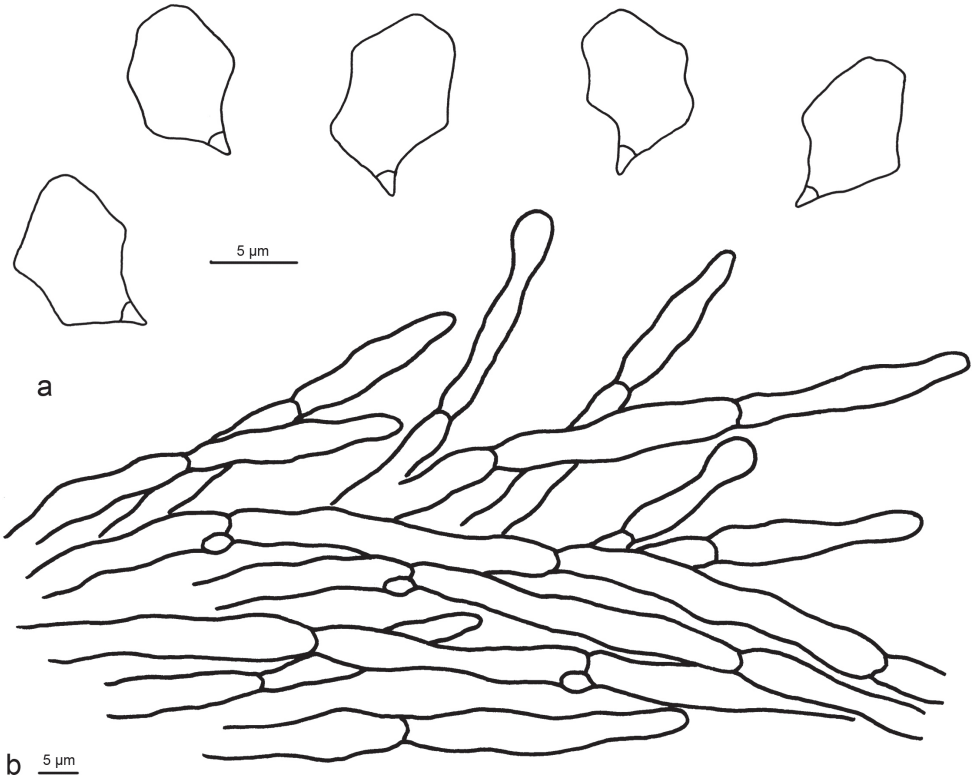

Figure 2. Microscopic structures of *Entoloma conchatum* (holotype) **a** Basidiospores **b** Basidia **c** Pileipellis.

2. *Entoloma flabellatum* Xiao L. He & E. Horak, sp. nov.
MycoBank No: 817516
Figures 1c, d, 3

Type. China. Guizhou Prov., Leishan County, Leigong Mountain, ca. 1600 m elev., 26°22'N, 108°12'E, on decaying stump of fagalean tree, 19 July 2014, *X.L. He* (*SAAS 1080*, holotype; *ZT 13612*, isotype).

Sequences ex holotype. KU312115 (ITS), KU534217 (nLSU), KU534470 (RPB2).

Etymology. *flabellatum* (Lat.), referring to the fan-like shape of the basidiomes.

Diagnosis. *Entoloma flabellatum* is separated from the sympatric *E. pleurotoides* by the more heterodiametric basidiospores.

Pileus 5–15 mm, conchate, broadly convex, becoming applanate with age, entirely matted-tomentose to matted-appressed fibrillose, membranous, whitish at first, becoming orange-white, yellowish-white to pale pinkish with age, weakly hygrophanous, non-striate to minutely sulcate-striate towards margin, dry. Lamellae 6–15, with 2–3 tiers of lamellulae, adnexed, distant, narrow, ventricose, up to 1.5 mm wide, white at first, becoming pinkish with age, entire edges concolorous. Stipe 1–2.5 × 0.5–1 mm,

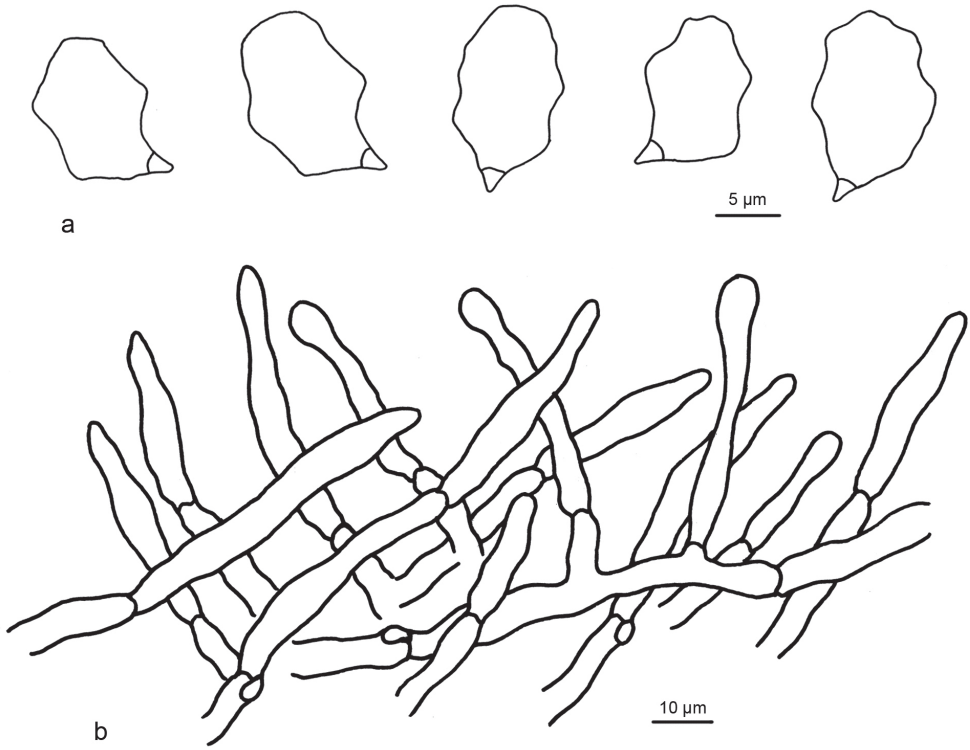

Figure 3. Microscopic structures of *Entoloma flabellatum* (holotype) **a** Basidiospores **b** Basidia **c** Pileipellis.

lateral, strongly reduced, pale grey-brown, covered with minute pale grey fibrils, base with white mycelium and prominent white rhizoids. Context thin, unchanging. Odour and taste not distinctive.

Basidiospores 8–10.5 (11) × 6–7 (7.5) µm (x = 8.9 ± 0.3 × 6.4 ± 0.3 µm), Q = 1.26–1.52, ***Q*** = 1.38 ± 0.04, 5–7-angled, heterodiametric in profile view. Basidia 28–38 × 7–8 µm, slender clavate, 4-spored, clampless. Lamellar edge fertile. Cheilocystidia, pleurocystidia and caulocystidia absent. Pileipellis a cutis composed of cylindrical hyphae, terminal cells (25–) 30–80 × 6–10 µm, repent or slightly uplifted, subclavate, non-gelatinised walls thin, smooth or minutely encrusted with yellowish pigment, subpellis composed of short-celled cylindrical hyphae, 6–20 µm diam. Oleiferous hyphae absent. Clamp connections present in pileipellis.

Habitat. On decaying stump of fagalean tree, in bamboo forest.

Additional materials examined. China. Guizhou Prov., Leishan County, Leigong Mountain, ca. 1600 m elev., 26°22'N, 108°12'E, on decaying stump of fagalean tree, 18 July 2014, *X.L. He* (*SAAS 1501*, *ZT 13605*).

Remarks. *Entoloma flabellatum* is distinguished by the small and pleurotoid basidiomes, prominent white rhizoids attached to the rudimentary lateral stipe and (5–) 6-angled basidiospores measuring 7.5–8.5 × 5.5–6.5 µm. The basidiomes are white at first but gradually change to yellowish or orange with age.

Numerous species of *Claudopus* recorded from SE-Asia and Australasia are characterised by white basidiomes, cf. Horak (1980), Manimohan et al. (2002), Noordeloos (2004), Largent et al. (2011) and Noordeloos and Gates (2012). The Chinese *E. flabellatum* closely resembles the following three taxa recently described from Australia viz. *E. pitereka* which differs by larger basidiospores (8–12 × 6–8 µm, Noordeloos and Gates 2012), spermatic odour and nutty taste. In addition, the ecology of *E. flabellatum* and *E. pitereka* differs distinctly: *E. pitereka* is reported to occur on rotten wood-bark in wet *Eucalyptus* forest, while *E. flabellatum* is found on rotten wood-bark in subtropical bamboo forest of SW-China. *C. minutoincanus* is also similar to the Chinese *E. flabellatum*, but is distinguished by more isodiameteric basidiospores (7.4–11.4 × 6.3–9.6 µm, Q = 1.08–1.44, Largent et al. 2011). In addition, the RPB2 sequence of *E. flabellatum* is 97% identical to that of *C. minutoincanus*, indicating that they are closely related, but separate species. Macroscopically and microscopically *C. viscosus* is difficult to separate from *E. flabellatum*. However, apart from different size of the basidiospores, the RPB2 sequences of the two species have no significant molecular similarity and thus indicate to represent different and not closely related species (Fig. 9).

3. *Entoloma gregarium* Xiao L. He & E. Horak, sp. nov.

MycoBank No: 817517
Figures 1e, f, 4

Type. China. Yunnan Prov.: Binchuan County, Jizu Mountain, ca. 2700 m elev., 25°58'N, 100°21'E, on stem base of living *Castanopsis*, 8 September 2015, *X.L. He* (*SAAS 1220*, holotype).

Sequences ex holotype. KU312122 (ITS), KU534237 (nLSU), KU534474 (RPB2), KU534423 (mtSSU).

Etymology. *gregarium* (Lat.), referring to gregarious habit.

Diagnosis. *Entoloma gregarium* resembles the Chinese *E. conchatum*, but differs by smaller basidiospores.

Pileus 5–10 mm, conchate, broadly convex, pure white, unchanging with age, entirely matted-tomentose to matted-depressed fibrillose, opaque, dry, not hygrophanous, margin not striate. Lamellae adnexed, subdistant to distant, subventricose, up to 2 mm wide, with two tiers of lamellulae, white at first, becoming pale pink, in moist condition with small red droplets at edges. Stipe 1–3 × 0.5–1 mm, strongly reduced, lateral, translucent, covered with minutely, white fibrils, equal, with white basal mycelium. Context white, unchanging, thin. Odour and taste not distinctive.

Basidiospores 7–9 (9.5) × 5.5–7 µm (x = 7.7 ± 0.3 × 6.3 ± 0.3 µm), Q = 1.16–1.47, $\boldsymbol{Q}$ = 1.25 ± 0.04, 5–6 (7)-angled, heterodiametric in profile view. Basidia (26–) 30–34 × 7–10 µm, subclavate, 4-spored, clampless. Lamellar edge fertile. Cheilocystidia, pleurocystidia and caulocystidia absent. Pileipellis a cutis of cylindrical hyphae, terminal cells (25–) 35–60 × 5–10 µm, subclavate or cylindrical (rarely also subfusoid), repent or slightly uplifted, non-gelatinised wall thin, smooth, with inconspicuous plas-

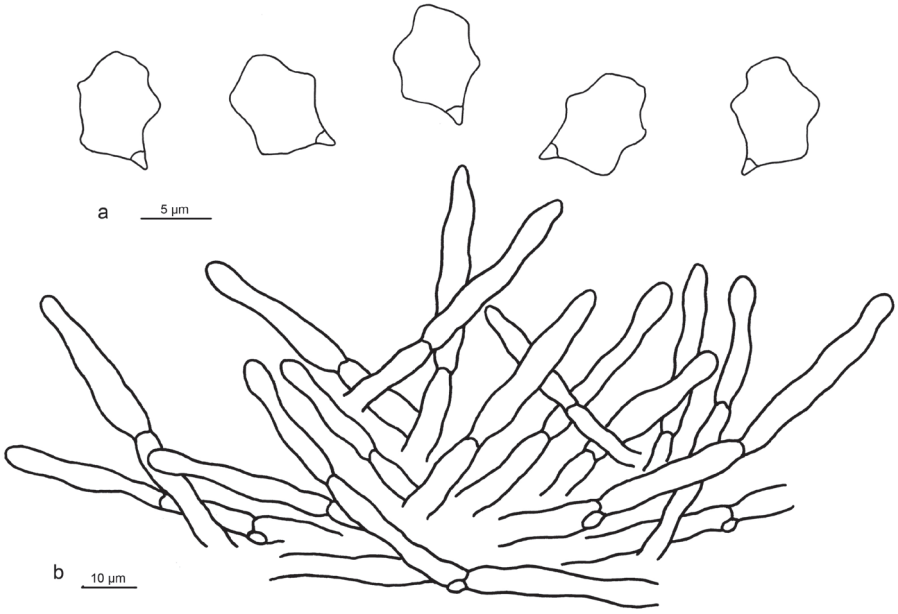

Figure 4. Microscopic structures of *Entoloma gregarium* (holotype) **a** Basidiospores **b** Basidia **c** Pileipellis.

matic pigment, subpellis composed of short-celled cylindrical hyphae, 6–14 µm diam. Oleiferous hyphae present in pileipellis. Clamp-connections present in all tissues.

Habitat. Amongst moss on stem base of living *Castanopsis* in fagalean forest.

Additional materials examined. China. Yunnan Prov.: Binchuan County, Jizu Mountain, ca. 2700 m elev., 25°58'N, 100°21'E, on stem base of living *Castanopsis*, 8 September 2015, *X.L. He* (*SAAS 1493*); *X.L. He* (*SAAS 1535*).

Remarks. As compared to other sympatric Chinese species, *E. gregarium* is unique due to the combination of the following characters viz. persistently white and gregarious basidiomes and small basidiospores.

The aforementioned taxa of *Claudopus* viz. *E. conchatum*, *E. indocarneum*, *E. crepidotoides*, *E. exiguum*, *E. jahnii*, *C. minutoincanus*, *C. pandanicola*, *E. parasiticum*, *E. pitereka*, *C. rupestris* and *C. viscosus* have white basidiomes and, accordingly, are macroscopically similar to *E. gregarium*. However, *E. gregarium* is separated from *E. conchatum*, *E. jahnii*, *C. minutoincanus*, *E. parasiticum*, *E. pitereka* and *C. viscosus* by smaller basidiospores; *C. rupestris* differs by the 4–5-angled basidiospores (Largent et al. 2011; Noordeloos 2004).

Based on macromorphological characters, *E. gregarium* is difficult to distinguish from *E. crepidotoides* (Deng et al. 2015); however, the different habitats allow the two species to be discriminated. Additionally, the molecular evidence (Figs 8, 9) of *E. crepidotoides* and *E. gregarium* clearly indicate that they are two distinctive species. *E. indocarneum* is characterised by smooth pileus and presence of mycelial rhizoids (Manimohan et al. 2002). *Claudopus pandanicola*, originally described from tropical Papua New Guinea, is separated by the striate pileus and the different shape of the basidiospores (7–8 × 6.5–7.5 µm, Horak 1980).

4. *Entoloma pleurotoides* Xiao L. He & E. Horak, sp. nov.
MycoBank No: 817514
Figures 1g, h, 5

Type. China. Yunnan Prov.: Jingdong County, Ailao Mountain, ca. 2500 m elev., 24°23'N, 100°47'E, amongst moss at base of living *Castanopsis* sp., 10 September 2015, *X.L. He* (*SAAS 1252*, holotype; *ZT 13610*, isotype).

Sequences ex holotype. KU312113 (ITS), KU534227 (nLSU), KU534468 (RPB2), KU534424 (mtSSU).

Etymology. *pleurotoides* (Lat.), referring to the pleurotoid shape of the basidiomes.

Diagnosis. *Entoloma pleurotoides* is close to the Australian *E. pitereka*, but differs by smaller and more isodiameteric basidiospores.

Pileus 5–15 mm, conchate, broadly convex, becoming applanate with age, entirely matted-tomentose to matted-appressed fibrillose, membranous, whitish at first, becoming orange-white, yellowish-white and finally pale pinkish with age, slightly hygrophanous, margin not transparent-striate. Lamellae 7–11, with 1–2 tiers of lamellulae, adnexed, distant, narrow, up to 1.5 mm wide, subventricose, white at first, becoming pinkish with age, entire edges concolorous. Stipe 1–2.5 × 0.5–1 mm, strongly reduced, lateral, pale grey brownish, covered with minutely, pale greyish fibrils, base with white mycelium, white basal rhizoids present. Context thin, unchanging. Odour absent. Taste not distinctive.

Basidiospores 8–10 × (7) 7.5–9.5 μm (x = 9.2 ± 0.2 × 8.4 ± 0.3 μm), Q = 1.0–1.25, $\boldsymbol{Q}$ = 1.1 ± 0.03, 5–6-angled, isodiametric to subisodiametric, 5–6-angled in profile view, with pronounced angles. Basidia 32–40 × 12–14 μm, clavate, 4-spored, clampless. Lamellar edge fertile. Cheilocystidia, pleurocystidia and caulocystidia absent. Pileipellis a cutis composed of cylindrical hyphae, terminal cells (25–) 30–40 × 3–8 μm, subclavate or cylindrical (rarely also subfusoid), repent or slightly uplifted, non-gelatinised wall thin, smooth, with inconspicuous plasmatic pigment, subpellis composed of short-celled cylindrical hyphae, 5–10 μm diam. Oleiferous hyphae present in pileipellis. Clamp-connections present.

Habitat. Amongst moss at base of living *Castanopsis* sp. or on decaying debris of *Castanopsis* sp.

Additional materials examined. China. Yunnan Prov.: Jingdong County, Ailao Mountain, ca. 2500 m elev., 24°23'N, 100°47'E, amongst moss at base of living *Castanopsis* sp., 10 September 2015, *X.L. He* (*SAAS 1354*); on decaying debris of *Castanopsis* sp., 10 September 2015, *X.L. He* (*SAAS 1215*; *ZT 13613*); Wuliang Mountain, ca. 2200 m elev., 24°45'N, 100°30'E, amongst moss at base of living *Castanopsis* sp., 9 September 2015, *X.L. He* (*SAAS 1007*).

Remarks. *Entoloma pleurotoides* is characterised by white, small and pleurotoid basidiomes, presence of basal rhizoids and isodiametric to subisodiametric basidiospores.

Macromorphologically, *E. pleurotoides* closely resembles *E. pitereka* which, however, differs by more heterodiametric basidiospores (Noordeloos and Gates 2012). Two other Australian species of *Claudopus* (*C. rupestris*, *C. viscosus*) possess basal rhizoids but, contrary to *E. pleurotoides*, are recognised by 4–5-angled, heterodiametric basidi-

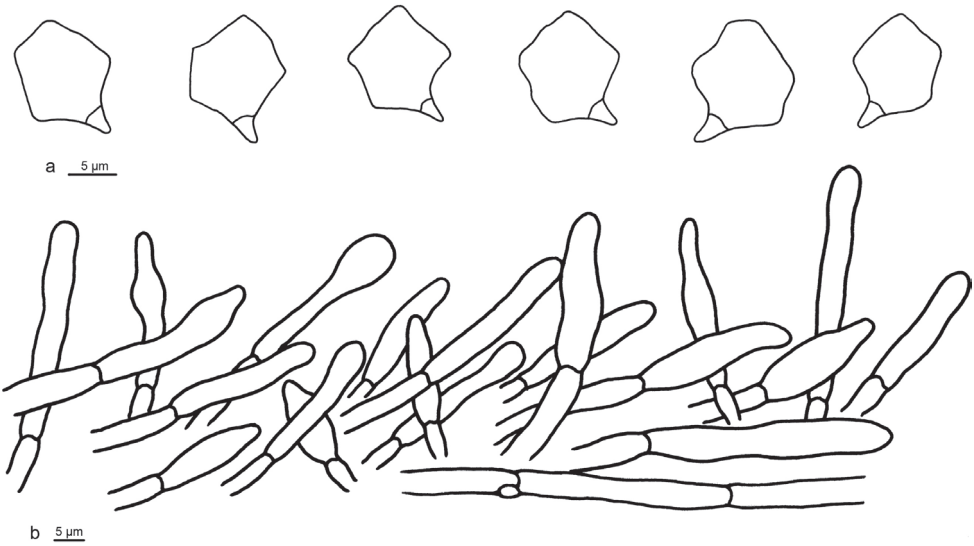

Figure 5. Microscopic structures of *Entoloma pleurotoides* (holotype): **a** Basidia **b** Basidiospores **c** Pileipellis.

ospores (Largent et al. 2011). Basal rhizoids are also reported for the Indian *E. indocarneum* (Manimohan et al. 2006), which is separated by smooth pileus and more pronounced heterodiametric basidiospores (7.5–10 × 5–7 µm, Manimohan et al. 2002). Concerning macromorphologic characters, *E. pleurotoides* is difficult to separate from the following *E. flabellatum* discovered in China; however, the latter differs by the more distinctive heterodiametric basidiospores. In addition, molecular evidence further confirms that the two taxa represent two defined species. The ITS sequences of *E. flabellatum* are 88% identical to those of *E. pleurotoides*.

5. *Entoloma reductum* Xiao L. He & E. Horak, sp. nov.

MycoBank No: 817513
Figures 1i, j, k, 6

Type. China. Yunnan Prov.: Binchuan County, Jizu Mountain, ca. 2600 m elev., 25°58'N, 100°21'E, on rotten stump of *Castanopsis* sp., 8 September 2015, *X.L. He* (*SAAS 1091*, holotype; *ZT 13607*, isotype).

Sequences ex holotype. KU312123 (ITS), KU534232 (nLSU), KU534480 (RPB2), KU534419 (mtSSU).

Etymology. *reductum* (Lat.), referring to the reduced stipe.

Diagnosis. *Entoloma reductum* is similar to *E. byssisedum* but differs by the size of the basidiospores.

Pileus 8–25 mm broad, conchate, broadly convex to applanate, greyish at first, becoming greyish-brown with age, entirely matted-tomentose or matted-fibrillose, fi-

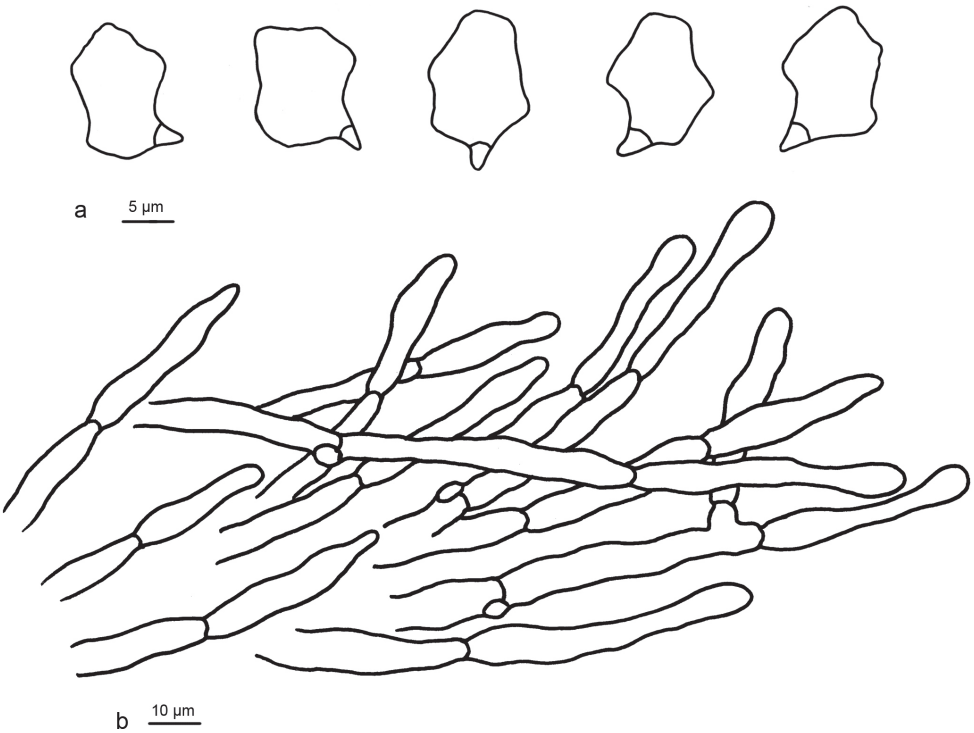

Figure 6. Microscopic structures of *Entoloma reductum* (holotype) **a** Basidiospores **b** Pileipellis.

brils greyish-white, slightly hygrophanous, margin weakly transparent-striate. Lamellae moderately close, with two tiers of lamellulae, adnate, ventricose, up to 4 mm wide, whitish or pale greyish at first, becoming pink or rust pinkish with age, entire edges concolorous. Stipe 1–2.5 × 0.5–1 mm, lateral, strongly reduced, pale grey brownish, covered with minute pale greyish fibrils, base with white mycelium. Rhizoids absent. Context thin, greyish, unchanging on exposure. Odour absent. Taste not distinctive.

Basidiospores 8–10.5 (12) × 6–7.5 µm (x = 8.8 ± 0.2 × 6.6 ± 0.3 µm), Q = 1.25–1.61, $\boldsymbol{Q}$ = 1.35 ± 0.05, 5–6-angled, heterodiametric in profile view. Basidia 20–34 × 8–11 µm, clavate, 4-spored, clampless. Lamellar edge fertile. Cheilocystidia, pleurocystidia and caulocystidia absent. Pileipellis a cutis composed of cylindric hyphae, terminal cells (25–) 40–65 × 5–7 µm, repent or slightly uplifted, cylindrical or slender clavate, non-gelatinised wall thin, smooth or minutely encrusted with slightly pale brown pigment. Oleiferous hyphae present in pileipellis. Clamp connections present in the pileipellis.

Habitat. On decayed stump of *Castanopsis* sp.; on soil or rock amongst moss in forest dominated by *Quercus* sp.

Additional materials examined. China. Sichuan Prov.: Yajiang County, Gexigou National Nature Reserve, ca. 2800 m elev., 30°03'N, 101°E, on rock amongst moss, 6 August 2015, *X.L. He* (*SAAS 1016*); on soil amongst moss, 3 August 2014, *X.L. He* (*SAAS 1897*); on rock amongst moss, 3 August 2014, *X.L. He* (*SAAS 2068*). Yunnan

Prov.: Binchuan County, Jizu Mountain, ca. 2600 m elev., 25°58'N, 100°21'E, on decayed stump of *Castanopsis* sp., 8 September 2015, *X.L. He* (*SAAS 1608*; *ZT 13606*).

Remarks. *Entoloma reductum* is unique by the combined features of pleurotoid, greyish-brown basidiomes, presence of brownish encrusting and intracellular pigment and presence of scattered clamp connections.

Entoloma reductum can be confused with *E. byssisedum* (Pers.) Donk; however, the latter species is separated by the larger basidiospores (9.5–12 × 6.5–8.0 μm, Noordeloos 2004). *E. byssisedum* var. *microsporum* is separated by the more reniform and paler coloured pileus and, in addition, the two species are well distinguished by their ITS and RPB2 sequences. *Claudopus dulcisaporus* Largent, described from North America, shares with *E. reductum* the brown basidiomes and the size of the basidiospores, but it can be distinguished not only by the presence of abundant cheilocystidia, but also the habitat (Largent 1994). *Claudopus graveolens* Largent is distinguished by smooth and bicolorous pileus, presence of cheilocystidia (Largent 1976); finally, *C. avellaneus* differs by the narrower basidiospores (8–10 × 5–6 μm, Murrill 1917).

6. *Entoloma byssisedum* var. *microsporum* Esteve-Rav. & Noordel.

Figures 1l, m, 7

Description of Chinese material. Pileus 5–20 mm, reniform, broadly convex, expanding to applanate, whitish-grey to greyish, entirely matted-tomentose to matted-appressed fibrillose, fibrils whitish, slightly hygrophanous, not striate. Lamellae with 2–3 tiers of lamellulae, adnexed, ventricose, up to 2.5 mm wide, moderately close, pale greyish at first, becoming greyish-pink, entire margin concolorous. Stipe 1–5 × 0.5–1 mm, strongly reduced, lateral, grey, covered with minutely, pale greyish fibrils, at base with white hairy mycelium. Basal rhizoids present, white. Context thin, unchanging. Odour absent. Taste not distinctive.

Basidiospores 8–10 × 5.5–7 (7.5) μm (x = 9 ± 0.3 × 6.5 ± 0.2 μm), Q = 1.29–1.52, $\boldsymbol{Q}$ = 1.39 ± 0.04, 5–6 (7)-angled, heterodiametric in profile view. Basidia 30–34 × 9–11 μm, clavate, 4-spored, rarely 2-spored, clampless. Lamellar edge fertile. Cheilocystidia, pleurocystidia and caulocystidia absent. Pileipellis a cutis composed of cylindrical hyphae, repent terminal cells (30–) 35–50 × 4–7 μm, cylindrical (or slender subclavate), non-gelatinised wall thin, smooth or minutely encrusted with pale brown pigment. Oleiferous hyphae numerous in pileipellis. Clamp-connections present in the pileipellis.

Habitat. On decaying stump of *Betula* sp. in deciduous forest dominated by *Betula* sp. and *Quercus* sp.

Materials examined. China. Sichuan Prov.: Kangding County, Mugecuo, ca. 2700 m elev., 30°13'N, 101°83'E, on decaying stump of *Betula* sp., 4 August 2015, *X.L. He* (*SAAS 1160*); on decaying stump of *Betula* sp., 3 September 2015, *X.L. He* (*SAAS 1828*); on decaying stump of *Betula* sp., 3 September 2015, *X.L. He* (*SAAS 1279*; *ZT 13608*). Xizang Autonomous Region (Tibet): Linzhi County, Kadinggou, ca.

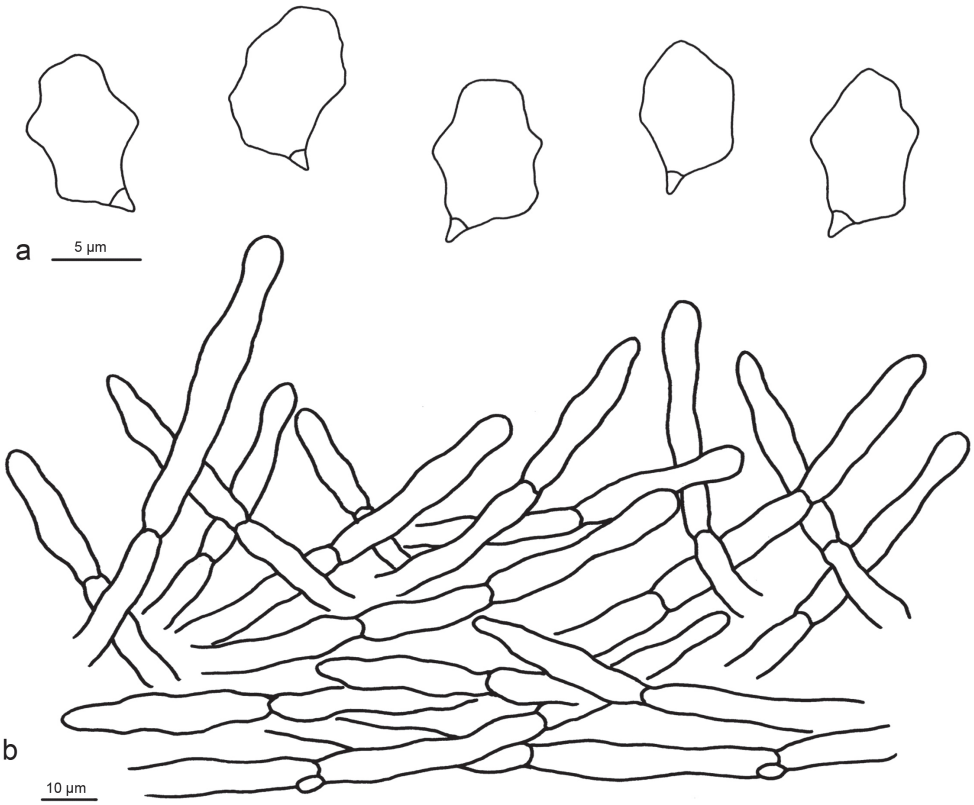

Figure 7. Microscopic structures of *Entoloma byssisedum* var. *microsporum* (SAAS 1279) **a** Basidiospores **b** Basidia **c** Pileipellis.

2980 m elev., 29°50'N, 93°25'E, on decaying stump of *Betula* sp., 25 September 2014, *X.L. He* (*SAAS 1025*); Linzhi County, Sejila Mountain, ca. 3600 m elev., 29°35'N, 94°25'E, on decaying stump of *Betula* sp., 24 September 2014, *X.L. He* (*SAAS 1953*).

Remarks. *Entoloma byssisedum* var. *microsporum* closely resembles typical *E. byssisedum* by its small crepidotoid pale greyish-brown basidiomes whose pileipellis is covered with fine, whitish arachnoid fibrils and lateral, strongly reduced to absent stipe. However, the basidiospores of the Chinese specimens are distinctly smaller as recorded for typical *E. byssisedum* and, thus, the morphotaxonomic characters correspond well with European collections of *E. byssisedum* var. *microsporum* (Noordeloos 2004). The identification is further supported by ITS sequences which demonstrate that the Chinese specimens of *E. byssisedum* var. *microsporum* are 99% identical as compared to those reported for European material (KJ001409). It is noteworthy that, in GenBank, there are two sequences labelled "*E. byssisedum*" (EU784209, KJ001413) which, however, are significantly different. The ITS sequences of the Chinese *E. byssisedum* var. *microsporum* are 97% identical to EU784209 but do not correspond with KJ001413. Accordingly, it could be speculated that *E. byssisedum* var. *microsporum* and *E. byssisedum* var. *byssisedum* actually represent two different species.

Key to the Chinese species of *Entoloma* subgenus *Claudopus* with pleurotoid basidiomes

1 Pileus grey to greyish-brown **2**
– Pileus white to pinkish-white **3**
2 Basidiospores 8–9.5 (–10) × (5.5) 6–7 µm. Occurring on bark-wood of *Castanopsis* and/or on soil ..... ***E. reductum***
– Basidiospores 9–10 × 6–6.5 µm. Occurring on decayed stumps of *Betula* ..... ***Entoloma byssisedum* var. *microsporum***
3 Basidiospores 8.5–10 (–10.5) × 7.5–9 µm, subisodiameteric to isodiametric ..... ***E. pleurotoides***
– Basidiospores smaller, heterodiameteric **4**
4 Reported from tropical lowland rain forest. Basidiospores 8–9 × 6–7 µm. On soil ..... ***E. crepidotoides***
– Reported from xerophytic or from montane habitat **5**
5 Basidiospores 8–10 × 6.5–7.5 µm. Basidiomes white at first becoming yellowish to orange with age. On living stem, on fallen branches of conifers or on soil ..... ***E. conchatum***
– Basidiospores narrower, on living or decaying hardwoods **6**
6 Basidiomes white at first becoming yellowish to orange with age. On decaying debris of fagalean tree ..... ***E. flabellatum***
– Basidiomes persistently white. Amongst moss at base of living *Castanopsis* ..... ***E. gregarium***

Molecular analyses

The new sequences presented in this study are deposited in GenBank with accession numbers KU312103–KU312125, KU534215–KU534217, KU534219–KU534238, KU534415–KU534436 and KU534459–KU534482. In the phylogenetic analysis, the final ITS dataset included 43 sequences; *E. omiense*, *E. stylophorum* and *E. subtenuicystidiatum* were designed as outgroups. The ITS dataset contained 702 nucleotide sites, of which 416 characters were constant, 175 were parsimony-informative characters and 111 variable characters were parsimony-uninformative. Two most parsimonious trees were recovered, based on ITS sequences and one of them is shown (Fig. 8). In the ITS tree, *E. conchatum* and *E. pleurotoides* grouped in the same monophyletic clade, while the remaining three species are placed in three different clades.

The combined dataset (ITS, nLSU, mtSSU and RPB2) consisted of 190 representatives and 4028 nucleotide bases were included. *Calocybe carnea* (Bull.) Donk, *Clitopilus cystidiatus* Hauskn. & Noordel. and *Lyophyllum leucophaeatum* (P. Karst.) P. Karst. were selected as outgroups. MP, ML and Bayesian analyses produced similar typologies except for some unsupported clades and the cladogram resulting from ML analysis is shown (Fig. 9). Ten monophyletic clades viz. *Claudopus* (Clade 1), *Leptonia* (Clade 2), *Nolanea* (Clade 3), *Cuboid-spored Inocephalus* (Clade 4), *"Alboleptonia"* (Clade 5), *Cyanula* (Clade

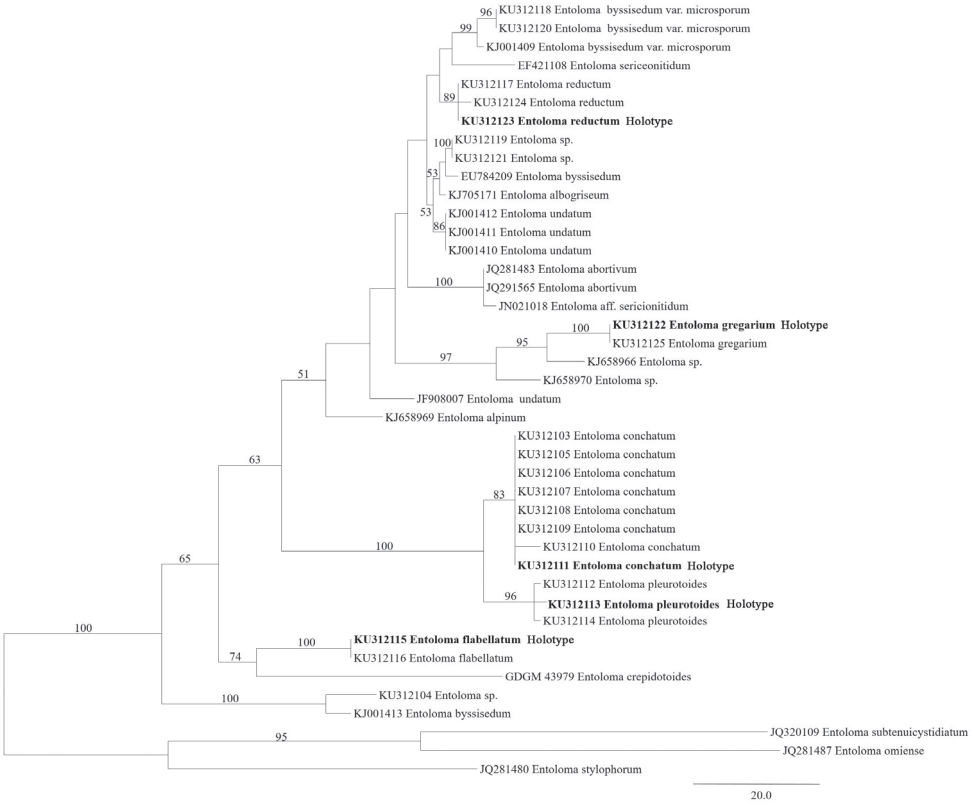

Figure 8. Phylogenetic reconstruction of *Claudopus* based on ITS sequences. Maximum parsimony bootstrap values (BS > 50%) are indicated above or below the branches, new species are in bold.

6), *Rusticoides* (Clade 7), *Pouzarella* (Clade 8), *Rhodopolia* (Clade 9) and *Prunnuloides* (Clade 10) were observed in the analyses. In Bayesian and ML analyses, *Nolanea*, *Leptonia* and *Claudopus* grouped in a large clade with significant support (0.99 pp and 93 RAxML BS, respectively). In the *Claudopus* clade, the five new species described above are clearly separated from each other. The traditional *Inocephalus* species (*E. griseolazulinum* Manim. & Noordel., *E. indigoticoumbrinum* G.M. Gates & Noordel., *E. tectonicola* Manim. & Noordel., *Inocephalus hypipamee* Largent and the cuboid-spored *Inocephalus*) are not placed in the same clade, and so for the sequestrate *Entoloma* (*E. prismaticum* Hir. Sasaki, A. Kinosh. & K. Nara, *E. hypogaeum* Hir. Sasaki, A. Kinosh. & K. Nara, *E. asterosporum* (Coker & Couch) Noordel. & Co-David and *Entoloma* sp.).

Discussion

Five new species of *Entoloma* subgenus *Claudopus* from China were described based on morphological and molecular data. Additionally, the phylogeny of *Entoloma* was also carried out, based on the combined ITS, LSU, mtSSU and RPB2 sequences. Co-David et al. (2009) presented a relatively comprehensive molecular phylogeny on

Entolomataceae (54 representatives of *Entoloma* were included). Since then, several molecular studies focusing on entolomatoid agarics have been reported (Baroni and Matheny 2011; Baroni et al. 2011; He et al. 2013; Kinoshita et al. 2012; Kokkonen 2015; Morgado et al. 2013; Morozova et al. 2014; Vila et al. 2014). Most of these studies were focused on one certain group or subgenus in *Entoloma* s.l. and samples used in phylogenetic analyses were mainly limited to the studied groups (He et al. 2013; Kokkonen 2015; Morgado et al. 2013; Morozova et al. 2014; Vila et al. 2014). This study provides a more comprehensive phylogeny, based on the sequences newly generated and includes almost all the representatives published in those previous studies (187 representatives of *Entoloma* were included). This is also the first contribution providing a relatively densely sampled systematic treatment of *Claudopus*. It is noteworthy that *Claudopus* in a traditional morphological sense is not monophyletic and the Rusticoides-group, previously considered within *Claudopus*, formed a separate clade; but the pleurotoid or crepidotoid *Claudopus* members, as well as *E. abortivum* (Berk. & Curt.) Donk, *E. undatum* and its related taxa, are placed in a distinctive monophyletic clade.

Phylogenetic analyses of combined datasets

In combined phylogenies, *Entoloma* s.l. is divided into ten monophyletic groups (Fig. 9). The majority of these groups are well defined regarding macro or micromorphology. The most distinctive group is the *Pouzarella*, whose taxonomic position as a monophyletic group is also supported by both morphologic and molecular evidence (Baroni and Matheny 2011; Co-David et al. 2009; He et al. 2013). In the previous studies, *Claudopus* species were nested in the nolanea-claudopus clade, based on very limited samples (Baroni and Matheny 2010; Co-David et al. 2009). However, on the basis of a more comprehensive sampling in the present study, it is obvious that *Claudopus* (*E. rusticoides* and relatives are excluded) is a monophyletic group clearly separated from *Nolanea*. *Claudopus* and *Nolanea* species are grouped as monophyletic groups, respectively, in different clades. In the present analysis, clade *Rusticoides* (traditionally considered within *Claudopus*) is also recognised to be monophyletic and is separated from *Claudopus*. Research data have indicated that traditional *Leptonia* (either as genus or subgenus) might be polyphyletic and species accommodated in section *Cyanula* are distantly related to section *Leptonia* (Baroni and Matheny 2011; Co-David et al. 2009). In Noordeloos and Gates (2012), section *Cyanula* was raised to subgeneric level and the concept of subgenus *Leptonia* was also emended. The present analysis further proved that the traditional concept of subgenus *Leptonia* is polyphyletic. In the previous studies, section *Leptonia* belonged to the /nolanea-claudopus clade, section *Cyanula* to the / inocephalus-cyanula clade, respectively. However, monophyly of section *Leptonia* and *Cyanula* are clearly demonstrated in this study. Section *Leptonia* is clearly separated from *Nolanea* and *Claudopus* and *Cyanula* is distinguished from *Inocephalus* (cuboid-spored *Inocephalus*), respectively. Two taxa in the traditional "*Alboleptonia*" (*A. stylophora* and *A.* aff. *sericella*) are grouped in the monophyletic clade *Cyanula*, while the following

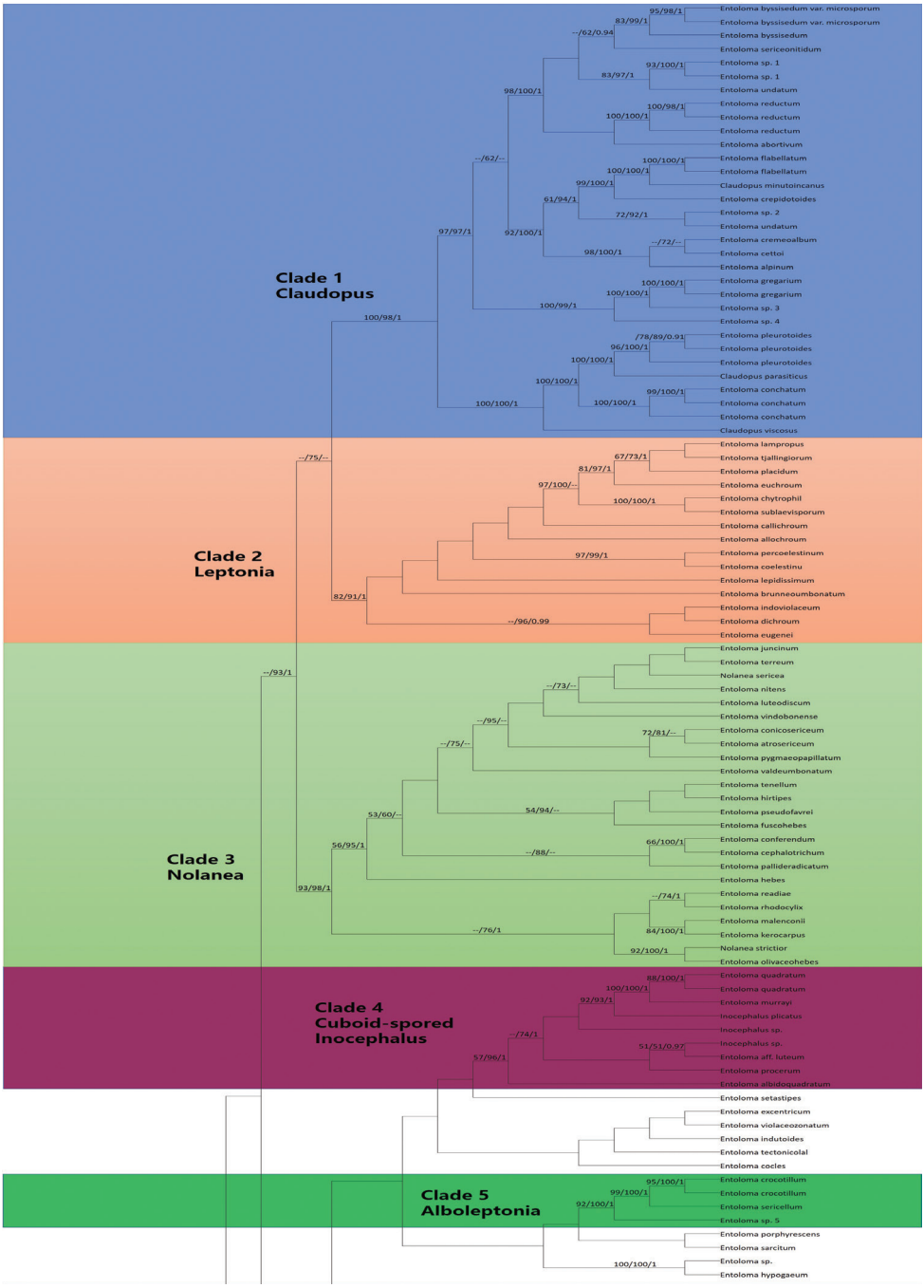

Figure 9. Cladogram based on the combined ITS, LSU, RPB2 and mtSSU sequences resulting from ML analysis. New species of *Entoloma* subgenus *Claudopus* are in bold. MP BS support values (> 50%), RAxML BS support values (> 50%) and Bayesian posterior probability values (BPP> 0.90) are indicated above or below branches as MP BS/RAxML BS/BPP.

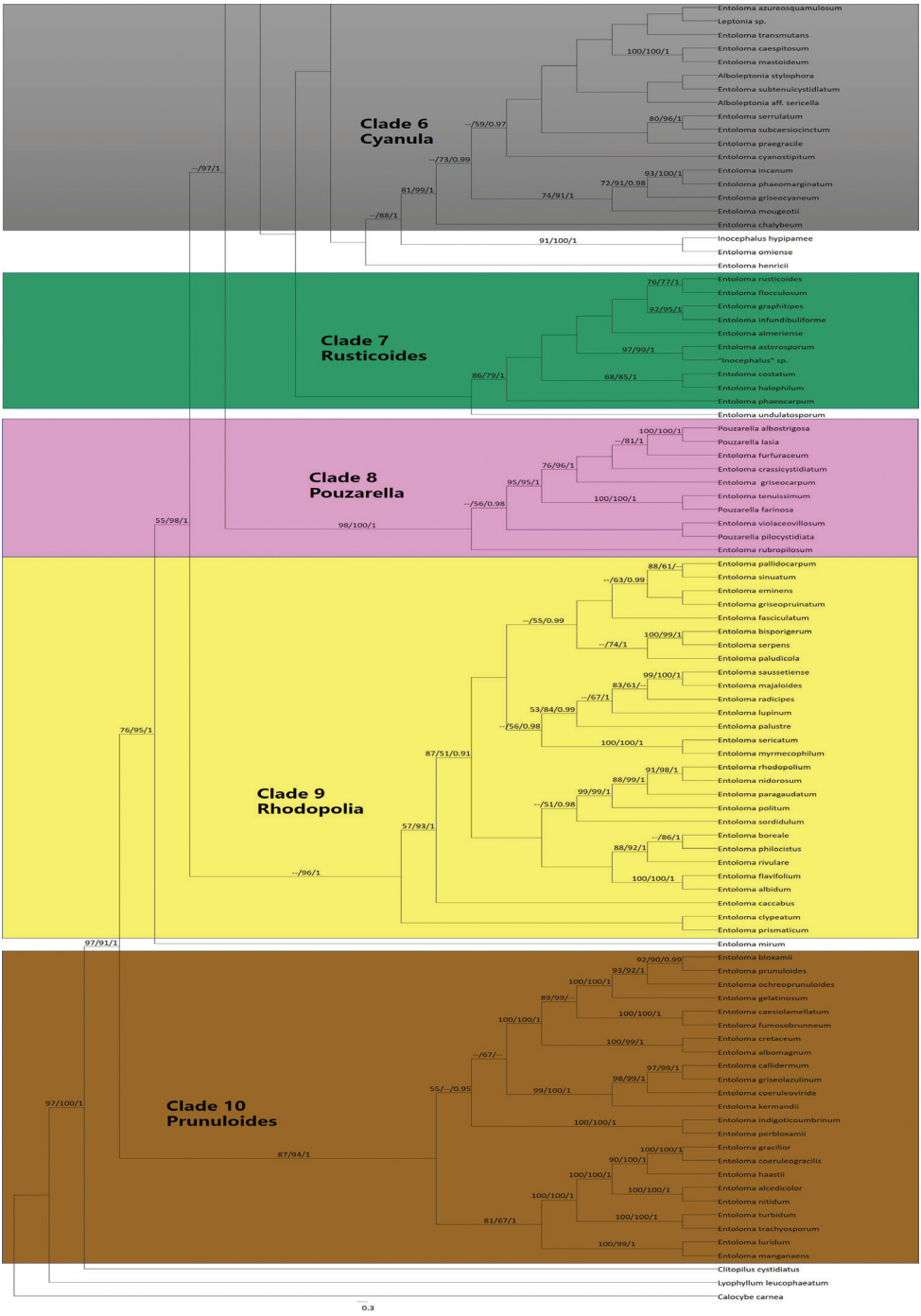

Figure 9. Continued.

species of "*Alboleptonia*" (*Entoloma crocotillum* Xiao L. He and *E. sericellum* (Fr.) P. Kumm.) are placed in a separated clade. These results suggest that "*Alboleptonia*" in the traditional circumscription might not be a well-defined genus or subgenus and the concept of *Cyanula* also needs to be revised. Polyphyly of the traditional *Inocephalus* is further confirmed in the present analyses. However, all analysed cuboid-spored species belonging to *Inocephalus* are clustered in a monophyletic clade, suggesting that these species may represent a distinct monophyletic group. The clade *Rhodopolia* (Clade 9) received strong support in the ML and Bayesian analysis which, however, is not supported by MP analysis. In the strongly supported *Prunuloides* clade, members in the emended subgenus *Entoloma* (Noordeloos and Gates 2012) were included and it is distant from the subgenus *Rhodopolia*, which is consistent with the previous studies (Baroni and Matheny 2011; Co-David et al. 2009). One internal clade includes 5 species of the traditional *Prunuloides* and 4 species [*E. haastii* G. Stev., *E. nitidum* Quél., *E. trachyosporum* Largent and *E. turbidum* (Fr.) Quél.] that belong to the genus *Entocybe* established by Baroni et al. (2011); however, it seems that it will cause subgenus *Prunuloides* to be paraphyletic if these entocyboid species are excluded from subgenus *Prunuloides* for the time being. The results also showed that sequestrate form (*E. prismaticum*, *E. hypogaeum*, *E. asterosporum* and *Entoloma* sp.) in *Entoloma* have multiple origins, which is consistent with the previous studies (Baroni and Matheny 2011; Kinoshita et al. 2012).

In conclusion: It can be safely predicted that, within entolomatoid agarics, further monophyletic lineages will be discovered as soon as the number of molecular information increases and, subsequently, the present classification of *Entoloma* s.l. is going to change fundamentally.

Phylogenetic species determination of *Claudopus*

The variation of macroscopic characters in many species of *Entoloma* subgenus *Claudopus* is limited and, accordingly, it is difficult or even impossible to identify morphologically similar taxa. In the future, it will be essential to recognise and describe new species of *Entoloma* subgenus *Claudopus* in combination with molecular data and morphological characters. Molecular analyses convincingly show that, regarding species of *Claudopus*, both ITS and RPB2 sequences have a high discriminating potential to separate species. In the present phylogenetic data, thirty-five sequences representing twenty-one phylogenetic species of *Entoloma* subgenus *Claudopus* are uncovered. It is herewith emphasised that nine species have now been recorded and four unidentified species have been collected from China which suggests that species diversity of *Entoloma* subgenus *Claudopus* is high in this country.

In the present ITS analysis (Fig. 8), two sequences labelled "*Entoloma byssisedum*" (EU784209, KJ001413) and one sequence referred to as *E. byssisedum* var. *microsporum* (KJ001409) are included. The relevant voucher material was collected in Europe. However, the molecular tree(s) demonstrates that the three sequences are nested in different clades: KJ001413 is distant from EU784209 and KJ001413. Consequently, it can be speculated that the European *E. byssisedum* var. *microsporum* could

be a distinctive species rather than a variety. Furthermore, the sequenced European materials, identified as *E. byssisedum*, is composed of a complex of as yet unnamed species or even more likely to misidentification of species of similar basidiomes. A similar situation is observed regarding *E. undatum*. In GenBank, sequences retrieved from several collections of *E. undatum* (ITS: KJ001412, JF908007; LSU: AF207199, GQ289202, KJ001455) are obviously different and belong to different species taxonomically not disentangled yet.

Ecology of Chinese taxa of *Claudopus*

Fieldwork demonstrated that the Chinese species of *Claudopus* are found in different habitats, characterised by distinctive ecology and substrates, (e.g. bark-wood of decaying debris of fallen or live broadleaf trees and conifers, soil in grassland or moss-covered rock). Unlike other entolomatoid species, the habitat on above-ground decaying wooden substrates is the rule for members of *Entoloma* subgenus *Claudopus*, while occurrence on bark-wood of live trees was not mentioned before in the relevant literature. The present results indicate, however, that growth on bark-wood of live trees is not uncommon for Chinese species of *Entoloma* subgenus *Claudopus*.

Based on present records, it is remarkable that, in China, the distribution of *Claudopus* stretches from tropical lowland forests (*E. crepidotoides*, from Hainan Prov.) to temperate and finally also to alpine localities in Sichuan Prov. (*E. alpinum*) or Xizang Autonomous Region, Tibet (*E. byssisedum* var. *microsporum*).

It must be emphasised that ecological data alone do not help to identify the Chinese taxa reported in the present contribution. As an example: based on available reports, *E. reductum* was found in different habitats and localities. The records from Sichuan Prov. were discovered on soil and moss-covered rock, but the specimens gathered in Yunnan Prov. are lignicolous. Despite different habitats, the microscopic examination and molecular data confirmed that the aforementioned records of *E. reductum* are identical. A similar observation was made regarding *E. conchatum* and *E. pleurotoides*. To confirm the identification of *Claudopus*, based on references relating to substrate/habitat, are not reliable unless morphotaxonomic characters and molecular data are also taken into consideration.

Diagnostic characters of *Claudopus* and the taxonomic position of *Entoloma* abortivum

In the large majority of entolomatoid species, the stipe is central and well developed. However, in some taxa of *Entoloma* subgenus *Claudopus*, the stipe is absent or strongly reduced and some species possess well-developed but eccentrically inserted stipes. In the tested *Claudopus* species, viz. *E. abortivum*, *E. alpinum*, *E. undatum*, *E. sericeonitidum* (P.D. Orton) Arnolds and an unidentified taxon (SAAS 1154), the stipes are well developed; while in other taxa strongly reduced and laterally attached stipes are observed. All of the above enumerated species are nested in the *Claudopus* clade with a strong

support. In the study of Vila et al. (2014), *E. korhonenii* Noordel., as well as several other *Claudopus* species, form a monophyletic group based on ITS sequences. The only common macro-character derived from the descriptions of these members, except for *E. undatum*, *E. korhonenii* and *E. sericeonitidum*, is that the stipes are off-centre which might be a key character for the recognition of *Claudopus*. It should be emphasised that the eccentric stipe should be a stabile and reliable character rather than an accidental adaptation to substrate in the habitats. During our field survey, we always found that the stipes of *E. abortivum*, *E. alpinum* and SAAS 1154 are off-centre or even eccentric.

Apparently, the stipe is also eccentrically inserted - but not properly mentioned in the relevant descriptions - in basidiomes of *E. undatum*, *E. sericeonitidum* and *E. korhoneni*. The eccentric position of the stipe can be observed in photographs of *E. undatum* and *E. korhonenii* (Noordeloos 2004). The picture of *E. sericeonitidum* (*Paraeccilia sericeonitida*) in Largent (1994) also showed that the stipe is slightly off-centre. In the future, the character "position of stipe" should be taken more carefully into consideration to support the hypothesis that this diagnostic feature is characteristic for the delimitation of *Entoloma* subgenus *Claudopus*.

Based on published records and collections from China, basidiomes of *E. abortivum* occur in two morphs viz. first with typical agaricoid and second with secotioid basidiomes. Regardless ofthe insertion of the stipe, the taxonomic position of *E. abortivum* was uncertain until molecular methods revealed that this taxon actually represents a typical species of *Entoloma* subgenus *Claudopus* (Baroni and Matheny 2011; Co-David et al. 2009; He et al. 2013; Vila et al. 2014). In the current descriptions of *E. abortivum*, the attachment of the stipe is not mentioned in particular. However, in our Chinese material, the position of the stipe of *E. abortivum* is always slightly but distinctly off-centre.

Acknowledgements

We express special thanks to Dr. Bao-Kai Cui (Beijing Forestry University, China), Bo Zhang (Jilin Agricultural University) and Dr. Hai-Xia Ma (Chinese Academy of Tropical Agricultural Sciences, China), for assistance in the field collection. Dr Wang-Qiu Deng (Guangdong Institute of Microbiology) is thanked for providing photos of *E. crepidotoides*. This research is financed by the National Natural Science Foundation of China (Nos. 31770020, 31400023), the Sichuan Provincial Innovation Ability Promotion Engineering (2016ZYPZ-028) and Project of Sichuan Microbiological Resources Infrastructure (2019JDPT0012).

References

Baroni TJ, Matheny PB (2011) A re-evaluation of gasteroid and cyphelloid species of Entolomataceae from eastern North America. Harvard Papers in Botany 16: 293–310. https://doi.org/10.3100/0.25.016.0205

Baroni TJ, Hofstetter V, Largent DL, Vilgalys R (2011) *Entocybe* is proposed as a new genus in the Entolomataceae (Agaricomycetes, Basidiomycota) based on morphological and molecular evidence. North Am Fungi 6(12): 1–19. https://doi.org/10.2509/naf2011.006.012

Chen JJ, Cui BK, Dai YC (2016) Global diversity and molecular systematics of *Wrightoporia* s. l. (Russulales, Basidiomycota). Persoonia 37: 21–36. https://doi.org/10.3767/003158516X689666

Co-David C, Langeveld D, Noordeloos ME (2009) Molecular phylogeny and spore evolution of Entolomataceae. Persoonia 23: 147–176. https://doi.org/10.3767/003158509X480944

Darriba D, Taboada GL, Doallo R, Posada D (2012) jModelTest 2: more models, new heuristics and parallel computing. Nature Methods 9: 772. https://doi.org/10.1038/nmeth.2109

Deng WQ, Li TH, Wang CQ, Li T, Shen YH (2015) A new crepidotoid *Entoloma* species from Hainan Island (China). Mycoscience 56: 340–344. https://doi.org/10.1016/j.myc.2014.11.002

Dennis RWG (1970) Fungus flora of Venezuela and adjacent countries. Kew Bulletin Additional Series 3: 1–531.

Edgar RC (2004) MUSCLE: multiple sequence alignment with high accuracy and high throughput. Nucleic Acids Research 32: 1792–1797. https://doi.org/10.1093/nar/gkh340

Esteve-Raventos F, De La Cruz M (1998) *Entoloma exiguum*, a new species of subgenus *Claudopus* (Entolomataceae, Agaricales) from Spain. Persoonia 17: 141–144.

Hall TA (1999) BioEdit: a user-friendly biological sequence alignment editor and analysis program for Windows 95/98/NT. Nucleic Acids Symposium Series 41: 95–98.

Han ML, Chen YY, Shen LL, Song J, Vlasák J, Dai YC, Cui BK (2016) Taxonomy and phylogeny of the brown-rot fungi: *Fomitopsis* and its related genera. Fungal Diversity 80: 343–373. https://doi.org/10.1007/s13225-016-0364-y

He XL, Li TH, Xi PG, Jiang ZD, Shen YH (2013) Phylogeny of *Entoloma* s.l. subgenus *Pouzarella*, with descriptions of five new species from China. Fungal Diversity 58: 227–243. https://doi.org/10.1007/s13225-012-0212-7

He XL, Peng WH, Gan BC (2015) Morphological and molecular evidence for a new species in *Entoloma* subgenus *Claudopus* from Sichuan Province, southwest China. Mycoscience 56: 326–331. https://doi.org/10.1016/j.myc.2014.10.001

Horak E (1980) *Entoloma* (Agaricales) in Indomalaya and Australasia. Beih. Nova Hedwigia 65: 1–352.

Horak E (2008) Agaricales of New Zealand 1: Pluteaceae (Pluteus, Volvariella), Entolomataceae (*Claudopus*, *Clitopilus*, *Entoloma*, *Pouzarella*, *Rhodocybe*, *Richoniella*). Fungi of New Zealand Volume 5. Hong Kong, Fungal Diversity Press.

Kinoshita A, Sasaki H, Nara K (2012) Multiple origins of sequestrate basidiomes within *Entoloma* inferred from molecular phylogenetic analyses. Fungal Biology 116: 1250–1262. https://doi.org/10.1016/j.funbio.2012.09.006

Kokkonen K (2015) A survey of boreal *Entoloma* with emphasis on the subgenus *Rhodopolia*. Mycological Progress 14: 116. https://doi.org/10.1007/s11557-015-1135-y

Kornerup A, Wanscher JH (1978) Methuen handbook of colour. 3rd ed. Chichester, Richard Clay Ltd.

Largent DL (1976) A new species of *Claudopus* from Northern California. Madroño 23: 376–378.

Largent DL (1994) Entolomatoid fungi of the western United States and Alaska. Mad River Press Inc, Eureka, CA.

Largent DL, Abell-Davis SE, Cummings GA, et al. (2011) Saxicolous species of *Claudopus* (Agaricales, Entolomataceae) from Australia. Mycotaxon 116: 253–264. https://doi.org/10.5248/116.253

Li YC, Feng B, Yang ZL (2011) *Zangia*, a new genus of Boletaceae supported by molecular and morphological evidence. Fungal Diversity 49: 125–143. https://doi.org/10.1007/s13225-011-0096-y

Manimohan P, Leelavathy KM, Noordeloos ME (2002) Three new species of *Entoloma* from Kerala State, India. Persoonia 17: 625–630.

Manimohan P, Noordeloos ME, Dhanya AM (2006) Studies on the genus *Entoloma* (Basidiomycetes, Agaricales) in Kerala State, India. Persoonia 19: 45–93.

Morgado LN, Noordeloos ME, Lamoureux Y, Geml J (2013) Multigene phylogenetic analysis reveals species limits, phylogenetic patterns and evolutionary histories of key morphological traits in *Entoloma* (Agaricales, Basidiomycota). Persoonia 31: 159–178. https://doi.org/10.3767/003158513X673521

Morozova OV, Noordeloos ME, Vila J (2014) *Entoloma* subgenus *Leptonia* in boreal-temperate Eurasia: towards a phylogenetic species concept. Persoonia 31: 141–169. https://doi.org/10.3767/003158514X681774

Morozova OV, Popov ES, Kovalenko AE (2012) Studies on mycobiota of Vietnam. I. Genus *Entoloma*: New records and new species. Mikologiya Fitopatologiya 46: 182–200.

Murrill WA (1917) Agaricaceae (pars), Agariceae (pars). North American Flora. 10: 78–80. https://doi.org/10.2307/3753039

Noordeloos ME (1981) Introduction to the taxonomy of the genus *Entoloma* sensu lato (Agaricales). Persoonia 11: 121–151.

Noordeloos ME (1992) *Entoloma* s.l. Fungi Europaei, vol. 5. Giovanna Biella, Saronno, Italy.

Noordeloos ME (2004) *Entoloma* s.l. Fungi Europaei, vol. 5a. Edizione Candusso, Italy.

Noordeloos ME, Gates GM (2012) The Entolomataceae of Tasmania. Fungal Diversity Research Series 22: 1–400. https://doi.org/10.1007/978-94-007-4679-4

Pegler DN (1983) Agaric flora of the Lesser Antilles. Kew Bulletin Additional Series 9: 1–668.

Ronquist F, Huelsenbeck JP (2003) MrBayes 3: Bayesian phylogenetic inference under mixed models. Bioinformatics 19: 1572–1574. https://doi.org/10.1093/bioinformatics/btg180

Stamatakis A (2014) RAxML version 8: a tool for phylogenetic analysis and post-analysis of large phylogenies. Bioinformatics 30: 1312–1313. https://doi.org/10.1093/bioinformatics/btu033

Swofford DL (2003) PAUP*: phylogenetic analysis using parsimony (*and other methods) version 4.0b10. Sinauer, Sunderland.

Vila J, Caballero F, Carbó J, et al. (2014) Preliminary morphologic and molecular study of the *Entoloma rusticoides* group (Agaricales-Basidiomycota). Revista Catalana de Micologia 35: 65–99.

White TJ, Bruns T, Lee S, Taylor J (1990) Amplification and direct sequencing of fungal ribosomal RNA genes for phylogenies. In: Innis MA, Gelfand DH, Sninsky JJ, White TJ (Eds) PCR protocols, a guide to methods and applications. Academic, San Diego. https://doi.org/10.1016/B978-0-12-372180-8.50042-1

MycoKeys 61: 27–37 (2019)
doi: 10.3897/mycokeys.61.36444
http://mycokeys.pensoft.net

RESEARCH ARTICLE

A peer-reviewed open-access journal
MycoKeys
Launched to accelerate biodiversity research

A novel sequestrate species from Mexico: *Aroramyces guanajuatensis* sp. nov. (Hysterangiaceae, Hysterangiales)

Rafael Peña-Ramírez[1,2], Zai-Wei Ge[2], Rigoberto Gaitán-Hernández[4], César Ramiro Martínez-González[4], Gonzalo Guevara-Guerrero[1]

1 *Instituto Tecnológico de Cd. Victoria, Av. Portes Gil 1301 Pte. C.P. 87010, Cd. Victoria Tam, Mexico* **2** *Kunming Institute of Botany, Chinese Academy of Sciences, 132, Lanhei Road, Kunming 650201, China* **3** *Instituto de Ecología, A.C., Carretera antigua a Coatepec # 351, El Haya, C.P. 91070, Xalapa, Veracruz, Mexico* **4** *Universidad Nacional Autónoma de México, Profesor de Asignatura B, Departamento de Biología, Facultad de Ciencias Ciudad Universitaria, Delegación Coyoacán, 04510, Ciudad de México, Mexico*

Corresponding author: *Gonzalo Guevara-Guerrero* (guevaragg@hotmail.com)

Academic editor: *Marc Stadler* | Received 23 May 2019 | Accepted 16 October 2019 | Published 11 December 2019

Citation: Peña-Ramírez R, Ge Z-W, Gaitán-Hernández R, Martínez-González CR, Guevara-Guerrero G (2019) A novel sequestrate species from Mexico: *Aroramyces guanajuatensis* sp. nov. (Hysterangiaceae, Hysterangiales). MycoKeys 61: 27–37. https://doi.org/10.3897/mycokeys.61.36444

Abstract

Knowledge of sequestrate Hysterangiaceae fungi in Mexico is very limited. In the present study, a new member of the family, *Aroramyces guanajuatensis* **sp. nov.**, is described. This speciesis closely related to *A. balanosporus*, but differs from the latter in possessing a tomentose peridium 165–240 µm thick, with occasional large terminal hyphae up to 170 µm, a variable mesocutis (isodiametric to angular), and distinct bright yellowish subcutis. In contrast, *A. balanosporus* possesses a fibrillose peridial surface with shorter hyphae, a peridium 200–450 µm thick, and a mainly hyaline isodiametric mesocutis with a slightly wider subcutis. The phylogenetic analysis of the LSU gene separated *A. guanajuatensis* from *A. balanosporus* with a Bayesian posterior probability (PP) = 1. This is the third *Aroramyces* species described for the American continent.

Keywords

Truffle, truffle-like, sequestrate fungi, hypogeous fungi

Introduction

Aroramyces Castellano and Verbeken was coined to settle *Hymenogaster radiatus* (Lloyd, 1925) and *Hysterangium gelatinosporum* (Cribb, 1957) from two different genera (Castellano et al. 2000). Phylogenetic analysis places *Aroramyces* near, but different to *Hysterangium* (Hosaka et al. 2006, 2008). *Aroramyces* is characterized by its unique combination of a brown gleba, spiny spores with distinctly inflated utricles, gelatinized gleba, and basidiome with a tomentose surface with numerous soil particles adhering to all sides. At present, there are four species in this group (Kirk 2018): *Aroramyces radiatus* (Lloyd) Castellano, Verbeken & Walleyn, *A. gelatinosporus* (J.W. Cribb) Castellano (Castellano et al. 2000), *A. balanosporus* G. Guevara & Castellano, and *A. herrerae* G. Guevara, Gomez-Reyes & Castellano (Guevara-Guerrero et al. 2016). *Aroramyces guanajuatensis* was discovered during a survey aiming to document the fugal diversity in Guanajuato, Mexico. It is therefore determined that the number of *Aroramyces* species described in the American continent is now three.

Materials and methods

Sampling and morphological characterization

The collections were discovered with a cultivator, digging around trees up to a depth of 15 cm. All encountered fruiting bodies were photographed fresh and then dried at 50 °C. The chosen material was cut by hand and rehydrated with 5% KOH for morphological studies. Thirty spores were measured. Peridial slices were made and observed under optical microscopy (Castellano et al. 1989). For scanning electron microscopy pictures (JSM5600LV, JOEL, Tokyo, Japan), the spores were coated with gold and palladium. Voucher collections are deposited at José Castillo Tovar (**ITCV**) Herbarium, Instituto Tecnólogico de Ciudad Victoria, Mexico.

DNA extraction, amplification, sequencing and phylogenetic analyses

Genomic DNA was obtained with CTAB (Martínez-González et al. 2017)) or using Fungal DNA extraction Kit (Bio Teke Corporation, China) from 2–3 mg of dry tissue. DNA quantification was performed with Nanodrop (Thermo, USA). Each sample was diluted to 20 ng/uL for PCR amplification. LR0R and LR5 primers were used to amplify the LSU gene (Vilgalys and Hester 1990). The PCR reaction contained the following: enzyme buffer 1×, *Taq* DNA polymerase, 0.8 mM deoxynucleoside triphosphates (0.2 mM each), 100 ng DNA, 20 pmol of each primer, and 2 units of Go*Taq* DNA (Promega, USA), with a final volume of 15 µL. The amplification program was run as follows: denaturalization at 96 °C for 2 min, 35 cycles of denaturalization at 94 °C for 1 min, annealing at 57 °C for 1 min, polymerization at 72 °C for 1 min, and final elongation at 72 °C for 5 min. All PCR reactions were carried out in a Peltier

Thermal Cycler PTC-200 (BIORAD, Mexico). The PCR products were verified by agarose gel electrophoresis run for 1 h at 95 V cm^{-3} in 1.5% agarose and 1× TAE buffer (Tris Acetate-EDTA). The products were then dyed with GelRed (Biotium, USA) and viewed in a transilluminator (Infinity 3000 Vilber, Loumat, Germany). Finally, the products were purified using the ExoSap Kit (Affymetrix, USA) according to the manufacturer's instructions and were prepared for the sequencing reaction using the BigDye Terminator Cycle Sequencing Kit v. 3.1 (Applied BioSystems).

Sequencing was carried out in a genetic analyzer (Model 3130XL, Applied BioSystems, USA) at the Biology Institute of the National Autonomous University of Mexico (UNAM). The sequences of both strains of each sample were analyzed, edited, and assembled using BioEdit v. 1.0.5 (Hall 1999) to create consensus sequences. The consensus sequences were compared with those in the GenBank database of the National Center for Biotechnology Information (NCBI) using the BLASTN 2.2.19 tool (Zhang et al. 2000). The LSU region was aligned using the online version of MAFFT v. 7 (Katoh et al. 2002, 2017; Katoh and Standley 2013). The alignment was revised in PhyDE (Müller et al. 2005), and small manual adjustments were then made to maximize the similarity between characters. The matrix was composed of 30 taxa (640 characters) (Table 1). *Ramaria gelatinosa* (access number AF213091) was used as the outgroup. The phylogeny was performed using Bayesian inference in MrBayes v. 3.2.6 64× (Huelsenbeck and Ronquist 2001). The information block matrix included two independent runs of the MC3 chains for ten million generations (standard deviation ≤ 0.01); the reversible-jump strategy was used (Huelsenbeck et al. 2004). An evolutionary model was used, so a proportion of invariable sites were designated, and the other proportion came from a gamma distribution (invgamma). The convergence of chains was visualized in Tracer v. 1 (Rambaut et al. 2014). The phylogram of maximum credibility for the clades was recovered in TreeAnotator v. 1.8 (Bouckaert et al. 2014) based on the burning of 2.5 million trees.

Table 1. List of NCBI accession numbers for LSU and ITS sequences of *Aroramyces guanajuatensis*.

Herbarium number	LSU NCBI number	ITS NCBI number
ITCV 1689	MK761021	MN392935
ITCV 1691	MK761022	MN392936
ITCV 1694	MK761023	MN392937
ITCV 1711	MK761024	MN392938
ITCV 1610	MK761025	MN392939
ITCV 1610	MK811035	–
ITCV 1613	MK761026	MN392940
ITCV 1613	MK811036	–
ITCV 1729	MK761027	MN392941
ITCV 1731	MK761028	MN392942
ITCV 1734	MK761029	MN392943
ITCV 1738	MK761030	MN392944
ITCV 1739	MK761031	MN392945
ITCV 1741	MK761032	MN392946

Results

Molecular analyses

ITS and LSU sequences of 12 samples *of A. guanajuatensis* were obtained (Table 1). ITS and LSU sequences are respectively identical. Based on this, only four sequences were selected for phylogenetic analysis. Then after, alignment was performed with 6 sequences of *Aroramyces* and 22 sequences of *Hysterangium* (Table 2). Phylogenetic results were as follows: According to the Bayesian analysis, after 10 million generations, 25% trees were discarder as the burn-in. The standard deviation between the chains stabilized at 0.002, indicating that MC3 reached a stationary phase. To confirm that the sample size was enough, the "parameter" file was analyzed using Tracer v. 1.6 (Rambaut et al. 2014), verifying that all parameters had an estimated sample size above 1,500. The subsequent probabilities (SP) were estimated based on the strict consensus rule produced by MrBayes and indicated on the maximum credibility clade tree. The Bayesian inference analysis recovered *A. guanajuatensis* as a monophyletic group, with a posterior probability of 1. (Fig. 1). *Ramaria gelatinosa* was used to root the tree. *Aroramyces balanosporus* and *A. guanajuatensis* showed the closest relationship but were branched with a probability of 1 and a dissimilarity of 2.19, supporting the existence of a new taxon. The *Hysterangium* species segregated and formed two different branches.

Taxonomy

Aroramyces guanajuatensis **Peña-Ramírez, Guevara-Guerrero, Z. W. Ge & Martínez-González, sp. nov.**
MycoBank No: 830329
Figures 2–4

Type. MEXICO. State of Guanajuato, municipality of Guanajuato, Cuenca de la Esperanza Protected Natural Area, 7 November. 2016Peña-Ramírez 108 (Holotype: ITCV 1613).

Diagnosis. *Aroramyces guanajuatensis* is characterized by a peridium 167–240 µm thick, of cotton-like hyphae, up to 170 µm, long, variably structured mesocutis, yellowish subcutis, spores with irregular and inflated utricle.

Etymology. "*guanajuatensis*" in reference to the site (Guanajuato state) where the new taxon was discovered.

Description. Basidiome 4.4–17×3.9–13.5×3.2–11.2 mm, globose or subglobose to irregular, sometimes compressed when growing together. Peridial surface white, pale brown, fibrillose or tomentose, often with cotton-like patches of white hyphae encompassing some debris soil, stones, leaves, and roots. Peridium Separable and fragile, exposing portions of the gleba. < 0.5 mm thick, mostly hyaline, outer portion pale

Table 2. List of *Aroramyces* and *Hysterangium* species, GenBank accession numbers, and references for LSU sequences used in the phylogenetic analysis. Sequences of new taxon are in bold.

Species	GenBank	Reference
Aroramyces balanosporus G. Guevara & Castellano	MK811031	This paper
A. guanajuatensis	MK761024	This paper
	MK811036	This paper
	MK811035	This paper
	MK761031	This paper
A. gelatinosporus (J.W. Cribb) Castellano	DQ218524	Hosaka et al. 2008
A. radiatus (Lloyd) Castellano, Verbeken & Walleyn	DQ218525	Hosaka et al. 2008
Aroramyces sp.	KY686203	Nuske & Abell unpublished
	DQ218527	Hosaka et al. 2008
	DQ218530	Hosaka et al. 2008
Hysterangium affine Mase & Rodway	DQ218546	Hosaka et al. 2008
H. album Zeller & C.W. Dodge	DQ218490	Hosaka et al. 2008
H. aureum Zeller	DQ218491	Hosaka et al. 2008
H. calcareum R. Hesse	DQ218492	Hosaka et al. 2008
H. clathroides Vittad	AF213121	Humpert et al. unpublished
H. coriaceum R. Hesse	AF213122	Humpert et al. unpublished
	AY574686	Giachini et al. 2010
H. crassum (Tul & C. Tul) E, Fisch	AY574687	Giachini et al. 2010
H. epiroticum Pacioni	DQ218495	Hosaka et al. 2008
H. fragile Vittad	DQ218496	Hosaka et al. 2008
H. hallingi Castellano & J.J. Muchovej	DQ218497	Hosaka et al. 2008
H. inflatun Rodway	DQ218549	Hosaka et al. 2008
H. membranaceum Vittad	DQ218498	Hosaka et al. 2008
H. neotunicatun Castellano & Beever	DQ218550	Hosaka et al. 2008
H. pompholyx Tul. & C. Tul.	DQ218499	Hosaka et al. 2008
H. rugisporum Castellano & Beever	DQ218500	Hosaka et al. 2008
H. salmonaceum G.W. Beaton, Pegler & T.W.K. Young	DQ218501	Hosaka et al. 2008
H. separabile Zeller	DQ974810	Smith et al. 2007
	DQ218502	Hosaka et al. 2008
H. spegazzinii Castellano & J.J. Muchovej	DQ218503	Hosaka et al. 2006
H. stoloniferum Tul. & C. Tul.	AF336259	Binder and Bresinsky 2002
H. strobilus Zeller & C.W. Dodge	DQ218504	Hosaka et al. 2006

brown, with a dark ring next to the gleba. Gleba brown, trama gelatinized, locules irregularly shaped, columella dendroid, translucent gray. Odor fungoid; taste not recorded. Basidiomata hard wen dried.

Peridium three layered, 165–240 µm thick. Epicutis 7.5–22.5 µm thick of hyaline to reddish brown, thin-walled, interwoven to repent or erect hyphae, 2–9 µm wide, forming scattered caespitose groups of erect, branched, setal hyphae up to 170 µm long, with abundant crystalline structures adherent on hyphal walls, clamp connections present. Mesocutis 55–105 µm thick, abundant hyaline, isodiametric, globose to subglobose, angular pseudoparenchyma like cells. 4–35×3–24 µm, also with some irregularly shaped, interwoven hyphae, 3–11 µm wide. walls 1–2 µm µm wide, clamp

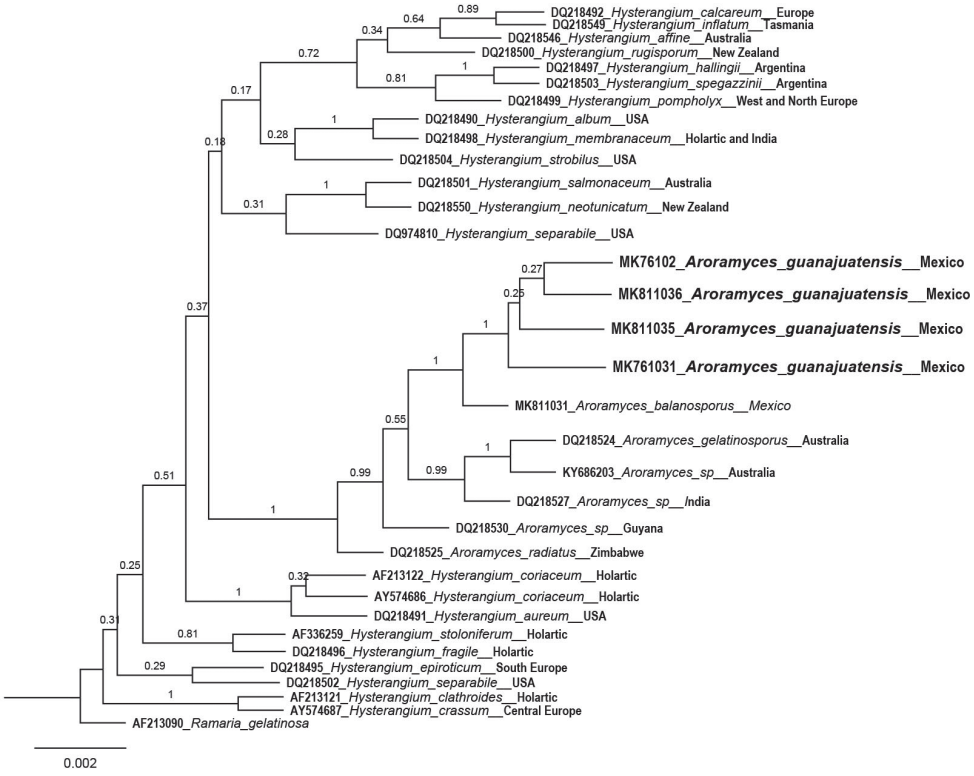

Figure 1. Maximum probability phylogram of clades obtained with Bayesian inference. The posterior probabilities for each clade are shown on the branches. The accession numbers in the sequence labels indicate the GenBank accession numbers.

connection absent. Subcutis 22.5–95 µm thick, of interwoven prostrate hyphae, 3–4 µm broad, with scattered large pseudoparenchyma like cells up to 37.5×30 µm, clamp connection absent.

Trama of hyaline, interwoven hyphae 4 µm wide, embedded in a gelatinized matrix, clamp connections present.

Basidia fusoid to clavate, hyaline, 14–48 × 9–12 µm, mean = 32.5 × 10.3 µm, wall 1 µm thick. Basidiospores ellipsoid to broadly ellipsoid, symmetrical, hyaline to pale brown, slightly reddish in KOH, pale brown in mass, excluding utricle 9–13 × 6–7 µm long, mean = 11 × 6.1 µm, Q range = 1.5–2.17, Q mean = 1.8; with utricle 12–17 × 7–10 µm long, mean = 14.47 × 8.27 µm, Q = 1.5–2.13, mean = 1.76. Ornamentation of irregular crest contained within an inflated utricle, hilar appendage in cross-section appears rectangular, 1–3 × 4–6 µm, mean = 1.97 × 5.2 µm. Apex obtuse. Utricle inflated up to 3 µm from spore wall, mean = 1.43 µm, occasionally the utricle is asymmetrically inflated.

Distribution, habit and ecology. MEXICO, state of Guanajuato. Cuenca de la Esperanza Protected Natural Area. Hypogeous, under *Quercus* spp. at 2530 m. 21°03.87'N, 101°13.193'W. October to December. The March collection was dried in situ.

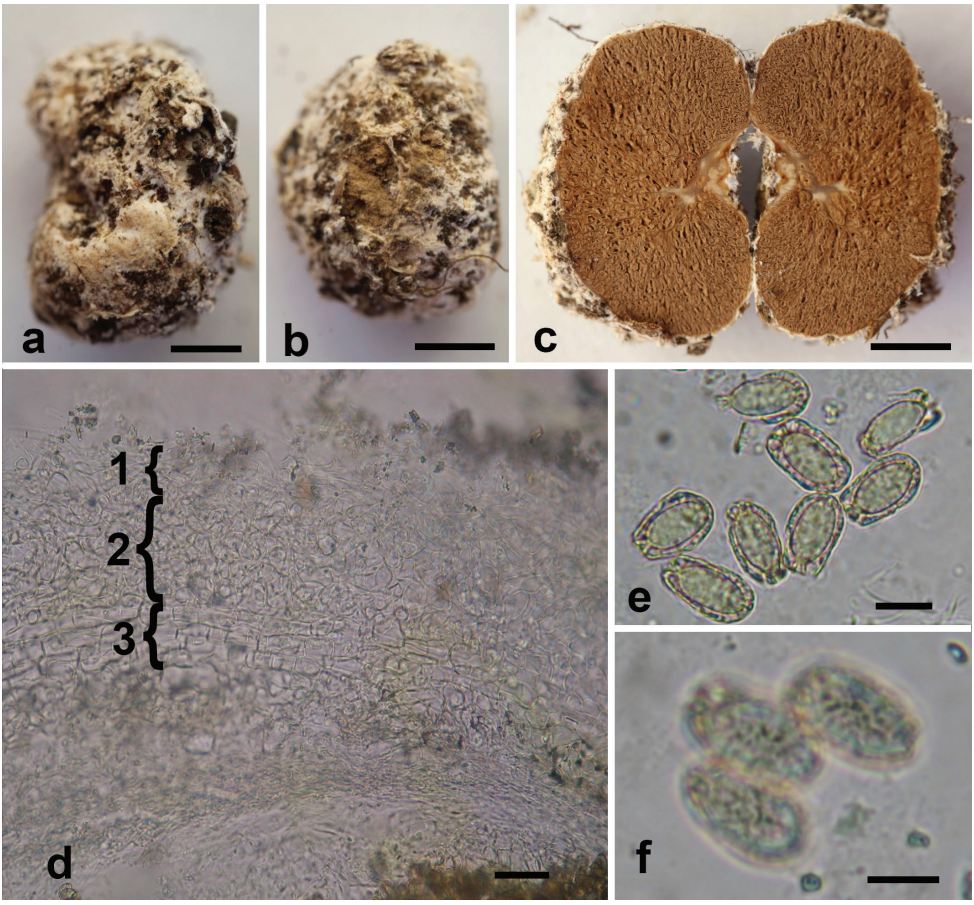

Figure 2. a–f *Aroramyces guanajuatensis* (holotype ITCV 1613) **a, b** basidiome showing the peridial surface **c** basidiome in cross-section showing glebal surface **d** cross-section of peridium showing three-layered peridium (1 epicutis, 2 mesocutis, 3 subcutis) at 400× **e–f** basidiospore 1000× **f** irregular crest contained within an inflated utricle. Scale bars: 0.5 cm (**a–c, f**), 20 µm (**d**), 5 µm (**e**).

Additional material examined. Mexico, state of Guanajuato, Cuenca de la Esperanza Protected Natural Area: 21°04.075'N, 101°13.193'W 2500 m, 26 October 2016, Peña-Ramírez 102, paratype (ITCV 1610). 21°03891'N, 101°13.531'W 2457 m, 5 October 2016, Peña-Ramírez 70 (ITCV 1689). 21°03.891'N, 101°13.533'W, 2464 m, 5 October 2016, Peña-Ramírez 72 (ITCV 1691). 21°03.88'N, 101°13.561'W, 2471 m, 5 October 2016, Peña-Ramírez 75 (ITCV 1694). 21°03.85'N, 101°13.278'W. 2533 m, 19 October 2016 Peña-Ramírez 92 (ITCV 1711). 21°03.741'N, 101°13.461'W. 2500 m, 14 November 2016, Peña-Ramírez 110 (ITCV 1729). 21°03.901'N, 101°13.551'W. 22 December 2016, Peña-Ramírez 119 (ITCV 1738). 21°03.905'N, 101°13.018'W. 2458 m. 22 December 2016, Peña-Ramírez 120 (ITCV 1739). 21°04.045'N, 101°13.018'W. 2508 m, 6 March 2017, Peña-Ramírez 122 (ITCV 1741).

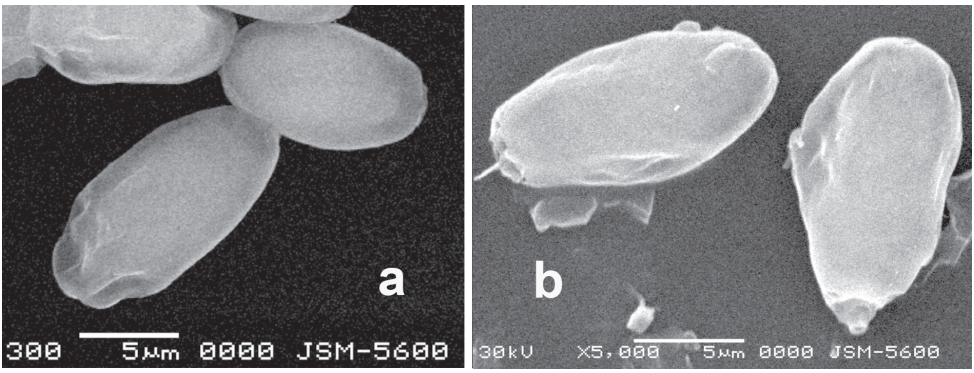

Figure 3. Electronic photomicrograph of basidiospores **a** *Aroramyces balanosporus* (ITCV 848) and **b** *Aroramyces guanajuatensis* (ITCV 1739). Scale bars: 5 µm.

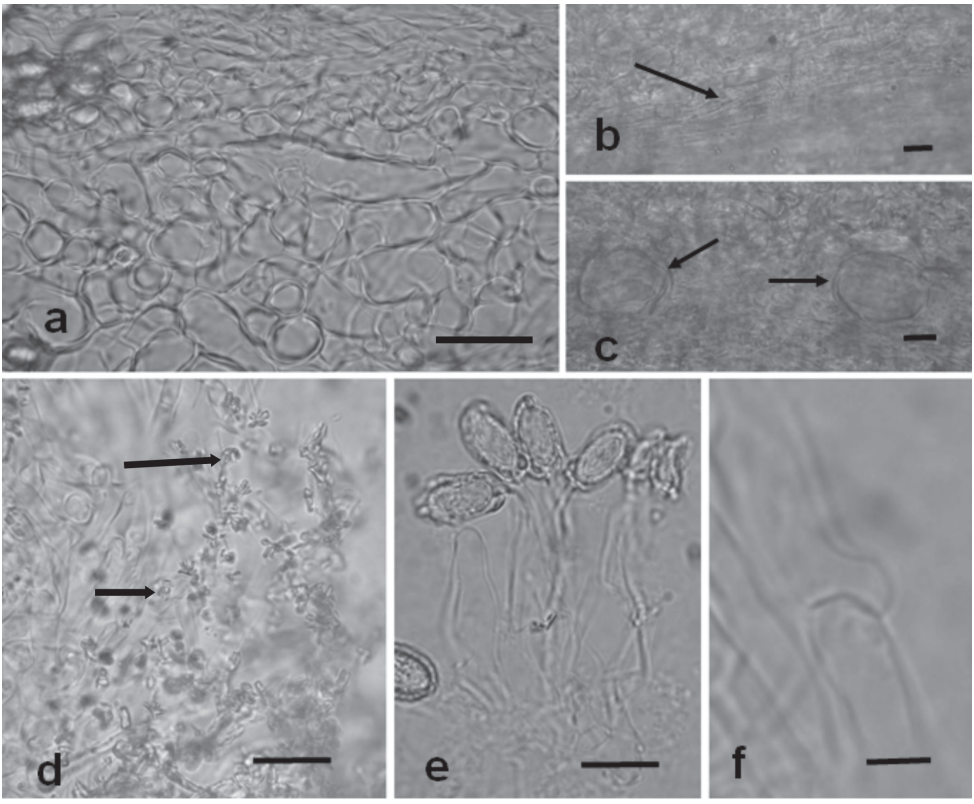

Figure 4. a–f *Aroramyces guanajuatensis* (holotype ITCV 1613) **a–c** Cross-section of peridium **a** epicutis of hyphae postrate cells and angular pseudoparenchyma like mesocutis **b** arrow head showing postrate cell subcutis **c** arrow head showing large cell scattered in subcutis **d** arrow head showing epicutis hyphae with attached crystals **e** basidia and basidioles **f** epicutis clamp connection. Scale bar: 10 µm (**a–c, e**), 25 µm (**d**), 5 µm (**f**).

Discussion

In the Bayesian inference analysis, Various *Aroramyces* nest together along with undescribed species mentioned in Nuske & Abell (unpublished) and Hosaka et al. (2008). The clade of the genus *Aroramyces* segregated between two clades that group species of *Hysterangium*. The close relationship of *Aroramyces* to *Hysterangium* in our study agrees with Hosaka et al. (2006, 2008). *Aroramyces balanosporus* and *A. guanajuatensis* are closely related but are morphologically and molecularly distinct (Figure 1). Although, the objective of the current assignment is not inferring the phylogenetic relationships in Hysterangiaceae, the result clearly supports *Aroramyces guanajuatensis* to be an independent species within the genus *Aroramyces* with a posterior probability of 1.

The hilar appendage is larger in *Aroramyces guanajuatensis* compared to *A. balanosporus*. The isodiametric mesocutis cells of *A. guanajuatensis* differ from the variously shaped cells in the mesocutis of *A. balanosporus*. The asymmetric utricle of *Aroramyces herrerae* up to 6 µm wide whereas the asymmetric utricle of *A. guanajuatensis* rarely reaches 3 µm wide. Mexican *Aroramyces* are associated with *Quercus* spp. Interestingly *A. radiatus* from Africa has smaller spores, 10–12(–13.5) × 6–7(–8) µm, and is associated with *Brachystegia spiciformis* (Caesalpinioideae) and *Upaca* sp. (Euphorbiaceae). *Aroramyces gelatinosporus* from Australia has similar sized spores but a single-layered peridium and is associated with *Eucalyptus* spp. (Myrtaceae) (Castellano et al. 2000; Lloyd 1925).

The collections were discovered in the Cuenca de la Esperanza Protected Natural Area in Guanajuato, Mexico, located north of Michoacán and east of Jalisco. The presence of unidentified species in this region highlights the importance of this protected natural area and as an area to search for additional new fungal taxa.

Acknowledgements

Peña-Ramírez acknowledges TecNM (Tecnológico Nacional de México) for fellowship PRODEP 1264-2015-2017. Guevara-Guerrero thanks CONACyT and TecNM for research support. Martínez-González acknowledges Laura Márquez y Nelly López, LaNaBio, of Instituto de Biología, Universidad Nacional Autónoma de México and to María Eugenia Muñiz Díaz de León, for giving us access to the Laboratory of Molecular Biology. Zai-Wei was supported by the National Natural Science Foundation of China (Nos. 31670024 and 31872619).

References

Binder M, Bresinsky A (2002) Derivation of a polymorphic lineage of Gasteromycetes from boletoid ancestors. Mycologia 94(1): 85–9. https://doi.org/10.1080/15572536.2003.11833251

Bouckaert R, Heled J, Kühnert D, Vaughan T, Wu C-H, Xie D, Suchard MA, Rambaut A, Drummond AJ (2014) BEAST 2: A software platform for Bayesian Evolutionary analy-

sis. PLOS Computational Biology 10: e1003537. https://journals.plos.org/ploscompbiol/article?id=10.1371/journal.pcbi.1003537

Castellano MA, Trappe JM, Maser Z, Maser C (1989) Key to spores of the genera of Hypogeous fungi of north temperate forest with special reference to animal mycophagy. Mad River press, Eureka, 186 pp.

Castellano MA, Verbeken A, Walleyn R, Thoen D (2000) Some new or interesting sequestrate Basidiomycota from African woodlands. Karstenia 40: 11–21. https://doi.org/10.29203/ka.2000.346

Cribb JW (1957) The Gasteromyces of Queensland – IV *Gautieria*, *Hysterangium* and *Gymnoglossum*. Papers of the Department of Botany University of Queensland 3[1958]: 153–159. The University of Queensland Press.

Giachini AJ, Hosaka K, Nouhra E, Spatafora J, Trappe JM (2010) Phylogenetic relationships of the Gomphales based on nuc-25S-rDNA, mit-12S-rDNA, and mit-atp6-DNA combined sequence. Fungal Biology 114(2–3): 224–234. http://doi.org/10.1016/j.funbio.2010.01.002

Guevara-Guerrero, G, Castellano MA, Gómez-Reyes V (2016) Two new *Aroramyces* species (Hysterangiaceae, Hysterangiales) from México. IMA Fungus 7(2): 235–238. https://imafungus.biomedcentral.com/articles/10.5598/imafungus.2016.07.02.02

Hall TA (1999) BioEdit: a user-friendly biological sequence alignment editor and analysis program for Windows 95/98/NT. Nucleic Acids Symposium Series 41: 95–98. http://brownlab.mbio.ncsu.edu/JWB/papers/1999hall1.pdf

Hosaka K, Bates ST, Beever RE, Castellano MA, Colgan W III, Dominguez LS, Nouhra ER, Geml J, Giachini AJ, Kenney SR, Simpson NB, Spatafora JW, Trappe JM (2006) Molecular phylogenetics of the gomphoid-phalloid fungi with an establishment of the new subclass Phallomycetidae and two new orders. Mycologia 98(6): 949–959. https://doi.org/10.1080/15572536.2006.11832624

Hosaka K, Castellano MA, Spatafora JW (2008) biogeography of Hysterangiales (Phallomycetidae, Basidiomycota). Mycological Research 112: 448–462. https://doi.org/10.1016/j.mycres.2007.06.004

Huelsenbeck J, Ronquist F (2001) MRBAYES: Bayesian inference of phylogenetic trees. Bioinformatics 17(8): 754–755. http://doi.org/10.1093/bioinformatics/17.8.754

Huelsenbeck JP, Larget B, Alfaro ME (2004) Bayesian phylogenetic model selection using reversible jump Markov Chain Montecarlo. Molecular Biology and Evolution 21: 1123–1133. https://doi.org/10.1093/molbev/msh123

Katoh K, Misawa K, Kuma K, Miyata T (2002) MAFFT: a novel method for rapid multiple sequence alignment based on fast Fourier transform. Nucleic Acids Research 30(14): 3059–3066. https://doi.org/10.1093/nar/gkf436

Katoh K, Standley DM (2013) MAFFT multiple sequence alignment software version 7: improvements in performance and usability. Molecular Biology and Evolution 30(4): 772–780. https://doi.org/10.1093/molbev/mst010

Katoh K, Rozewicki J, Yamada KD (2017) MAFFT online service: multiple sequence alignment, interactive sequence choice and visualization. Briefings in Bioinformatics 20(4): 1160–1166. https://doi.org/10.1093/bib/bbx108

Kirk P (2018) Index fungorum. http://www.indexfungorum.org

Lloyd CG (1925) Mycological Writings, Mycological Notes 7: 1304. https://ia600501.us.archive.org/6/items/indexofmycologic07lloy/indexofmycologic07lloy.pdf

Martínez-Gonzalez CR, Ramírez-Mendoza R, Jiménez-Ramírez J, Gallegos-Vázquez C, Luna-Vega I (2017) Improved method for Genomic DNA Extraction for *Opuntia* Mill. (Cactaceae). Plant Methods 13: 1–82. http://doi.org/10.1186/s13007-017-0234-y

Müller K, Quandt D, Müller J, Neinhuis C (2005) PhyDE-Phylogenetic data editor. Program distributed by the authors, version 10.0. https://www.phyde.de

Rambaut A, Suchard MA, Xie D, Drummond AJ (2014) Tracer v1.6. http://beast.bio.ed.ac.uk/Tracer

Smith ME, Douhan GW, Rizzo DM (2007) Ectomycorrhizal community structure in a xeric *Quercus* Woodland based on rDNA sequence analysis of sporocarps and pooled roots. New Phytologist 174(4): 847–863. http://doi.org/10.1111/j.1469-8137.2007.02040.x

Vilgalys R, Hester M (1990) Rapid Genetic Identification and mapping of enzymatically amplified ribosomal DNA from several *Cryptococcus* species. Journal of Bacteriology 172(8): 4238–4246. https://doi.org/10.1128/jb.172.8.4238-4246.1990

Zhang Z, Schwartz S, Wagner L, Miller W (2000) A greedy algorithm for aligning DNA sequences. Journal of Computational Biology 7: 203–214. https://doi.org/10.1089/10665270050081478

MycoKeys 61: 39–74 (2019)
doi: 10.3897/mycokeys.61.38175
http://mycokeys.pensoft.net

RESEARCH ARTICLE

A peer-reviewed open-access journal
MycoKeys
Launched to accelerate biodiversity research

Morphology and secondary chemistry in species recognition of *Parmelia omphalodes* group – evidence from molecular data with notes on the ecological niche modelling and genetic variability of photobionts

Emilia Ossowska[1*], Beata Guzow-Krzemińska[1*], Marta Kolanowska[2,3], Katarzyna Szczepańska[4], Martin Kukwa[1]

1 *Department of Plant Taxonomy and Nature Conservation, Faculty of Biology, University of Gdańsk, Wita Stwosza 59, PL-80-308, Gdańsk, Poland* **2** *Department of Geobotany and Plant Ecology, Faculty of Biology and Environmental Protection, University of Łódź, Banacha 12/16, 90-237, Łódź, Poland* **3** *Department of Biodiversity Research, Global Change Research Institute AS CR, Bělidla 4a, 603 00, Brno, Czech Republic* **4** *Department of Botany and Plant Ecology, Wroclaw University of Environmental and Life Sciences, pl. Grunwaldzki 24a, PL-50–363, Wrocław, Poland*

Corresponding author: *Emilia Ossowska* (emilia.ossowska@ug.edu.pl)

Academic editor: *T. Lumbsch* | Received 11 July 2019 | Accepted 22 November 2019 | Published 11 December 2019

Citation: Ossowska E, Guzow-Krzemińska B, Kolanowska M, Szczepańska K, Kukwa M (2019) Morphology and secondary chemistry in species recognition of *Parmelia omphalodes* group – evidence from molecular data with notes on the ecological niche modelling and genetic variability of photobionts. MycoKeys 61: 39–74. https://doi.org/10.3897/mycokeys.61.38175

Abstract

To evaluate the importance of morphological and chemical characters used in the recognition of species within the *Parmelia omphalodes* group, we performed phylogenetic, morphological and chemical analyses of 335 specimens, of which 34 were used for molecular analyses. Phylogenetic analyses, based on ITS rDNA sequences, show that *P. pinnatifida* is distinct from *P. omphalodes* and the most important difference between those species is the development of pseudocyphellae. In *P. pinnatifida*, they are mostly marginal and form white rims along lobes margins, but laminal pseudocyphellae can develop in older parts of thalli and are predominantly connected with marginal pseudocyphellae. In contrast, in *P. omphalodes* laminal pseudocyphellae are common and are predominantly not connected to marginal pseudocyphellae. Chemical composition of secondary lichen metabolites in both analysed species is identical and therefore this feature is not diagnostic in species recognition. Few samples of *P. discordans*, species morphologically similar to *P. omphalodes* and *P. pinnatifida*, were also included in the analyses and they are nested within

* Contributed equally as the first authors.

the clade of *P. omphalodes*, despite the different chemistry (protocetraric acid present versus salazinic acid in *P. omphalodes*). All taxa of the *P. omphalodes* group occupy similar niches, but their potential distributions are wider than those currently known. The absence of specimens in some localities may be limited by the photobiont availability. *Parmelia omphalodes* and *P. pinnatifida* are moderately selective in photobiont choice as they form associations with at least two or three lineages of *Trebouxia* clade S. *Parmelia pinnatifida*, as well as *P. discordans* are associated with *Trebouxia* OTU S02 which seems to have a broad ecological amplitude. Other lineages of *Trebouxia* seem to be rarer, especially *Trebouxia* sp. OTU S04, which is sometimes present in *P. pinnatifida*. This study indicates the importance of extensive research including morphology, chemistry and analysis of molecular markers of both bionts in taxonomical studies of lichens.

Keywords

Ascomycota, Parmeliaceae, parmelioid lichens, ITS rDNA, secondary metabolites, morphology, photobiont, ecological niche modelling

Introduction

The genus *Parmelia* Ach. (Parmeliaceae, Ascomycota) currently comprises ca. 40 species (Crespo and Lumbsch 2010; Thell et al. 2012; Molina et al. 2017) and was divided, based on the presence and type of vegetative diaspores, into three groups: the *P. saxatilis* group with isidiate species, the *P. sulcata* group containing sorediate species and the *P. omphalodes* group without vegetative propagules (Thell et al. 2017). To date, research has focused mainly on the isidiate and sorediate species (e.g. Molina et al. 2004, 2011, 2017; Divakar et al. 2005; Thell et al. 2008; Ossowska et al. 2018; Corsie et al. 2019; Haugan and Timdal 2019). The phylogenetic position of species of the *P. omphalodes* group and their taxonomic status have not been fully understood and required more detailed study as suggested by Molina et al. (2004) and Thell et al. (2008).

The *P. omphalodes* group includes three taxa, often treated at the species level, i.e. *P. discordans* Nyl., *P. omphalodes* (L.) Ach. and *P. pinnatifida* Kurok. (Hale 1987; Molina et al. 2004; Thell et al. 2008), but the distinction between them and their taxonomic status remain a long-term debate, especially in the case of *P. omphalodes* and *P. pinnatifida*. The first controversy concerns the taxonomic position of these species. Kurokawa (1976) presented the description of three species, *P. omphalodes*, *P. discordans* and *P. pinnatifida*, while Skult (1984) proposed a different concept and classified them as subspecies within *P. omphalodes*. Hale (1987) did not agree with Skult's concept and distinguished two species within this group, i.e. *P. discordans* and *P. omphalodes*. He did not recognise *P. pinnatifida* as a separate species and included it in *P. omphalodes*.

The second issue is related to the differences between the species. Kurokawa (1976) noted that species of the *P. omphalodes* group differed in the shape of lobes and orientation of pseudocyphellae, which were mostly marginal in *P. pinnatifida*, whereas, in *P. discordans* and *P. omphalodes*, these were both laminal and marginal. In the case of the lobe shape, Kurokawa (1976) reported that *P. pinnatifida* has repeatedly branched lobes with narrow lobules, which are similar to those of *P. omphalodes*. *Parmelia discordans* has wider lobes than *P. pinnatifida* and without lobules, while

P. omphalodes has the widest lobes with lobules. The descriptions in Skult (1984) indicated the same differences. The variation in lobe shape between *P. discordans* and *P. omphalodes* was also confirmed by Hale (1987), who classified both species in the group of taxa with marginal pseudocyphellae. Molina et al. (2004) and Thell et al. (2008) considered the shape of lobes and the orientation of pseudocyphellae as diagnostic features that distinguish both species; however, their conclusions were based mainly on published data, a limited number of specimens and few details about the species presented. In the discussion, they emphasised that those species required further studies. According to some works (e.g. Kurokawa 1976; Skult 1984; Hale 1987; Thell et al. 2008, 2011), differences in the secondary chemistry appear more diagnostic in the recognition of species within this group. Atranorin, salazinic and consalazinic acids, lobaric acid and protolichesterinic acid were reported as present in *P. omphalodes*. *Parmelia pinnatifida* is chemically similar, but lacks lobaric acid, whereas in *P. discordans* salazinic and consalazinic acids are replaced by protocetraric acid (e.g. Kurokawa 1976; Skult 1984; Thell et al. 2011).

The species of the *Parmelia omphalodes* group are rare in most parts of their distributional ranges. *Parmelia discordans* is reported from Europe only (Hale 1987; Hawksworth et al. 2008, 2011), whereas *P. omphalodes* and *P. pinnatifida* have wider geographical distributions and have been reported from Asia, Africa, Europe, South and North Americas (e.g. Hafellner 1995; Diederich and Sérusiaux 2000; Calvelo and Liberatore 2002; Hawksworth et al. 2008, 2011; Knežević and Mayrhofer 2009; Seaward 2010; Guttová et al. 2013; Esslinger 2015). Nevertheless, both those taxa are rarer than other members of the genus *Parmelia*. Furthermore, these species occupy similar habitats and grow mainly on siliceous rocks (Hale 1987; Thell et al. 2011).

According to literature, all *Parmelia* species form associations with green algae of the genus *Trebouxia* de Puymaly (Hale 1987; Friedl 1989; Nash 2008; Thell et al. 2011; Leavitt et al. 2015). Unfortunately, all studies to date focused mainly on species from *P. saxatilis* and *P. sulcata* groups and there are relatively fewer data on photobionts within the *P. omphalodes* group. Recent results showed that interactions between myco- and photobionts are not random, but depend on ecological or environmental factors, such as exposure or type of substratum, in addition to evolutionarily-determined specificity (Helms 2003; Peksa and Škaloud 2011; Leavitt et al. 2015). The prevailing view of symbiotic associations in lichens is that the mycobiont tends to form associations with photobionts best adapted to the local habitat conditions (Peksa and Škaloud 2011). Moreover, ecologically similar co-existing lichens may share the same pool of photobiont species (Rikkinen et al. 2002; Yahr et al. 2006). As species of *P. omphalodes* group grow mainly on rocks, one hypothesis, therefore, might be that the species should contain the same pool of *Trebouxia* species.

During our study of *P. omphalodes* and *P. pinnatifida* specimens, important differences between published data and the results of our own studies were observed. For example, lobaric acid was identified in the specimens with marginal pseudocyphellae (thus morphologically similar to *P. pinnatifida*) or both lobaric acid and fatty acids were absent in specimens with marginal and laminal pseudocyphellae (thus morphologi-

cally similar to *P. omphalodes*). The differences between our results and literature data prompted more detailed morphological, chemical and phylogenetic studies on those two species, which are also relatively common and thus easy to be sampled for molecular analyses. We also included a few samples of *P. discordans* to better understand the differences amongst all three species of *P. omphalodes* group, especially in the case of photobiont associations. In the study, we used the nuclear ribosomal internal transcribed spacer region (ITS), which is considered as a universal barcode marker for fungi in many taxonomic groups (e.g. Schoch et al. 2012; Leavitt et al. 2014; Divakar et al. 2016).

The main goals of this paper are to study the phylogenetic relationships between *P. discordans*, *P. omphalodes* and *P. pinnatifida*, to determine, based on molecular evidence, the diagnostic characters separating *P. omphalodes* and *P. pinnatifida* and to study the photobionts genetic variation in all three species. As not much is known about their ecology, the evaluation of the 'ecological niche similarity' is also presented.

Materials and methods

Taxon sampling

In total, 335 herbarium specimens deposited in B, H, HBG, LD, S, UGDA and UPS were used for morphological, chemical and ecological niche modelling (ENM) study: 61 of *P. discordans*, 113 of *P. pinnatifida* and 161 of *P. omphalodes*. A total of 34 specimens were selected for molecular study using the nuclear internal transcribed spacer region (ITS rDNA). Thirty four ITS rDNA sequences of the mycobionts and 17 ITS rDNA sequences of their photobionts were newly generated (Table 1). Additionally, 22 sequences from 10 *Parmelia* taxa and 67 representative sequences of *Trebouxia* OTUs, as proposed by Leavitt et al. (2015), were downloaded from GenBank. The specimens deposited in MAF herbarium, which sequences were also used here, have been morphologically and chemically analysed. Newly obtained ITS rDNA sequences were subjected to BLAST search (Altschul et al. 1997) in order to check their identity. All sequences have been deposited in GenBank (see Table 1).

Morphology

The upper surfaces of all specimens were examined to determine the type of pseudocyphellae orientation such as: only marginal, marginal with few laminal in older parts of thalli and marginal and laminal in young and older parts of thalli. Pseudocyphellae were analysed on the whole thalli surfaces. Moreover, the length (distance between points of lobe branching) and width (distance between two adjacent lobe edges at the point of their branching) of lobes were also measured. Based on morphology and chemistry (see below), the studied specimens were divided into groups, which are characterised in Table 2. From each group (see Table 2) the samples were selected for DNA analysis.

Table 1. Specimens used in this study with the locality, voucher information, references and GenBank accession numbers. Sequences generated during this study are in bold.

Species/OTU	Voucher/ References	Fungal ITSrDNA	Algal ITSrDNA
Parmelia discordans	Sweden, S-F284965, Odelvik 15-293	**MN412798**	**MN412816**
	Sweden, S-F252494, Odelvik 13-147 et al.	**MN412800**	**MN412815**
	Sweden, UGDA L-23627, Kukwa 12278	**MN412799**	–
	UK, MAF-Lich 10232, (Molina et al. 2011)	AY583212	–
Parmelia ernstiae	Germany, HBG 4619 (Feuerer and Thell 2002)	AF410833	–
	Latvia, UGDA L-19917 (Ossowska et al. 2018)	KU845673	–
Parmelia imbricaria	Canada, TG 08-108 (Molina et al. 2017)	KT625503	–
Parmelia mayi	USA, MAF 15765 (Molina et al. 2011)	JN609439	–
	USA, MAF 15766 (Molina et al. 2011)	JN609438	–
	USA, MAF 15767 (Molina et al. 2011)	JN609437	–
Parmelia omphalodes	Sweden, S-F236118, Odelvik 12163	**MN412792**	**MN412806**
	Sweden, S-F300480, Odelvik 16-490	**MN412794**	**MN412805**
	Sweden, S-F252845, Odelvik 13-113	**MN412793**	**MN412808**
	UK, 2240 (Thell et al. 2008)	EF611295	–
	Finland (Thell et al. 2008)	AY251440	–
	Spain, MAF 7062 (Molina et al. 2004)	AY036998	–
	Spain, MAF 7044, (Molina et al. 2004)	AY036999	–
	Sweden, S-F238139, Odelvik 12238	**MN412796**	**MN412803**
	Sweden, UGDA L- 23632, Kukwa 12283	**MN412795**	**MN412817**
Parmelia pinnatifida	Norway, S-F254099, Odelvik 13-439	**MN412790**	**MN412804**
	Sweden, S-F299936, Odelvik 16-276	**MN412791**	–
	Sweden, S-F252763, Odelvik 13-225 et al.	**MN412797**	**MN412807**
	Sweden, S-F285120, Odelvik 15-294 et al.	**MN412789**	**MN412802**
	Poland, UGDA L-24300, Ossowska 118 et al.	**MN412774**	–
	Poland, UGDA L-24301, Ossowska 119 et al.	**MN412775**	**MN412813**
	Poland, UGDA L-24302, Ossowska 120 et al.	**MN412776**	–
	Poland, UGDA L-24304, Ossowska 123 et al.	**MN412777**	–
	Poland, UGDA L-24305, Ossowska 124 et al.	**MN412778**	**MN412814**
	Poland, UGDA L-24306, Ossowska 127 et al.	**MN412779**	–
	Poland, UGDA L-24307, Ossowska 132 et al.	**MN412780**	–
	Poland, UGDA L-24308, Ossowska 133 et al.	**MN412781**	–
	Poland, UGDA L-24310, Ossowska 137 et al.	**MN412783**	–
	Poland, UGDA L-24311, Ossowska 138 et al.	**MN412782**	–
	Poland, UGDA L-24318, Ossowska 150 et al.	**MN412785**	**MN412812**
	Poland, UGDA L-24319, Ossowska 152 et al.	**MN412784**	**MN412818**
	Poland, UGDA L-24313, Ossowska 143 et al.	**MN412786**	–
	Poland, UGDA L-24312, Ossowska 139 et al.	**MN412787**	**MN412811**
	Poland, UGDA L-24316, Ossowska 147 et al.	**MN412788**	–
	Poland, UGDA L-24294, Szczepańska s.n.	**MN412772**	**MN412810**
	Poland, UGDA L-24293, Szczepańska 1040	**MN412770**	**MN412809**
	Poland, UGDA L-24296, Szczepańska 1049	**MN412767**	–
	Poland, UGDA L-24297, Szczepańska 1052	**MN412768**	–
	Poland, UGDA L-24298, Szczepańska 1080	**MN412769**	–
	Poland, UGDA L-24295, Szczepańska 1126	**MN412773**	–
	Poland, UGDA L-24299, Szczepańska 1135	**MN412771**	–
	Austria (Thell et al. 2008)	EF611300	–
	Russia, MAF 7272 (Molina et al. 2004)	AY036988	–
	Russia, MAF 7274 (Molina et al. 2004)	AY036987	–
Parmelia saxatilis	Czech Republic, UGDA L-21245 (Ossowska et al. 2018)	KU845667	–
	Sweden, S-F300671, Odelvik 16-669 & Hedenäs	**MN412801**	–
	Sweden, MAF 6882 (Crespo et al. 2002)	AF350028	–
Parmelia serrana	Poland, UGDA L-21210 (Ossowska et al. 2018)	KU845669	–
	Spain, MAF 9756 (Molina et al. 2004)	AY295109	–
Parmelia skultii	Canada, LD 795 (Thell et al. 2004)	AY251456	–
	Greenland, 311C (Thell et al. 2004)	FJ425881	–

Species/OTU	Voucher/ References	Fungal ITSrDNA	Algal ITSrDNA
Parmelia submontana	Poland, UGDA L-21213 (Ossowska et al. 2018)	KU845664	–
	Morocco, MAF 15440 (Molina et al. 2011)	JN609434	–
Parmelia sulcata	Ireland, MAF 15421 (Molina et al. 2011)	JN118597	–
OTU I01	USA, I01_RH_shus_usa_UT_saxi_544 (Leavitt et al. 2015)	–	KR913803
OTU I02	USA, I02_ME_subau_usa_MI_cort_4176 (Leavitt et al. 2015)	–	KR913865
OTU I03	Estonia, I03_MH_exata_estonia_unk_cort_4110 (Leavitt et al. 2015)	–	KR913991
OTU I04	Russia, I04_RH_chryC_russia_Orenb_saxi_6890 (Leavitt et al. 2015)	–	KR914011
OTU I05	USA, I05_PUN_rud_usa_OH_cort_3157 (Leavitt et al. 2015)	–	KR914027
OTU I06	Canada, I06_MH_infum_canada_BC_saxi_4834 (Leavitt et al. 2015)	–	KR914029
OTU I07	USA, I07_ME_elber_usa_MN_cort_5773 (Leavitt et al. 2015)	–	KR914035
OTU I08	China, I08_MH_subexata_china_richuan_cort_3649 (Leavitt et al. 2015)	–	KR914042
OTU I09	USA, I09_MH_halei_usa_NC_cort_4008 (Leavitt et al. 2015)	–	KR914044
OTU I10	Argentina, I10_MH_ushua_argentina_unk_saxi_6045 (Leavitt et al. 2015)	–	KR914047
OTU I11	Russia, I11_MH_oliva_russia_Prim_cort_6012 (Leavitt et al. 2015)	–	KR914050
OTU I12	Russia, I12_MH_oliva_russia_Prim_cort_5998 (Leavitt et al. 2015)	–	KR914053
OTU I13	USA, I13_PUN_cas_usa_OH_cort_3161 (Leavitt et al. 2015)	–	KR914054
OTU I14	Russia, I14_MH_oliva_russia_Prim_cort_5973 (Leavitt et al. 2015)	–	KR914055
OTU I15	Kenya, I15_PUN_rud_kenya_unk_cort_1195 (Leavitt et al. 2015)	–	KR914056
OTU S01	Canada, S01_LE_lupina_canada_BC_cort_FJ170511 (Altermann 2009)	–	FJ170511
OTU S02	UK, S02_CE_acul_ant_shetland_terr_GQ375315 (Ruprecht et al. 2012)	–	GQ375315
OTU S03	Canada, S03_LE_vulpina_canada_BC_cort_FJ170752 (Altermann 2009)	–	FJ170752
OTU S04	Canada, S04_MH_exula_canada_BC_cort_5194 (Leavitt et al. 2015)	–	KR914114
OTU S05	USA, S05_LE_vulpina_usa_CA_cort_FJ170727 (Altermann 2009)	–	FJ170727
OTU S06	USA, S06_MH_eltula_usa_CO_cort_4212 (Leavitt et al. 2015)	–	KR914169
OTU S07	USA, S07_MH_eltula_usa_WA_cort_4343 (Leavitt et al. 2015)	–	KR914185
OTU S08	Spain, S08_CE_acul_spain_unk_terr_GQ375345 (Ruprecht et al. 2012)	–	GQ375345
OTU S09	Turkey, S09_CE_acul_turkey_unk_terr_GQ375351 (Ruprecht et al. 2012)	–	GQ375351
OTU S10	S10_TRE_simplex_SAG101_80_cult_FJ626735 (del Campo et al. 2010)	–	FJ626735
OTU S11	S11_TRE_australis_SAG2250_cult_FJ626726 (del Campo et al. 2010)	–	FJ626726
OTU S12	USA, S12_CE_acul_usa_AK_terr_GU124701 (Seifried 2009)	–	GU124701
OTU S13	S13_TRE_brindabellae_SAG2206_FJ626727 (del Campo et al. 2010)	–	FJ626727
OTU G01	Canaries, G01_PMT_pse_CANAR_gome_cort_3730 (Leavitt et al. 2015)	–	KR913271
OTU G02	Canaries, G02_PMT_per_CANAR_gome_cort_3751 (Leavitt et al. 2015)	–	KR913285
OTU G03	G03_TRE_usneae_UTEX2235_cult_AJ249573 (Friedl et al. 2000)	–	AJ249573
OTU G04	Canaries, G04_PMT_per_CANAR_gome_cort_3746 (Leavitt et al. 2015)	–	KR913286
OTU G05	G05_TRE_galapagensis_UTEX2230_AJ249567 (Friedl et al. 2000)	–	AJ249567
OTU A01	USA, A01_LEC_garov_usa_ID_saxi_078 (Leavitt et al. 2015)	–	KR912351
OTU A02	USA, A02_LEC_garov_usa_ID_saxi_108 (Leavitt et al. 2015)	–	KR912568
OTU A03	Sweden, A03_ME_fulig_swe_Skane_cort_3935 (Leavitt et al. 2015)	–	KR912760
OTU A04	USA, A04_XA_chE2_usa_ID_terr_201 (Leavitt et al. 2015)	–	KR912832
OTU A05	Mexico, A05_ORO_bicolor_mexico_OAX_cort_4043 (Leavitt et al. 2015)	–	KR912913
OTU A06	USA, A06_XA_coE3_usa_CO_saxi_6618 (Leavitt et al. 2015)	–	KR912989
OTU A07	USA, A07_XA_chE2_usa_UT_terr_008 (Leavitt et al. 2015)	–	KR913034
OTU A08	USA, A08_RH_mela_usa_UT_saxi_614 (Leavitt et al. 2015)	–	KR913115
OTU A09	USA, A09_XA_coE3_usa_UT_saxi_064 (Leavitt et al. 2015)	–	KR913162
OTU A10	Canada, A10_XA_cuF1_canada_BC_saxi_1007 (Leavitt et al. 2015)	–	KR913184
OTU A11	USA, A11_XA_idBX_usa_WY_terr_787 (Leavitt et al. 2015)	–	KR913199
OTU A12	USA, A12_XA_chE3_usa_UT_terr_126 (Leavitt et al. 2015)	–	KR913203
OTU A13	UK, A13_LEC_disp_uk_unk_saxi_6407 (Leavitt et al. 2015)	–	KR913212
OTU A14	USA, A14_XA_maricopF2_usa_A2_saxi_6699 (Leavitt et al. 2015)	–	KR913215
OTU A15	A15_TRE_gigantea_UTEX2231_cult_AF242468 (Kroken and Taylor 2000)	–	AF242468
OTU A16	Canada, A16_XA_caB1_canada_BC_terr_901 (Leavitt et al. 2015)	–	KR913224
OTU A17	Peru, A17_ORO_unk_peru_unk_cort_1602 (Leavitt et al. 2015)	–	KR913235
OTU A18	USA, A18_LEC_garov_usa_UT_saxi_140 (Leavitt et al. 2015)	–	KR913237
OTU A19	Canaries, A19_PMT_per_CANAR_gome_cort_3742 (Leavitt et al. 2015)	–	KR913241
OTU A20	USA, A20_XA_meF2_usa_A2_saxi_147 (Leavitt et al. 2015)	–	KR913248
OTU A21	USA, A21_XA_caB3_usa_ID_terr_334 (Leavitt et al. 2015)	–	KR913250

Species/OTU	Voucher/ References	Fungal ITSrDNA	Algal ITSrDNA
OTU A22	USA, A22_XA_chE2_usa_UT_terr_007 (Leavitt et al. 2015)	–	KR913255
OTU A23	A23_TRE_showmanii_UTEX2234_cult_AF242470 (Kroken & Taylor 2000)	–	AF242470
OTU A24	USA, A24_ME_calif_usa_CA_cort_4088 (Leavitt et al. 2015)	–	KR913251
OTU A25	USA, A25_XA_mariF2_usa_A2_saxi_6698 (Leavitt et al. 2015)	–	KR913259
OTU A26	USA, A26_XA_coE3_usa_UT_saxi_073 (Leavitt et al. 2015)	–	KR913261
OTU A27	USA, A27_XA_chE3_usa_WY_terr_110 (Leavitt et al. 2015)	–	KR913264
OTU A28	Mexico, A28_XA_diA1_mex_PU_saxi_098 (Leavitt et al. 2015)	–	KR913265
OTU A29	Japan, A29_MO_predis_japan_Shinano_saxi_8597 (Leavitt et al. 2015)	–	KR913266
OTU A30	USA, A30_XA_cuE2_usa_UT_saxi_036 (Leavitt et al. 2015)	–	KR913267
OTU A31	USA, A31_XA_coE1_usa_UT_saxi_030 (Leavitt et al. 2015)	–	KR913268
OTU A32	USA, A32_XA_cuE1_usa_UT_saxi_075 (Leavitt et al. 2015)	–	KR913269
OTU A33	A33_TRE_decolorans_UTEXB781_cult_FJ626728 (del Campo et al. 2010)	–	FJ626728
OTU A34	USA, A34_XA_mariF2_usa_AZ_saxi_6702 (Leavitt et al. 2015)	–	KR913270

Chemistry

Secondary lichen compounds were identified using thin-layer chromatography (TLC) in solvents A and C (Orange et al. 2001). The presence or absence of fatty acids was checked on two types of TLC plates: glass and aluminium. In order to check the differences in the concentration of lobaric acid in different parts of thalli, samples from marginal and central parts of thalli were analysed using TLC.

DNA extraction, PCR amplification and sequencing

Total genomic DNA was extracted using the Sherlock AX Kit (A&A Biotechnology, Poland) in accordance with the manufacturer's protocol, with slight modifications described by Ossowska et al. (2018).

Fungal ITS rDNA was amplified using the primers ITS1F and ITS4A (White et al. 1990; Gardes and Bruns 1993), while algal ITS rDNA was amplified using the following primers: LR3, ITS4M, ITS1T, ITS4T and AL1500bf (Friedl and Rokitta 1997; Kroken and Taylor 2000; Helms et al. 2001; Guzow-Krzemińska 2006). Amplification was performed in a total volume of 25 µl containing 1.0 µl of 10 µM of each primer, 12.5 µl of Start-Warm HS-PCR Mix Polymerase (A&A Biotechnology, Poland), 1.0 µl of dimethyl sulphoxide (DMSO), 3.0 µl of template DNA (~10–100 ng) and water.

The amplifications were performed in an Eppendorf thermocycler and carried out using the following programme: for fungal ITS rDNA marker: initial denaturation at 94 °C for 3 min and 33 cycles of: 94 °C for 30 sec; annealing at 52 °C for 45 sec; extension at 72 °C for 1 min and final extension at 72 °C for 10 min. For green-algal ITS: initial denaturation at 94 °C for 3 min and 35 cycles of: 94 °C for 45 sec; annealing at 55 °C for 45 sec; extension at 72 °C for 90 sec and final extension at 72 °C for 7 min.

The PCR products were purified using Wizard SV Gel and PCR Clean Up System (Promega, US), according to the manufacturer's instruction. The cleaned DNA was sequenced using Macrogen sequencing service (http://www.macrogen.com).

Table 2. Diagnostic morphological and chemical features in species from *Parmelia omphalodes* group analysed in this study with their classification after molecular research (ATR – atranorin, SAL – salazinic acid with consalazinic acid, LOB – lobaric acid, PRC – protocetraric acid, LICH – lichesternic acid, PRL – protolichesterinic acid).

Chemistry	Orientation of pseudocyphellae	Lenght (L) and width (W) of lobes (mm)	Voucher of specimens used in molecular research	Classification after molecular research
ATR, SAL, LOB	marginal	L 1.5–2; W 1	S-F299936 S-F254099	*Parmelia pinnatifida*
ATR, SAL, LOB	marginal, laminal in older lobes	L 2; W 2	UGDA L-24310 S-F252763	*Parmelia pinnatifida*
ATR, SAL, LOB, LICH, PRL	marginal	L 1–2; W 0.5–1.5	UGDA L-24295 UGDA L-24311 UGDA L-24319 UGDA L-24294 UGDA L-24296 UGDA L-24298 UGDA L-24305 UGDA L-24306	*Parmelia pinnatifida*
ATR, SAL, LOB, LICH, PRL	marginal, laminal in older lobes	L 1.5–2; W 1.5–2	UGDA L-24313 UGDA L-24308 UGDA L-24293 UGDA L-24297	*Parmelia pinnatifida*
ATR, SAL, LOB, PRL	marginal	L 0.5–2; W 0.5–1	UGDA L-24299 UGDA L-24300 UGDA L-24307 UGDA L-24318	*Parmelia pinnatifida*
ATR, SAL	marginal	L 1; W 1	UGDA L-24304 MAF 7274	*Parmelia pinnatifida*
ATR, SAL	marginal, laminal in older lobes	L 1.5 ,W 1	UGDA L-24312	*Parmelia pinnatifida*
ATR, SAL, LICH, PRL	marginal	L 2; W 1	UGDA L-24301	*Parmelia pinnatifida*
ATR, SAL, PRL	marginal	L 1.5–2; W 1.5–1	UGDA L-24302 S-F285120	*Parmelia pinnatifida*
ATR, SAL, PRL	marginal, laminal in older lobes	L 1.5; W 1	UGDA L-24316	*Parmelia pinnatifida*
ATR, PRC, LOB	marginal	L 3; W 1–2	S-F284965 S-F252494 MAF 10232	*Parmelia discordans*
ATR, PRC	marginal and laminal on young thalli	L 3; W 2	UGDA L-23627	*Parmelia discordans*
ATR, SAL, LOB	marginal, laminal	L 3–4; W 2–3	S-F300480 S-F252845 S-F238139 S-F236118 UGDA L-23632 MAF 7044	*Parmelia omphalodes*
ATR, SAL	marginal, laminal	L 2; W 1.5	MAF 7062	*Parmelia omphalodes*

Phylogenetic analyses

The newly generated mycobiont sequences, together with selected representatives of *Parmelia* spp., were automatically aligned in Seaview (Galtier et al. 1996; Gouy et al. 2010) using the algorithm MUSCLE (Edgar 2004), followed by manual correction and elimination of terminal ends. Then, selection of unambiguously aligned positions was performed using Gblocks 0.91b (Castresana 2000) employing less stringent conditions. The final alignment of mycobionts consisted of 58 ITS rDNA sequences and 444 characters. A sequence of *P. sulcata* (JN118597) was used as an outgroup.

The newly generated photobiont sequences, together with representative *Trebouxia* OTUs, downloaded from Dryad database (Dryad Digital Repository) (Leavitt et al. 2015) and described in Leavitt et al. (2015), were automatically aligned using MAFFT – Multiple Alignment using Fast Fourier Transform (Katoh et al. 2002), as implemented in UGENE (Okonechnikov et al. 2012). It was followed with a selection of unambiguously aligned positions using Gblocks 0.91b (Castresana 2000) with less stringent settings (i.e. allowing smaller final blocks, gap positions within the final blocks and less strict flanking positions).

The final alignment of photobionts consisted of 84 ITS rDNA sequences and 580 characters. The names of operational taxonomic units (OTU) for *Trebouxia* ITS rDNA sequences were given according to Leavitt et al. (2015).

The GTR+I+G best-fit evolutionary model was selected for the mycobiont dataset, based on Akaike Information Criterion (AIC) (Akaike 1973) as implemented in MrModelTest2 (Nylander 2004). For photobionts, we used Partition Finder 2 (Lanfear et al. 2016), implemented at CIPRES Science Gateway (Miller et al. 2010) to determine the best substitution model for each partition under Akaike Information Criterion (AIC) and greedy search algorithm (Lanfear et al. 2012). Two different models were found for partitions, i.e. TRNEF+I+G for 5.8S and GTR+I+G+X for both ITS regions.

Bayesian analysis was carried out using the Metropolis-coupled Markov chain Monte Carlo (MCMCMC) method by using the Markov chain Monte Carlo (MCMC) method, in MrBayes v. 3.2.6 (Huelsenbeck and Ronquist 2001; Ronquist and Huelsenbeck 2003) on the CIPRES Web Portal (Miller et al. 2010) using best models. Two parallel MCMCMC runs were performed, each using four independent chains and 2 million generations for the mycobiont tree and 10 million generations for the photobiont tree, sampling every 1000th tree. Tracer v. 1.6 (Rambaut and Drummond 2007) was used by plotting the log-likelihood values of the sample points against generation time. Convergence between runs was also verified using the Potential Scale Reduction Factor (PSRF) with all values equal or close to 1.000. Posterior Probabilities (PP) were determined by calculating a majority-rule consensus tree after discarding the initial 25% trees of each chain as the burn-in.

A Maximum Likelihood (ML) analysis was performed using RAxML-HPC2 v.8.2.10 (Stamatakis 2014) with 1000 ML bootstrap iterations (BS) and the GTRGAMMAI model for both analyses.

Phylogenetic trees were visualised using FigTree v. 1.4.2 (Rambaut 2012). Since the RAxML tree did not contradict the Bayesian tree topology for the strongly supported branches, only the latter was shown with the bootstrap support values, together with posterior probabilities of the Bayesian analysis (Figures 1, 2). BS ≥ 70 and PP ≥ 0.95 were considered to be significant and are shown near these branches.

Haplotype network

Sequences of ITS rDNA from specimens belonging to *P. discordans* and *P. omphalodes* were aligned using Seaview software (Galtier et al. 1996; Gouy et al. 2010) and the

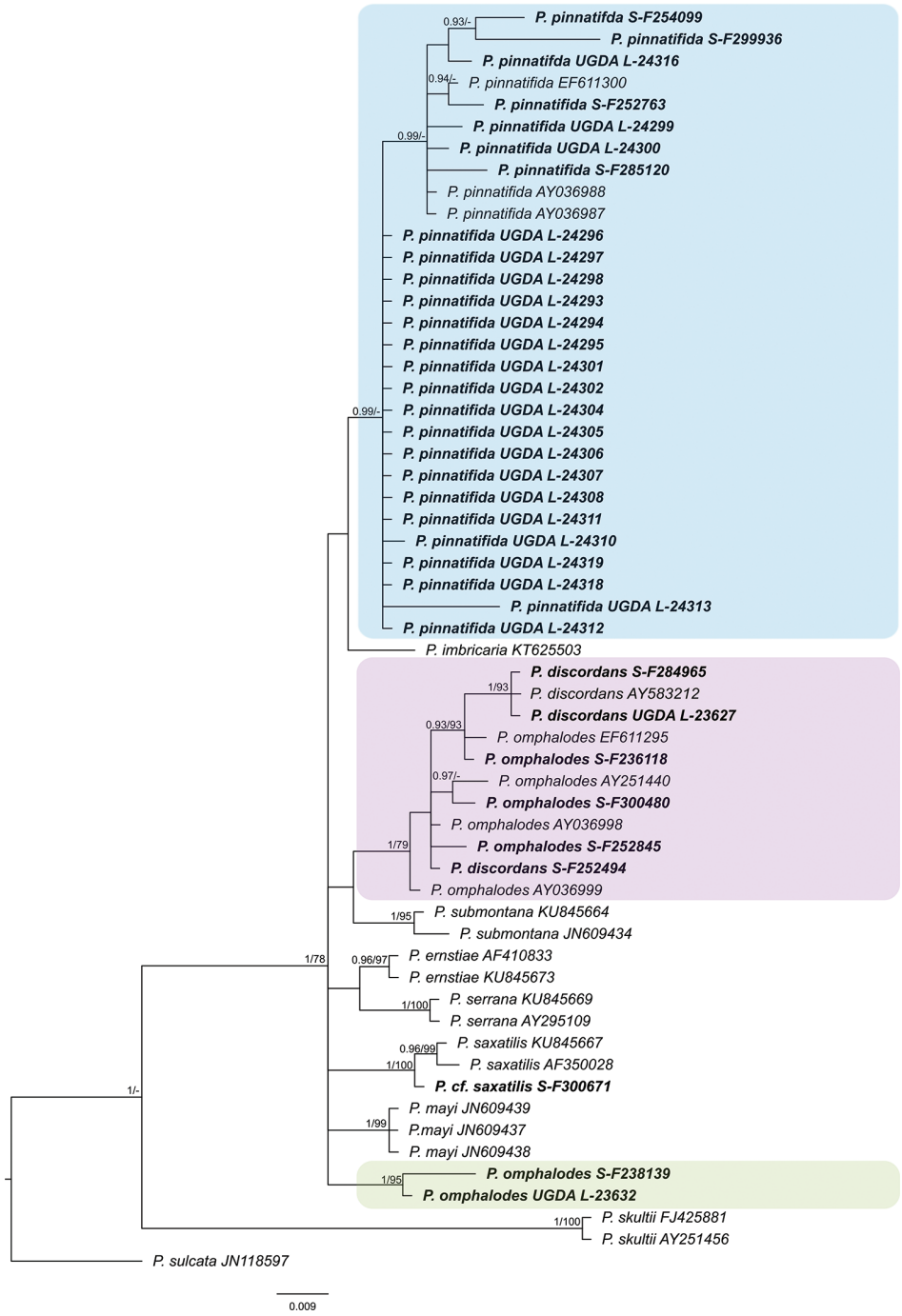

Figure 1. Phylogenetic relationships of *Parmelia discordans*, *P. omphalodes* and *P. pinnatifida*, based on Bayesian analysis of the ITS rDNA dataset. Posterior probabilities and maximum likelihood bootstrap values are shown near the internal branches. Newly generated sequences are described with herbarium numbers following the species names. GenBank Accession numbers of sequences downloaded from GenBank follow the species names. Clades with *Parmelia discordans*, *P. omphalodes* and *P. pinnatifida* are highlighted.

Figure 2. Phylogenetic placement of *Trebouxia* photobionts from selected *Parmelia* spp., based on Bayesian analysis of the ITS rDNA dataset. Posterior probabilities and maximum likelihood bootstrap values are shown near the internal branches. Newly generated sequences are in bold, with collecting numbers preceding the species names. Representative *Trebouxia* OTUs, as described in Leavitt et al. (2015), were downloaded from Dryad database (Dryad Digital Repository, Leavitt et al. 2015). Clades with photobionts from *Parmelia discordans*, *P. omphalodes* and *P. pinnatifida* are highlighted.

terminal ends were deleted. The alignment consisted of 13 sequences and 463 sites. The TCS network (Clement et al. 2002) was created using PopART software (http://popart.otago.ac.nz) (Figure 3).

Niche similarity

To evaluate the similarity of niches occupied by all studied taxa, ecological niche modelling (ENM) was applied.

The database of localities of *P. discordans*, *P. omphalodes* and *P. pinnatifida* was compiled, based on information provided on labels of herbarium specimens. The geographic coordinates provided on the herbarium sheet labels were verified. If there were no information about the latitude and longitude on the herbarium sheet label, we followed the description of the collection site and assigned coordinates as precisely as possible to this location. Google Earth (Google Inc.) was used to validate all gathered information. In total, 61 records of *P. discordans*, 161 of *P. omphalodes* and 113 of *P. pinnatifida* were used to perform ENM analysis (Figure 4 and Suppl. material 1: Table S1).

The maximum entropy method, as implemented in Maxent version 3.3.2 software, was used to create models of the suitable niche distribution (Phillips et al. 2004, 2006). This application has been proved to provide the most robust response across the number of environmental variables tested (Duque-Lazo et al. 2016) and it has been shown to work better with a small number of samples than with other approaches (Hernandez et al. 2006). MaxEnt settings previously used in research where limited samples were available (e.g. Pietras and Kolanowska 2019) were used in our computations. To assess the high level of specificity of the analysis, the maximum iterations of the optimisation algorithm were established as 10000 and the convergence threshold as 0.00001. The neutral (= 1) regularisation multiplier value and auto features were used. The "random seed" option was used for selecting training points. The run was performed with 1000 bootstrap replications and the default logistic model was used. The Area Under the Receiver Operating Characteristic (AUC) was used to evaluate the reliability of analyses. This is a commonly used threshold independent metric for evaluation of species distribution models (Hosmer and Lemeshow 2000; Elith et al. 2006; Evangelista et al. 2008) which was also used in studies involving a small number of samples (Pietras and Kolanowska 2019). Using more specific metrics, which could evaluate the possible overfitting of the model, would require implementing absence points and, in the case of our study object, such a dataset could not be prepared due to the lack of comprehensive studies on the distribution of genus representatives.

Twelve bioclimatic variables in 2.5 minutes developed by Hijmans et al. (2005; http://www.worldclim.org) were used as input data (Table 3). The study area which was used to evaluate the global identity of niches occupied by *P. discordans*, *P. omphalodes* and *P. pinnatifida* extended from 86.583°N to 17.83°N. As some previous studies (Barve et al. 2011) indicated that usage of a restricted area in ENM analysis is more reliable than calculating habitat suitability on the global scale, the similarity of niches occupied in America was calculated for an area that extended from 180°W to 31.749°W

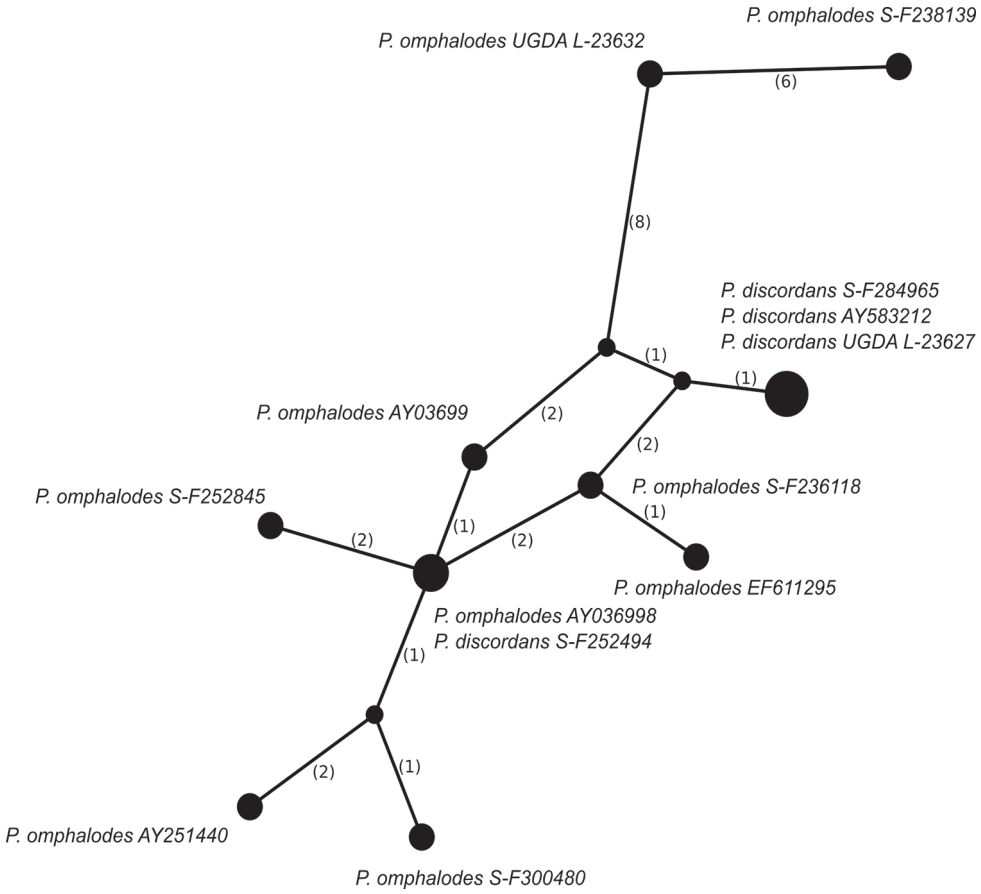

Figure 3. Haplotype network showing relationships between ITS rDNA sequences from *Parmelia discordans* and *P. omphalodes*. The names of species are followed with herbarium numbers of specimens or GenBank Accession Numbers. Mutational changes are presented as numbers in brackets near lines between haplotypes.

and from 85.292°N to 17.833°N and the study area of all three species occurring in Eurasia was reduced to 84.83–17.83°N and 17.833°W-180°E.

The differences amongst the niches occupied by the populations of three studied lichens were evaluated using the niche identity indices: Schoener's D (D) and I statistic (I) as available in ENMTools v1.3 (Schoener 1968; Warren et al. 2008, 2010). Additionally, the predicted niche occupancy (PNO) profiles were plotted to visualise differences in the preferred climatic factors amongst all taxa. PNO integrates species probability (suitability) distributions derived with MaxEnt with respect to a single climatic variable (Heibl and Calenge 2015).

Principal components analysis (PCA) was performed to explain the general variation pattern amongst the studied species, based on 12 bioclimatic factors used in ENM analysis. Statistical computations were performed with the programme PAST v. 3.0 (Hammer et al. 2001).

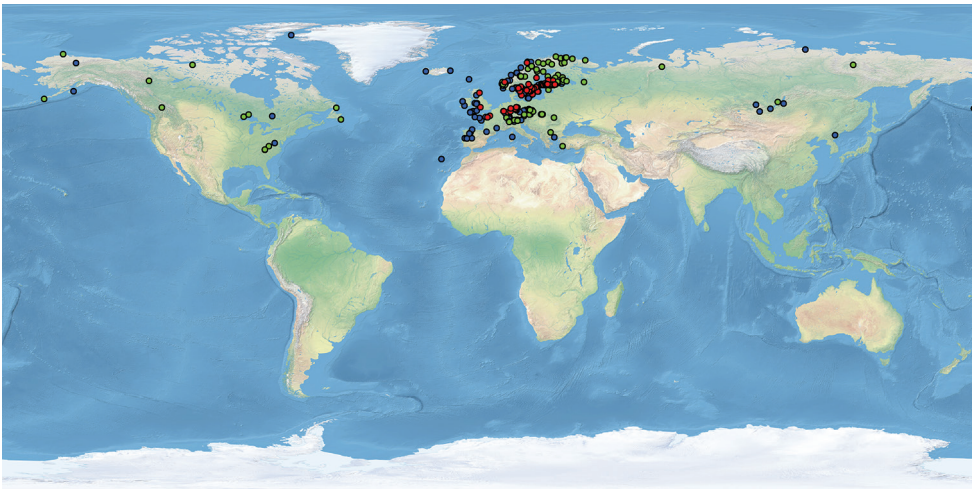

Figure 4. Localities of *Parmelia discordans* (red), *P. omphalodes* (blue) and *P. pinnatifida* (green) used in ENM analysis.

Table 3. Variables used in the ENM analysis.

bio1	annual mean temperature
bio2	mean diurnal range (mean of monthly (max temp - min temp))
bio3	isothermality (mean diurnal range / temperature annual range * 100)
bio4	temperature seasonality (standard deviation *100)
bio5	max temperature of the warmest month
bio8	mean temperature of the wettest quarter
bio12	annual precipitation
bio13	precipitation of the wettest month
bio14	precipitation of the driest month
bio15	precipitation seasonality (coefficient of variation)
bio18	precipitation of the warmest quarter
bio19	precipitation of coldest quarter

Results and discussion

Phylogeny, morphology and chemistry of species of *Parmelia omphalodes* group

Trees of similar topologies were generated using the maximum likelihood method (RaxML; best tree likelihood LnL = –1512.540166) and the Bayesian approach (BA; harmonic mean was –1667.09). The Bayesian tree is presented in Figure 1 with added bootstrap supports from the RaxML analysis and posterior probabilities from the BA. The phylogenetic analyses showed that, despite morphological similarities of species, the *P. omphalodes* group is not monophyletic. Specimens are separated into three distinct clades. One clade (0.99 PP) is related to *P. imbricaria* Goward et al. (Figure 1). In this clade, specimens containing salazinic acid, but variable in fatty and lobaric acids content (Table 2), are grouped with sequences labelled as *P. pinnatifida*, downloaded from GenBank. Analysis of morphological features revealed that all specimens in this

clade have predominantly marginal pseudocyphellae. Specimens with similar chemical variation (Table 2), but having both marginal and laminal pseudocyphellae and, thus, referable to *P. omphalodes*, form two distinct clades (Figure 1), one containing the majority of the studied specimens and also the sequences downloaded from GenBank (1 PP and 79 BS) and the second (1 PP and 95 BS) grouping only two samples (specimens S-F238139 and UGDA L-23632). The latter clade consists of specimens indistinguishable in all morphological and chemical features from other specimens of *P. omphalodes* used in this study. This lineage may represent a cryptic species, but more specimens and additional molecular markers are necessary to be analysed before it is described.

Within the larger clade of *P. omphalodes*, four sequences obtained from specimens containing protocetraric acid and determined as *P. discordans* are nested. Three of those specimens form a highly supported lineage (1 PP and 93 BS), while the fourth sample of *P. discordans* is placed outside this subclade (Figure 1). Moreover, to better understand the phylogenetic position and genetic variation of the ITS rDNA marker within *P. omphalodes* s.l., we generated a haplotype network for specimens of both *P. discordans* and *P. omphalodes* (Figure 3). There is no significant difference between specimens of those two taxa, except two samples of *P. omphalodes* (specimens S-F238139 and UGDA L-23632) representing the second lineage found in our study (see above), that differ from other representatives of this species in at least 10 sites. One specimen of *P. discordans* (S-F252494) shares the same haplotype with *P. omphalodes* (AY036998), which differs from other haplotypes of the former taxon in 5 sites. Moreover, three other specimens of *P. discordans* share the same haplotype, which differs from haplotypes of *P. omphalodes* in at least 3 positions.

So far, the taxonomy of *P. omphalodes* group was unclear. Kurokawa (1976) recognised three species within this group: *P. discordans*, *P. omphalodes* and *P. pinnatifida*, whereas Skult (1984) classified *P. discordans* and *P. pinnatifida* as subspecies within *P. omphalodes*. On the other hand, Hale (1987) recognised two species, *P. discordans* and *P. omphalodes*. However, our results agree to a certain point with those presented by Molina et al. (2004) and Thell et al. (2008), who showed that *P. pinnatifida* is a taxon well-separated from *P. omphalodes*. In the case of *P. discordans*, Thell et al. (2008) used only a single sequence of this species (AY583212), which was nested within the *P. omphalodes* clade. In the discussion, those authors concluded that the status of *P. discordans* as a separate taxon required further molecular analyses (Thell et al. 2008). In our study, sequences of *P. discordans* are also nested in the clade of *P. omphalodes*. Perhaps the former should be synonymised with *P. omphalodes*, as some specimens of both taxa share the same ITS rDNA haplotypes (Figure 3). However, the final conclusions should await more data from other molecular markers as the use of a single genetic marker to delimit species might be inappropriate (e.g. Leavitt et al. 2011, 2013a; Pino-Bodas et al. 2013). However, in the case of many taxonomic groups, ITS rDNA helps to discriminate species, for example, in *Parmeliaceae*, including *Parmelia*, and has been shown to be effective and proposed to be used as a primary fungal barcode (e.g. Crespo and Lumbsch 2010; Leavitt et al. 2014; Divakar et al. 2016; Corsie et al. 2019).

The distinguishing character between *P. omphalodes* and *P. pinnatifida* is the development of pseudocyphellae; however, the determination of the type and orientation of

pseudocyphellae requires checking of the entire thallus surface, not only marginal or central parts of the thalli. We concluded that *P. pinnatifida* has mostly marginal pseudocyphellae forming white rims around lobes margins (Figure 5C), in some samples with few laminal ones in older parts of thalli. Laminal pseudocyphellae, in this species, predominantly start at the edge of lobes and are connected to the marginal pseudocyphellae and only very few are separated from the marginal ones (Figures 5C, D). Thalli of *P. omphalodes* always have marginal and laminal pseudocyphellae and, in the case of the latter, many are not connected to the margins of lobes (Figure 5B). We also checked the orientation of pseudocyphellae in *P. discordans*. In young thalli, they may be exclusively marginal, but in most cases laminal ones are also developed (Figure 5A), as in the case of *P. omphalodes*.

The presence of lobaric and fatty acids cannot be treated as diagnostic for the separation of *P. omphalodes* and *P. pinnatifida*, as it does not correspond with molecular data. Until now, *P. pinnatifida* was characterised as a species lacking lobaric acid (Kurokawa 1976; Skult 1984; Molina et al. 2004; Ossowska and Kukwa 2016). In this study, the specimens with morphology of pseudocyphellae typical for this species and with or without lobaric acid are grouped in one clade. The same variation in the

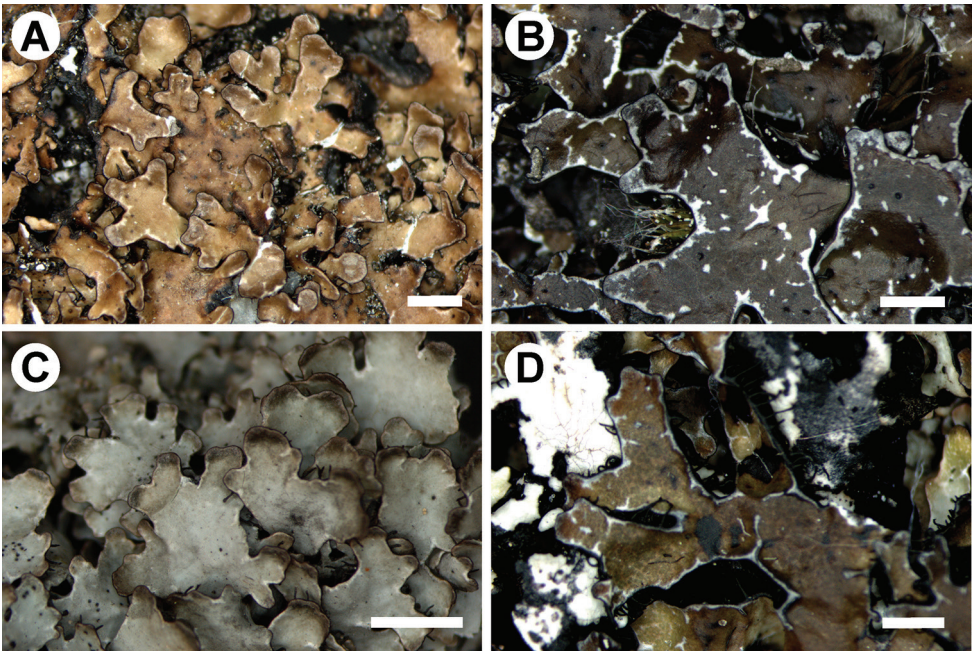

Figure 5. A *Parmelia discordans*, with marginal and laminal pseudocyphellae, laminal pseudocyphellae mostly not connected with marginal ones (S F-252494) **B** *P. omphalodes*, with marginal and laminal pseudocyphellae, laminal pseudocyphellae mostly not connected with marginal ones (S F-252845) **C** *P. pinnatifida*, with marginal pseudocyphellae (UGDA L-24298) **D** *P. pinnatifida*, with marginal and laminal pseudocyphellae, laminal pseudocyphellae starting predominantly from pseudocyphellae formed at the edge of lobes (S F-239397). Scale bars: 200 μm (**A, B, D**), 150 μm (**C**).

presence of lobaric acid was noted in *P. omphalodes*, which was reported as constantly containing this substance (Kurokawa 1976; Skult 1984; Ossowska and Kukwa 2016). A similar issue was noted in the *P. saxatilis* group. The presence or absence of lobaric acid was treated as a diagnostic character to differentiate species (e.g. Feuerer and Thell 2002; Molina et al. 2004; Thell et al. 2011; Ossowska et al. 2014), but the recent results obtained by Thell et al. (2017), Ossowska et al. (2018), Corsie et al. (2019) and Haugan and Timdal (2019), revealed that the production of this substance is variable, for example, *P. serrana* A. Crespo et al., typically lacking lobaric acid, may also produce this substance (Ossowska et al. 2018; Corsie et al. 2019; Haugan and Timdal 2019). Similar variation in lobaric acid production was also observed in *Stereocaulon condensatum* Hoffm. (Oset 2014). Moreover, lobaric acid was detectable in *P. omphalodes* and *P. pinnatifida* only when lobes from the central parts of the thalli were taken for TLC.

Kurokawa (1976) reported that *P. omphalodes* and *P. pinnatifida* also differ in the production of fatty acids (absent in *P. omphalodes*, present in *P. pinnatifida*), but both species also showed intraspecific variation in this character (Table 2). Moreover, the detection of fatty acids may differ due to the type of TLC plates used. The glass TLC plates are better suited for the detection of these substances than aluminium plates (Orange et al. 2001) and, for example, protolichesterinic acid was undetectable on aluminium plates, but visible on glass plates.

Morphological and chemical characteristics of all taxa of the group are summarised in Table 4 and the determination key is presented below (see also Table 2).

Phylogenetic analyses of photobionts

Trees of similar topologies were generated using maximum likelihood (RaxML; best tree likelihood LnL = -7013.073328) and Bayesian analysis (BA; harmonic mean was -6996.31). The Bayesian tree is presented in Figure 2 with added bootstrap supports from RaxML and posterior probabilities from BA. The phylogenetic analyses showed that photobionts of *P. discordans*, *P. omphalodes* and *P. pinnatifida* belong to the *Trebouxia* S clade (*T. simplex*/*lethariil jamesii* group) sensu Leavitt et al. (2015) and represent at least five different lineages (Figure 2). The most common photobiont in the species analysed in this work is *Trebouxia* OTU S02, which was found in one specimen of *P. discordans* and most specimens of *P. pinnatifida* (Figure 6). Additionally, we detected *Trebouxia* OTU S04 in a single specimen of *P. pinnatifida* (UGDA L-24293) and one specimen of this species (S-F252763) has an unnamed *Trebouxia* species (SUn2). Therefore, *P. pinnatifida* associates with at least three different photobiont taxa of which, based on the BLAST search, OTU S04 seems to be very rare. We also found some variation in photobionts of *P. omphalodes* which associates with two lineages of *Trebouxia*, i.e. OTU S05 (two specimens) and an unnamed *Trebouxia* lineage (three specimens) (SUn1), closely related to the photobiont present in one sample of *P. pinnatifida* (S-F252763). Moreover, *Trebouxia* OTU S05 was also detected in *P. discordans*. In Leavitt et al. (2015), it was reported that, based on 98% sequence similarity, *Parmelia* species

Table 4. Historical and present overview of species delimitations within the *Parmelia omphalodes* group with their morphological and chemical characteristics (ATR – atranorin, SAL – salazinic acid with consalazinic acid, LOB – lobaric acid, PRC – protocetraric acid, PRL – protolichesterinic acid, FAT – fatty acids; + present in all specimens; ± sometimes present).

	Taxa	Morphology	Chemistry
Kurokawa (1976)	*P. discordans*	pseudocyphellae marginal and laminal; lobules absent; lobes 1–2.5 mm wide	ATR (+), PRC (+), LOB (+), FAT (±)
	P. omphalodes	pseudocyphellae marginal and laminal; lobules present	ATR (+), SAL (+), LOB (+)
	P. pinnatifida	pseudocyphellae marginal; narrow lobules present; lobes repeatedly branched	ATR (+), SAL (+), FAT (+)
Skult (1984)	*P. omphalodes* subsp. *discordans*	pseudocyphellae sparse and marginal in young lobes; lobes diameter 0.13–2.8 mm	ATR (+), PRC (+), LOB (+), PRL (+)
	P. omphalodes subsp. *omphalodes*	pseudocyphellae marginal and laminal; lobes up to 3.5 mm diameter	ATR (+), SAL (+), LOB (+), PRL (±)
	P. omphalodes subsp. *pinnatifida*	pseudocyphellae marginal, in old lobes laminal; lobes narrow, 0.13–2.9 mm diameter	ATR (+), SAL (+), PRL (±)
Hale (1987)	*P. discordans*	pseudocyphellae marginal, few also laminal; lobes 1–3 mm wide	ATR (+), PRC (+), LOB (+), unidentified FAT (±)
	P. omphalodes	pseudocyphellae mostly marginal; lobes wide 1–4 mm	ATR (+), SAL (+), LOB (±), PRL (+)*
Molina et al. (2004)	*P. discordans*	pseudocyphellae linear; lobes overlapping, 1–3 mm wide	PRC (+), LOB (+)
	P. omphalodes	lobes 4 mm wide	ATR (+), SAL (+), LOB (+), PRC (±)
	P. pinnatifida	pseudocyphellae restricted to the margins; lobes narrow, repeatedly branched and overlapping	ATR (+), SAL (+), PRL (+)
Thell et al. (2008)	*P. discordans*	pseudocyphellae indistinct; lobes narrow	ATR (+), PRC (+), LOB (+)
	P. omphalodes	–	ATR (+), SAL (+), LOB (+), PRL (+), PRC (±)
	P. pinnatifida	pseudocyphellae marginal; lobes narrow	ATR (+), SAL (+), PRL (+), PRC (±)
This study	*P. discordans*	pseudocyphellae marginal and laminal, laminal pseudocyphellae at least partly not starting from the lobe margins; lobes narrow and sublinear, about 1–3 mm wide and 1–3 mm length	ATR (+), PRC (+), LOB (±), FAT (±)
	P. omphalodes	pseudocyphellae marginal and laminal, laminal pseudocyphellae mostly not starting from the lobe margins; lobes broad and sublinear, about 2–3 mm wide and 3–4 mm length	ATR (+), SAL (+), LOB (±), FAT (±)
	P. pinnatifida	pseudocyphellae marginal, in older parts of thalli with few laminal connected to the lobes margins; lobes narrow, sublinear, about 1–2 mm wide and 0.5–2 mm length	ATR (+), SAL (+), LOB (±), FAT (±)

* Author described the lack of lobaric acid in 96% of analysed samples, but morphologically they were similar to *P. omphalodes*. Hale (1987) did not classified them as a *P. pinnatifida*.

form associations with *Trebouxia* OTU I02, belonging to the *T. impressa/galapagensis* group, but this group of photobionts might only be characteristic for *P. saxatilis* and *P. sulcata* groups, as we have not found this lineage in the studied specimens.

According to Beck et al. (2002), 'selectivity' refers to the taxonomic range of partners that are selected by one of the bionts, while 'specificity' should be used for the symbiotic association and depends on the range and taxonomic relatedness of acceptable partners. Lichens with high selectivity may associate with a limited number of photobionts. Numerous mycobionts, belonging to Parmeliaceae, have been shown to associate with identical species of *Trebouxia*, while others exhibited higher photobiont flexibility

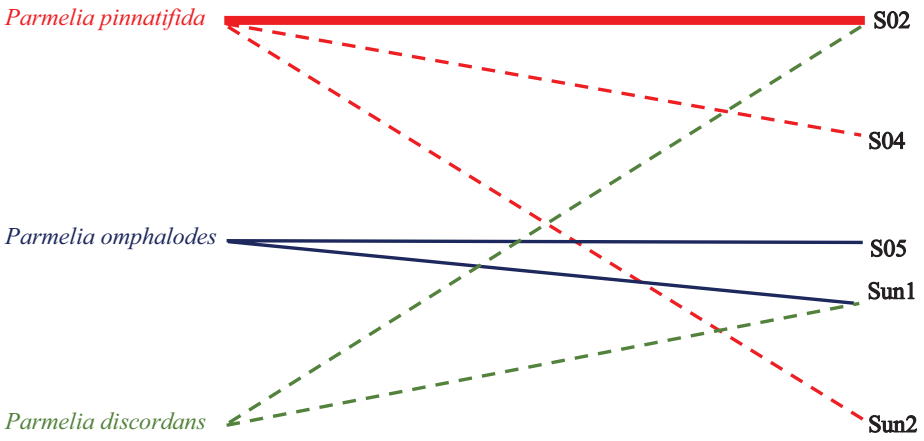

Figure 6. Association network between lichen mycobionts of *P. omphalodes* group (i.e. *Parmelia discordans*, *P. omphalodes* and *P. pinnatifida*) and photobiont OTUs. The line width is proportional to the number of specimens forming the association with the particular OTU. SUn1 and SUn2 represent unnamed lineages of *Trebouxia* belonging to clade S.

(e.g. Kroken and Taylor 2000; Ohmura et al. 2006, 2018; Doering and Piercey-Normore 2009; Leavitt et al. 2013b, 2015; Lindgren et al. 2014). Our results indicate that taxa from *P. omphalodes* group are moderately selective in their photobionts choice, as these taxa associate with at least two or three *Trebouxia* lineages (Figure 6).

Lichens that reproduce sexually via independent dispersal of fungal spores, undergo a process of re-lichenisation. This means that the germinating spore of the mycobiont can easily exchange its autotrophic partner, in contrast to asexually reproducing lichens distributing both partners together, which allows continuation of the symbiosis without the need to re-associate with another biont (Beck et al. 1998, 2002; Romeike et al. 2002; Sanders and Lücking 2002). However, even asexually reproducing lichens, such as the *Lepraria* species, have been shown to switch their algal partners (Nelsen and Gargas 2008). Moreover, in populations of *Physconia grisea* (Lam.) Poelt with a vegetative propagation strategy, mycobionts associate with more than one photobiont genotype (Wornik and Grube 2010). It was also reported that both sexual and vegetative reproduction allows lichens to generate almost the same amount of diversity to adapt to their environments (Cao et al. 2015). Moreover, *Protoparmeliopsis muralis* (Schreb.) M.Choisy, which does not produce vegetative propagules, exhibited a low selectivity level (Guzow-Krzemińska 2006; Muggia et al. 2013); however, *P. muralis* has wider geographical distribution and occurs on a wider range of substrata and ecological conditions than taxa from the analysed group.

The ecological 'lichen guilds' hypothesis, i.e. communities of lichens growing on the same type of habitat and forming associations with the same photobiont species, have been proposed for cyanobacterial lichens (Rikkinen et al. 2002). This hypothesis

was tested by Peksa and Škaloud (2011) for the eukaryotic genus *Asterochloris* Tschermak-Woess. These authors showed that ecological niches available to lichens may be limited by algal preferences for environmental factors and thus can lead to the existence of specific lichen guilds, but their results were based only on selected species of *Lepraria* Ach. and *Stereocaulon* Hoffm. On the other hand, results obtained by Leavitt et al. (2015) indicated that ecologically specialised lichens from different genera form associations with different *Trebouxia* OTUs in the same habitat. Moreover, observations made by Deduke and Piercey-Normore (2015) for species of *Xanthoparmelia* (Vain.) Hale, growing on different rock types, did not support the photobiont guild hypothesis. However, they suggested that the range of rock substrata type in their study may have been too narrow to differentiate algal preference. On the other hand, they indicated that Peksa and Škaloud (2011) compared broadly defined types of substrata (defined as a 'bark of tree' and 'rock').

In this study, we found that the most common photobiont in *P. pinnatifida* was *Trebouxia* OTU S02. All samples of *P. pinnatifida* were collected from rocks; however, some authors previously reported the same *Treboxia* OTU S02 from terricolous, saxicolous and corticolous Parmeliaceae (i.e. genera *Cetraria* Ach., *Melanohalea* O.Blanco et al., *Montanelia* Divakar et al., *Protoparmelia* M.Choisy and *Rhizoplaca* Zopf and species *Xanthoparmelia coloradoensis* Hale and *Vulpicida juniperinus* (L.) J.-E.Mattsson & M.J.Lai) (Lindgren et al. 2014; Leavitt et al. 2015; Singh et al. 2017), but it may also occur in lichen genera representing other families, for example, *Chaenotheca* (Th. Fr.) Th.Fr., *Circinaria* Link and *Umbilicaria* Hoffm. (Beck 2002; Romeike et al. 2002; Molins et al. 2018). On the other hand, *Trebouxia* OTU S04, which corresponds to *T. jamesii* (UBT-86.156C3), was identified in a single specimen of *P. pinnatifida* (UGDA L-24293). It was previously reported exclusively from corticolous *Melanohalea* and *Bryoria* species (Lindgren et al. 2014; Leavitt et al. 2015) and seems to be very rare or at least rarely sampled, as it is poorly represented in GenBank. Moreover, the unnamed lineage of *Trebouxia* (SUn2) was detected in a single specimen of *P. pinnatifida* and, based on 99% identity, we found that it may also associate with, for example, *Bryoria simplicior* (Vain.) Brodo & D.Hawksw., *Cetraria aculeata* (Schreber) Fr., *Evernia divaricata* L. (Ach.) (Piercey-Normore 2009; Domaschke et al. 2012; Lindgren et al. 2014). Some variation in photobionts was also found in specimens of *P. omphalodes* which associate with *Trebouxia* OTU S05 and an unnamed lineage (SUn1). Leavitt et al. (2015) reported *Trebouxia* OTU S05, which corresponds to *Trebouxia suecica* (SAG2207), from terricolous and corticolous Parmeliaceae (i.e. *Cetraria aculeata* (Schreber) Fr., *Letharia vulpina* (L.) Hue and *Melanohalea* spp.). Photobionts, very similar to *Trebouxia* OTU S05 (100% identity), were additionally found in, for example, *Bryoria fremontii* (Tuck.) Brodo & D.Hawksw., *Lasallia hispanica* (Frey) Sancho & Crespo, *Lecanora rupicola* (L.) Zahlbr. and *Tephromela atra* (Huds.) Hafellner (Blaha et al. 2006; Lindgren et al. 2014; Muggia et al 2014; Paul et al. 2018). Moreover, the unnamed lineage of *Treboxia* (SUn1) was detected in three specimens of *P. omphalodes* and, based on 99% identity, we found that it may also associate with, for example, *Bryoria* spp., *Cetraria* spp., *Evernia mesomorpha* Nyl. *Flavocetraria nivalis* (L.) Kärnefelt

& A.Thell and *Vulpicida pinastrii* (Scop.) J.-E.Mattsson & M.J.Lai (Opanowicz and Grube 2004; Piercey-Normore 2009; Lindgren et al. 2014; Onuț-Brännström et al. 2018). Therefore, the results obtained, based on our dataset, do not support the ecological guild hypothesis; however, our sampling was rather limited and we did not analyse co-occurring species. Although the type of substrata seems not to correspond to any of *Trebouxia* OTUs, bioclimatic factors, such as annual mean temperature, maximum temperature of warmest month or precipitation, may influence the patterns of photobionts distribution. However, to perform such an analysis, a larger set of specimens should be examined.

Interestingly, although *P. omphalodes* was found to associate with two lineages of *Trebouxia* photobionts (i.e. OTU S05 and an unidentified lineage SUn1), it does not associate with *Trebouxia* OTU S02, which, on the other hand, was found to associate with *P. discordans* (two samples). However, *P. discordans* also associates with *Trebouxia* OTU S05. As those species differ in morphology and chemistry, we suggest that those differences might be related to the photobiont type. Although some researchers did not find any correlation between different chemotypes and the associated photobionts (e.g. Blaha et al. 2006; Lindgren et al. 2014), recent studies suggested that the production of certain secondary metabolites might be triggered by the environment, for example, climate, edaphic factors or associated symbionts (e.g. Spribille et al. 2016; Lutsak et al. 2017). However, due to limited sampling, we cannot confirm this hypothesis for *Parmelia* spp. analysed in this study.

Ecological niche modelling of species of *Parmelia omphalodes* group

The created models, derived from MaxEnt, received high AUC scores, indicating high reliability of analyses (Table 5). Generated maps of distribution of suitable niches of the three lichen species were wider than the known geographical range of these lichens (Figures 7–9).

The distribution of *P. discordans* is limited mainly by precipitation of the driest month (bio14), but two other factors that can influence the occurrence of this taxon, varied in analyses conducted for the Northern Hemisphere and Eurasia separately. While in the former analysis, annual mean temperature (bio1) and mean diurnal range (bio2) gave important contributions to the model, the latter analysis indicated maximum temperature of the warmest month (bio5) and temperature seasonality (bio4) as significant limiting factors. Additionally, in cases of *P. omphalodes* and *P. pinnatifida*, different variables gave various contributions to the models created for different study

Table 5. The average training AUC for created models.

	Northern Hemisphere	Eurasia	America
P. discordans	0.993 (SD = 0.001)	0.992 (SD = 0.001)	–
P. omphalodes	0.980 (SD = 0.003	0.982 (SD = 0.002)	0.767 (SD = 0.101)
P. pinnatifida	0.981 (SD = 0.003	0.986 (SD = 0.002)	0.819 (SD = 0.064)

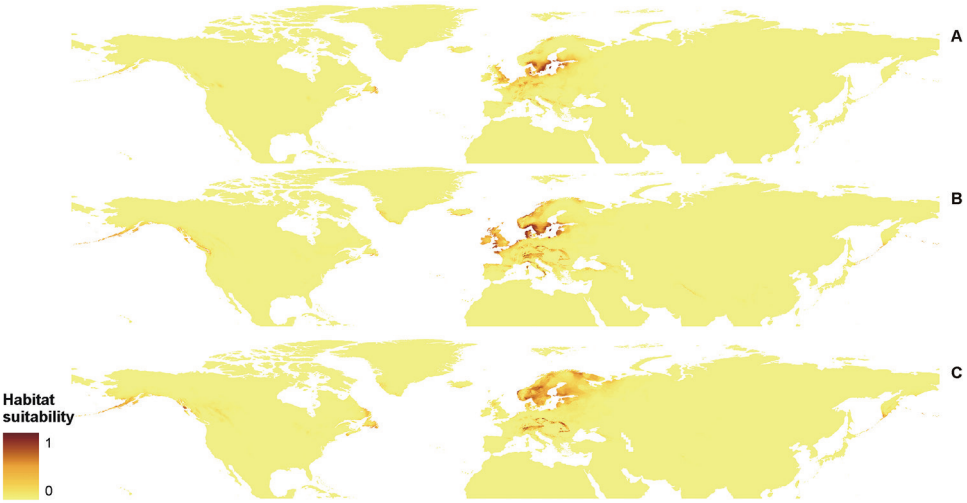

Figure 7. Distribution of suitable niches of *P. discordans* (**A**), *P. omphalodes* (**B**) and *P. pinnatifida* (**C**) in the Northern Hemisphere.

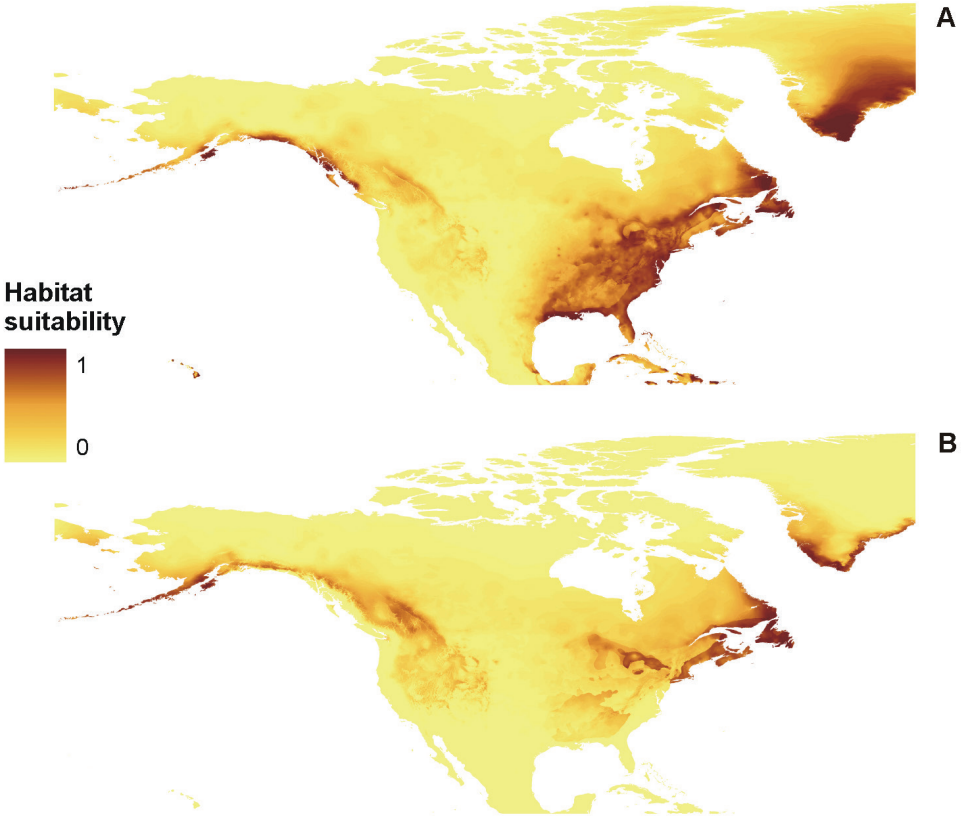

Figure 8. Distribution of suitable niches of *P. omphalodes* (**A**) and *P. pinnatifida* (**B**) in America.

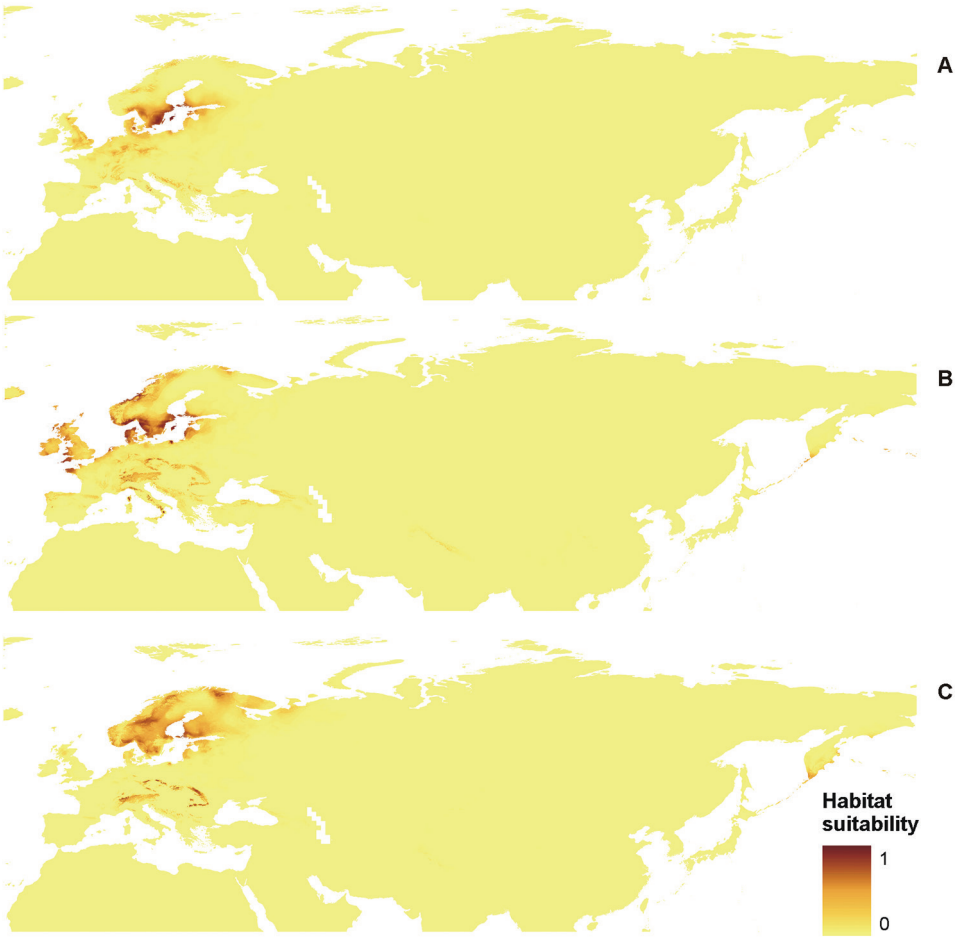

Figure 9. Distribution of suitable niches of *P. discordans* (**A**), *P. omphalodes* (**B**) and *P. pinnatifida* (**C**) in Eurasia.

areas. Mean diurnal range (bio2) was the crucial limiting factor for Eurasian populations of *P. omphalodes*, while within the American range of this species, its occurrence depends on precipitation of the driest month (bio14). For the American distribution of *P. pinnatifida*, the annual mean temperature (bio1) significantly influenced the model and the distribution of Eurasian populations appears limited by the maximum temperature of the warmest month (bio5) (Table 6).

The PCA diagram (Figure 10) showed that the highest bioclimatic variation is observed in *P. omphalodes* and that niches of *P. discordans* and *P. pinnatifida* are embedded in this highly flexible bioclimatic tolerance of *P. omphalodes*. The overall high similarity in bioclimatic preferences of all three studied taxa is presented in PNO profiles created for various geographic areas (Suppl. material 2: Figure S2, Suppl. material 3: Figure S3, Suppl. material 4: Figure S4). On a global scale, *P. pinnatifida* and *P. omphalodes* occupy similar niches (D = 0.581, I = 0.840), while bioclimatic preferences of *P. discordans* are

Table 6. Estimates of relative contributions of the environmental variables to the Maxent model.

	Northern Hemisphere	Eurasia	America
P. discordans	bio14 (25.6)	bio14 (35.9)	–
	bio1 (18.8)	bio5 (15.2)	
	bio2 (15.4)	bio4 (14.6)	
P. omphalodes	bio19 (21.1)	bio2 (27.8)	bio14 (48.2)
	bio4 (21)	bio19 (24.8)	bio15 (20.3)
	bio2 (17.7)	bio4 (14.2)	bio2 (10.9)
P. pinnatifida	bio5 (17.7)	bio5 (24.6)	bio1 (42.2)
	bio14 (17.3)	bio14 (19.1)	bio14 (18)
	bio4 (14.1)	bio4 (15.7)	bio8 (11.1)

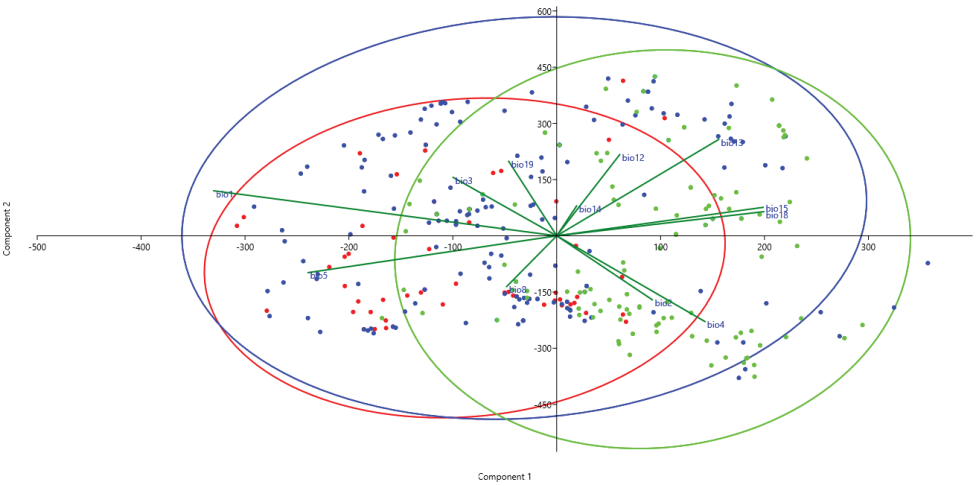

Figure 10. Principal components analysis (PCA) of *P. discordans* (red), *P. omphalodes* (blue) and *P. pinnatifida* (green), based on the bioclimatic factors from individuals.

more similar to *P. omphalodes* than to *P. pinnatifida* (Table 7). In the American range, *P. omphalodes* and *P. pinnatifida* occupy very similar habitats (D = 0.821, I = 0.968; Table 8). Within Eurasian populations, the highest similarity is observed for *P. omphalodes* and *P. discordans* (D = 0.587, I = 0.828); however, *P. pinnatifida* and *P. omphalodes* also occupy similar niches (D = 0.564, I = 0.820; Table 9).

According to published data (Sanders and Lücking 2002; Büdel and Scheidegger 2008), lichens without vegetative propagules, dispersing both bionts independently, require the contact of the mycobiont with a compatible photobiont species in suitable environmental conditions to establish new thalli. Results of ecological niche modelling, presented here, confirmed that species from the analysed group occupy similar niches. In Figure 2, one sequence of photobionts, associating with *P. discordans*, belong to *Trebouxia* OTU S05 and the second to *Trebouxia* OTU S02. The latter is the most common photobiont of *P. pinnatifida* which, on the other hand, was also found to associate with *Trebouxia* OTU S04 and an unnamed *Trebouxia* lineage SUn2. However, none of photobionts from *P. omphalodes* belongs to *Trebouxia* OTU S02 and OTU S04, but this taxon associates with two lineages of *Trebouxia* photobionts (i.e.

Table 7. Niche identity indexes calculated for Northern Hemisphere.

D\I	*P. discordans*	*P. omphalodes*	*P. pinnatifida*
P. discordans	x	0.791	0.703
P. omphalodes	0.544	x	0.840
P. pinnatifida	0.441	0.581	x

Table 8. Niche identity indexes calculated for America.

D\I	*P. omphalodes*	*P. pinnatifida*
P. omphalodes	x	0.968
P. pinnatifida	0.821	x

Table 9. Niche identity indexes calculated for Eurasia.

D\I	*P. discordans*	*P. omphalodes*	*P. pinnatifida*
P. discordans	x	0.828	0.729
P. omphalodes	0.587	x	0.820
P. pinnatifida	0.468	0.564	x

OTU S05 and an unnamed lineage SUn1). These results show that, despite the species from *P. omphalodes* group differing in associated photobiont species, they exhibit similar niche preferece.

PCA (Figure 10) results showed that *P. omphalodes* is characterised by the highest bioclimatic variation in comparison with other species from the *P. omphalodes* group. On the other hand, the ENM method has shown that the potential distribution of *P. omphalodes* is wider than its known current occurrence range (Figures 4, 6–8). The absence of this taxon in the potential niches may be caused by the lack of suitable photobiont species in those areas or that the model did not capture the relevant variation and so overestimates the niche. Two *Trebouxia* lineages are found in this species, i.e. OTU S05 and an unnamed lineage. Such flexibility in the photobiont choice may facilitate the mycobiont colonisation of new niches; however, some of those photobionts may be relatively rare. *Trebouxia* OTU S05, which corresponds to the generalist *Trebouxia suecica*, was previously reported from numerous terricolous and corticolous species in temperate, boreal and alpine climates, while the unnamed lineage of *Trebouxia* (SUn1, Table 10), present in three specimens, probably also occurs in selected terricolous and corticolous species (Table 10). Probably the latter is characterised by narrower ecological amplitude, but it needs further studies. On the other hand, *P. pinnatifida* forms associations with three *Trebouxia* lineages, i.e. OTUs S02 and S04 and an unnamed lineage (SUn2, Table 10). Most photobiont sequences from *P. pinnatifida* were grouped in OTU S02 clade. They were collected from different localities in Poland (Beskidy Mts, Sudety Mts, Stołowe Mts), Norway and Sweden. Moreover, the same *Trebouxia* OTU S02 was found in terricolous, saxicolous and corticolous lichens (e.g. Leavitt et al. 2015). It suggests that *Trebouxia* OTU S02 has a broad ecological amplitude and worldwide distribution. Therefore *P. pinnatifida* may also have wider geographical distribution than current data suggest. The absence of those species in some localities may be caused by the lack of unambiguous morphological and chemi-

Table 10. *Trebouxia* OTUs associating with species from *P. omphalodes* group with the information about their distribution, substrata preferences and references.

OTUs	Distribution	Substrata	References
S02	Antarctica, Austria, Canada, Chile, Germany, Greenland, Iceland, Morocco, Norway, Poland, Portugal, Russia, Slovakia, Spain, Sweden, UK, USA	corticolous, saxicolous and terricolous	Muggia et al. 2014, Leavitt et al. 2015, Singh et al. 2017, this study
S04	Canada, Estonia, Germany, Netherlands, Poland, Sweden, Turkey, USA	corticolous and saxicolous	Leavitt et al. 2015, this study
S05	Canada, Finland, Italy, Norway, Spain, Sweden, Turkey, USA	corticolous, saxicolous and terricolous	Blaha et al. 2006, Muggia et al. 2014, Leavitt et al. 2015, Singh et al. 2017, Dal Grande et al. 2018, Paul et al. 2018, this study
SUn1	Canada, Finland, Spain, Sweden	corticolous and terricolous	Opanowicz and Grube 2004, Piercey-Normore 2009, Lindgren et al. 2014, Onuț-Brännström et al. 2018, this study
SUn2	Canada, Norway, Russia, Sweden	corticolous and terricolous	Piercey-Normore 2009, Domaschke et al. 2012, Lindgren et al. 2014, this study

cal features necessary for their identification. For this reason, herbarium material from the group *P. omphalodes* requires re-determination. On the other hand, the possible overestimation of the MaxEnt models may be due to additional, ecological factors (e.g. interaction with other organisms) which were not included in our analyses, but limit the distribution of the studied lichens.

Key to *Parmelia species* from the non-vegetative propagules group

1 Pseudocyphellae marginal **2**
– Pseudocyphellae marginal and laminal (at least in older parts of thalli) **3**
2 Salazinic acid present ..... ***P. pinnatifida***
– Protocetraric acid present ..... ***P. discordans*** **(young thalli, rare)**
3 Lobes 0.5–2 mm long and 1–2 mm wide, laminal pseudocyphellae predominantly connected with marginal pseudocyphellae, very few pseudocyphellae not starting from the lobe edges ..... ***P. pinnatifida***
– Lobes 1–4 mm long and 1–3 mm wide, laminal pseudocyphellae predominantly not connected to the lobe margins **4**
4 Protocetraric present ..... ***P. discordans***
– Salazinic acid present ..... ***P. omphalodes***

Acknowledgements

We are grateful to the curators of all herbaria for the loan of specimens and reviewers for their helpful comments, Agnieszka Jabłońska and Magdalena Kosecka for help with molecular study, Paulina Dygner for help with TLC study and Andrzej Szczepański for help during field research. The research was supported by the Ministry of Science and Higher Education, project no. 2012/07/N/NZ8/00061 and BW/538-L150-B257-16 from the University of Gdansk, granted to EO.

References

Akaike H (1973) Information theory and an extension of the maximum likelihood principle. In: Petrov BN, Csaki F (Eds) Proceedings of the 2nd International Symposium on Information Theory. Akademiai Kiado, Budapest, 267–281.

Altermann S (2009) Geographic Structure in a Symbiotic Mutualism. University of California, Santa Cruz.

Altschul SF, Madden TL, Schäffer AA, Zhang J, Zhang Z, Miller W, Lipman J (1997) Gapped BLAST and PSI-BLAST: a new generation of protein database search programs. Nucleic Acids Research 25: 3389–3402. https://doi.org/10.1093/nar/25.17.3389

Barve N, Barve V, Jimenez-Valverde A, Lira-Noriega A, Maher SP, Peterson AT, Soberóna J, Villalobos F (2011) The crucial role of the accessible area in ecological niche modeling and species distribution modeling. Ecological Modelling 222: 1810–1819. https://doi.org/10.1016/j.ecolmodel.2011.02.011

Beck A (2002) Morphological variation, photobiont association and ITS phylogeny of *Chaenotheca phaeocephala* and *C. subroscida* (Coniocybaceae, lichenized ascomycetes). Nordic Journal of Botany 21: 651–660. https://doi.org/10.1111/j.1756-1051.2001.tb00824.x

Beck A, Friedl T, Rambold G (1998) Selectivity of photobiont choice in a defined lichen community: inferences from cultural and molecular studies. New Phytologist 139: 709–720. https://doi.org/10.1046/j.1469-8137.1998.00231.x

Beck A, Kasalicky T, Rambold G (2002) Myco-photobiontal selection in a Mediterranean cryptogam community with *Fulgensia fulgida*. New Phytologist 153: 317–326. https://doi.org/10.1046/j.0028-646X.2001.00315.x

Blaha J, Baloch E, Grube M (2006) High photobiont diversity associated with the euryoecious lichen-forming ascomycete *Lecanora rupicola* (Lecanoraceae, Ascomycota). Biological Journal Linnean Society London 88(2): 283–293. https://doi.org/10.1111/j.1095-8312.2006.00640.x

Büdel B, Scheidegger C (2008) Thallus morphology and anatomy. In: Nash TH (Ed.) Lichen Biology (2nd ed.). Cambridge University Press, Cambridge, 40–68. https://doi.org/10.1017/CBO9780511790478.005

Cao S, Zhang F, Liu C, Hao Z, Tian Y, Zhu L, Zhou Q (2015) Distribution patterns of haplotypes for symbionts from *Umbilicaria esculenta* and *U. muehlenbergii* reflect the importance of reproductive strategy in shaping population genetic structure. BMC Microbiology 15: 1–212. https://doi.org/10.1186/s12866-015-0527-0

Calvelo S, Liberatore S (2002) Catálogo de los líquenes de la Argentina. Kurtziana 29(2): 7–170.

Castresana J (2000) Selection of conserved blocks from multiple alignments for their use in phylogenetic analysis. Molecular Biology and Evolution 17(4): 540–552. https://doi.org/10.1093/oxfordjournals.molbev.a026334

Clement M, Snell Q, Walker P, Posada D, Crandall K (2002) TCS: Estimating gene genealogies. Parallel and Distributed Processing Symposium, International Proceedings 2: 1–184. https://doi.org/10.1109/IPDPS.2002.1016585

Corsie EI, Harrold P, Yahr R (2019) No combination of morphological, ecological or chemical characters can reliably diagnose species in the *Parmelia saxatilis* aggregate in Scotland. Lichenologist 51: 107–121. https://doi.org/10.1017/S0024282919000069

Crespo A, Lumbsch HT (2010) Cryptic species in lichen-forming fungi. IMA Fungus 1: 167–170. https://doi.org/10.5598/imafungus.2010.01.02.09

Crespo A, Molina MC, Blanco O, Schroeter B, Sancho LG, Hawksworth DL (2002) rDNA ITS and β-tubulin gene sequence analyses reveal two monophyletic groups within the cosmopolitan lichen *Parmelia saxatilis*. Mycological Research 106: 788–795. https://doi.org/10.1017/S095375620200610X

Dal Grande F, Rolshausen G, Divakar PK, Crespo A, Otte J, Schleuning M, Schmitt I (2018) Environment and host identity structure communities of green algal symbionts in lichens. New Phytologist 217: 277–289. https://doi.org/10.1111/nph.14770

del Campo EM, Hoyo A del, Casano LM, Martínez-Alberola F, Barreno E (2010) A rapid and cost-efficient DMSO-based method for isolating DNA from cultured lichen photobionts. Taxon 59: 588–591. https://doi.org/10.1002/tax.592023

Deduke C, Piercey-Normore MD (2015) Substratum preference of two species of *Xanthoparmelia*. Fungal Biology 119: 812–822. https://doi.org/10.1016/j.funbio.2015.05.005

Diederich P, Sérusiaux E (2000) The Lichens and Lichenicolous Fungi of Belgium and Luxembourg. An annotated checklist. Musée National d'Histoire, Luxembourg.

Divakar PK, Molina MC, Lumbsch HT, Crespo A (2005) *Parmelia barrenoae*, a new lichen species related to *Parmelia sulcata* (Parmeliaceae) based on molecular and morphological data. Lichenologist 37: 37–46. https://doi.org/10.1017/S0024282904014641

Divakar PK, Leavitt SD, Molina MC, Del-Prado R, Lumbsch HT, Crespo, A (2016[2015]) A DNA barcoding approach for identification of hidden diversity in Parmeliaceae (Ascomycota): *Parmelia* sensu stricto as a case study. Botanical Journal of the Linnean Society 180: 21–29. https://doi.org/10.1111/boj.12358

Doering M, Piercey-Normore MD (2009) Genetically divergent algae shape an epiphytic lichen community on Jack Pine in Manitoba. Lichenologist 41: 69–80. https://doi.org/10.1017/S0024282909008111

Domaschke S, Fernández-Mendoza F, Garcia M, Martín M, Printzen C (2012) Low genetic diversity in Antarctic populations of the lichen-forming ascomycete *Cetraria aculeata* and its photobiont. Polar Research 31: 1–13. https://doi.org/10.3402/polar.v31i0.17353

Duque-Lazo J, van Gils H, Groen TA, Navarro-Cerrillo RM (2016) Transferability of species distribution models: The case of *Phytophthora cinnamomi* in Southwest Spain and Southwest Australia. Ecological Modelling 320: 62–70. https://doi.org/10.1016/j.ecolmodel.2015.09.019

Edgar RC (2004) MUSCLE: multiple sequence alignment with high accuracy and high throughput. Nucleic Acids Research 32: 1792–1797. https://doi.org/10.1093/nar/gkh340

Elith J, Graham CH, Anderson RP, Dudik M, Ferrier S, Guisan A, Hijmans RJ, Huettmann F, Leathwick JR, Lehmann A, Li J, Lohmann LG, Loiselle BA, Manion G, Moritz C, Nakamura M, Nakazawa Y, Overton JM, Peterson AT, Phillips SJ, Richardson K, Scachetti-Pereira R, Schapire RE, Soberon J, Williams S, Wisz M, Zimmermann NE (2006) Novel methods improve prediction of species' distributions from occurrence data. Ecography 29(2): 129–151. https://doi.org/10.1111/j.2006.0906-7590.04596.x

Esslinger TL (2015) A cumulative checklist for the lichen-forming, lichenicolous and allied fungi of the continental United States and Canada. Opuscula Philolichenum 15: 136–390.

Evangelista PH, Kumar S, Stohlgren TJ, Jarnevich CS, Crall AW, Norman III JB, Barnett DT (2008) Modelling invasion for a habitat generalist and a specialist plant species. Diversity and Distributions 14: 808–817. https://doi.org/10.1111/j.1472-4642.2008.00486.x

Feuerer T, Thell A (2002) *Parmelia ernstiae* – a new macrolichen from Germany. Mitteilungen des Instituts für Allgemeine Botanik, Hamburg 30–32: 49–60.

Friedl T (1989) Systematik und Biologie von *Trebouxia* (Microthamniales, Chlorophyta) als Phycobiont der Parmeliaceae (lichenisierte Ascomyceten). Universität Bayreuth, Bayreuth.

Friedl T, Rokitta C (1997) Species relationships in the lichen alga *Trebouxia* (Chlorophyta, Trebouxiophyceae): molecular phylogenetic analyses of nuclear-encoded large subunit rRNA gene sequences. Symbiosis 23: 125–148.

Friedl T, Besendahl A, Pfeiffer P, Bhattacharya D (2000) The distribution of group I introns in lichen algae suggests that lichenization facilitates intron lateral transfer. Molecular Phylogenetics and Evolution 14: 342–352. https://doi.org/10.1006/mpev.1999.0711

Galtier N, Gouy M, Gautier C (1996) SeaView and Phylo_win: two graphic tools for sequence alignment and molecular phylogeny. Computer applications in the biosciences 12: 543–548. https://doi.org/10.1093/bioinformatics/12.6.543

Gardes M, Bruns TD (1993) ITS primers with enhanced specificity for basidiomycetes-application to the identification of mycorrhizae and rust. Molecular Ecology 2: 113–118. https://doi.org/10.1111/j.1365-294X.1993.tb00005.x

Gouy M, Guindon S, Gascuel O (2010) SeaView version 4: a multiplatform graphical user interface for sequence alignment and phylogenetic tree building. Molecular Biology and Evolution 27: 221–224. https://doi.org/10.1093/molbev/msp259

Guttová A, Lackovičová A, Pišút I (2013) Revised and updated checklist of lichens of Slovakia. Biologia 68: 845–850. https://doi.org/10.2478/s11756-013-0218-y

Guzow-Krzemińska B (2006) Photobiont flexibility in the lichen *Protoparmeliopsis muralis* as revealed by ITS rDNA analyses. Lichenologist 38(5): 469–476. https://doi.org/10.1017/S0024282906005068

Hafellner J (1995) A new checklist of lichens and lichenicolous fungi of insular Laurimacaronesia including a lichenological bibliography for the area. Fritschiana 5: 1–132.

Hale ME (1987) A monograph of the lichen genus *Parmelia* Acharius sensu stricto (Ascomycotina: Parmeliaceae). Smithsonian Contributions to Botany 66: 1–55. https://doi.org/10.5479/si.0081024X.66

Hammer Ø, Harper DAT, Ryan PD (2001) PAST: Paleontological statistics software package for education and data analysis. Palaeontologia Electronica 4(1): 1–9.

Haugan R, Timdal E (2019) The morphologically cryptic lichen species *Parmelia ernstiae* and *P. serrana* new to Norway. Graphis Scripta 31: 5–13.

Hawksworth DL, Blanco O, Divakar PK, Ahti T, Crespo A (2008) A first checklist of parmelioid and similar lichens in Europe and some adjacent territories, adopting revised generic circumscriptions and with indications of species distributions. Lichenologist 40: 1–21. https://doi.org/10.1017/S0024282908007329

Hawksworth DL, Divakar PK, Crespo A, Ahti T (2011) The checklist of parmelioid and similar lichens in Europe and some adjacent territories: additions and corrections. Lichenologist 43: 639–645. https://doi.org/10.1017/S0024282911000454

Heibl C, Calenge C (2015) Phyloclim: integrating phylogenetics and climatic niche modeling package version 0.9-4. https://cran.r-project.org/web/packages/phyloclim/phyloclim.pdf

Helms G (2003) Taxonomy and Symbiosis in Associations of Physciaceae and *Trebouxia*. Inauguraldissertation am Albrecht-von-Haller Institut für Pflanzenwissenschaften, Experimentelle Phykologie und Sammlung von Algenkulturen der Georg-August-Universität Göttingen, Göttingen, 156 pp.

Helms G, Friedl T, Rambold G, Mayrhofer H (2001) Identification of photobionts from the lichen family *Physciacea* using algal-specific ITS rDNA sequencing. Lichenologist 33: 73–86. https://doi.org/10.1006/lich.2000.0298

Hernandez PA, Graham CH, Master LL, Albert DL (2006) The effect of sample size and species characteristics on performance of different species distribution modeling methods. Ecography 29: 773–785. https://doi.org/10.1111/j.0906-7590.2006.04700.x

Hijmans RJ, Cameron SE, Parra JL, Jones PG, Jarvis A (2005) Very high resolution interpolated climate surfaces for global land areas. International Journal of Climatology 25: 1965–1978. https://doi.org/10.1002/joc.1276

Hosmer DW, Lemeshow S (2000) Applied Logistic Regression. John Wiley and Sons, New York, 397 pp. https://doi.org/10.1002/0471722146

Huelsenbeck JP, Ronquist F (2001) MRBAYES: Bayesian inference of phylogenetic trees. Bioinformatics 17: 754–755. https://doi.org/10.1093/bioinformatics/17.8.754

Katoh K, Misawa K, Kuma K., Miyata T (2002) MAFFT: a novel method for rapid multiple sequence alignment based on fast Fourier transform. Nucleic Acids Research 30: 3059–3066. https://doi.org/10.1093/nar/gkf436

Knežević B, Mayrhofer H (2009) Catalogue of the lichenized and lichenicolous fungi of Montenegro. Phyton (Horn, Austria) 48: 283–328.

Kroken S, Taylor JW (2000) Phylogenetic species, reproductive mode, and specificity of the green alga *Trebouxia* forming lichens with the fungal genus *Letharia*. Bryologist 103: 645–660. https://doi.org/10.1639/0007-2745(2000)103[0645:PSRMAS]2.0.CO;2

Kurokawa S (1976) A note on *Parmelia omphalodes* and its related species. Journal of Japanese Botany 51: 377–380.

Lanfear R, Calcott B, Ho SY, Guindon S (2012) PartitionFinder: combined selection of partitioning schemes and substitution models for phylogenetic analyses. Molecular Biology and Evolution 29(6): 1695–1701. https://doi.org/10.1093/molbev/mss020

Lanfear R, Frandsen PB, Wright AM, Senfeld T, Calcott B (2016) PartitionFinder 2: new methods for selecting partitioned models of evolution for molecular and morphological phylogenetic analyses. Molecular Biology and Evolution 34(3): 772–773. https://doi.org/10.1093/molbev/msw260

Leavitt SD, Johnson LA, Goward T, St Clair LL (2011) Species delimitation in taxonomically difficult lichen-forming fungi: an example from morphologically and chemically diverse *Xanthoparmelia* (Parmeliaceae) in North America. Molecular Phylogenetics and Evolution 60: 317–332. https://doi.org/10.1016/j.ympev.2011.05.012

Leavitt SD, Lumbsch HT, Stenroos S, St Clair LL (2013a) Pleistocene speciation in North American lichenized fungi and the impact of alternative species circumscriptions and rates

of molecular evolution on divergence estimates. PLoS ONE 8(12): e85240. https://doi.org/10.1371/journal.pone.0085240

Leavitt SD, Nelsen MP, Lumbsch HT, Johnson LA, St Clair LL (2013b) Symbiont flexibility in subalpine rock shield lichen communities in the Southwestern USA. Bryologist 116: 149–161. https://doi.org/10.1639/0007-2745-116.2.149

Leavitt SD, Esslinger TL, Hansen ES, Divakar PK, Crespo A, Loomis BF, Lumbsch HT (2014) DNA barcoding of brown *Parmeliae* (Parmeliaceae) species: a molecular approach for accurate specimen identification, emphasizing species in Greenland. Organisms Diversity and Evolution 14: 11–20. https://doi.org/10.1007/s13127-013-0147-1

Leavitt SD, Kraichak E, Nelsen MP, Altermann S, Divakar PK, Alors D, Esslinger TL, Crespo A, Lumbsch HT (2015) Fungal specificity and selectivity for algae play a major role in determining lichen partnerships across diverse ecogeographic regions in the lichen-forming family Parmeliaceae (Ascomycota). Molecular Ecology 24: 3779–3797. https://doi.org/10.1111/mec.13271

Lindgren H, Velmala S, Högnabba F, Goward T, Holien H, Myllys L (2014) High fungal selectivity for algal symbionts in the genus *Bryoria*. Lichenologist 46: 681–695. https://doi.org/10.1017/S0024282914000279

Lutsak T, Fernández-Mendoza F, Nadyeina O, Şenkardeşler A, Printzen C (2017) Testing the correlation between norstictic acid content and species evolution in the *Cetraria aculeata* group in Europe. Lichenologist 49: 39–56.https://doi.org/10.1017/S0024282916000566

Miller MA, Pfeiffer W, Schwartz T (2010) Creating the CIPRES Science Gateway for Inference of Large Phylogenetic Trees. Proceedings of the Gateway Computing Environments Workshop (GCE), 14 November, 2010, New Orleans, 8 pp. https://doi.org/10.1109/GCE.2010.5676129

Molina MC, Crespo A, Blanco O, Lumbsch HT, Hawksworth DL (2004) Phylogenetic relationships and species concepts in *Parmelia* s. str. (Parmeliaceae) inferred from nuclear ITS rDNA and β-tubulin sequences. Lichenologist 36: 37–54. https://doi.org/10.1017/S0024282904013933

Molina MC, Del-Prado R, Divakar PK, Sanchez-Mata D, Crespo A (2011) Another example of cryptic diversity in lichen-forming fungi: the new species *Parmelia mayi* (Ascomycota: Parmeliaceae). Organisms Diversity and Evolution 11: 331–342. https://doi.org/10.1007/s13127-011-0060-4

Molina MC, Divakar PK, Goward T, Millanes AM, Lumbsch HT, Crespo A (2017) Neogene diversification in the temperate lichen-forming fungal genus *Parmelia* (Parmeliaceae, Ascomycota). Systematics and Biodiversity 15: 166–181. https://doi.org/10.1080/14772000.2016.1226977

Molins A, Moya P, García-Breijo FJ, Reig-Armiñana J, Barreno E (2018) Molecular and morphological diversity of *Trebouxia* microalgae in sphaerothallioid *Circinaria* spp. lichens. Journal of Phycology 54: 494–504. https://doi.org/10.1111/jpy.12751

Muggia L, Vancurova L, Škaloud P, Peksa O, Wedin M, Grube M (2013) The symbiotic playground of lichen thalli – a highly flexible photobiont association in rock-inhabiting lichens. FEMS Microbiology Ecology 85: 313–323. https://doi.org/10.1111/1574-6941.12120

Muggia L, Pérez-Ortega S, Kopun T, Zellnig G, Grube M (2014) Photobiont selectivity leads to ecological tolerance and evolutionary divergence in a polymorphic complex of lichenized fungi. Annals of Botany 114: 463–75. https://doi.org/10.1093/aob/mcu146

Nash TH (2008) Lichen Biology (2nd edn). Cambridge University Press, Cambridge, 486 pp.

Nelsen M, Gargas A (2008) Dissociation and horizontal transmission of codispersing lichen symbionts in the genus *Lepraria* (Lecanorales: Stereocaulaceae). New Phytologist 177: 264–275. https://doi.org/10.1111/j.1469-8137.2007.02241.x

Nylander JAA (2004) MrModeltest v2. Program distributed by the author. Evolutionary Biology Centre, Uppsala University, Uppsala.

Ohmura Y, Kawachi M, Kasai F, Watanabe MM, Takeshita S (2006) Genetic combinations of symbionts in a vegetatively reproducing lichen, *Parmotrema tinctorum*, based on ITS rDNA sequences. Bryologist 109: 43–59. https://doi.org/10.1639/0007-2745(2006)109[0043:GCOSIA]2.0.CO;2

Ohmura Y, Takeshita S, Kawachi M (2018) Photobiont diversity within populations of a vegetatively reproducing lichen, *Parmotrema tinctorum*, can be generated by photobiont switching. Symbiosis 77: 59–72. https://doi.org/10.1007/s13199-018-0572-1

Okonechnikov K, Golosova O, Fursov M, UGENE team (2012) Unipro GENE: a unified bioinformatics toolkit. Bioinformatics 28: 1166–1167. https://doi.org/10.1093/bioinformatics/bts091

Onuț-Brännström I, Benjamin M, Scofield DG, Heiðmarsson S, Andersson MGI, Lindström ES, Johannesson H (2018) Sharing of photobionts in sympatric populations of *Thamnolia* and *Cetraria* lichens: evidence from high-throughput sequencing. Scientific Reports 8: 4406. https://doi.org/10.1038/s41598-018-22470-y

Opanowicz M, Grube M (2004) Photobiont genetic variation in *Flavocetraria nivalis* from Poland (Parmeliaceae, lichenized Ascomycota). Lichenologist 36: 125–131. https://doi.org/10.1017/S0024282904013763

Orange A, James PW, White FJ (2001) Microchemical Methods for the Identification of Lichens. British Lichen Society, London, 101 pp.

Oset M (2014) The lichen genus *Stereocaulon* (Schreb.) Hoffm. in Poland – a taxonomic and ecological study. Monographiae Botanicae 104: 1–81. https://doi.org/10.5586/mb.2014.001

Ossowska E, Bohdan A, Szymczyk R, Kukwa M (2014) The lichen family Parmeliaceae in Poland. III. *Parmelia serrana*, new to Poland. Acta Societatis Botanicorum Poloniae 83: 81–84. https://doi.org/10.5586/asbp.2014.006

Ossowska E, Kukwa M (2016) *Parmelia barrenoae* and *P. pinnatifida*, two lichen species new to Poland. Herzogia 29: 198–203. https://doi.org/10.13158/heia.29.1.2016.198

Ossowska E, Guzow-Krzemińska B, Dudek M, Oset M, Kukwa M (2018) Evaluation of diagnostic chemical and morphological characters in five *Parmelia* species (Parmeliaceae, lichenized Ascomycota) with special emphasis on the thallus pruinosity. Phytotaxa 383: 165–180. https://doi.org/10.11646/phytotaxa.383.2.3

Paul F, Otte J, Schmitt I, Dal Grande F (2018) Comparing Sanger sequencing and high-throughput metabarcoding for inferring photobiont diversity in lichens. Scientific Reports 8(1): 8624. https://doi.org/10.1038/s41598-018-26947-8

Peksa O, Škaloud P (2011) Do photobionts influence the ecology of lichens? A case study of environmental preferences in symbiotic green alga *Asterochloris* (Trebouxiophyceae). Molecular Ecology 20: 3936–3948. https://doi.org/10.1111/j.1365-294X.2011.05168.x

Phillips SJ, Dudík M, Schapire RE (2004) A maximum entropy approach to species distribution modeling. ICML '04 Proceedings of the twenty-first international conference on Machine learning. ACM, New York, 655–662. https://doi.org/10.1145/1015330.1015412

Phillips SJ, Anderson R, Schapire RE (2006) Maximum entropy modeling of species geographic distributions. Ecological Modelling 190: 231–259. https://doi.org/10.1016/j.ecolmodel.2005.03.026

Piercey-Normore MD (2009) Vegetatively reproducing fungi in three genera of the *Parmeliaceae* show divergent algal partners. Bryologist 112: 773–785. https://doi.org/10.1639/0007-2745-112.4.773

Pietras M, Kolanowska M (2019) Predicted potential occurrence of the North American false truffle *Rhizopogon salebrosus* in Europe. Fungal Ecology 39: 225–230. https://doi.org/10.1016/j.funeco.2018.12.002

Pino-Bodas R, Martin MP, Burgaz AR, Lumbsch HT (2013) Species delimitation in *Cladonia* (Ascomycota): a challenge to the DNA barcoding philosophy. Molecular Ecology Resources 13: 1058–1068. https://doi.org/10.1111/1755-0998.12086

Rambaut A (2012) FigTree v1.4.2. http://tree.bio.ed.ac.uk/software/figtree/

Rambaut A, Drummond AJ (2007) Tracer v1.6. http://beast.bio.ed.ac.uk/

Rikkinen J, Oksanen I, Lohtander K (2002) Lichen guilds share related cyanobacterial symbionts. Science 297: 1–357. https://doi.org/10.1126/science.1072961

Romeike J, Friedl T, Helms G, Ott S (2002) Genetic diversity of algal and fungal partners in four species of *Umbilicaria* (Lichenized Ascomycetes) along a transect of the Antarctic Peninsula. Molecular Biology and Evolution 19: 1209–1217. https://doi.org/10.1093/oxfordjournals.molbev.a004181

Ronquist H, Huelsenbeck JP (2003) MrBayes 3: Bayesian phylogenetic inference under mixed models. Bioinformatics 19: 1572–1574. https://doi.org/10.1093/bioinformatics/btg180

Ruprecht U, Brunauer G, Printzen C (2012) Genetic diversity of photobionts in Antarctic lecideoid lichens from an ecological view point. Lichenologist 44: 661–678. https://doi.org/10.1017/S0024282912000291

Sanders WB, Lücking R (2002) Reproductive strategies, relichenization and thallus development observed in situ in leaf-dwelling lichen communities. New Phytologist 155: 425–435. https://doi.org/10.1046/j.1469-8137.2002.00472.x

Schoch CL, Seifert KA, Huhndorf S, Robert V, Spouge JL, Levesque CA, Chen W, Fungal Barcoding Consortium (2012) Nuclear ribosomal internal transcribed spacer (ITS) region as a universal DNA barcode marker for Fungi. Proceedings of the National Academy of Sciences of the United States of America 109: 6241–6246. https://doi.org/10.1073/pnas.1117018109

Schoener TW (1968) The anolis lizards of bimini: Resource partitioning in a complex fauna. Ecology 49: 704–726. https://doi.org/10.2307/1935534

Seaward MRD (2010) Census catalogue of Irish Lichens (3rd edn.). National Museums Northern Ireland, Belfast, 64 pp.

Seifried J (2009) Genetische Diversität in beringischen und extraberingischen arktischen Populationen der Strauchflechte *Cetraria aculeata*. Thesis, Goethe-Universität, Frankfurt am Main.

Singh G, Dal Grande F, Divakar PK, Otte J, Crespo A, Schmitt I (2017) Fungal-algal association patterns in lichen symbiosis linked to macroclimate. New Phytologist 214: 317–329. https://doi.org/10.1111/nph.14366

Skult H (1984) The *Parmelia omphalodes* (Ascomycetes) complex in the Eastern Fennoscandia. Chemical and morphological variation. Annales Botanici Fennici 21: 117–142.

Spribille T, Tuovinen V, Resl P, Vanderpool D, Wolinski H, Aime MC, Schneider K, Stabentheiner E, Toome-Heller M, Thor G, Mayrhofer H, Johannesson H, McCutcheon JP (2016) Basidiomycete yeasts in the cortex of ascomycete macrolichens. Science 353: 488–492. https://doi.org/10.1126/science.aaf8287

Stamatakis A (2014) RAxML Version 8: A tool for Phylogenetic Analysis and Post-Analysis of Large Phylogenies. Bioinformatics 30(9): 1312–1313. https://doi.org/10.1093/bioinformatics/btu033

Thell A, Feuerer T, Karnefelt L, Myllys L, Stenroos S (2004) Monophyletic groups within the Parmeliaceae identified by ITS rDNA, β-tubulin and GAPDH sequences. Mycological Progress 3(4): 297–314. https://doi.org/10.1007/s11557-006-0100-1

Thell A, Elix JA, Feuerer T, Hansen ES, Karnefelt I, Schuler N, Westberg M (2008) Notes on the systematics, chemistry and distribution of European *Parmelia* and *Punctelia* species (lichenized ascomycetes). Sauteria 15: 545–559.

Thell A, Thor G, Ahti T (2011) *Parmelia* Ach. In: Thell A, Moberg R (Eds) Nordic Lichen Flora. Nordic Lichen Society, 83–90.

Thell A, Crespo A, Divakar PK, Karnefelt I, Leavitt SD, Lumbsch HT, Seaward MRD (2012) A review of the lichen family Parmeliaceae – history, phylogeny and current taxonomy. Nordic Journal of Botany 30: 64–664. https://doi.org/10.1111/j.1756-1051.2012.00008.x

Thell A, Tsurykau A, Persson PE, Hansson M, Åsegård E, Kärnefelt I, Seaward MRD (2017) *Parmelia ernstiae*, *P. serrana* and *P. submontana*, three species increasing in the Nordic countries. Graphis Scripta 29: 24–32.

Warren DL, Glor RE, Turelli M (2008) Environmental niche equivalency versus conservatism: Quantitative approaches to niche evolution. Evolution 62: 2868–2883. https://doi.org/10.1111/j.1558-5646.2008.00482.x

Warren DL, Glor RE, Turelli M (2010) ENMTools: a toolbox for comparative studies of environmental niche models. Ecography 33: 607–611. https://doi.org/10.1111/j.1600-0587.2009.06142.x

White TJ, Bruns T, Lee S, Taylor J (1990) Amplification and direct sequencing of fungal ribosomal RNA genes for phylogenetics. In: Innis MA, Gelfand DH, Sninsky JJ, White TJ (Eds) PCR Protocols: a Guide to Methods and Applications Academic Press, New York, 315–322. https://doi.org/10.1016/B978-0-12-372180-8.50042-1

Wornik S, Grube M (2010) Joint Dispersal Does Not Imply Maintenance of Partnerships in Lichen Symbioses. Microbial Ecology 59: 150–157. https://doi.org/10.1007/s00248-009-9584-y

Yahr R, Vilgalys R, DePriest PT (2006) Geographic variation in algal partners of *Cladonia subtenuis* (Cladoniaceae) highlights the dynamic nature of a lichen symbiosis. New Phytologist 171: 847–860. https://doi.org/10.1111/j.1469-8137.2006.01792.x

Supplementary material 1

Table S1. Database of localities used in the analyses with the bioclimatic values for each record

Authors: Emilia Ossowska, Beata Guzow-Krzemińska, Marta Kolanowska, Katarzyna Szczepańska, Martin Kukwa

Data type: occurrence

Link: https://doi.org/10.3897/mycokeys.61.38175.suppl1

Supplementary material 2

Figure S2. PNO profiles created for *P. discordans* (A), *P. omphalodes* (B) and *P. pinnatifida* (C) in Northern Hemisphere

Authors: Emilia Ossowska, Beata Guzow-Krzemińska, Marta Kolanowska, Katarzyna Szczepańska, Martin Kukwa

Data type: multimedia

Link: https://doi.org/10.3897/mycokeys.61.38175.suppl2

Supplementary material 3

Figure S3. PNO profiles created for *P. discordans* (A), *P. omphalodes* (B) and *P. pinnatifida* (C) in Eurasia

Authors: Emilia Ossowska, Beata Guzow-Krzemińska, Marta Kolanowska, Katarzyna Szczepańska, Martin Kukwa

Data type: multimedia

Link: https://doi.org/10.3897/mycokeys.61.38175.suppl3

Supplementary material 4

Figure S4. PNO profiles created for *P. omphalodes* (A) and *P. pinnatifida* (B) in America

Authors: Emilia Ossowska, Beata Guzow-Krzemińska, Marta Kolanowska, Katarzyna Szczepańska, Martin Kukwa

Data type: multimedia

Link: https://doi.org/10.3897/mycokeys.61.38175.suppl3

MycoKeys 61: 75–89 (2019)
doi: 10.3897/mycokeys.61.46799
http://mycokeys.pensoft.net

RESEARCH ARTICLE

A peer-reviewed open-access journal
MycoKeys
Launched to accelerate biodiversity research

Two new species of *Fuscoporia* (Hymenochaetales, Basidiomycota) from southern China based on morphological characters and molecular evidence

Qian Chen[1,2], Yu-Cheng Dai[1,2]

1 *Beijing Advanced Innovation Center for Tree Breeding by Molecular Design, Beijing Forestry University, Beijing 100083, China* **2** *Institute of Microbiology, Beijing Forestry University, Beijing 100083, China*

Corresponding author: *Yu-Cheng Dai* (yuchengd@yahoo.com)

Academic editor: *Bao-Kai Cui* | Received 24 September 2019 | Accepted 20 November 2019 | Published 12 December 2019

Citation: Chen Q, Dai Y-C (2019) Two new species of *Fuscoporia* (Hymenochaetales, Basidiomycota) from southern China based on morphological characters and molecular evidence. MycoKeys 61: 75–89. https://doi.org/10.3897/mycokeys.61.46799

Abstract

Fuscoporia (Hymenochaetaceae) is characterized by annual to perennial, resupinate to pileate basidiocarps, a dimitic hyphal system, presence of hymenial setae, and hyaline, thin-walled, smooth basidiospores. Phylogenetic analyses based on the nLSU and a combined ITS, nLSU and RPB2 datasets of 18 species of *Fuscoporia* revealed two new lineages that are equated to two new species; *Fuscoporia ramulicola* **sp. nov.** grouped together with *F. ferrea*, *F. punctatiformis*, *F. subferrea* and *F. yunnanensis* with a strong support; *Fuscoporia acutimarginata* **sp. nov.** formed a strongly supported lineage distinct from other species. The individual morphological characters of the new species and their related species are discussed. A key to Chinese species of *Fuscoporia* is provided.

Keywords

Hymenochaetaceae, phylogeny, taxonomy, wood-rotting fungi

Introduction

Fuscoporia Murrill (1907) was established based on *F. ferruginosa* (Schrad.) Murrill. However, the genus has been unconsidered for a long time, reduced as a synonym of *Phellinus* Quél. (e.g., Overholts 1953; Ryvarden and Johansen 1980; Larsen and Cobb-Poulle 1990). Fiasson and Niemelä (1984) firstly used morphological features to segre-

gate some members of *Phellinus* into distinct taxonomic entities, including *Fomitiporia* Murrill, *Fulvifomes* Murrill, *Phellinus* Murrill, *Porodaedalea* Murrill and *Fuscoporia*.

Fiasson and Niemelä (1984) defined *Fuscoporia* by annual to perennial, resupinate to pileate basidiocarps, a dimitic hyphal system with generative hyphae in the dissepiment edge and the tube trama often encrusted with crystals, presence of hymenial setae and hyaline, thin-walled, smooth basidiospores. Later on, phylogenetic studies based on nuclear large subunit (nLSU) ribosomal RNA-based phylogeny confirmed that *Fuscoporia* formed a lineage distinct from *Phellinus* s. s. (Wagner and Fischer 2001, 2002). Previous studies on *Fuscoporia* were mostly based on morphological characteristics (Groposo et al. 2007; Baltazar et al. 2009; Baltazar and Gibertoni 2010; Raymundo et al. 2013) but, recently, more new taxa were described based on both molecular analyses and morphology (Niemelä et al. 2001; Jang et al. 2012; Pires et al. 2015; Chen and Yuan 2017; Chen et al. 2019).

In our study, phylogenetic analyses were carried out based on the nLSU and combined ITS, nLSU and RPB2 datasets including 99 (60 newly generated) sequences representing 18 species of *Fuscoporia*. From the analyses, two new species of *Fuscoporia* were found and described. In addition, a key to Chinese species in the genus was provided.

Materials and methods

Morphological studies

The studied specimens are deposited in the herbarium of the Institute of Microbiology, Beijing Forestry University (BJFC). Macro-morphological descriptions are based on field observations and notes and dry herbarium specimens. The microscopic analyses followed that described by Cui et al. (2019). Sections were studied at ultimate magnification ×1000 applying Nikon Eclipse 80i microscopy and phase contrast illumination. Drawings were made with the aid of a drawing tube. The measurements and drawings were made from slide preparations stained with Cotton Blue. In recording spore size variation, 5% of measurements were excluded from each end of the range and given in parentheses. The following abbreviations are used in the article: KOH = 5% potassium hydroxide, CB = Cotton Blue, CB- = acyanophilous, IKI = Melzer's reagent, IKI- = neither amyloid nor dextrinoid, L = mean spore length (arithmetic average of all spores), W = mean spore width (arithmetic average of all spores), Q = variation in the L/W ratios between specimens studied, and n (a/b) = number of spores (a) measured from given number of specimens (b). Special color terms are cited from Petersen (1996).

DNA extraction and sequencing

Extract total genomic DNA was extracted from dried specimens by CTAB rapid plant genome extraction kit (Aidlab Biotechnologies Co., Ltd., Beijing, China) according to the manufacturer's instructions with some modifications (Chen et al. 2016; Han et al. 2016).

To generate PCR amplicons, the following primer pairs were used: ITS4 and ITS5 (White et al. 1990) for the internal transcribed spacer (ITS), LR0R and LR7 (Vilgalys and Hester 1990) for nuclear large submit (nLSU) and bRPB2-6F and bRPB2-7.1R (Matheny 2005) for partial RNA polymerase II, second largest submit (RPB2). The PCR procedures followed Song and Cui (2017) and Zhu et al. (2019). DNA sequencing was performed at Beijing Genomics Institute and the sequences are deposited in GenBank and listed in Table 1.

Phylogenetic analyses

Sixty new sequences (nineteen ITS, seventeen nLSU and twenty-four RPB2) of *Fuscoporia* species were newly generated (Table 1). All sequences of ITS+nLSU+RPB2 analysis (Fig. 2) were shown in Table 1. Additional sequences of representatives genera of Hymenochaetaceae included in nLSU analysis (Fig. 1) were downloaded from GenBank to explore the phylogenetic relationships of *Fuscoporia*, which were used in the previous phylogenetic study (Zhou et al. 2016; Chen et al. 2019), thus not shown in Table 1. *Oxyporus corticola* (Fr.) Ryvarden, *Oxyporus populinus* (Schumach.) Donk, and *Hyphodontia pallidula* (Bres.) J. Erikss. were included as outgroups in nLSU analysis based on previous studies (Zhou et al. 2016; Chen et al. 2019). The outgroups selected for ITS+nLSU+RPB2 analysis were *Coniferiporia weirii* (Murrill) L.W. Zhou & Y.C. Dai and *Coniferiporia sulphurascens* (Pilát) L.W. Zhou & Y.C. Dai because *Coniferiporia* resulted as a sister group of *Fuscoporia* in previous studies (Fig. 1; Zhou et al. 2016; Chen and Yuan 2017; Chen et al. 2019).

Sequences were aligned with BioEdit (Hall 1999) and ClustalX (Thompson et al. 1997). Prior to phylogenetic analysis, ambiguous sequences at the start and the end were deleted and gaps were manually adjusted to optimize the alignment. Sequence alignment was deposited at TreeBase (http://purl.org/phylo/treebase; submission ID 22620). Phylogenetic analysis was carried out according to previous studies (Zhou 2015; Shen et al. 2019; Zhu et al. 2019). Maximum parsimony (MP), bayesian inference (BI) and maximum likelihood (ML) methods were employed to perform phylogenetic analysis of the two aligned datasets. MP analysis were performed using PAUP* 4.0b10 (Swofford 2002); BI was calculated with MrBayes3.1.2 (Ronquist and Huelsenbeck 2003); RAxML v.7.2.6 (Stamatakis 2006) was used for ML analysis. The three phylogenetic methods resulted in similar topologies for each dataset, and, thus, only the topology from the MP tree is presented along with statistical values from the ML/BI/MP algorithms (simultaneous MP/BI not less than 75 % and BPP not less than 0.9) at the nodes.

Results

The nLSU datasets included 23 representatives genera of Hymenochaetaceae and the combined ITS+nLSU+RPB2 datasets included 41 fungal specimens representing 20 species. In addition to sequences of new species, 14 new sequences of three species without published DNA sequences were uploaded – *F. punctatiformis* (Murrill) Zmitr., Malysheva & Spirin, *F. setifer* (T. Hatt.) Y.C. Dai and *F. yunnanensis* Y.C. Dai.

Table 1. Taxa and GenBank accession numbers for ITS, nLSU and RPB2 sequences used in the phylogenetic analyses (Fig. 2).

Species	Sample no.	Locality	GenBank accession no.		
			ITS	nLSU	RPB2
Fuscoporia acutimarginata	Dai 15137	China	**MH050751**	**MH050765**	**MN159384**
	Dai 16892	China	**MH050752**	**MH050766**	**MH079393**
	Dai 15115	China	**MN121764**	**MN121823**	**MN159385**
F. atlantica	SP 445618	Brazil	KP058515	KP058517	–
	SP 465829	Brazil	KP058514	KP058516	–
F. callimorpha	Dai 17388	Brazil	**MN121765**	**MN121824**	–
	Dai 17389	Brazil	**MN121766**	**MN121825**	–
F. contigua	Dai 16025	USA	MG008401	MG008454	**MH079406**
	JV 1204/22.6-J	USA	MG008403	MG008456	**MH079407**
	Dai 13567A	Romania	**MG008402**	**MG008455**	**MN159386**
F. ferrea	MUCL 45984	France	KX961112	KY189112	–
	Cui 11801	China	KX961101	KY189101	**MN159387**
	JV 1105/3-J	USA	**MH050760**	**MH050770**	**MH079392**
F. ferruginosa	JV 1309/4	Slovakia	KX961102	KY189102	**MH079405**
	JV 1507/11-CN	Europe	MG008400	MG008453	**MH079404**
F. gilva	Cui 11209	China	**MN121767**	**MN121826**	**MN159388**
	Dai 15681	China	**MN121768**	**MN121827**	**MN159389**
F. insolita	SP 5251	Russia	KJ677113	–	–
	SP 5208	Russia	**MN121769**	**MN121828**	–
F. punctatiformis	Doll#872	USA	**MH050753**	–	–
	Dai 17443	Brazil	**MH050755**	**MH050764**	–
F. ramulicola	Dai 15723	China	**MH050749**	**MH050762**	**MH079398**
	Dai 16155	China	**MH050750**	**MH050763**	**MH079399**
F. rufitincta	JV 1008/25	USA	KJ940029	KX058575	–
	JV 0904/142	USA	KJ940030	KX058574	–
F. senex	KUC 20110922-13	Korea	JX463658	JX463652	–
	MEL:2382630	Australia	KP012992	KP012992	–
F. setifer	Dai 15710	China	**MH050758**	**MH050767**	**MN159390**
	Dai 15706	China	**MH050759**	**MH050769**	**MN159391**
F. subferrea	Dai 16326	China	KX961097	KY053472	**MH079400**
	Dai 16327	China	KX961098	KY053473	**MH079401**
F. torulosa	JV 1405/2	Czech	KX961106	KY189106	**MN159392**
	JV 1312/19-Kout	Spain	KX961107	KY189107	**MN159393**
F. viticola	JV 0911/6	Czech	KX961110	KY189110	–
	He 2081	USA	**MN121770**	**MN121829**	–
F. wahlbergii	Dai 15636	China	MG008397	MG008450	**MH079402**
	Dai 15659	China	MG008398	MG008451	**MH079403**
F. yunnanensis	Cui 8182	China	**MH050756**	–	**MN159394**
	Dai 15637	China	**MH050757**	**MH050768**	**MN159395**
Coniferiporia sulphurascens	Cui 10429	China	KR350565	KR350555	–
C. weirii	CFS 504	Canada	AY829341	AY829345	–

Note: New sequences produced by this work are in bold.

The nLSU dataset had an aligned length of 1386 characters, of which 996 were constant, 96 were variable but parsimony-uninformative, and 294 were parsimony-informative. Maximum Parsimony (MP) analysis yielded four equally most parsimonious trees (TL = 1639, CI = 0.350, RI = 0.733, RC = 0.256, HI = 0.650). Bayesian

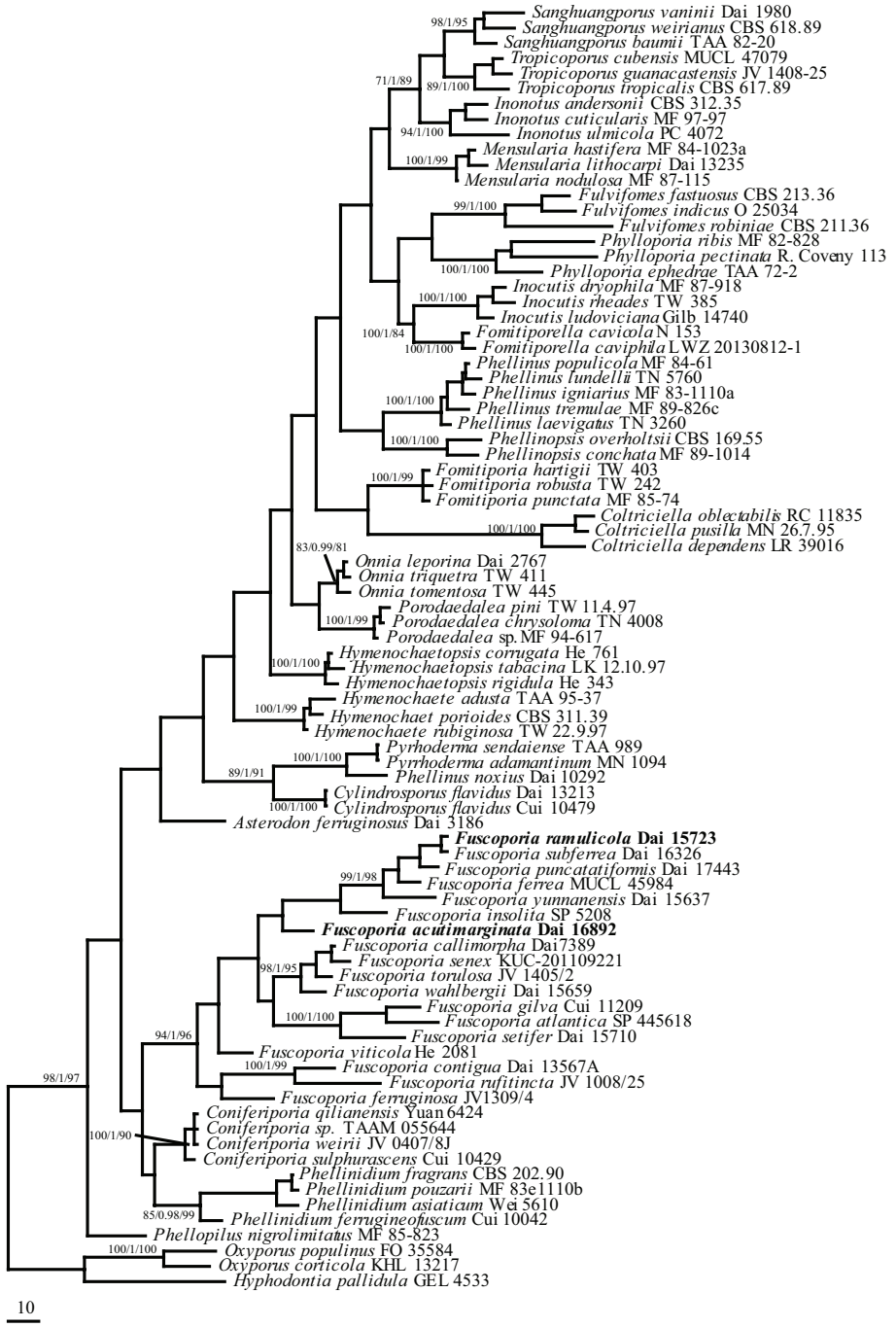

Figure 1. Phylogenetic positions of *Fuscoporia* and the new species within the Hymenochaetaceae inferred from the nLSU sequences. Topology is from MP tree and statistical values (MP/BI/ML) are indicated for each node that simultaneously received BS from ML and MP not below 75%, and BPP from BI not below 0.9. Names of new species are in bold.

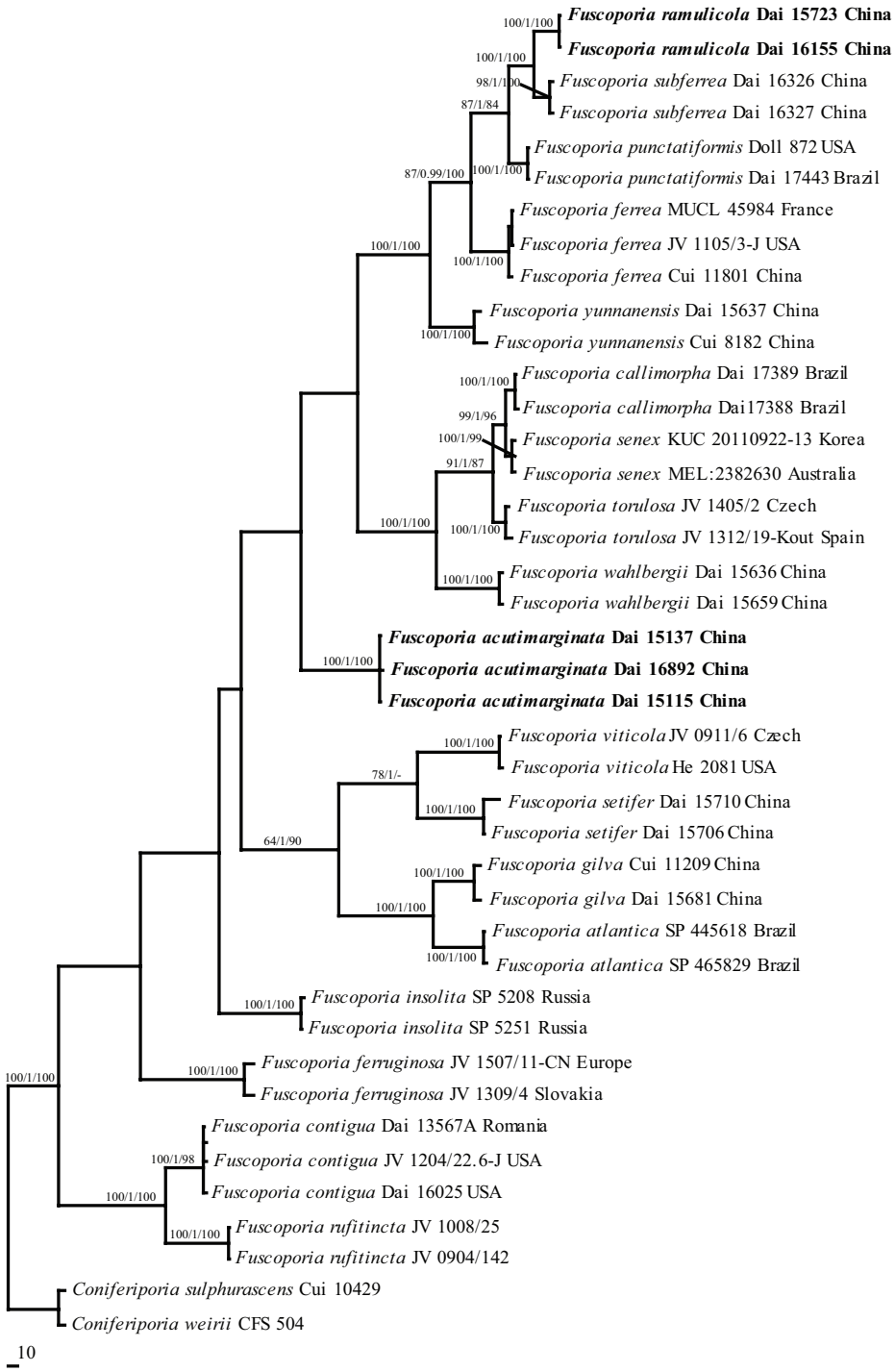

Figure 2. Phylogeny of *Fuscoporia* inferred from ITS+nLSU+RPB2 sequences. Topology is from MP tree and statistical values (MP/BI/ML) are indicated for each node that simultaneously received BS from ML and MP not below 75%, and BPP from BI not below 0.9. Names of new species are in bold.

(BI) resulted in a similar consensus tree to that of the Maximum Parsimony (MP) and Maximum Likelihood (ML) analysis, with 1 million generations and an average standard deviation of split frequencies = 0.009570.

The three-gene dataset had an aligned length of 2950 characters, of which 1990 were constant, 90 were variable but parsimony-uninformative, and 870 were parsimony-informative. Maximum Parsimony (MP) analysis yielded 4 most parsimonious trees with near-identical topologies (TL = 2631, CI = 0.569, RI = 0.807, RC = 0.459, HI = 0.431). Bayesian (BI) resulted in a similar consensus tree to that of the Maximum Parsimony (MP) and Maximum Likelihood (ML) analysis, with 1 million generations and an average standard deviation of split frequencies = 0.005640.

Eighteen species of *Fuscoporia* formed a well-supported clade (94/1/96 in Fig. 1) within the Hymenochaetaceae. *Fuscoporia* is a sister genus to *Coniferiporia*. Two samples from southern China are clustered into a new highly supported lineage (100/1/100 in Fig. 2) and in a clade with *F. ferrea* (Pers.) G. Cunn., *F. punctatiformis*, *F. subferrea* Q. Chen & Y. Yuan, and *F. yunnanensis* with high support (99/1/98 in Fig. 1; 100/1/100 in Fig. 2); it is described as *F. ramulicola* sp. nov. Another three specimens formed a distinct lineage with strong support (100/1/100 in Fig. 2) in *Fuscoporia*. This clade is interpreted as a new species, *F. Acutimarginata* sp. nov.

Taxonomy

***Fuscoporia acutimarginata* Y.C. Dai & Q. Chen, sp. nov.**
MycoBank MB 824732
Figs 3A, 4

Type. China. Yunnan Province: Kunming, Wild Duck Park, 2 August 2016, on fallen angiosperm branch, Dai 16892 (holotypes: BJFC 022998).

Etymology. *"Acutimarginata"* (Latin): referring to the species with a sharp margin of fruiting body.

Description. Basidiocarps annual, effused-reflexed to pileate, broadly attached, without taste or odor and soft corky when fresh. Pilei conchate, laterally fused, convex towards margin, projecting up to 1.5 cm, 7 cm wide and 6 mm thick at base. Pileal surface yellowish brown to dark brown, velutinate, concentrically sulcate with zoned; margin acute, yellowish brown. Pore surface yellowish brown when dry, glancing; margin distinct, yellowish, up to 2 mm wide; pores circular to angular, 5–7 per mm; dissepiments thin, entire. Context yellowish brown to dull brown, corky, up to 3 mm thick. Tubes yellowish brown, paler than context, corky, up to 3 mm long.

Hyphal structure. Hyphal system dimitic; generative hyphae simple septate; tissue darkening but otherwise unchanged in KOH.

Subiculum. Generative hyphae rare, hyaline to pale yellowish, thin- to slightly thick-walled, occasionally branched, 2–3.5 μm in diam; skeletal hyphae dominant, yellowish brown, thick-walled with a wide lumen, unbranched, aseptate, interwoven, 2–4.3 μm in diam.

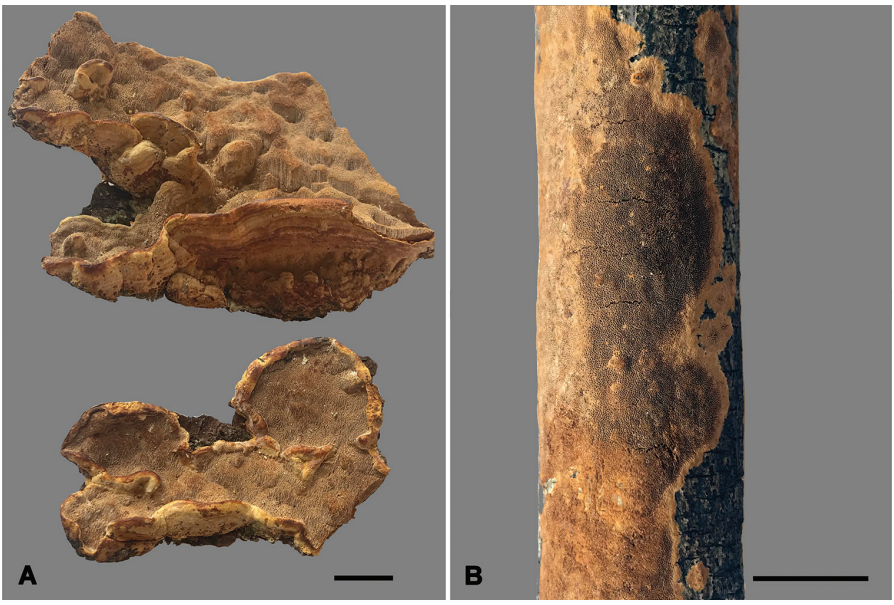

Figure 3. Basidiocarps of *Fuscoporia*. **A** *F. acutimarginata* (Dai 15137) **B** *F. ramulicola* (Dai 16155). Scale bars: 10 mm.

Tubes. Generative hyphae hyaline, thin-walled, occasionally branched, 2–3 μm in diam, occasionally encrusted at dissepiment edges; skeletal hyphae dominant, yellowish brown, thick-walled with a wide lumen, unbranched, aseptate, straight, subparallel along the tubes, 2–4 μm in diam. Irregular crystals occasionally present among trama and hymenia.

Hymenium. Hymenial setae rare, mostly originating from tramal hyphae, subulate, dark brown, thick-walled, 20–40 × 3–7 μm; cystidioles frequent, fusoid, sometimes covered with crystals, hyaline, thin-walled, 16.5–26 × 4–6.5 μm; basidia broadly clavate, with four sterigmata and a simple septum at the base, 14–17 × 4.8–6.5 μm; basidioles similar in shape to basidia, but slightly smaller. Basidiospores cylindrical, hyaline, thin-walled, smooth, IKI–, CB–, (7–)7.5–9(–9.8) × (2.2–)2.5–3.2 μm, L = 8.12 μm, W = 2.87μm, Q = 2.73–2.95 (n = 60/2).

Additional specimens examined (paratypes). China. Hunan Province: Yizhang County, Mangshan Nature Reserve, Guizizhai, 16 Aug 2014, on fallen angiosperm trunk, Dai 15115 (BJFC 018227), Dai 15137 (BJFC 018253).

Fuscoporia ramulicola **Y.C. Dai & Q. Chen, sp. nov.**
MycoBank MB 824734
Figs 3B, 5

Type. China. Yunnan Province: Binchuan County, Jizushan Park, 30 August 2015, on fallen angiosperm branch, Dai 15723 (holotypes: BJFC 019827).

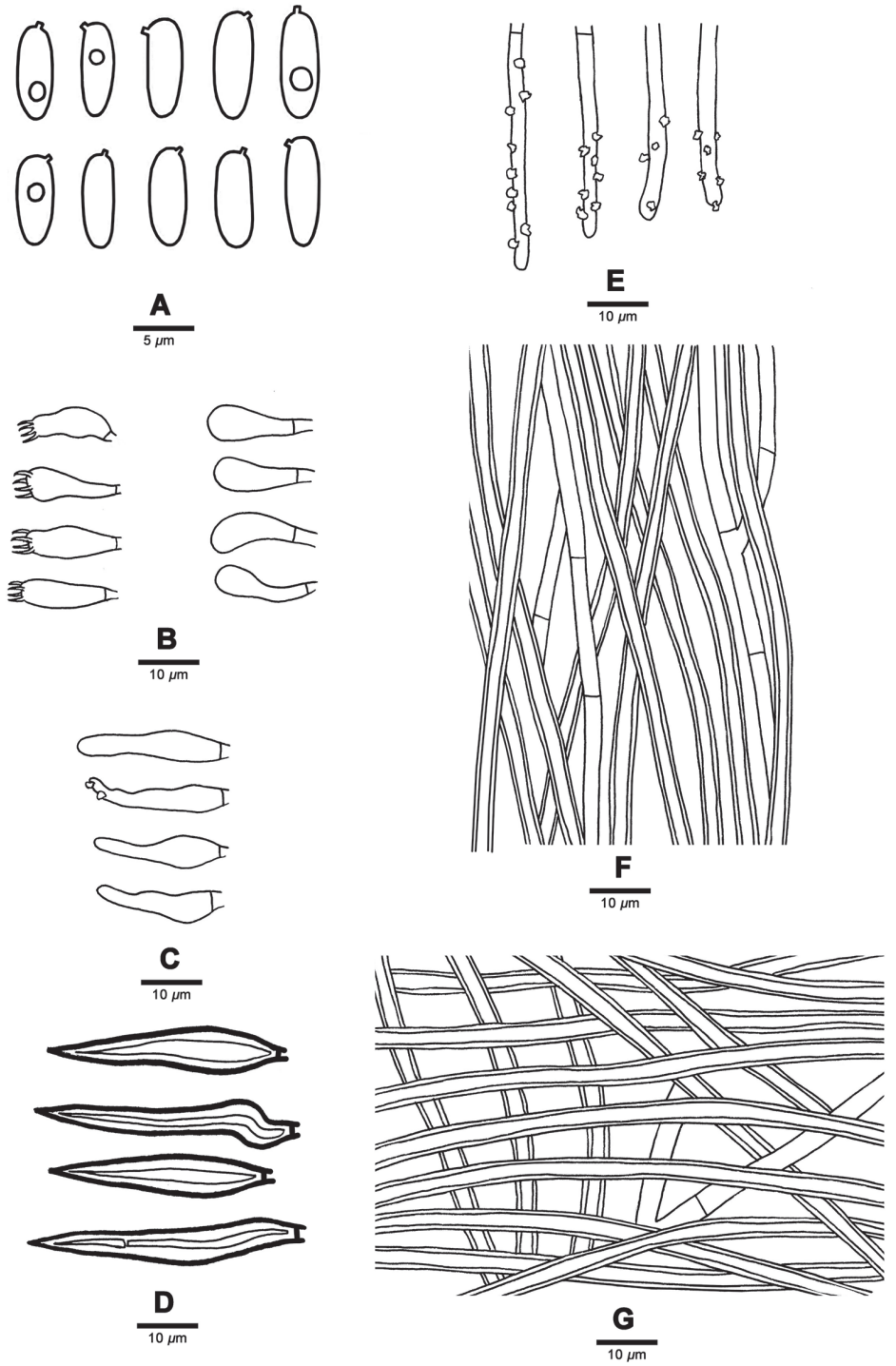

Figure 4. Microscopic structures of *Fuscoporia acutimarginata* (Holotype, Dai 16892) **A** basidiospores **B** basidia and basidioles **C** cystidioles **D** hymenial setae **E** generative hyphae at dissepiment edge **F** hyphae from trama **G** hyphae from subiculum.

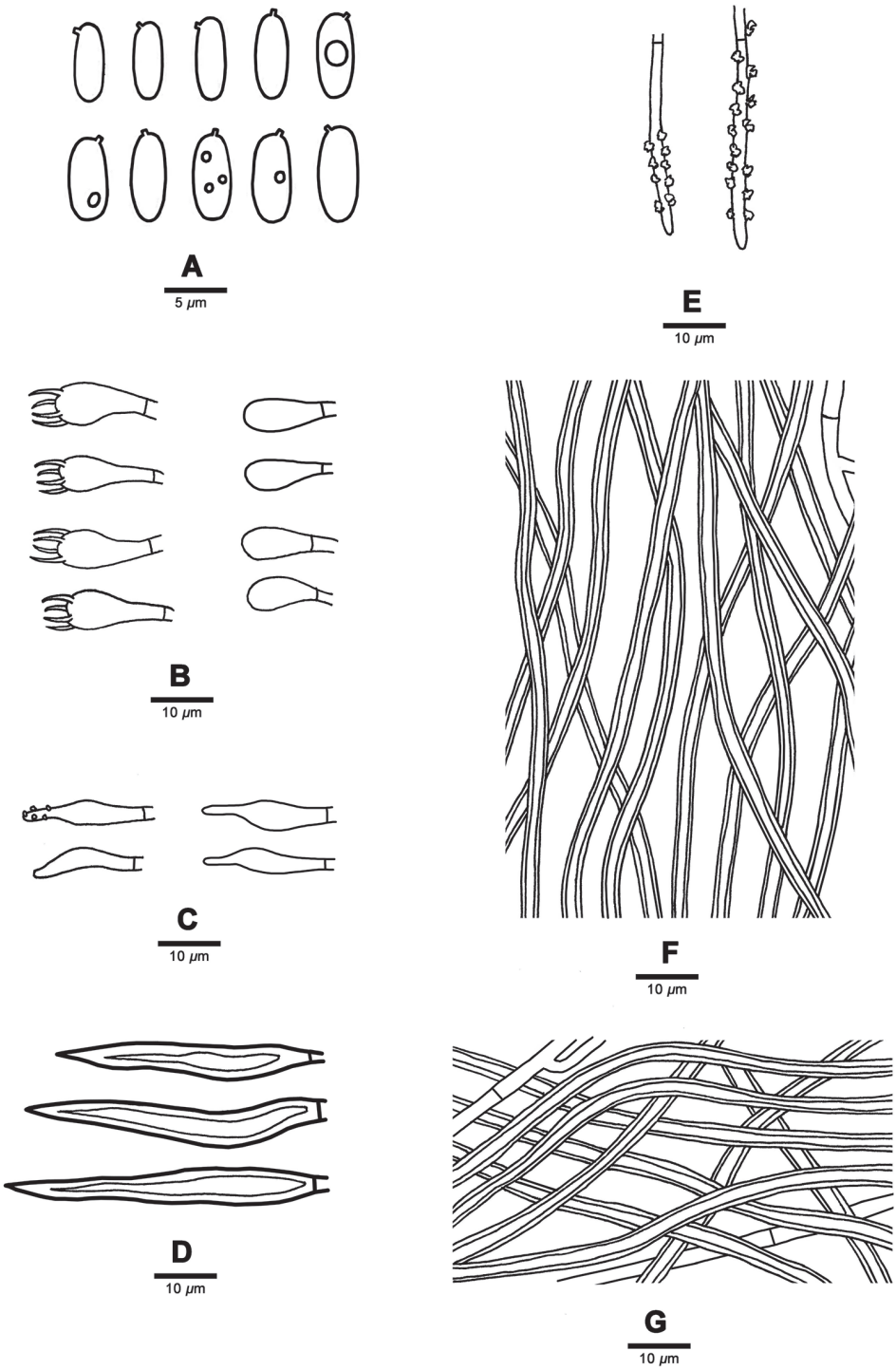

Figure 5. Microscopic structures of *Fuscoporia ramulicola* (Holotype, Dai 15723) **A** basidiospores **B** basidia and basidioles **C** cystidioles **D** hymenial setae **E** generative hyphae at dissepiment edge **F** hyphae from trama **G** hyphae from subiculum.

Etymology. *"Ramulicola"* (Latin) referring to the species growing on branches.

Description. Basidiocarps annual, resupinate, effused, inseparable, without taste or odor and corky when fresh, light-weight and hard corky when dry, up to 10 cm long, 2.2 cm wide and 1 mm thick at center. Pore surface grayish brown, fawn, cracked with age; sterile margin yellowish brown to olivaceous buff, distinctly paler than tubes, up to 1 mm wide; pores more or less angular, 6–7 per mm; dissepiments thin, sometimes irregular to slightly lacerate; abundant setae seen in tube cavities (under lens). Subiculum reddish brown, corky, very thin, about 0.1 mm thick. Tubes olivaceous buff, paler contrasting with pores and subiculum, hard corky, up to 0.9 mm long.

Hyphal structure. Hyphal system dimitic; generative hyphae simple septate; tissue darkening but otherwise unchanged in KOH.

Subiculum. Generative hyphae rare, hyaline, thin-walled, occasionally branched and simple septate, 2.5–3 μm in diam; skeletal hyphae dominant, rust-brown, thick-walled with a wide lumen, unbranched, aseptate, flexuous, loosely interwoven, 3–3.8 μm in diam.

Tubes. Generative hyphae rare, mostly present at dissepiment edges and subhymenium, hyaline, thin-walled, occasionally branched and frequently simple septate, 1.8–2.8 μm in diam, some of them at dissepiment edges and in the hymenium encrusted with small crystals; skeletal hyphae dominant, yellowish brown, thick-walled with a wide lumen, unbranched, aseptate, flexuous to more or less straight, subparallel along the tubes, 2.5–3.8 μm in diam. Irregular crystals usually present among trama and hymenia.

Hymenium. Hymenial setae frequent, mostly originating from hymenium, subulate, dark brown, thick-walled, 35–60 × 4.5–7 μm; cystidioles fusoid, sometimes covered with crystals, hyaline and thin-walled, 15–22 × 3–5 μm; basidia barrel-shaped, with four sterigmata and a simple septum at the base, 9–11 × 4.5–5.5 μm; basidioles frequently in hymenium, similar in shape to the basidia, but slightly smaller. Basidiospores cylindrical, hyaline, thin-walled, smooth, usually glued in tetrads, IKI–, CB–, with some small guttules, (5.2–)5.8–7(–7.2) × (1.8–)2–2.5(–2.8) μm, L = 6.37 μm, W = 2.28 μm, Q = 2.57–2.88 (n = 60/2).

Additional specimen examined (paratype). China. Hainan Province: Wuzhishan County, Wuzhishan Nature Reserve, 14 Nov 2015, on fallen angiosperm branch, Dai 16155 (BJFC 020252).

Discussion

In the study, sixteen previously accepted species of *Fuscoporia* were referred to morphological examination and phylogenetic analyses. Two species of *Fuscoporia* from China, *F. acutimarginata* and *F. ramulicola*, are described as new on the basis of molecular data and morphology. *F. acutimarginata* is characterized by annual, effused-reflexed to pileate basidiocarps, small pores (5–7 per mm), a dimitic hyphal structure, hymenial setae rarely present, originating from tramal hyphae, the presence of cystidioles, and cylindrical basidiospores measuring 7.5–9 × 2.5–3.2 μm. Phylogenetically, samples of

F. acutimarginata formed a well-supported monophyletic lineage distinct from other *Fuscoporia* species (Fig. 2). *F. acutimarginata* is very similar to *F. setifer* in having annual, effused-reflexed basidiocarps and the presence of cystidioles, but the latter has bigger pores (3–4 per mm) and smaller basidiospores (5.8–7 × 2–2.5 μm, Dai 2010). *F. acutimarginata* has a similar macromorphology to *F. gilva* (Schwein.) T. Wagner & M. Fisch., but the latter has frequently septate skeletal hyphae and ellipsoid to ovoid basidiospores (4–5 × 3–3.5 μm, Ryvarden 2004).

Fuscoporia ramulicola is distributed in southern China and characterized by annual and resupinate basidiocarps, small pores (6–7 per mm), a dimitic hyphal system, subulate hymenial setae, the presence of cystidioles, and cylindrical basidiospores measuring 5.8–7 × 2–2.5 μm. *F. ferrea*, *F. subferrea*, *F. yunnanensis* and *F. ramulicola* have overlapping distribution in China and clustered together with *F. punctatiformis* in a clade with strong support (99/1/98 in Fig. 1, 100/1/100 in Fig. 2). They are distinguishable according to their morphology and molecular data: *F. ferrea* is distinguished from *F. ramulicola* by its perennial basidiocarps and widely distributed in northern China, Europe and North America (Ryvarden and Gilbertson 1994, Lowe 1966, Chen et al. 2019); *F. subferrea* has smaller pores (7–10 per mm) and shorter basidiospores (4.2–6.2 × 2–2.6 μm, Chen and Yuan 2017); *F. yunnanensis* has larger pores (2–4 per mm) and wider basidiospores (6–8.3 × 2.4–3 μm, Dai 2010); *F. punctatiformis* has shorter hymenial setae (18–25 μm vs. 35–60 μm), subcylindrical basidiospores with a pointed apex (4–6 × 1.5–2 μm, Ryvarden and Johansen 1980) and is reported from America, Brazil and USA (Ryvarden 2004; Groposo et al. 2007). *Fuscoporia ramulicola* is similar to *F. contigua* and *F. ferruginosa* in having resupinate basidiocarps; however, *F. contigua* and *F. ferruginosa* have mycelial, extrahymenial setae (Chen et al. 2019); in addition, the three species are distantly related in our phylogenies (Figs 1, 2). *Fuscoporia montana* Y.C. Dai & Niemelä and *F. chrysea* (Lév.) Baltazar & Gibertoni are also similar to *F. ramulicola* in sharing resupinate basidiocarps, abundant subulate hymenial setae, absence of mycelial setae and distributed in southern China. *Fuscoporia montana* differs from *F. ramulicola* in having ovoid basidiospores 6.5–8.2 × 3.2–4.2 μm (Niemelä et al. 2001) whereas *F. chrysea* is different from *F. ramulicola* by its smaller pores (9–10 per mm) and shorter basidiospores (3–4 × 2–2.5 μm, Dai 2010).

Key to *Fuscoporia* species in China

1	Basidiocarps usually laterally stipitate; hymenial setae absent	***F. discipes***
–	Basidiocarps sessile; hymenial setae present	**2**
2	Basidiocarps completely resupinate	**3**
–	Basidiocarps effuse-reflexed to pileate	**11**
3	Mycelial setae present in the decayed wood and margin of basidiocarps (by hand lens)	**4**
–	Mycelial setae absent from the decayed wood and margin of basidiocarps (by hand lens)	**5**
4	Pores 7–8 per mm	***F. ferruginosa***
–	Pores 2–3 per mm	***F. contigua***

5 Basidiocarps perennial....**6**
– Basidiocarps annual....**9**
6 Pores 5–7 per mm....**7**
– Pores 7–10 per mm....**8**
7 Basidiospores cylindrical, 6–7.8 × 2–2.5 µm....***F. ferrea***
– Basidiospores subcylindrical, 4–6 × 1.5–2 µm....***F. punctatiformis***
8 Pores 9–10 per mm; basidiospores ellipsoid, < 5 µm long....***F. chrysea***
– Pores 7–8 per mm; basidiospores narrowly ovoid, > 5 µm long....***F. montana***
9 Pores 2–4 per mm....***F. yunnanensis***
– Pores 6–10 per mm....**10**
10 Pores 7–10 per mm; basidiospores 4.2–6.2 µm long....***F. subferrea***
– Pores 6–7 per mm; basidiospores 6–7 µm long....***F. ramulicola***
11 Hymenial setae usually hooked....***F. wahlbergii***
– Hymenial setae straight....**12**
12 Pores 3–4 per mm....***F. setifera***
– Pores 5–11 per mm....**13**
13 Basidiocarps annual, margin acute....**14**
– Basidiocarps perennial, margin obtuse....**15**
14 Skeletal hyphae septate, spores ellipsoid, 3.3–4.2 × 2.2–3 µm....***F. gilva***
– Skeletal hyphae aseptate, spores cylindrical, 7.5–9 × 2.5–3.2 µm....
....***F. acutimarginata***
15 Basidiocarps subungulate; contextual skeletal hyphae aseptate....***F. torulosa***
– Basidiocarps usually applanate; contextual skeletal hyphae septate....**16**
16 Basidiospores 3.3–4.1 × 2.1–2.4 µm, skeletal hyphae unchanged in KOH....
....***F. rhabarbarina***
– Basidiospores 4–4.8 × 3.6–3.9 µm, skeletal hyphae swelling in KOH....***F. senex***

Acknowledgements

We are grateful to Dr. Shuang-Hui He (BJFC, China) for his companionship on field trips. The research is financed by the National Natural Science Foundation of China (Project Nos. U1802231 & 31530002).

References

Baltazar JM, Gibertoni TB (2010) New combinations in *Phellinus* s.l. and *Inonotus* s.l. Mycotaxon 111: 205–208. https://doi.org/10.5248/111.205

Baltazar JM, Trierveiler-Pereira L, Loguercio-Leite C, Ryvarden L (2009) Santa Catarina Island mangroves 3: a new species of *Fuscoporia*. Mycologia 100: 859–863. https://doi.org/10.3852/08-082

Chen JJ, Cui BK, Dai YC (2016) Global diversity and molecular systematics of *Wrightoporia* s.l. (Russulales, Basidiomycota). Persoonia 37: 21–36. https://doi.org/10.3767/003158516X689666

Chen Q, Wu F, Ji XH, Si J, Zhou LW, Tian XM, Vlasák J, Dai YC (2019) Phylogeny of the genus *Fuscoporia* and taxonomic assessment of the *F. contigua* group. Mycologia 111: 423–444. https://doi.org/10.1080/00275514.2019.1570749

Chen Q, Yuan Y (2017) A new species of *Fuscoporia* (Hymenochaetales, Basidiomycota) from southern China. Mycosphere 8: 1238–1245. https://doi.org/10.5943/mycosphere/8/6/9

Cui BK, Li HJ, Ji X, Zhou JL, Song J, Si J, Yang ZL, Dai YC (2019) Species diversity, taxonomy and phylogeny of Polyporaceae (Basidiomycota) in China. Fungal Diversity 97: 137–392. https://doi.org/10.1007/s13225-019-00427-4

Dai YC (2010) Hymenochaetaceae (Basidiomycota) in China. Fungal Diversity 45: 131–343. https://doi.org/10.1007/s13225-010-0066-9

Dai YC, Cui BK, Si J, He SH, Hyde KD, Yuan HS, Liu XY, Zhou LW (2015) Dynamics of the worldwide number of fungi with emphasis on fungal diversity in China. Mycological Progress 14: 62. https://doi.org/10.1007/s11557-015-1084-5

Fiasson JL, Niemelä T (1984) The Hymenochaetales: a revision of the European poroid taxa. Karstenia 24: 14–28. https://doi.org/10.29203/ka.1984.224

Gilbertson RL (1979) The genus *Phellinus* (Aphyllophorales: Hymenochaetaceae) in western North America. Mycotaxon 9: 51–89.

Groposo C, Loguercio-Leite C, Góes-Neto A (2007) *Fuscoporia* (Basidiomycota, Hymenochaetales) in southern Brazil. Mycotaxon 101: 55–63.

Hall TA (1999) Bioedit: a user-friendly biological sequence alignment editor and analysis program for Windows 95/98/NT. Nucleic Acids Symposium Series 41: 95–98.

Han ML, Chen YY, Shen LL, Song J, Vlasák J, Dai YC, Cui BK (2016) Taxonomy and phylogeny of the brown-rot fungi: *Fomitopsis* and its related genera. Fungal Diversity 80: 343–373. https://doi.org/10.1007/s13225-016-0364-y

Jang Y, Lee SW, Jang S, Lim YW, Lee JS, Kim JJ (2012) Four unrecorded wood decay fungi from Seoul in Korea. Mycobiology 40: 195–201. https://doi.org/10.5941/MYCO.2012.40.3.195

Larsen MJ, Cobb-Poulle LA (1990) *Phellinus* (Hymenochaetaceae). A survey of the world taxa. Synopsis Fungorum 3: 1–206. https://doi.org/10.2307/3760175

Lowe JL (1966) Polyporaceae of North America. The genus *Poria*. Technical Publication of the State University College of Forestry at Syracuse University 90: 1–183.

Matheny PB (2005) Improving phylogenetic inference of mushrooms with RPB1 and RPB2 nucleotide sequences (*Inocybe*; Agaricales). Molecular Phylogenetics and Evolution 35: 1–20. https://doi.org/10.1016/j.ympev.2004.11.014

Murrill WA (1907) Polyporaceae 1. North American Flora 9: 1–72.

Niemelä T, Wagner T, Fischer M, Dai YC (2001) *Phellopilus* gen. nov. and its affinities within *Phellinus* s. lato and *Inonotus* s. lato (Basidiomycetes). Annales Botanici Fennici 38: 51–62. http://www.jstor.org/stable/23726833

Overholts LD (1953) The Polyporaceae of the United States, Alaska and Canada. Ann Arbor: University of Michigan Press. https://doi.org/10.2307/2481836

Petersen JH (1996) The Danish Mycological Society's colour-chart. Greve: Foreningen til Svampekundskabens Fremme.

Pires RM, Motatovásquez V, De Gugliotta AM (2015) *Fuscoporia atlantica* sp. nov., a new polypore from the Brazilian Atlantic Rainforest. Mycotaxon 130: 843–855. https://doi.org/10.5248/130.843

Raymundo T, Valenzuela R, Esqueda M (2013) Hymenochaetaceae from Mexico 6. A new *Fuscoporia* species from the Sonoran Desert. Mycotaxon 125: 37–43. https://doi.org/10.5248/125.37

Ryvarden L (2004) Neotropical polypores 1. Introduction, Hymenochaetaceae and Ganodermataceae. Synopsis Fungorum 19: 1–227.

Ryvarden L, Johansen I (1980) A preliminary polypore flora of East Africa. Oslo: Fungiflora. https://doi.org/10.2307/3759822

Ryvarden L, Gilbertson RL (1994) European polypores. Part 2. Synopsis Fungorum 7: 394–743.

Ryvarden L, Melo I (2017) Poroid fungi of Europe, 2nd edition. Synopsis Fungorum 37: 1–431.

Shen LL, Wang M, Zhou JL, Xing JH, Cui BK, Dai YC (2019) Taxonomy and phylogeny of *Postia*. Multi-gene phylogeny and taxonomy of the brown-rot fungi: *Postia* (Polyporales, Basidiomycota) and related genera. Persoonia 42: 101–126. https://doi.org/10.3767/persoonia.2019.42.05

Song J, Cui BK (2017) Phylogeny, divergence time and historical biogeography of *Laetiporus* (Basidiomycota, Polyporales). BMC Evolutionary Biology 17: 102. https://doi.org/10.1186/s12862-017-0948-5

Thompson JD, Gibson TJ, Plewniak F, Jeanmougin F, Higgins DG (1997) The clustal_X windows interface: Flexible strategies for multiple sequence alignment aided by quality analysis tools. Nucleic Acids Research 25: 4876–4882. https://doi.org/10.1093/nar/25.24.4876

Vilgalys R, Hester M (1990) Rapid genetic identification and mapping of enzymatically amplified ribosomal DNA from several Cryptococcus species. Journal of Bacteriology 172: 4238–4246. https://doi.org/10.1128/jb.172.8.4238-4246.1990

Wagner T, Fischer M (2001) Natural groups and a revised system for the European poroid Hymenochaetales (Basidiomycota) supported by nLSU rDNA sequence data. Mycological Research 105: 773–782. https://doi.org/10.1017/S0953756201004257

Wagner T, Fischer M (2002) Proceedings towards a natural classification of the worldwide taxa *Phellinus* s.l. and *Inonotus* s.l., and phylogenetic relationships of allied genera. Mycologia 94: 998–1016. https://doi.org/10.2307/3761866

White TJ, Bruns T, Lee S, Taylor J (1990) Amplification and direct sequencing of fungal ribosomal RNA genes for phylogenetics. In: Innis MA, Gefand DH, Sninsky JJ, White JT (Eds) PCR Protocols: a guide to methods and applications. Academic Press, San Diego, 315–322. https://doi.org/10.1016/B978-0-12-372180-8.50042-1

Zhou LW (2015) *Fulvifomes imbricatus* and *F. thailandicus* (Hymenochaetales, Basidiomycota): Two new species from ailand based on morphological and molecular evidence. Mycological Progress 14: 89. https://doi.org/10.1007/s11557-015-1116-1

Zhou LW, Vlasák J, Dai YC (2016) Taxonomy and phylogeny of *Phellinidium* (Hymenochaetales, Basidiomycota): a redefinition and the segregation of *Coniferiporia* gen. nov. for forest pathogens. Fungal Biology 120: 988–1001. https://doi.org/10.1016/j.funbio.2016.04.008

Zhu L, Song J, Zhou JL, Si J, Cui BK (2019) Species diversity, phylogeny, divergence time and biogeography of the genus *Sanghuangporus* (Basidiomycota). Frontiers in Microbiology 10: 812. https://doi.org/10.3389/fmicb.2019.00812

MycoKeys 61: 91–109 (2019)
doi: 10.3897/mycokeys.61.47056
http://mycokeys.pensoft.net

RESEARCH ARTICLE

A peer-reviewed open-access journal
MycoKeys
Launched to accelerate biodiversity research

Additions to Chaetothyriaceae (Chaetothyriales): *Longihyalospora* gen. nov. and *Ceramothyrium longivolcaniforme*, a new host record from decaying leaves of *Ficus ampelas*

Danushka S. Tennakoon[1,2,3], Kasun M. Thambugala[4], Rajesh Jeewon[5], Sinang Hongsanan[6], Chang-Hsin Kuo[1], Kevin D. Hyde[2,3]

1 *Department of Plant Medicine, National Chiayi University, 300 Syuefu Road, Chiayi City 60004, Taiwan* **2** *Center of Excellence in Fungal Research, Mae Fah Luang University, Chiang Rai, 57100, Thailand* **3** *Key Laboratory for Plant Biodiversity and Biogeography of East Asia (KLPB), Kunming Institute of Botany, Chinese Academy of Science, Kunming 650201, Yunnan, China* **4** *Industrial Science and Management (International Program), Faculty of Science and Technology, Thammasat University (Rangsit Center), Klong Luang, Pathumthani 12121, Thailand* **5** *Department of Health Sciences, Faculty of Science, University of Mauritius, Reduit, Mauritius* **6** *Shenzhen Key Laboratory of Microbial Genetic Engineering, College of Life Sciences and Oceanography, Shenzhen University, Shenzhen 518000, China*

Corresponding author: *Chang-Hsin Kuo* (chkuo@mail.ncyu.edu.tw)

Academic editor: *A. Miller* | Received 4 October 2019 | Accepted 19 November 2019 | Published 16 December 2019

Citation: Tennakoon DS, Thambugala KM, Jeewon R, Hongsanan S, Kuo C-H, Hyde KD (2019) Additions to Chaetothyriaceae (Chaetothyriales): *Longihyalospora* gen. nov. and *Ceramothyrium longivolcaniforme*, a new host record from decaying leaves of *Ficus ampelas*. MycoKeys 61: 91–109. https://doi.org/10.3897/mycokeys.61.47056

Abstract

A novel ascomycete genus, *Longihyalospora*, occurring on leaf litter of *Ficus ampelas* in Dahu Forest Area in Chiayi, Taiwan is described and illustrated. *Longihyalospora* is characterized by dark mycelium covering the upper leaf surface, elongate mycelial pellicle with ring of setae, pale brown to brown peridium, broadly obovoid, short pedicellate asci and hyaline, fusiform, elongated (tapering ends) and multi-septate ascospores with a thin mucilaginous sheath. Phylogenetic analyses of combined ITS, LSU and SSU sequence data revealed *Longihyalospora* as a distinct genus within the Chaetothyriaceae with high bootstrap support. Moreover, based on morphological similarities, *Chaetothyrium vermisporum* transferred to the new genus. In addition, *Ceramothyrium longivolcaniforme* is reported for the first time on *Ficus ampelas*. Newly added species are compared with other similar species and comprehensive descriptions and micrographs are provided.

Keywords

Moraceae, multi-gene phylogeny, mycelium pellicle, sooty mould, taxonomy

Introduction

The family Chaetothyriaceae was established by Hansford (1946) with the generic type *Chaetothyrium* Speg., and the members of this family are characterized by a loose network of dark mycelium over the substrate, ascomata produced beneath a mycelial pellicle, and forming beneath an external hyphal mat with or without setae (Batista and Ciferri 1962; von Arx and Müller 1975; Hughes 1976; Pereira et al. 2009; Chomnunti et al. 2012; Tian et al. 2014; Zeng et al. 2016). Due to some morphological similarities (i.e. bitunicate asci), Eriksson (1982) referred this family to the order Dothideales in Dothideomycetes, but subsequently, taxonomic studies have established its placement in Eurotiomycetes with support of molecular data (Chomnunti et al. 2012, 2014; Tian et al. 2014; Crous et al. 2015; Maharachchikumbura et al. 2018; Yang et al. 2018). Currently, 16 genera are accepted in Chaetothyriaceae, viz. *Actinocymbe* Höhn., *Aphanophora* Réblová & Unter., *Beelia* F. Stevens & R.W. Ryan, *Camptophora* Réblová & Unter., *Ceramothyrium* Bat. & H. Maia, *Ceratocarpia* Rolland, *Chaetothyriomyces* Pereira-Carvalho et al., *Chaetothyrium* Speg., *Cyphellophoriella* Crous & A.J. Sm., *Euceramia* Bat. & Cif., *Microcallis* Syd., *Phaeosaccardinula* P. Henn., *Stanhughesia* Constant., *Treubiomyces* Höhn., *Vonarxia* Bat. and *Yatesula* Syd. & P. Syd. (Wijayawardene et al. 2018).

During our survey of the taxonomy and diversity of leaf litter microfungi, two interesting fungal species were collected from Dahu forest, Chiayi in Taiwan. Morphological and multi-gene phylogenetic analyses were performed to establish their taxonomic placement.

Materials and methods

Sample collection, morphological studies and isolation

Decaying leaf litter samples of *Ficus ampelas* Burm.f. were collected from Dahu forest area in Chiayi, Taiwan and brought to the laboratory in plastic bags. The samples were incubated in plastic boxes at 25–30 °C for 3 days and examined following the methods described by Tian et al. (2014). Morphological observations were made using an Axioskop 2 Plus compound microscope and images were taken with an Axioskop 2 Plus compound microscope equipped with a Canon Axiocam 506 Color digital camera. Permanent slides were prepared by mounting fungal material in lactoglycerol and sealed by applying nail-polish around the margins of cover slips. All measurements were made with ZEN2 (blue edition) and images used for figures were processed with Adobe Photoshop CS3 Extended version 10.0 software (Adobe Systems, USA).

Isolates (for *Ceramothyrium longivolcaniforme* Zeng, T.C. Wen & K.D. Hyde) were obtained from single ascospores following the methods described in Chomnunti et al. (2014). Germinated ascospores were transferred to potato dextrose agar (PDA) and incubated at 25 °C in normal light. Subsequent sub culturing was done carefully to ensure no contaminants are used to generate DNA sequence data. Culture characteristics were observed after two weeks. Type specimens were deposited in the Mae Fah Luang

University Herbarium (MFLU) and living cultures were deposited in Mae Fah Luang University Culture Collection (MFLUCC). Faces of Fungi and Index Fungorum numbers were provided as in Jayasiri et al. (2015) and Index Fungorum (2019).

DNA extraction and PCR amplification

Fresh mycelia were scraped (for *Ceramothyrium longivolcaniforme*) using a sterile scalpel from pure cultures growing on PDA medium at 25 °C and kept in a 1.5 ml microcentrifuge tube and used as starting material for DNA extraction. When fungi failed to germinate in a culture medium, DNA was extracted directly from ascomycete fruiting bodies (for *Longihyalospora ampeli*) by following a modified protocol of Zeng et al. (2018) protocol: 15–20 fruiting bodies (> 500 µm diam., 10 fruiting bodies) were removed from the host substrate using a sterilized needle and transferred to a drop of sterile water, placed in a sterile Eppendorf tube (1.5 mL) under aseptic conditions.

The genomic DNA was extracted using a DNA extraction kit (E.Z.N.A Fungal DNA Mini Kit, D3390-02, Omega Bio-Tek) following the manufacturer's protocol. The DNA product was kept at 4 °C for DNA amplification and maintained at -20 °C for long-term storage. DNA was amplified by Polymerase Chain Reaction (PCR) for three genes, the large subunit (28S, LSU), small subunit (18S, SSU) and internal transcribed spacers (ITS1-5.8S-ITS2). The LSU gene was amplified by using the primers LR0R and LR5 (Vilgalys and Hester 1990; Rehner and Samuels 1994); SSU gene was amplified using the primers NS1 and NS4 (White et al. 1990); nuclear ITS was amplified by using the primers ITS5 and ITS4 (White et al. 1990). The amplification reactions were performed in 25µl of total reaction that contained 9.5 µl of sterilized water, 12.5 µl of 2×Power Taq PCR MasterMix (Tri-I Biotech, Taipei, Taiwan), 1 µl of each forward and reverse primers and 1 µl of DNA template. PCR thermal cycle program for ITS, LSU and SSU were as detailed by Tian et al. (2016). The PCR products were analyzed by 1.5% agarose gels containing the Safeview DNA stain (GeneMark, Taipei, Taiwan) to confirm the expected molecular weight of a single amplification product. PCR products were purified and sequenced with primers mentioned above by Tri-I Biotech, Taipei, Taiwan. Nucleotide sequences were deposited in GenBank (Table 1).

Phylogenetic analysis

Phylogenetic analyses were performed based on a combined ITS, LSU and SSU DNA sequence data. Newly generated sequences were subjected to a standard BLAST search of GenBank to aid in phylogenetic taxon sampling. Other sequences used in the analyses (Table 1) were obtained from GenBank based on recently published data (Zeng et al. 2016; Maharachchikumbura et al. 2018; Yang et al. 2018). The multiple alignments were made with MAFFT v. 7 at the web server (http://mafft.cbrc.jp/alignment/server), using default settings (Katoh and Standley 2013). The alignment was refined manually with BioEdit v. 7.0.5.2 (Hall 1999) where necessary. The tree topologies obtained

Table 1. GenBank and culture collection accession numbers of species included in the present phylogenetic study. The newly generated sequences are shown in bold.

Species	Strain/Voucher no.	GenBank accession no.		
		ITS	LSU	SSU
Aphanophora eugeniae	CBS 124105	FJ839617	FJ839652	–
Brycekendrickomyces acaciae	CBS 124104	MH863350	MH874874	–
Camptophora hylomeconis	IFRDCC 2661	MF285228	MF285230	–
C. hylomeconis	CBS 113311	EU035415	–	KC455295
Capronia fungicola	CBS 614.96	KY484990	FJ358224	FJ225722
C. mansonii	CBS 101.67	AF050247	MH870591	AF346422
Ceramothyrium aquaticum	LC306299	LC360299	LC360296	–
C. carniolicum	AFTOL-ID 1063	–	EF413628	EF413627
C. carniolicum	CBS 175.95	KC978733	KC455251	KC455294
C. exiguum	LC306297	LC360297	LC360295	–
C. ficus	MFLUCC 15-0228	KT588601	KT588599	–
C. ficus	MFLUCC 15-0229	KT588602	KT588600	–
C. longivolcaniforme	MFLU 16-1306	KP324929	KP324931	–
C. longivolcaniforme	**MFLUCC 19-0252**	**MN219715**	**MN238770**	**MN238773**
C. melastoma	CPC 19837	KC005771	KC005793	–
C. menglunense	MFLU 16-1874	KX524148	KX524146	–
C. phuquocense	LC306298	LC360298	LC360294	–
C. podocarpi	CPC 19826	KC005773	KC005795	–
C. thailandicum	MFLUCC 10-0008	KP324928	HQ895835	–
C. thailandicum	MFLU 13-0632	HQ895838	KP324930	–
Chaetothyrium agathis	MFLUCC 12-0113	KP744437	KP744480	–
C. brischoficola	MFLUCC 10-0012	HQ895839	HQ895836	–
Cladophialophora minourae	CBS 556.83	AY251087	FJ358235	FJ225734
C. emmonsii	CBS 640.96	KX822192	KC809995	KX822192
Cyphellophoriella pruni	CPC 25120	KR611878	–	–
Leptoxyphium fumago	CBS 123.26	MH854862	GU214430	GU214535
L. madagascariense	CBS 124766	MH863407	GQ303308	–
Longihyalospora ampeli	**MFLU 19-0824**	**MN219716**	**MN238771**	**MN238774**
L. ampeli	**MFLU 19-0825**	**MN219717**	**MN238772**	**MN238775**
Knufia cryptophialidica	DAOM 216555	–	JN040500	EF137364
K. cryptophialidica	DAOM 216553	JN040504	–	EF137363
K. perforans	CBS 885.95	MH862564	MH874191	–
K. perforans	CBS 726.95	KC978746	KC978741	KC978739
Minimelanolocus asiaticus	MFLUCC 15-0237	KR215604	KR215610	KR215615
M. melanicus	MFLUCC 15-0415	KR215608	KR215613	KR215618
Phaeosaccardinula dendrocalami	IFRDCC 2663	KF667243	KF667246	–
P. dendrocalami	IFRDCC 2649	KF667242	KF667245	–
P. ficus	MFLUCC 10-0009	HQ895840	HQ895837	–
P. multiseptata	IFRDCC 2639	KF667241	KF667244	–
Trichomerium deniqulatum	MFLUCC 10-0884	JX313654	JX313660	–
T. follicola	MFLUCC 10-0058	JX313653	JX313659	–
T. gleosporum	MFLUCC 10-0087	JX313656	JX313662	–
Vonarxia vagans	CBS 123533	FJ839636	FJ839672	KC455310
V. vagans	CPC 15152	FJ839637	FJ839673	–

from a single gene sequence data were compared prior to the combined gene analysis for checking the incongruence in overall topology of the phylogenetic tree.

Maximum likelihood trees were generated using the RAxML-HPC2 on XSEDE (8.2.8) (Stamatakis et al. 2008; Stamatakis 2014) in the CIPRES Science Gateway platform (Miller et al. 2010) using GTRGAMMA model with 1,000 bootstrap replicates. Maximum parsimony analysis (MP) was performed in PAUP v. 4.0b10 (Swofford 2002), with the heuristic search option and 1,000 random replicates. Maxtrees was set to 1,000 and branches of zero length were collapsed and all multiple parsimonious trees were saved. Descriptive tree statistics for parsimony (Tree Length [TL], Consistency Index [CI], Retention Index [RI], Relative Consistency Index [RC] and Homoplasy Index [HI] were calculated.

A Bayesian analysis (GTR+I+G model) was conducted with MrBayes v. 3.1.2 (Huelsenbeck and Ronqvist 2001) to evaluate posterior probabilities (PP) (Rannala and Yang 1996; Zhaxybayeva and Gogarten 2002) by Markov Chain Monte Carlo sampling (BMCMC). Six simultaneous Markov chains were run for 1,000,000 generations and trees were sampled every 100th generation, thus 10,000 trees were obtained. The suitable burn-in phases were determined by inspecting likelihoods and parameters in Tracer version 1.6 (Rambaut et al. 2014). Based on the tracer analysis, the first 1,000 trees representing 10% were discarded as the burn-in phase in the analysis. The remaining trees were used to calculate posterior probabilities in the majority rule consensus tree (critical value for the topological convergence diagnostic set to 0.01). Phylograms were visualized with FigTree v1.4.0 (Rambaut 2012) and annotated in Microsoft Power Point (2010). The final alignment and trees were deposited in TreeBASE, submission ID: 24826.

Results

Phylogenetic analysis

The combined dataset of ITS, LSU and SSU sequences comprised 2531 characters, of which 1492 characters are constant, 801 characters are parsimony-informative, while 238 variable characters are parsimony-uninformative in the maximum parsimony (MP) analysis (TL = 3011, CI = 0.515, RI = 0.698, RC = 0.360, HI = 0.485). LSU contains 900 total characters (constant = 645, informative = 217, uninformative = 38), ITS contains 759 total characters (constant = 332, informative = 364, uninformative = 63) and SSU contains 872 characters (constant = 515, informative = 220, uninformative = 137). The RAxML analysis of the combined dataset yielded a best scoring tree (Figure 1) with a final ML optimization likelihood value of -17222.496803. The matrix had 1040 distinct alignment patterns, with 37.84 % of undetermined characters or gaps. All analyses (ML, MP and BYPP) gave similar results and in agreement with previous studies based on multi-gene analyses (Zeng et al. 2016; Maharachchikumbura et al. 2018).

The phylogeny recovered herein also agrees with previously established ones in that *Ceramothyrium* is within the Chaetothyriales (Zeng et al. 2016; Maharachchikumbura

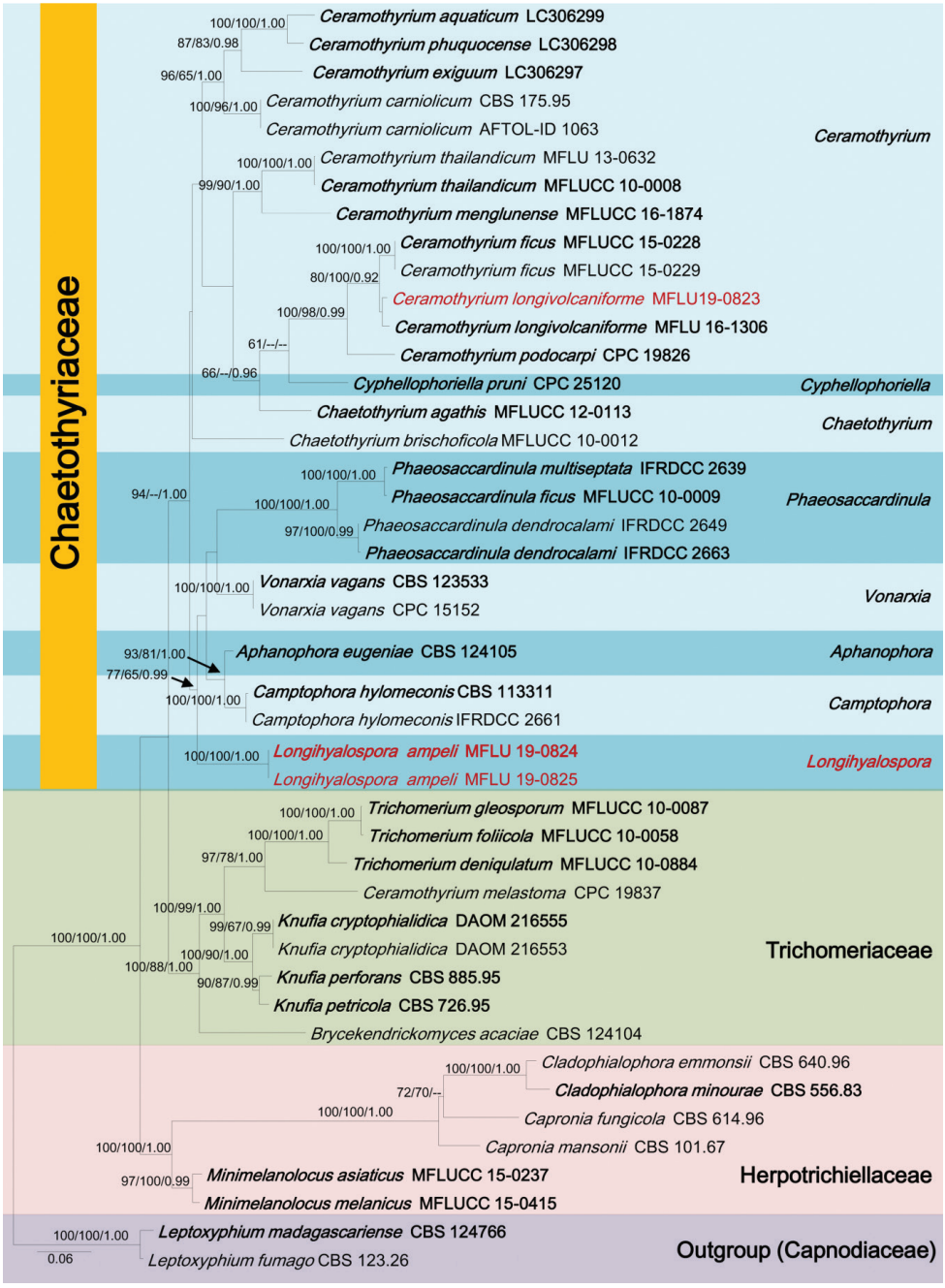

Figure 1. RAxML tree based on a combined dataset of ITS, LSU and SSU partial sequences of 45 taxa. Bootstrap support values for maximum likelihood (ML and, maximum parsimony (MP) values higher than 60 % and Bayesian posterior probabilities (BYPP) greater than 0.90 are given above each branch respectively. The new isolates are in red. Ex-type strains are in bold. The tree is rooted by *Leptoxyphium fumago* (CBS 123.26) and *L. madagascariense* (CBS 124766).

et al. 2018; Yang et al. 2018). Our new collection (MFLUCC19-0252) grouped in a well-supported clade (80% ML, 100% MP and 0.92 BYPP) with other *Ceramothyrium* species (Figure 1). In particular, it shows a close affinity to *Ceramothyrium longivolcaniforme* (holotype, MFLU16-1306). MFLU 19-0824 and MFLU 19-0825 constitute in a strongly supported subclade and is phylogenetically distinct from other genera in family (77% ML, 65% MP, 0.99 BYPP) (Figure 1).

Taxonomy

***Ceramothyrium longivolcaniforme* X.Y. Zeng, T.C. Wen & K.D. Hyde, Phytotaxa 267(1): 54 (2016)**
Fungorum Number: IF 811216
Facesoffungi number: FoF0047
Figure 2

Description. *Epiphytic* on decaying leaves of *Ficus ampelas* Burm.f. Covering the upper leaf surface with dark mycelium without penetrating host tissues. *Mycelial pellicle* elongate, subiculum-like, comprising hyphae that are mostly narrow, 3.5–4.5 µm wide ($\bar{x}$ = 3.8 µm, n= 20), brownish, slightly constricted at the septa, dense, radiating outward, anastomosing at the tips with cells of the hyphal network. ***Sexual morph***: *Ascomata* 130–180 µm high, 200–250 µm diam. ($\bar{x}$ = 155 × 220 µm, n = 10) in diameter, superficial, solitary, pale brown, globose to subglobose, coriaceous, somewhat flattened when dry, covered by a mycelial pellicle, with a circumferential space filled with sparse mycelium around the mature ascomata. *Peridium* 18–25 µm wide ($\bar{x}$ = 23.5 µm, n= 20), light brown, with compressed, hyaline, inner cells of *textura angularis* and light brown outer cells of *textura angularis*. *Asci* (62–)70–90 × 30–60 µm ($\bar{x}$ = 81 × 44 µm, n = 20), 8-spored, bitunicate, broadly obovoid, short pedicellate, apically rounded, with well-developed ocular chamber. *Ascospores* 30–45(–47) × 8–16 µm ($\bar{x}$ = 36 × 12 µm, n = 30), crowded or overlapping, irregularly triseriate, hyaline, oblong to ellipsoid, muriform, with 7 transversal septa and 6 longitudinal septa, slightly constricted at the septa, smooth-walled, surrounded by a mucilaginous sheath. ***Asexual morph***: Not observed.

Culture characteristics. Colonies on PDA reaching 3 mm diameter after 2 weeks at 25–30 °C, slow growing, spreading, with folded, velvety, wavy margin, consist of dark mycelium, colony color from above: olivaceous green; colony color from below: dark brown to black, not producing pigments in PDA.

Material examined. Taiwan, Chiayi, Fanlu Township area, Dahu forest, decaying leaves of *Ficus ampelas* Burm.f (Moraceae), 20 June 2018, D.S. Tennakoon, H10 (MFLU19-0823), living culture (MFLUCC19-0252).

Notes. In this study, a sample of *Ceramothyrium longivolcaniforme* was collected from dead leaves of *Ficus ampelas* (Moraceae) in Taiwan. The new collection shares a close phylogenetic relationship with *Ceramothyrium longivolcaniforme* (MFLU16-1306) (Figure 1). The morphology of our collection (MFLUCC19-0252) fits with the

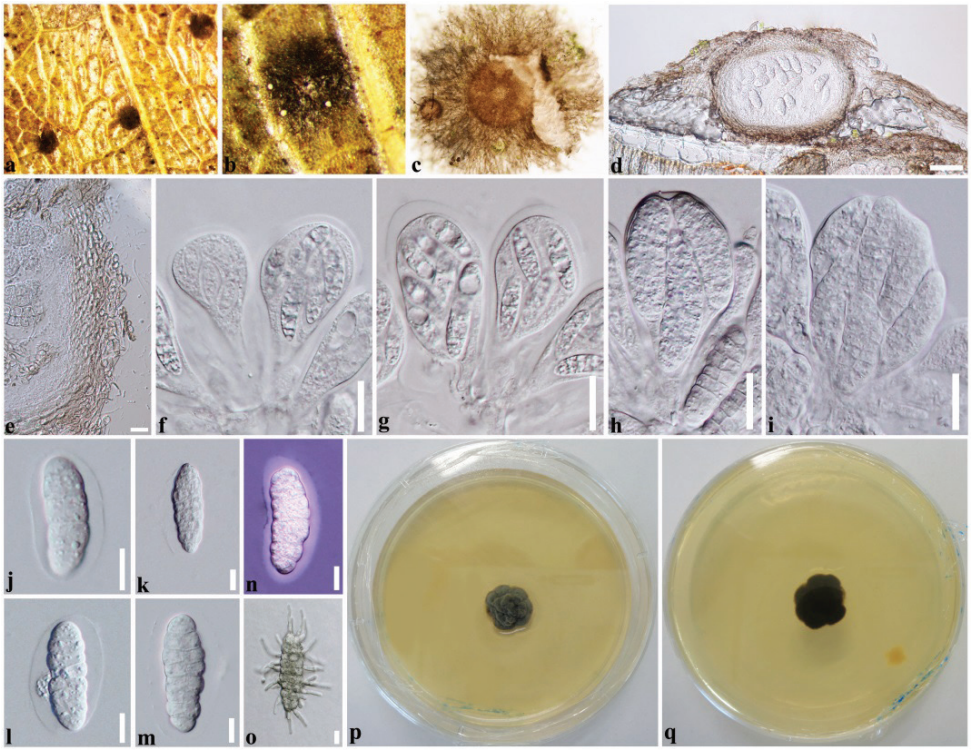

Figure 2. *Ceramothyrium longivolcaniforme* (MFLU19-0823, new host record). **a, b** Appearance of colony (black spots) on host leaf **c** mycelial pellicle **d** vertical section through ascoma **e** section of peridium **f–i** asci **j–m** ascospores **n** ascospore stained in Indian ink showing mucilaginous sheath **o** germinating ascospore **p, q** colony from above and below. Scale bars: 50 µm (**d**), 10 µm (**e**), 20 µm (**f–i**), 10 µm (**j–o**).

type material of *Ceramothyrium longivolcaniforme* (MFLU16-1306) in having elongate mycelial pellicle, broadly obovoid, short pedicellate asci and hyaline, oblong to ellipsoid, muriform ascospores with a mucilaginous sheath (Zeng et al. 2016). However, the ascospores are slightly larger (30–45 × 8–16 µm) than MFLU16-1306 (28–37 × 7–13 µm) (Table 2). *Ceramothyrium longivolcaniforme* has been previously reported from Thailand on unidentified sp. (not *F. ampelas*) and thus, we provide the new host record of *Ceramothyrium longivolcaniforme* on *Ficus ampelas* (Moraceae). Remarkably, this is the first *Ceramothyrium* species collected from Taiwan.

Longihyalospora **Tennakoon, C.H Kuo & K. D Hyde, gen. nov.**
Index Fungorum number: IF 556715
Facesoffungi number: FoF06136

Etymology. Referring to the long, hyaline ascospores.

Table 2. Comparison of ascospore characters among species of *Ceramothyrium*.

Species	Numbers of septa	Host /Locality	Size (µm)	References
C. anacardii	3	–	33–50 × 7–9.5	Batista and Maia (1956)
C. aurantii	3–6	–	18.9–27 × 5.4–8	Batista and Maia (1956)
C. biseptatum	2	*Macaranga tanarius*/ Philippines	14–16 × 4.5–5.5	Batista and Ciferri (1962)
C. boedijnii	3	*Theobroma cacao*/ Papua New Guinea	15–20 × 5–7	Batista and Ciferri (1962)
C. calycanthi	6–10	*Calycanthus* sp./ Georgia	24.5–37 × 6.5–9.5	Batista and Ciferri (1962)
C. carniolicum	3	*Pyrola rotundifolia*/ Sweden	18–20 × 4–5.5	Eriksson (1992)
C. cinereum	7	–	35–42 × 7–9	Batista and Maia (1956)
C. citricola	3–4	*Citrus aurantium*/ Brazil	14–30 × 2.5–11	Mendes et al. (1998)
C. coffeanum	3	*Coffea robusta*/ New Guinea	12–16 × 4–6	Batista and Ciferri (1962)
C. cordiae	3	*Cordia rufescens*/ Brazil	10–13.5 × 4–5.4	Eriksson (1992)
C. europaeum	3	*Pogonophora schomburgkiana*/ Brazil	16–20 × 4–5.5	Eriksson (1992)
C. globosum	6–9 transversal	–	50–58 × 5–6	Batista and Maia (1956)
C. griseolum	4–6	*Aleurites moluccana*/ Brazil	19–25 × 4–5	Eriksson (1992)
C. gustaviae	3–5	*Gustavia augusta*/ Brazil	22–25 × 3.7–5	Eriksson (1992)
C. gymnopogonis	2	*Alyxia scandens*/ Samoa	15 × 5	Dingley et al. (1981)
C. jambosae	–	*Eugenia malaccensis*/ Brazil	–	Eriksson 1992
C. linnaeae	3–4	*Lycopodium annotinum*/ Sweden	12–18 × 3–5	Constantinescu et al. 1989
C. longivolcaniforme (MFLU 16-1306)	7 transversal 6 longitudinal	Unidentified/ Thailand	28–37 × 7–13	Zeng et al. (2016)
***C. longivolcaniforme* (MFLU 19-0823)**	**7 transversal 6 longitudinal**	***Ficus ampelas* / Taiwan**	**30–45 × 8–16**	**This study (New host record)**
C. lycopodii	7	*Lycopodium annotinum*/ Sweden	45 × 4	Constantinescu et al. (1989)
C. martinii	5–7	–	20–27 × 7–9	Barr (1993)
C. moravicum	2–3	–	10–14 × 3–5	Petrak (1961)
C. paiveae	1–4	*Paivaea langsdorffii*/ Brazil	12.5–22 × 3.7–6	Mendes et al. (1998)
C. paraense	3–7	*Anacardium* sp./ Brazil	20–30 × 3.5–4	Mendes et al. 1998
C. parenchymaticum	5–7	*Didymopanax morototoni*/ Cuba	30–40 × 8–10	Batista and Ciferri 1962
C. peltatum	6–9	–	28–32 × 4.5–6.5	Batista and Maia (1956)
C. philodendri	1–7	*Philodendron imbe*/ Brazil	17.5–32.5 × 5–7.5	Mendes et al. (1998)
C. thailandicum	7–9 transversal	*Lagerstroemia* sp./ Thailand	24.7–35.5 × 5.7–8.7	Chomnunti et al. (2012)

Description. *Epiphytic* on the upper surface decaying leaves, appearing as small black dots. Covering the upper leaf surface with dark mycelium without penetrating host tissues. *Mycelial pellicle* elongate, subiculum-like, comprising hyphae that are mostly narrow, dense, dark brown. *Mycelial setae* broad, dark brown, scattered, discrete, arranged as a ring around the pellicle, unbranched, formed on dense, dark hyphae. ***Sexual morph***: *Ascomata* superficial, solitary, dark brown to black, globose to subglobose, coriaceous, uni-locular, somewhat flattened when dry, covered by a mycelial pellicle. *Peridium* pale brown to brown, with compressed, hyaline, inner cells of *textura angularis* and dark brown outer cells of *textura angularis*, fusing and indistinguishable from the host tissues. *Asci* 8-spored, bitunicate, broadly obovoid, slightly stalked, apically rounded, with a well-developed ocular chamber. *Ascospores* overlapping, irregularly triseriate, hyaline, fusiform, elongated, multi-septate, slightly constricted at the septa, tapering to the ends, smooth-walled, surrounded by a thin mucilaginous sheath. ***Asexual morph***: Not observed.

Type species. *Longihyalospora ampeli* Tennakoon, C.H Kuo & K. D Hyde.

Longihyalospora ampeli **Tennakoon, C.H Kuo & K.D. Hyde, sp. nov.**
Index Fungorum number: IF 556716
Facesoffungi number: FoF06137
Figure 3

Etymology. Species name based on the host *Ficus ampelas*, from which it was collected.

Holotype. MFLU 19-0824

Description. *Epiphytic* on the upper surface decaying leaves, appearing as small black dots. Covering the upper leaf surface with dark mycelium without penetrating host tissues. *Mycelial* pellicle (190–) 200–250 (–258) µm diam., elongate, subiculum-like, comprising hyphae that are mostly narrow, 1–2 µm wide ($\bar{x}$ = 1.5 µm, n= 20), dense, dark brown. *Mycelial setae* (197–) 200–225 (–231) µm long, at base 10–12 µm

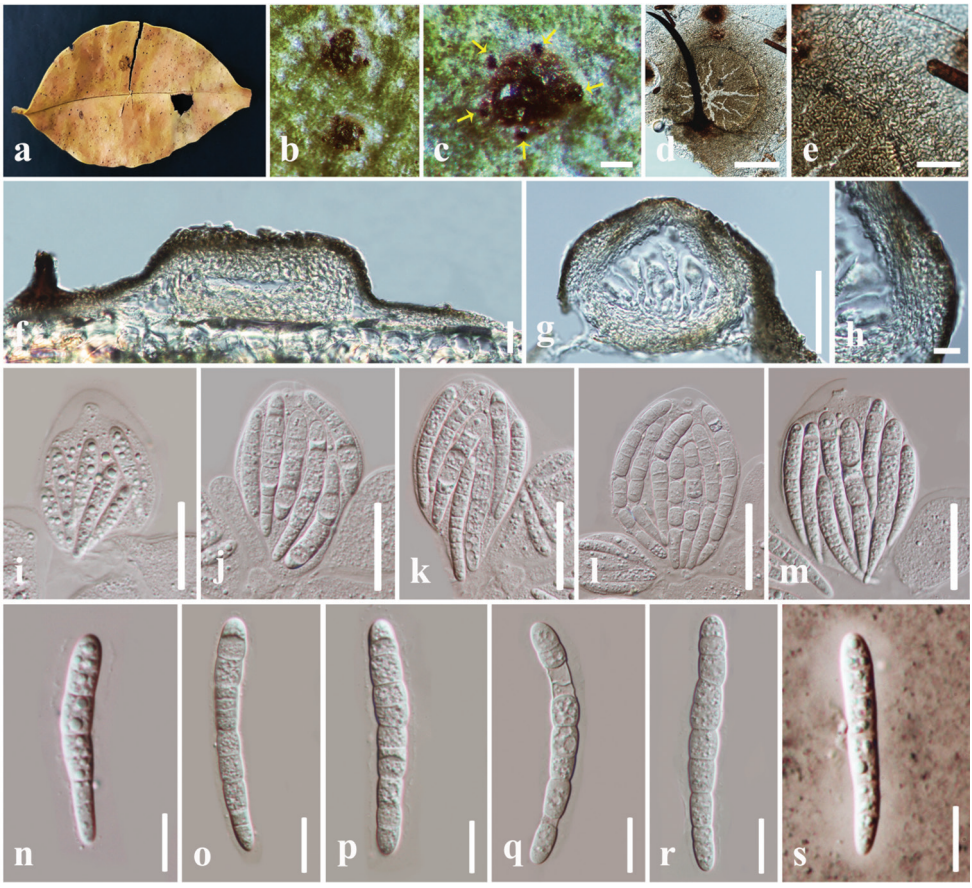

Figure 3. *Longihyalospora ampeli* (MFLU 19-0824, holotype). **a** Host leaf **b** appearance of colony (black spots) on leaf **c** ring of setae around the pellicle **d** mycelial pellicle with setae **e** mycelial pellicle cells **f, g** vertical section through ascoma **h** section of peridium **i–m** asci **n–r** ascospores **s** ascospore stained in Indian ink showing a mucilaginous sheath. Scale bars: 100 µm (**c**), 75 µm (**d**), 20 µm (**e, f**), 50 µm (**g**), 10 µm (**h**), 50 µm (**i–m**), 20 µm (**n–s**).

wide, at apex 2–3 µm wide, dark brown, scattered, discrete, arranged as a ring around the pellicle, unbranched, formed on dense, dark hyphae. ***Sexual morph***: *Ascomata* 55–90 µm high, 150–200 µm diam. ($\bar{x}$ = 76 × 168 µm, n = 10) in diameter, superficial, solitary, dark brown to black, globose to subglobose, coriaceous, uni-locular, somewhat flattened when dry, covered by a mycelial pellicle. *Peridium* 18–25 µm wide ($\bar{x}$ = 23.5 µm, n= 20), pale brown to brown, with compressed, hyaline, inner cells of *textura angularis* and dark brown outer cells of *textura angularis*. *Asci* (82–) 90–115 (–120) × 52–62 µm ($\bar{x}$ = 106 × 57 µm, n = 20), 8-spored, bitunicate, broadly obovoid, slightly stalked, apically rounded, with well-developed ocular chamber. *Ascospores* (74–) 76–98(–105) × 10–12 µm ($\bar{x}$ =84 × 10.8 µm, n = 30), overlapping, irregularly triseriate hyaline, elongate fusiform, (6–) 8–11 (–12) septa, slightly constricted at the middle septum, tapering to the ends, smooth-walled, surrounded by a 3.5–5 µm wide mucilaginous sheath. ***Asexual morph***: Not observed.

Material examined. Taiwan, Chiayi, Fanlu Township area, Dahu forest, decaying leaves of *Ficus ampelas* (Moraceae), 20 June 2018, D.S. Tennakoon, H50B1 (MFLU 19-0824, **holotype**), H50B2 (MFLU19-0825, **isotype**).

Notes. *Longihyalospora* is described herein as a new monotypic genus in Chaetothyriaceae. *Longihyalospora* differs from other genera in Chaetothyriaceae by a combination of a dark mycelium covering the upper leaf surface, an elongate mycelial pellicle, ring of setae around the pellicle, pale brown to brown peridium with hyaline inner layers, broadly obovoid, short pedicellate asci and hyaline, elongate fusiform and 8–11-septate ascospores, with tapering ends and a thin mucilaginous sheath. In our phylogenetic analyses, *Longihyalospora ampeli* species constitutes a strongly supported sub clade, which is nested independently from other genera in Chaetothyriaceae (Figure 1).

Longihyalospora vermisporum **(Hansf.) Tennakoon, C.H. Kuo & K.D. Hyde, comb. nov.**
Index Fungorum number: IF 556717
Facesoffungi number: FoF01679

≡ *Chaetothyrium vermisporum* Hansf., Mycol. Pap. 15: 151 (1946)
Morphological description: See Hansford (1946), Hofmann and Piepenbring (2006).

Recorded hosts. *Canthium* sp. (Rubiaceae) Hansford no. 1327; *Hugonia platysepalae* (Linaceae) Hansford no. 1384; *Ventilago africana* (Rhamnaceae), Hansford no. 2930 (Hansford, 1946).

Known distribution. Uganda (Hansford, 1946), Panama (Hofmann and Piepenbring 2006).

Notes. *Chaetothyrium vermisporum* was introduced by Hansford (1946) which was collected from Uganda based on morphological characteristics. Subsequently, it has been collected from Panama by Hofmann and Piepenbring (2006). After in-depth morphological investigations, we found that *Chaetothyrium vermisporum* shares some similar morphology

with *Longihyalospora ampeli* by having mycelial pellicle with ring of setae, pale brown to brown peridium and hyaline, fusiform, elongated and multi-septate ascospores (Hansford (1946). However, *Chaetothyrium vermisporum* can be distinguished from *Longihyalospora ampeli* by having hyaline surface mycelium, smaller asci (60 × 30 µm) and ascospores (35–50 × 5–6 µm) without a mucilaginous sheath, whereas *Longihyalospora ampeli* has dark brown mycelium, larger asci (90–115 × 52–62 µm) and ascospores (76–98 × 10–12 µm) with mucilaginous sheath. Therefore, we synonymized *Chaetothyrium vermisporum* under *Longihyalospora* based on high morphological similarities. Fresh collections with molecular data are needed to clarify the phylogenetic affinity of *Longihyalospora vermisporum*.

Additionally, we compared our collection with *Chaetothyrium guaraniticum* Speg. (type species of *Chaetothyrium*). *Longihyalospora ampeli* can be distinguished from *Chaetothyrium guaraniticum* by many morphological characters, viz. *C. guaraniticum* has 1-septate shorter ascospores (10–14 × 4–5 µm) and lacks a mucilaginous sheath (Spegazzini 1888), whereas *L. ampeli* has multi-septate (8–11), longer (84 × 10.8 µm) ascospores with a mucilaginous sheath. Further collections are needed to resolve the phylogenetic position and relationships between members of *Chaetothyrium* and *Longihyalospora* species.

Discussion

Sooty molds are an interesting group of fungi in tropical and temperate regions in worldwide (Chomnunti et al. 2014; Hongsanan et al. 2015; Farr and Rossman 2019; Kwon et al. 2019). Their morphology has been well-studied but their phylogenetic relationships are poorly understood due to the difficulty of obtaining good-quality DNA samples (Chomnunti et al. 2011, 2014; Zeng et al. 2016; Zeng et al. 2019). Currently, seven sooty mold forming families have been reported, viz. Antennulariellaceae Woron., Capnodiaceae Höhn., Euantennariaceae S. Hughes & Corlett ex S. Hughes, Metacapnodiaceae S. Hughes & Corlett (Dothideomycetes) and Chaetothyriaceae Hansf. ex M.E. Barr, Coccodiniaceae Höhn. ex O.E. Erikss., and Trichomeriaceae Chomnunti & K.D. Hyde (Eurotiomycetes) (Reynolds 1998; Winka et al. 1998; Hughes and Seifert 2012; Hyde et al. 2013; Chomnunti et al. 2014; Hongsanan et al. 2016).

Chaetothyriaceae species are widespread in tropical and temperate regions (Hofmann and Piepenbring 2006; Chomnunti et al. 2011, 2014; Hongsanan et al. 2015; Zeng et al. 2016; Maharachchikumbura et al. 2018; Yang et al. 2018; Farr and Rossman 2019). Wijayawardene et al. (2018) accepted 16 genera in Chaetothyriaceae, but currently only seven genera (*Aphanophora*, *Camptophora*, *Ceramothyrium*, *Chaetothyrium*, *Cyphellophoriella*, *Phaeosaccardinula* and *Vonarxia*) have DNA sequence data. The main morphological differences of Chaetothyriaceae genera are mentioned in Table 3.

Batista and Maia (1956) established the genus *Ceramothyrium* and designated *Ceramothyrium paiveae* Bat. & H. Maia as the type species, which has been collected from Brazil. *Ceramothyrium* species are characterized by a mycelial pellicle that covers the ascomata with a circumferential space around the maturing ascomata, lack of setae and hyaline, transversely pluriseptate ascospores (Batista and Maia 1956; Chomnunti et al.

Table 3. Synopsis of sexual morphs of Chaetothyriaceae genera discussed in this study.

Genus name	Ascomata or mycelium setose/ glabrous	Asci		Ascospores				References
		Shape	Number of spores/ ascus	Shape	Color	Septation	Sheath	
Actinocymbe Höhn.	Glabrous	straight to sickle shape	8	club shaped	hyaline to light brown	9		Verma and Kamal (1987)
Beelia F. Stevens & R.W. Ryan	Glabrous	broadly ellipsoidal	8	cylindrical	hyaline	5	yes	Li et al. (2011)
Camptophora Réblová & Unter.	Glabrous	long-ellipsoid to obovoid	8	obovoid to pyriform	hyaline	1–3 or muriform	no	Yang et al. (2018)
Ceramothyrium Bat. & H. Maia	Glabrous	clavate or pyriform	8	oblong to ellipsoid or cylindrical clavate	hyaline	3–10 or muriform	yes	Zeng et al. (2016), Chomnunti et al. (2012)
Ceratocarpia Rolland	Glabrous	clavate to broadly clavate	8	ellipsoid to fusiform	light brown	muriform	no	Tian et al. (2014)
Chaetothyrium Speg.	Setose	broadly ovoid or oblong	8	oblong to ellipsoidal or obovoid	hyaline	4–7 or muriform	no	Chomnunti et al. (2012), Liu et al. (2015)
Chaetothyriomyces Pereira-Carv et al.	Glabrous	broadly clavate	16	elliptical	hyaline	1	no	Pereira et al. (2009)
Euceramia Bat. & Cif.	Glabrous	ellipsoid to pyriform	8	clavate-fusoid	hyaline	4–5	no	Batista and Ciferri (1962)
***Longihyalospora* Tennakoon, C.H. Kuo & K.D. Hyde**	**Setose**	**broadly obovoid**	**8**	**fusiform and elongated**	**hyaline**	**8–11**	**yes**	**This study**
Microcallis Syd.	Glabrous	clavate	8	oblong to clavate	hyaline	1	no	Sydow (1926), Chomnunti et al. (2011)
Phaeosaccardinula Henn.	Glabrous	obovoid to oval	4–6	oblongellipsoid to reniform	hyaline or pale brown	muriform	yes	Yang et al. (2014), Maharachchikumbura et al. (2018)
Treubiomyces Höhn.	setose	clavate	8	oblong to clavate	hyaline	muriform	no	Höhnel (1909), Pohlad (1989)
Yatesula Syd. & P. Syd.	Glabrous	clavate	4–8	oblong to clavate	brownish yellow	3–4 or muriform	no	Ellis and Everhart, (1893), Sydow and Sydow (1917)

2012; Tsurumi et al. 2018). Most *Ceramothyrium* species have been collected from terrestrial habitats and their asexual morph has been recorded as *Stanhughesia* Constant. (Chomnunti et al. 2012; Réblová et al. 2013; Wijayawardene et al. 2017; Tsurumi et al. 2018). *Ceramothyrium* species seem to have a diverse distribution since they have been recorded from both temperate and tropical countries (i.e. Brazil, Canada, Georgia, Indonesia, Thailand, Panama, Philippines, South Africa, Sweden, Vietnam) (Hofmann and Piepenbring 2006; Chomnunti et al. 2012; Crous et al. 2012; Zeng et al. 2016; Tsurumi et al. 2018; Farr and Rossman 2019). Host-specificity of the taxa in this group has not yet been proven, since they have been recorded from various plant families (i.e. Arecaceae, Anacardiaceae, Ericaceae, Lycopodiaceae, Lythraceae, Melastomataceae, Podocarpaceae, Rubiaceae) (Batista and Maia 1956; Chomnunti et al. 2012; Hongsanan et al. 2015; Farr and Rossman 2019). Combined phylogenetic analyses with a larger taxon sampling provide a better resolution of interspecific relationships of *Ceramothyrium* within Chaetothyriaceae (Chomnunti et al. 2014; Zeng et al. 2016; Maharachchikumbura et al. 2018; Yang et al. 2018).

Recent studies have revealed that *Ceramothyrium* is a species rich genus. For instance, in the last few years, numerous *Ceramothyrium* species have been described. *Ceramothyrium longivolcaniforme*, *C. menglunense* were introduced by Zeng et al. (2016) and Hyde et al. (2016) respectively. Yen et al. (2018) introduced three *Ceramothyrium* species, viz. *C. aquaticum*, *C. phuquocense* and *C. exiguum*. Currently, there are 41 *Ceramothyrium* epithets in Index Fungorum (2019).

Most previous Chaetothyriaceae studies have been based on brief descriptions with line drawings and without DNA sequence data (i.e. *Actinocymbe*, *Beelia*, *Ceratocarpia*, *Chaetothyriomyces*, *Euceramia*, *Microcallis*, *Stanhughesia*, *Treubiomyces* and *Yatesul*a). Therefore, it is essential to focus on DNA sequence data to clarify the phylogenetic affinity of above genera in Chaetothyriaceae in future studies. Thus, it is necessary to collect more fungi similar to Chaetothyriaceae in different geographic regions and hosts, isolate them into cultures, describe their morphology, analyze their DNA sequences and investigate their phylogenetic relationships for a better identification and classification.

Acknowledgments

We thank the Department of Plant Medicine, National Chiayi University (NCYU) for providing facilities for DNA molecular experiment. We also thank Mae Fah Luang University grant number 56101020032 for supporting studies on Dothideomycetes. We also extend our gratitude to Dr. Shaun Pennycook for checking species' names. The authors would like to thank N.I de Silva, Wilawan Punyaboon, Chada Norphanphoun and Dr. Samantha Karunarathne for their valuable suggestions and help. K.D. Hyde thanks Chiang Mai University for the award of Visiting Professorship. R. Jeewon thanks the University of Mauritius for research support.

References

Barr ME (1993) Redisposition of some taxa described by JB Ellis. Mycotaxon 46: 45–76.

Batista AC, Ciferri R (1962) The Chaetothyriales. Beihefte zur Sydowia 3: 1–129.

Batista AC, Maia HS (1956) *Ceramothyrium*, a new genus of the family Phaeosaccardinulaceae. Atti dell'Istituto Botanico e Laboratorio Crittogamico dell'Universita di Pavia 14: 23–52.

Chomnunti P, Schoch CL, Aguirre-Hudson B, Ko-Ko TW, Hongsanan S, Jones EG, Kodsueb R, Phookamsak R, Chukeatirote E, Bahkali AH, Hyde KD (2011) Capnodiaceae. Fungal Diversity 51: 103–134. https://doi.org/10.1007/s13225-011-0145-6

Chomnunti P, Ko TWK, Chukeatirote E, Hyde KD, Cai L, Jones EG, Kodsueb R, Hassan BA, Chen H (2012) Phylogeny of Chaetothyriaceae in northern Thailand including three new species. Mycologia 104: 382–395. https://doi.org/10.3852/11-066

Chomnunti P, Hongsanan S, Aguirre-Hudson B, Tian Q, Peršoh D, Dhami MK, Alias AS, Xu J, Liu X, Stadler M, Hyde KD (2014) The sooty moulds. Fungal Diversity 66: 1–36. https://doi.org/10.1007/s13225-014-0278-5

Constantinescu O, Holm K, Holm L (1989) Teleomorph-anamorph connections in ascomycetes. 1–3. *Stanhughesia* (Hyphomycetes) new genus, the anamorph of *Ceramothyrium*. Studies in Mycology 31: 69–84.

Crous PW, Shivas RG, Wingfield MJ, Summerell BA, Rossman AY, Alves JL, Adams GC, Barreto RW, Bell A, Coutinho ML, Flory SL (2012) Fungal Planet description sheets: 128–153. Persoonia 29: 146–201. https://doi.org/10.3767/003158512X661589

Crous PW, Schumacher RK, Wingfield MJ, Lombard L, Giraldo A, Christensen M, Gardiennet A, Nakashima C, Pereira OL, Smith AJ, Groenewald JZ (2015) Fungal systematics and evolution: FUSE 1. Sydowia 67: 81–118. http://hdl.handle.net/2263/52749

Dingley JM, Fullerton RA, and McKenzie EHC (1981) Survey of Agricultural Pests and Diseases. Technical Report Volume 2. Records of Fungi, Bacteria, Algae, and Angiosperms Pathogenic on Plants in Cook Islands, Fiji, Kiribati, Niue, Tonga, Tuvalu, and Western Samoa. FAO, 485 pp.

Ellis JB, Everhart BM (1893) New species of North American fungi from various localities. Proceedings of the Academy of Natural Sciences of Philadelphia 45, 128–172.

Eriksson OE (1982) Notes on ascomycete systematics. System Ascomycete 11: 49–82.

Eriksson OE (1992) The non-lichenized pyrenomycetes of Sweden. Btjtryck, Lund, 208 pp.

Farr DF, Rossman AY (2019) Fungal databases, Systematic mycology and microbiology laboratory, ARS, USDA. http://nt.ars-grin.gov/fungaldatabases [retrieved May 10, 2019]

Hall TA (1999) BioEdit: a user-friendly biological sequence alignment editor and analysis program for Windows 95/98/NT. Nucleic Acids Symposium Series 41: 95–98.

Hansford CG (1946) The foliicolous ascomycetes, their parasites and associated fungi. Mycological Papers 15: 1–240.

Hofmann TA, Piepenbring M (2006) New records and host plants of fly-speck fungi from Panama. Fungal Diversity 22: 55–70.

Höhnel F von (1909) Fragmente zur Mykologie: VIII. Mitteilung (Nr. 354 bis 406). Sitzungsberichte der Kaiserlichen Akademie der Wissenschaften Math.-naturw. Klasse Abt. I. 118: 1157–1246.

Hongsanan S, Hyde KD, Bahkali AH, Camporesi E, Chomnunti P, Ekanayaka H, Gomes AA, Hofstetter V, Jones EG, Pinho DB, Pereira OL (2015) Fungal biodiversity profiles 11–20. Cryptogamie mycologie 36: 355–381. https://doi.org/10.7872/crym/v36.iss3.2015.355

Hongsanan S, Sánchez-Ramírez S, Crous PW, Ariyawansa HA, Zhao RL, Hyde KD (2016) The evolution of fungal epiphytes. Mycosphere 7: 1690–1712. https://doi.org/10.5943/mycosphere/7/11/6

Hongsanan S, Maharachchikumbura S, Hyde K, Samarakoon M, Jeewon R, Zhao Q, Bahkali A (2017) An updated phylogeny of Sordariomycetes based on phylogenetic and molecular clock evidence. Fungal Diversity 84: 25–41. https://doi.org/10.1007/s13225-017-0384-2

Huelsenbeck JP, Ronquist F (2001) MRBAYES: Bayesian inference of phylogenetic trees. Bioinformatics 17: 754–755. https://doi.org/10.1093/bioinformatics/17.8.754

Hughes SJ (1976) Sooty moulds. Mycologia 68: 693–820. https://doi.org/10.1080/00275514.1976.12019958

Hughes SJ, Seifert KA (2012) Taxonomic and nomenclatural notes on sooty mould name based on species mixtures: *Hormiscium handelii* and *Torula lecheriana*. Mycoscience 53: 17–24. https://doi.org/10.1007/s10267-011-0133-4

Hyde KD, Jones EBG, Liu JK, Ariyawansa H, Boehm E, Boonmee S, Braun U, Chomnunti P, Crous PW, Dai DQ, Diederich P, Dissanayake A, Doilom M, Doveri F, Hongsanan S, Jayawardena R, Lawrey JD, Li YM, Liu YX, Lücking R, Monka J, Muggia L, Nelsen MP, Pang KL, Phookamsak R, Senanayake IC, Shearer CA, Suetrong S, Tanaka K, Thambugala KM, Wijayawardene NN, Wikee S, Wu HX, Zhang Y, Begoña AH, Alias SA, Aptroot A, Bahkali AH, Bezerra JL, Bhat DJ, Camporesi E, Chukea E, Gueidan C, Hawksworth DL, Hirayama K, Hoog SD, Kang JK, Knudsen K, Li WJ, Li XH, Liu ZY, Mapook A, Mckenzie EHC, Miller AN, Mortimer PE, Phillips AJL, Raja HA, Scheuer C, Schumm F, Taylor JE, Tian Q, Tibpromma S, Wanasinghe DN, Wang Y, Xu JC, Yacharoen S, Yan JY, Zang M (2013) Families of Dothideomycetes. Fungal Divers 63: 1–313. https://doi.org/10.1007/s13225-013-0263-4

Hyde KD, Hongsanan S, Jeewon R, Bhat DJ, McKenzie EHC, Jones EBG, Phookamsak R, Ariyawansa HA, Boonmee S, Zhao Q, Abdel-Aziz FA, Abdel-Wahab MA, Banmai S, Chomnunti P, Cui BK, Daranagama DA, Das K, Dayarathne MC, de Silva NI, Dissanayake AJ, Doilom M, Ekanayaka AH, Gibertoni TB, Go´es-Neto A, Huang SK, Jayasiri SC, Jayawardena RS, Konta S, Lee HB, Li WJ, Lin CG, Liu JK, Lu YZ, Luo ZL, Manawasinghe IS, Manimohan P, Mapook A, Niskanen T, Norphanphoun C, Papizadeh M, Perera RH, Phukhamsakda C, Richter C, de Santiago ALCMA, Drechsler-Santos ER, Senanayake IC, Tanaka K, Tennakoon TMDS, Thambugala KM, Tian Q, Tibpromma S, Thongbai B, Vizzini A, Wanasinghe DN, Wijayawardene NN, Wu HX, Yang J, Zeng XY, Zhang H, Zhang JF, Bulgakov TS, Camporesi E, Bahkali AH, Amoozegar AM, Araujo-Neta LS, Ammirati JF, Baghela A, Bhatt RP, Bojantchev S, Buyck B, da Silva GA, de Lima CLF, de Oliveira RJV, de Souza CAF, Dai YC, Dima B, Duong TT, Ercole E, Mafalda-Freire F, Ghosh A, Hashimoto A, Kamolhan S, Kang JC, Karunarathna SC, Kirk PM, Kytovuori I, Lantieri A, Liimatainen K, Liu ZY, Liu XZ, Lu¨cking R, Medardi G, Mortimer PE, Nguyen TTT, Promputtha I, Raj KNA, Reck MA, Lumyong S, Shahzadeh-Fazeli SA, Stadler M, Soudi MR, Su HY, Takahashi T, Tangthirasunun N, Uniyal P, Wang Y, Wen TC, Xu JC, Zhang ZK, Zhao YC, Zhou JZ, Zhu L (2016) Fungal diversity notes 367–490: taxonomic and phylogenetic contributions to fungal taxa. Fungal Divers 80: 1–270. https://doi.org/10.1007/s13225-016-0373-x

Index Fungorum (2019) http://www.indexfungorum.org/names/Names.asp [accessed 6 May 2019]

Jayasiri SC, Hyde KD, Ariyawansa HA, Bhat J, Buyck B, Cai L, Dai YC, Abd-Elsalam KA, Ertz D, Hidayat I, Jeewon R, Jones EBG, Bahkali AH, Karunarathna SC, Liu JK, Luangsa-ard JJ, Lumbsch HT, Maharachchikumbura SSN, McKenzie EHC, Moncalvo JM, Ghobad-Nejhad M, Nilsson H, Pang KA, Pereira OL, Phillips AJL, Raspé O, Rollins AW, Romero AI, Etayo J, Selçuk F, Stephenson SL, Suetrong S, Taylor JE, Tsui CKM, Vizzini A, Abdel-Wahab MA, Wen TC, Boonmee S, Dai DQ, Daranagama DA, Dissanayake AJ, Ekanayaka AH, Fryar SC, Hongsanan S, Jayawardena RS, Li WJ, Perera RH, Phookamsak R, de Silva NI, Thambugala KM, Tian Q, Wijayawardene NN, Zhao RL, Zhao Q, Kang JC, Promputtha I (2015) The Faces of Fungi database: fungal names linked with morphology, phylogeny and human impacts. Fungal Diversity 74: 3–18. https://doi.org/10.1007/s13225-015-0351-8

Katoh K, Standley K (2013) MAFFT Multiple Sequence Alignment Software Version 7: Improvements in Performance and Usability. Molecular Biology. Evolution 30: 772–780. https://doi.org/10.1093/molbev/mst010

Kwon JH, Park K, Lee Y, Choi O, Kim J (2019) The Occurrence of Sooty Mold of Blueberry Caused by *Cladosporium sphaerospermum* in Korea. Agricultural Life Science Research 53: 151–156. https://doi.org/10.14397/jals.2019.53.1.151

Li Y, Wu H, Chen H, Hyde KD (2011) Morphological studies in Dothideomycetes: *Elsinoë* (Elsinoaceae), *Butleria*, and three excluded genera. Mycotaxon 115: 507–520. https://doi.org/10.5248/115.507

Liu JK, Hyde KD, Jones EBG, Ariyawansa HA, Bhat DJ, Boonmee S, Maharachchikumbura SSN, McKenzie EHC, Phookamsak R, Phukhamsakda C, Shenoy BD, Abdel-Wahab MA, Buyck B, Chen J, Chethana KWT, Singtripop C, Dai DQ, Dai YC, Daranagama DA, Dissanayake AJ, Doilom M, D'souza MJ, Fan XL, Goonasekara ID, Hirayama K, Hongsanan S, Jayasiri SC, Jayawardena RS, Karunarathna SC, Li WJ, Mapook A, Norphanphoun C, Pang KL, Perera RH, Peršoh D, Pinruan U, Senanayake IC, Somrithipol S, Suetrong S, Tanaka K, Thambugala KM, Tian Q, Tibpromma S, Udayanga D, Wijayawardene NN, Wanasinghe DN, Wisitrassameewong K, Zeng XY, Abdel-Aziz FA, Adamčík S, Bahkali AH, Boonyuen N, Bulgakov T, Callac P, Chomnunti P, Greiner K, Hashimoto A, Hofstetter V, Kang JC, Lewis D, Li XH, Liu XZ, Liu ZY, Matsumura M, Mortimer PE, Rambold G, Randrianjohany E, Sato G, Sri-Indrasutdhi V, Tian CM, Verbeken A, von Brackel W, Wang Y, Wen TC, Xu JC, Yan JY, Zhao RL, Camporesi E (2015) Fungal diversity notes 1–110: taxonomic and phylogenetic contributions to fungal species. Fungal Divers 72: 1–197. https://doi.org/10.1007/s13225-015-0324-y

Maharachchikumbura SSN, Haituk S, Pakdeeniti P, Al-Sadi AM, Hongsanan S, Chomnunti P, Cheewangkoon R (2018) *Phaeosaccardinula coffeicola* and *Trichomerium chiangmaiensis*, two new species of Chaetothyriales (Eurotiomycetes) from Thailand. Mycosphere 9: 769–778. https://doi.org/10.5943/mycosphere/9/4/5

Mendes MAS, da Silva VL, Dianese JC, Ferreira MASV, Santos CEN, Urben AF, Castro C (1998) Fungos em Plants no Brasil. Embrapa-SPI/Embrapa-Cenargen, Brasilia, 555 pp.

Miller MA, Pfeiffer W, Schwartz T (2010) Creating the CIPRES Science Gateway for Inference of Large Phylogenetic Trees. In: SC10 Workshop on Gateway Computing Environments (GCE10). https://doi.org/10.1109/GCE.2010.5676129

Petrak F (1961) Mykologische Bemerkungen. Sydowia 15: 204–217.

Pereira-Carvalho RC, Dornelo-Silva D, Inácio CA, Dianese JC (2009) *Chaetothyriomyes*: a new genus in family Chaetothyriaceae. Mycotaxon 107: 483–488. https://doi.org/10.5248/107.483

Pohlad BR (1989) Morphology of *Treubiomyces pulcherrimus* (Chaetothyriaceae). Canadian journal of botany 67: 40–45. https://doi.org/10.1139/b89-006

Rambaut A (2012) FigTree version 1.4.0. http://tree.bio.ed.ac.uk/software/figtree/ [accessed 10 May 2019]

Rambaut A, Suchard M, Xie W, Drummond A (2014) Tracer v. 1.6. University of Edinburgh, Edinburgh.

Rannala B, Yang Z (1996) Probability distribution of molecular evolutionary trees: a new method of phylogenetic inference. Journal of Molecular Evolution 43: 304–311. https://doi.org/10.1007/BF02338839

Réblová M, Untereiner WA, Réblová K (2013) Novel evolutionary lineages revealed in the Chaetothyriales (Fungi) based on multigene phylogenetic analyses and comparison of ITS secondary structure. PLoS One 8: 63547. https://doi.org/10.1371/journal.pone.0063547

Rehner SA, Samuels GJ (1994) Taxonomy and phylogeny of *Gliocladium* analysed from nuclear large subunit ribosomal DNA sequences. Mycological Research 98: 625–634. https://doi.org/10.1016/S0953-7562(09)80409-7

Reynolds DR (1998) Capnodiaceous sooty mold phylogeny. Canadian Journal of Botany 76: 2125–2130. https://doi.org/10.1139/b98-155

Spegazzini C (1888) Fungi Guarinitici. Pugillus II. Anales de la Sociedad Científica Argentina 26: 5–74.

Stamatakis A, Hoover P, Rougemont J (2008) A rapid bootstrap algorithm for the RAxML web servers. Systematic Biology 57: 758–771. https://doi.org/10.1080/10635150802429642

Stamatakis A (2014) RAxML version 8: a tool for phylogenetic analysis and post-analysis of large phylogenies. Bioinformatics 30: 1312–1313. https://doi.org/10.1093/bioinformatics/btu033

Swofford DL (2002) PAUP: phylogenetic analysis using parsimony, version 4.0 b10. Sinauer Associates, Sunderland.

Sydow H (1926) Fungi in intinere costaricensi collecti, pars secunda. Annales Mycologici 24: 283–426.

Sydow H, Sydow P (1917) Beitrag zur Kenntniss der Pilzflora der Philippinen-Inseln. Annales Mycologici 15: 165–268.

Tian Q, Chomnunti P, Bhat JD, Alias SA, Mortimer PE, Hyde KD (2014) Towards a natural classification of Dothideomycetes 5: The genera *Ascostratum*, *Chaetoscutula*, *Ceratocarpia*, *Cystocoleus*, and *Colensoniella* (Dothideomycetes incertae sedis). Phytotaxa 176: 42–54. https://doi.org/10.11646/phytotaxa.176.1.7

Tian Q, Doilom M, Luo ZL, Chomnunti P, Bhat JD, Xu JC, Hyde KD (2016) Introducing *Melanoctona tectonae* gen. et sp. nov. and *Minimelanolocus yunnanensis* sp. nov.(Herpotrichiellaceae, Chaetothyriales). Cryptogamie Mycologie 37: 477–493. https://doi.org/10.7872/crym/v37.iss4.2016.477

Tsurumi Y, Van Hop D, Ando K (2018) Three New Anamorph of *Ceramothyrium* from Fallen Leaves in Vietnam. Advances in Microbiology 8: 314–323. https://doi.org/10.4236/aim.2018.84021

Verma RK, Kamal R (1987) Studies on foliicolous ascomycotina – III. Some interesting bitunicati. Indian Phytopathology 40: 410–413.

Vilgalys R, Hester M (1990) Rapid genetic identification and mapping of enzymatically amplified ribosomal DNA from several *Cryptococcus* species. Journal of Bacteriology 172: 4238–4246. https://doi.org/10.1128/jb.172.8.4238-4246.1990

Von Arx JA, Müller E (1975) A re-evaluation of the bitunicate ascomycetes with keys to families and genera. Studies in Mycology 9: 1–159.

White TJ, Bruns T, Lee SJWT, Taylor JW (1990) Amplification and direct sequencing of fungal ribosomal RNA genes for phylogenetics. PCR protocols: a guide to methods and applications 18: 315–322. https://doi.org/10.1016/B978-0-12-372180-8.50042-1

Wijayawardene NN, Hyde KD, Rajeshkumar KC, Hawksworth DL, Madrid H, Kirk PM, Braun U, Singh RV, Crous PW, Kukwa M, Lucking R, Kurtzman CP, Yurkov A, Haelewaters D, Aptroot A, Lumbsch HT, Timdal E, Ertz D, Etayo J, Phillips AJL, Groenewald JZ, Papizadeh M, Selbmann L, Dayarathne MC, Weerakoon G, Jones EBG, Suetrong S, Tian Q, Castanéda-Ruiz RF, Bahkali AH, Pang KL, Tanaka K, Dai DQ, Sakayaroj J, Hujslová M, Lombard L, Shenoy BD, Suija A, Maharachchikumbura SSN, Thambugala KM, Wanasinghe DN, Sharma BO, Gaikwad S, Pandit G, Zucconi L, Onofri S, Egidi E, Raja HA, Kodsueb R, Caceres MES, Perez-Ortega S, Fiuza PO, Monteiro JS, Vasilyeva LN, Shivas RG, Prieto M, Wedin M, Olariaga I, Lateef AA, Agrawal Y, Fazeli SAS, Amoozegar MA, Zhao GZ, Pfliegler WP, Sharma G, Oset M, Abdel MA, Takamatsu S, Bensch K, Silva NI, De Kesel A, Karunarathna A, Boonmee S, Pfister DH, Lu YZ, Luo ZL, Boonyuen N, Daranagama DA, Senanayake IC, Jayasiri SC, Samarakoon MC, Zeng XY, Doilom M, Quijada L, Rampadarath S, Heredia G, Dissanayake AJ, Jayawardana RS, Perera PH, Tang LZ, Phukhamsakda C, Hernández-Restrepo M, Ma XY, Tibpromma S, Gusmao LFP, Weerahewa D, Karunarathna SC (2017) Notes for genera: Ascomycota. Fungal Diversity 86: 1–594. https://doi.org/10.1007/s13225-017-0386-0

Wijayawardene NN, Hyde KD, Lumbsch HT, Liu JK, Maharachchikumbura SSN, Ekanayaka AH, Tian Q, Phookamsak R (2018) Outline of Ascomycota. Fungal Diversity 88: 167–263. https://doi.org/10.1007/s13225-018-0394-8

Winka K, Eriksson O, Bång A (1998) Molecular evidence for recognizing the Chaetothyriales. Mycologia 90: 822–830. https://doi.org/10.1080/00275514.1998.12026976

Yang H, Chomnunti P, Ariyawansa HA, Wu HX, Hyde KD (2014) The genus *Phaeosaccardinula* (Chaetothyriales) from Yunnan, China, introducing two new species. Chaing Mai Journal of Science 41: 873–884.

Yang H, Hyde KD, Karunarathna SC, Deng C, Gu CH, Yang SA, Zhang ZC (2018) New species of *Camptophora* and *Cyphellophor*a from China, and first report of sexual morphs for these genera. Phytotaxa 343: 149–159. https://doi.org/10.11646/phytotaxa.343.2.5

Yen LTH, Tsurumi Y, Van Hop D, Ando K (2018) Three new anamorph of *Ceramothyrium* from fallen leaves in Vietnam. Advances in Microbiology 8: 314–323. https://doi.org/10.4236/aim.2018.84021

Zeng XY, Wen TC, Chomnunti PR, Liu JK, Boonme S, Hyde KD (2016) *Ceramothyrium longivolcaniforme* sp nov., a new species of Chaetothyriaceae from northern Thailand. Phytotaxa 267: 51–60. https://doi.org/10.11646/phytotaxa.267.1.5

Zeng XY, Jeewon R, Wen TC, Hongsanan S, Boonmee S, Hyde KD (2018) Simplified and efficient DNA extraction protocol for Meliolaceae specimens. Mycological Progress 17: 403–415. https://doi.org/10.1007/s11557-017-1361-6

Zeng XY, Wu HX, Hongsanan S, Jeewon R, Wen TC, Maharachchikumbura SS, Chomnunti P, Hyde KD (2019) Taxonomy and the evolutionary history of Micropeltidaceae. Fungal Diversity 97(1): 1–44. https://doi.org/10.1007/s13225-019-00431-8

Zhaxybayeva O, Gogarten JP (2002) Bootstrap, Bayesian probability and maximum likelihood mapping: exploring new tools for comparative genome analyses. BMC Genomics 3: 4. https://doi.org/10.1186/1471-2164-3-4

MycoKeys 61: 111–145 (2019)
doi: 10.3897/mycokeys.61.47520
http://mycokeys.pensoft.net

REVIEW ARTICLE

A peer-reviewed open-access journal
MycoKeys
Launched to accelerate biodiversity research

Phylogenetic overview of *Aureoboletus* (Boletaceae, Boletales), with descriptions of six new species from China

Ming Zhang[1], Tai-Hui Li[1], Chao-Qun Wang[1], Nian-Kai Zeng[2], Wang-Qiu Deng[1]

1 *State Key Laboratory of Applied Microbiology Southern China, Guangdong Provincial Key Laboratory of Microbial Culture Collection and Application, Guangdong Institute of Microbiology, Guangdong Academy of Sciences, Guangzhou 510070, China* **2** *Department of Pharmacy, Hainan Medical University, Haikou 571101, China*

Corresponding author: *Tai-Hui Li* (mycolab@263.net)

Academic editor: *M. P. Martín* | Received 23 October 2019 | Accepted 29 November 2019 | Published 17 December 2019

Citation: Zhang M, Li T-H, Wang C-Q, Zeng N-K, Deng W-Q (2019)Phylogenetic overview of *Aureoboletus* (Boletaceae, Boletales), with descriptions of six new species from China. MycoKeys 61: 111–145. https://doi.org/10.3897/mycokeys.61.47520

Abstract

In this study, species relationships of the genus *Aureoboletus* were studied, based on both morphological characteristics and a four-gene (nrLSU, *tef1-a*, *rpb1* and *rpb2*) phylogenetic inference. Thirty-five species of the genus have been revealed worldwide, forming eight major clades in the phylogenetic tree, of which twenty-four species have been found in China, including six new species: *A. glutinosus*, *A. griseorufescens*, *A. raphanaceus*, *A. sinobadius*, *A. solus*, *A. velutipes* and a new combination *A. miniatoaurantiacus* (Bi & Loh) Ming Zhang, N.K. Zeng & T.H. Li proposed here. A key to 24 known Chinese species has been provided.

Keywords

Boletes, molecular phylogeny, morphology, species identification, taxonomy

Introduction

Aureoboletus Pouzar was circumscribed in 1957, based on the type species *A. gentilis* (Quél.) Pouzar (Pouzar 1957). It was characterised by its slimy basidiomata, glabrous to subglabrous pileus and golden yellow hymenophore unchanging when dry (Quélet 1884; Saccardo 1888; Pouzar 1957). To date, 35 species have been described worldwide, 15 of which were originally described in China (Patouillard 1895; Shi and Liu 2013; Zhang et al. 2014, 2015a, b, 2017; Zeng et al. 2015; Li et al. 2016; Wu et al. 2016; Fang et al. 2019). *Aureoboletus* species can be found in tropical, subtropical and temperate regions of different continents, but most known species appear to exist in Asia and North America. Interestingly, they are strongly implicated as symbionts with an array of ectotrophic plants of the Fagaceae and Pinaceae families (Pouzar 1957; Yang et al. 2003; Klofac 2010; Shi and Liu 2013; Halling et al. 2015; Zeng et al. 2015; Wu et al. 2016; Zhang et al. 2017).

The establishment and acceptance of the genus *Aureoboletus* has a long history. *Xerocomus* section *Auripori* Singer (1942) was established to accommodate *Aureoboletus*-like taxa. Later, *Auripori* species were transferred to the genus *Pulveroboletus* Murrill (Singer 1947). For a long time, the genus *Aureoboletus* was not accepted as an independent genus by some mycologists (Smith and Thiers 1971; Corner 1972; Singer 1986; Both 1993; Bessette et al. 2000; Šutara 2005) and species with viscid basidiomata and vivid yellow hymenophores were variously placed in genera *Boletellus* Murrill, *Boletus* L., *Pulveroboletus* and *Xerocomus* Quél. (Singer 1942, 1947, 1986; Smith and Thiers 1971; Corner 1972; Both 1993; Bessette et al. 2000); However, *Aureoboletus* was accepted as an independent genus by other mycologists and the features of the genus were redefined (Watling 1965; Watling 2008; Hongo 1973; Zang 1993; Šutara 2008; Klofac 2010). A world-wide survey of the genus, based on morphological characteristics, was conducted and a key was designed to aid in the identification of 11 global *Aureoboletus* species (Klofac 2010).

Recently, broad-scale molecular phylogenetic studies have been used to investigate phylogenetic relationships amongst the genera and species in Boletes. *Aureoboletus* was strongly supported as a genus in the Boletaceae, subfamily Xerocomoideae and has been shown to be closely related to *Boletellus*, *Hemileccinum* Šutara, *Heimioporus* E. Horak, *Xerocomus* etc. (Binder 1999; Binder and Hibbett 2006; Nuhn et al. 2013; Wu et al. 2014, 2016). The genus *Sinoboletus* M. Zang, originally described in southwestern China, was proven to be a synonym of *Aureoboletus* (Zang 1992; Wu et al. 2014); *Boletellus projectellus* (Murrill) Singer, *B. mirabilis* (Murrill) Singer, *B. russellii* (Frost) E.-J. Gilbert and *Pulveroboletus auriflammeus* (Berk. & M.A. Curtis) Singer) were transferred into the genus *Aureoboletus*, based on both morphological and molecular data (Halling et al. 2015; Wu et al. 2016).

Numerous *Aureoboletus* specimens have been recently obtained in China, increasing the species diversity of *Aureoboletus*. In this study, the species richness and phylogenetic relationships were re-evaluated, based on detailed morphological observations and a four-gene phylogenetic inference. The aims were to 1) evaluate the phylogenetic relationships within the genus; 2) redefine the characteristics of *Aureoboletus*; 3) elucidate the species diversity of *Aureoboletus* in China; 4) describe the newly discovered species.

Materials and methods

Morphological studies

Photographs and records of basidiomata were obtained in the field. Specimens were dried in an electric drier and finally deposited in the Fungarium of Guangdong Institute of Microbiology (**GDGM**) or the Fungal Herbarium of Hainan Medical University (**FHMU**), Haikou City, Hainan Province, China. Descriptions of macro-morphological characters and habitats were obtained with photographs and field notes. Colours were described in general terms with serial numbers, for example, reddish-brown (9D8–9E8), following Kornerup and Wanscher (1978). Micro-morphological features were observed from dried materials after sectioning and mounting in 5% potassium hydroxide (KOH) solution and 1% Congo Red or Melzer's reagent under a light microscope (Olympus BX51, Tokyo, Japan). For basidiospore descriptions, an abbreviation [n/m/p] denotes n spores measured from m basidiomata of p collections; a notation (a–)b–c(–d) describes basidiospore dimensions, where the range b–c represented 90% or more of the measured values and 'a' and 'd' were the extreme values; Q referred to the length/width ratio of an individual basidiospore and Qm referred to the average Q value of all basidiospores ± sample standard deviation. All line-drawings of microstructures were made, based on rehydrated materials.

DNA extraction, PCR amplification and sequencing

Genomic DNA was extracted from the voucher specimens using the Sangon Fungus Genomic DNA Extraction kit (Sangon Biotech Co. Ltd., Shanghai, China), according to the manufacturer's instructions. Primer pairs LR0R/LR5 or LR0R/LR7 (Vilgalys and Hester 1990), EF1-B-F1/EF1-B-R, RPB1-B-F/RPB1-B-R and RPB2-B-F1/RPB2-B-R (Wu et al. 2014) were used for the amplification of the large subunit nuclear ribosomal RNA (nrLSU) region, the translation elongation factor 1-alpha subunit (*tef1-a*), the largest subunit of RNA polymerase II (*rpb1*) and the second largest subunit of RNA polymerase II (*rpb2*), respectively. Polymerase Chain Reaction was performed in a total volume of 25 µl containing 1 µl template DNA, 9.5 µl distilled water, 1 µl of each primer and 12.5 µl PCR mix [DreamTaqtm Green PCR Master Mix (2×), Fermentas]. Amplification reactions were performed in a Tprofessional Standard thermocycler (Biometra, Göttingen, Germany) under the following conditions: at 95 °C for 4 min, then 35 cycles of denaturation at 95 °C for 60 s, annealing at 53 °C (LSU) /55 °C (*tef1-a*, *rpb1* and *rpb2*) for 60 s and extension at 72 °C for 80 s, with a final extension at 72 °C for 8 min. The PCR products were electrophoresed on 1% agarose gels with known standard DNA markers and sequences were performed on an ABI Prism 3730 Genetic Analyzer (PE Applied Biosystems, Foster, CA, USA) at Beijing Genomic Institute (BGI) using the same primers. The raw sequences were assembled with SeqMan implemented in Lasergene v7.1 (DNASTAR Inc., USA). The assembled sequences of the specimens were submitted to GenBank.

Phylogenetic analyses

Newly generated sequences and related sequences downloaded from GenBank were used to reconstruct phylogenetic trees. Detailed information of samples, including species name, voucher, locality, GenBank accession numbers and references, are given in Table 1. Four sequence datasets (nrLSU, *tef1-a*, *rpb1* and *rpb2*) were separately aligned with MAFFT v6.853 using the E-INS-i strategy (Katoh et al. 2002) and examined in Bioedit v7.0.9 (Hall 1999). The four datasets were analysed independently using the Maximum Likelihood (ML) method to detect the topologies of the four genes. Since no significant incongruence was detected (BS > 70%), the four single-gene alignments were concatenated using Phyutility 2.2 (Smith and Dunn 2008). Missing fragments of some gene markers of several specimens were coded as missing data, intron regions of protein-coding genes were retained in the final analyses and the ambiguously aligned regions were detected and excluded with Gblocks (Castresana 2000).

The combined final dataset was analysed using RAxML v7.2.6 (Stamatakis 2006) and MrBayes v3.1.2 (Ronquist and Huelsenbeck 2003) for Maximum Likelihood (ML) and Bayesian Inference (BI), respectively. For both BI and ML analyses, the substitution model, suitable for each gene partition, was determined using the Akaike Information Criterion (AIC), complemented in MrModeltest v2.3 (Nylander 2004). All parameters in the ML analysis were kept as defaults except for choosing GTR-GAMMAI as the model and statistical supports were obtained using rapid non-parametric bootstrapping with 1000 replicates; BI analysis using 4 chains were conducted by setting generations to 80 million and stoprul command with the value of stopval set to 0.01, trees were sampled every 100 generations, the first 25% generations were discarded as burn-ins and posterior probabilities (PP) were then calculated from the posterior distribution of the retained Bayesian trees. *Phylloporus imbricatus* N.K. Zeng, Zhu L. Yang & L.P. Tang and *Xerocomus subtomentosus* (L.) Quél. were selected as outgroups, based on Wu et al. (2016) and Zhang et al. (2017).

Results

Molecular phylogenetic results

For phylogenetic analyses, 304 (102 nrLSU, 59 *tef1-a*, 71 *rpb1* and 72 *rpb2*) new sequences from 105 *Aureoboletus* collections and 171 GenBank downloaded sequences from 68 *Aureoboletus* samples were used as ingroups. Four sequences of *P. imbricatus* and *X. subtomentosus*, respectively, retrieved from GenBank were used as outgroups. The combined matrix of 175 samples with 3018 nucleotide sites was submitted to TreeBASE (Submission ID 25249). HKY+G, GTR+I+G, SYM+I and SYM+G were chosen as the best substitution models for nrLSU, *tef1-a*, *rpb1* and *rpb2*, respectively. ML and BI analyses generated almost identical tree topologies with minimal variations in statistical support values. Thus, only a ML tree is displayed (Fig. 1).

Table 1. Information of samples used in this study.

Taxon	Voucher	Country	LSU	tef1	rpb1	rpb2	Reference
A. auriflammeus	DD973	USA	AY612818	_	_	_	GenBank
A. auriporus	MAN020	Costa Rica	JQ003659	_	_	_	Neves et al. 2012
	BDCR0431	Costa Rica	HQ161871	_	HQ161840	_	Dentinger et al. 2010
A. cf. *auriporus*	GDGM 44404	USA	MN410705	_	_	_	This study
A. catenarius	GDGM 45142	China	MN204514	_	MN473157	_	This study
	HKAS54463	China	KT990509	KT990710	KT990890	KT990348	Wu et al. 2016
	HKAS54467	China	KT990510	KT990711	_	KT990349	Wu et al. 2016
A. citriniporus	REH8719	USA	KF030298	_	_	_	Nuhn et al. 2013
A. clavatus	GDGM42992	China	MK123462	MK165847	_	_	Zeng et al. 2015
	GDGM42962	China	KR052045	MK165846	KR052056	_	Zeng et al. 2015
	GDGM42963	China	KR052046	KR052054	KR052057	_	Zeng et al. 2015
	GDGM42984	China	KR052047	KR052055	_	_	Zeng et al. 2015
A. duplicatoporus	GDGM 49451	China	MN204515	_	MN473160	_	This study
	GDGM 53135	China	MN204517	MN549677	MN473167	_	This study
	GDGM 53134	China	MN204516	_	MN473166	MN549707	This study
	GDGM 52898	China	MN410708	_	MN473164	_	This study
	GDGM 53181	China	MN204518	MN549669	MN473168	_	This study
	GDGM 71293	China	MN204519	_	MN473173	_	This study
	GDGM 71724	China	MN204520	_	MN473175	_	This study
	HKAS50498	China	KF112361	KF112230	KF112561	KF112754	Wu et al. 2016
	HKAS63009	China	KT990511	KT990712	KT990891	KT990350	Wu et al. 2016
	HKAS83115	China	KT990512	KT990713	KT990892	KT990351	Wu et al. 2016
	GDGM45133	China	MK123455	MK165834	_	MN549697	This study
	GDGM52889	China	MK123456	MK165835	MN473163	_	This study
A. formosus	GDGM44441	China	KT291749	KT291744	MN473152	KT291751	Zhang et al. 2015
	GDGM44444	China	KT291750	MK165833	MN473153	KT291752	Zhang et al. 2015
A. gentilis	Pug1	Germany	DQ534635	KF030399	_	_	Nuhn et al. 2013
	MG372a	Italy	KF112344	KF134014	KF112557	KF112741	Wu et al. 2014
A. glutinosus	GDGM 55717	China	MN204522	_	_	_	This study
	GDGM 45927	China	MN204521	_	-	MN549699	This study
	GDGM44476	China	MH670254	MH700192	_	MH700228	This study
	GDGM44477	China	MH670255	MH700205	_	MH700229	This study
	GDGM44479	China	MH670256	MH700204	_	MH700230	This study
	GDGM44733	China	MH670257	MH700203	_	MH700231	This study
	GDGM44821	China	MH670258	_	_	MH700232	This study
A. griseolorufescens	GDGM28490	China	MH670278	_	_	MH700241	This study
	ZhangM131	China	MH670279	_	MH700220	MH700242	This study
A. innixus	136/98	USA	DQ534639	_	_	_	Binder and Hibbett 2007
	MB03-104	USA	KF030239	KF030400	_	_	Nuhn et al. 2013
	136	USA	KF030240	_	_	_	Nuhn et al. 2013
A. liquidus	TNS:F-39710	Japan	AB972886	_	_	_	Terashima et al. 2016
	TNS:F-52265	Japan	AB972884	_	_	_	Terashima et al. 2016
	TNS:F-52267	Japan	AB972885	_	_	_	Terashima et al. 2016
A. longicollis	GDGM 70547	China	MN204526	_	MN473172	_	This study
	GDGM 75292	China	MN204527	_	MN473179	_	This study
	GDGM 49735	China	MN204525	_	MN473161	_	This study
	GDGM 43502	China	MN204524	_	MN473150	MN549688	This study
	ZhangM56	China	MN204528	_	MN473187	_	This study
	GDGM43239	China	MK123459	MK165843	MN473147	_	This study
	HKAS80127	China	KT990515	KT990719	_	_	Zeng et al. 2015
	GDGM42849	China	KR052051	_	KR052058	_	Zeng et al. 2015
	HKAS53398	China	KF112376	KF112238	KF112625	KF112755	Zeng et al. 2015
	HKAS84679	China	KT990514	KT990718	_	KT990356	Zeng et al. 2015
	HKAS80489	China	KT990523	KT990727	_	KT990364	Zeng et al. 2015
	GDGM44734	China	MK123458	MK165842	MN473155	MN549692	This study
	GDGM53336	China	MK123460	MK165844	MN473170	MN5497018	This study
	GDGM44739	China	MK123461	MK165845	MN473156	MN549693	This study
A. marronius	GDGM43288	China	KJ488958	KT291746	_	KT291753	Zhang et al. 2014

Taxon	Voucher	Country	LSU	tef1	rpb1	rpb2	Reference
A. miniatoaurantiacus	GDGM 75495	China	MN204533	_	MN473181	MN549711	This study
	GDGM 53350	China	MN204532	MN549678	MN473171	MN549709	This study
	GDGM 43437	China	MN204530	_	MN473149	MN549687	This study
	GDGM 43282	China	MN204529	MN549671	MN473148	MN549686	This study
	GDGM 44727	China	MN204531	_	MN473154	MN549691	This study
	GDGM53501	China	MH670262	MH700199	MH700217	_	This study
	Zeng1625	China	MH670263	_	_	_	This study
	Zeng1294	China	MH670264	MH700198	_	_	This study
	Zeng1323	China	MH670265	MH700197	_	_	This study
	Zeng1339	China	MH670266	MH700196	_	_	This study
	Zeng664	China	MH670267	MH700195	_	_	This study
	HKAS59694	China	KT990513	KT990714	KT990893	KT990352	Wu et al. 2016
	GDGM42855	China	MH670259	MH700202	MH700214	MH700233	This study
	GDGM53274	China	MH670260	MH700201	MH700215	MH700234	This study
	GDGM52888	China	MH670261	MH700200	MH700216	MH700235	This study
A. mirabilis	REH9765	USA	KP327661	KP327661	_	_	Halling et al. 2015
	CBS-136.60	Germany	AF050652	_	_	_	Binder and Fischer 1997
	HKAS57776	China	KF112360	KF112229	KF112624	KF112743	Wu et al. 2014
	REH8717	USA	KF030299	_	_	_	Nuhn et al. 2013
A. moravicus	Xle1	Germany	_	KF030403	_	_	Nuhn et al. 2013
	MG374a	Italy	KF112421	KF112232	KF112559	KF112745	Wu et al. 2014
A. nephrosporus	HKAS67931	China	KT990516	KT990720	KT99089	KT990357	Wu et al. 2016
	HKAS74929	China	KT990517	KT990721	KT990896	KT990358	Wu et al. 2016
A. novoguineensis	K-A/7	Japan	DQ534637	_	_	_	Binder and Hibbett 2007
A. projectellus	MB-03-118	USA	NG027638	_	_	_	GenBank
	NYBG13392	USA	KP327622	KP327675	_	_	Halling et al. 2015
	Sn2Hor	USA	KF030300	_	_	_	Nuhn et al. 2013
	NYBG13393	USA	KP327623	KP327676	_	_	Halling et al. 2015
	ID-713	USA	DQ534582	AY879116	AY788850	AY787218	Binder and Hibbett 2007
A. quercus-spinosae	GDGM 43757	China	KY039966	MK165839	KY039962	KY039957	Zhang et al. 2017
	GDGM43757	China	KY039966	MK165839	KY039962	KY039957	Zhang et al. 2017
	GDGM43755	China	KY039967	MK165836	KY039963	KY039958	Zhang et al. 2017
	GDGM43758	China	KY039968	MK165837	KY039964	KY039959	Zhang et al. 2017
	GDGM43786	China	KY039969	MK165838	KY039965	KY039960	Zhang et al. 2017
A. raphanaceus	GDGM 45966	China	MN204536	MN549673	_	MN549700	This study
	GDGM 52266	China	MN204538	MN549674	_	MN549702	This study
	GDGM 45911	China	MN204535	_	_	MN549698	This study
	GDGM 52908	China	MN204539	MN549675	_	_	This study
	GDGM 49634	China	MN204537	_	_	MN549701	This study
	GDGM 53127	China	MN204540	MN549676	MN473165	MN549706	This study
	GDGM 75476	China	MN204541	_	MN473166	MN549707	This study
	GDGM 42937	China	MN204534	_	MN473146	MN549685	This study
	GDGM52543	China	MH670271	_	_	_	This study
	GDGM44832	China	MH670268	MH700194	MH700218	MH700236	This study
	GDGM50266	China	MH670269	_	_	MH700237	This study
	GDGM46333	China	MH670270	_	_	MH700238	This study
	GDGM52590	China	MH670272	MH700193	MH700219	MN549704	This study
A. roxanae	DS626-7	USA	KF030311	KF030402	KF030381	_	Nuhn et al. 2013
A. rubellus	GDGM52382	China	MH670273	_	_	MH700239	This study
	GDGM52367	China	MH670274	_	_	MH700240	This study
A. shichianus	HKAS43373	China	AY647211	_	_	_	GenBank
	HKAS76852	China	KF112419	KF112237	KF112562	KF112756	Wu et al. 2014
A. sinobadius	GDGM75499	China	MN204551	_	MN473182	_	This study
	GDGM 70666	China	MN204547	_	_	_	This study
	GDGM 49747	China	MN204546	_	_	_	This study
	GDGM 49670	China	MN204545	_	_	_	This study
	GDGM 71932	China	MN204548	_	MN473176	_	This study

Taxon	Voucher	Country	LSU	tef1	rpb1	rpb2	Reference
A. sinobadius	GDGM 49482	China	MN204544	_	_	_	This study
	GDGM 72253	China	MN204549	_	MN473177	_	This study
	GDGM 49432	China	MN204543	_	MN473159	_	This study
	GDGM 75477	China	MN204550	_	MN473180	_	This study
	GDGM44473	China	MH670250	MH700189	MH700211	_	This study
	GDGM43275	China	MH6702464	MH700185	MH700208	MH700221	This study
	GDGM44732	China	MH670247	MH700186	MH700207	MH700222	This study
	GDGM44730	China	MH670248	MH700187	MH700209	MH700223	This study
	GDGM44736	China	MH670249	MH700188	MH700210	MH700224	This study
A. solus	GDGM46222	China	MH670275	_	_	_	This study
	GDGM44759	China	MH670276	MH700206	_	_	This study
	GDGM42822	China	MH670277	_	_	_	This study
	GDGM 49600	China	MN410707	_	_	_	This study
	GDGM 49404	China	MN204553	_	_	_	This study
	GDGM 46807	China	MN204552	_	_	_	This study
	GDGM 72441	China	MN204555	_	_	_	This study
	GDGM 70342	China	MN204554	_	_	_	This study
Aureoboletus sp.	GDGM 49259	China	MN410706	_	MN473158	_	This study
	GDGM 71707	China	MN204556	_	MN473174	MN549710	This study
	GDGM 75305	China	MN204513	_	_	_	This study
	GDGM 70474	China	MN204511	_	_	_	This study
	GDGM 72473	China	MN204512	_	_	_	This study
	GDGM 44470	China	MN204509	MN549672	_	MN549680	This study
	GDGM 52298	China	MN204523	_	MN473162	MN549703	This study
	LAM-0466	Malaysia	KY091058	_	_	_	GenBank
	HKAS53458	China	KF112456	KF112231	KF112558	KF112742	This study
	GDGM44829	China	KY039970	_	_	KY039961	This study
	GDGM44831	China	KY039971	MK165840	_	MN549696	This study
	GDGM44469	China	KP319028	MK165841	_	MN549690	This study
A. tenuis	GDGM42601	China	KF534789	KT291745	_	KT291754	Zhang et al. 2013
A. thibetanus	HKAS76655	China	KF112420	KF112236	KF112626	KF112752	Wu et al. 2014
	GDGM43283	China	KJ907380	KT291747	_	KT291755	Zhang et al. 2014
	GDGM43284	China	KJ90738	KT291748	_	KT291756	Zhang et al. 2014
	HKAS57692	China	KT990524	KT990728	KT990901	KT990365	Wu et al. 2016
	HKAS89494	China	KT990525	KT990729	KT990902	KT990366	Wu et al. 2016
A. velutipes	GDGM52409	China	MH670252	_	_	MH700225	This study
	GDGM44713	China	MH670253	MH700191	MH700213	MH700226	This study
	GDGM42608	China	MH670251	MH700190	MH700212	MN549683	This study
A. cf. *venustus*	ZhangM142	China	MN204558	MN549668	MN473186	MN549714	This study
	A-2	China	MN204557	MN549679	MN473185	MN549713	This study
	GDGM42800	China	MK123463	_	MN473187	MN549684	This study
A. venustus	HKAS82183	China	KU321705	_	_	_	Li et al. 2016
	HKAS77700	China	KU321703	_	_	_	Li et al. 2016
A. viridiflavus	DD972	USA	AY612805	_	_	_	GenBank
A. viscidipes	GDGM 44818	China	MN204510	_	_	MN549694	This study
	HKAS77103	China	KT990519	KT990723	_	KT990360	Wu et al. 2016
	GDGM44820	China	MK123457	_	_	MN549695	This study
A. yunnanensis	GDGM 26359	China	MN204560	MN549670	MN473145	MN549681	This study
	GDGM 24560	China	MN204559	_	MN473144	MN549682	This study
	HKAS57581	China	KF112422	KF112233	KF112560	KF112746	Wu et al. 2016
	HKAS75050	China	KT990520	KT990724	KT990898	KT990361	Wu et al. 2016
A. zangii	GDGM 75881	China	MN204563	-	MN473183	MN549712	This study
	GDGM 28577	China	MN204561	_	_	_	This study
	GDGM 44406	China	MN204562	_	MN473151	MN549689	This study
	HKAS63217	China	KT990526	_	_	_	Wu et al. 2016
	HKAS74751	China	KT990521	KT990725	KT990899	KT990362	Wu et al. 2016
	HKAS74766	China	KT990522	KT990726	KT990900	KT990363	Wu et al. 2016
P. imbricatus	HKAS68642	China	KF112398	KF112299	KF112637	KF112786	Wu et al. 2014
X. aff. *subtomentosus*	HKAS58865	China	KF112389	KF112294	KF112630	KF112784	Wu et al. 2014

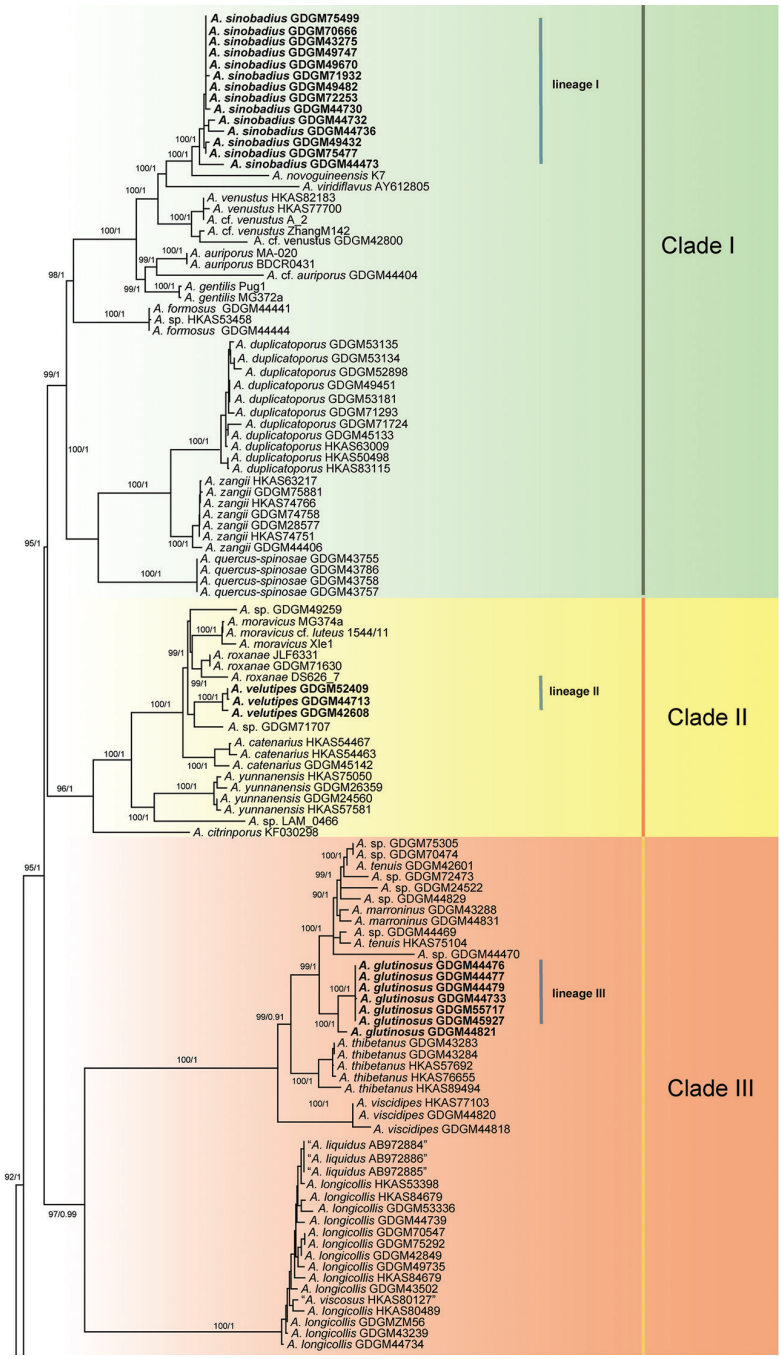

Figure 1. Maximum likelihood tree from a RAXML search using the GTRGAMMA model, illustrating the phylogeny of *Aureoboletus* and related taxa in Boletales, based on a multilocus (nrLSU, *tef1-a*, *rpb1* and *rpb2*) dataset. *Phylloporus imbricatus* N.K. Zeng, Zhu L. Yang & L.P. Tang and *Xerocomus subtomentosus* (L.) Quél. are chosen as outgroups. The lineages with new species and new combination are bold in the tree. Branches are labelled with maximum likelihood bootstrap higher than 70% and Bayesian posterior probabilities more than 0.95.

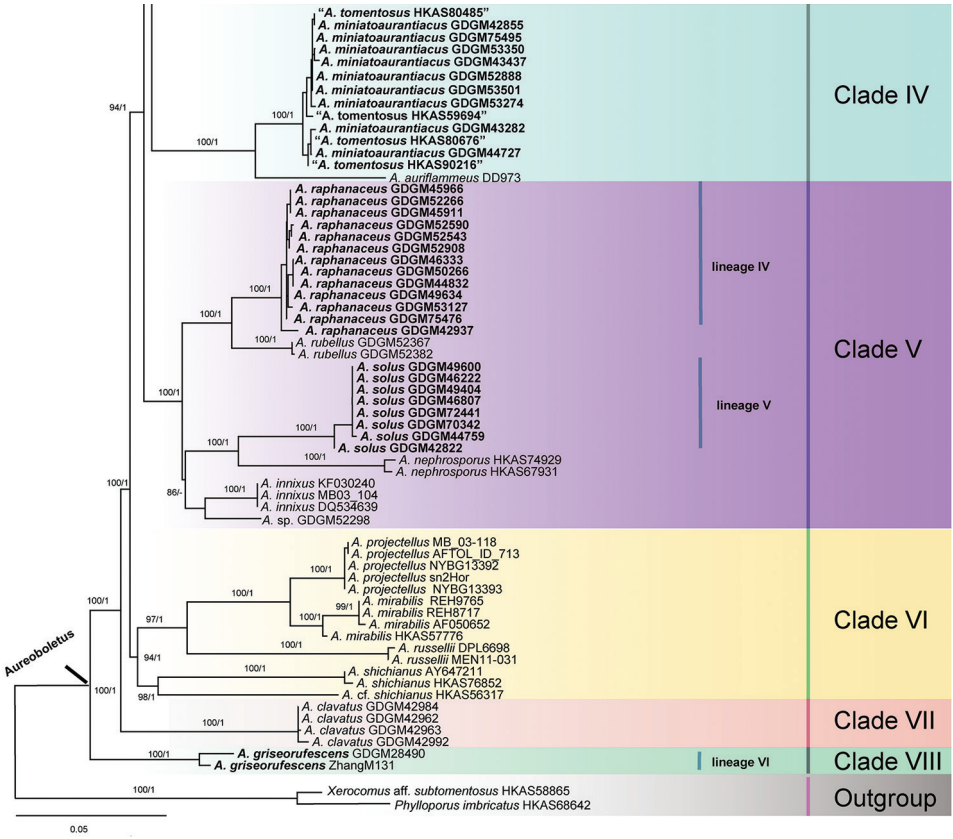

Figure 1. Continued.

In the multi-gene phylogenetic trees, the monophyly of *Aureoboletus* was statistically strongly supported (BS = 100, PP = 1); eight well supported main clades, labelled as Clade I to VIII, are shown and six well supported (BS = 100, PP = 1) new species lineages were recognised. In Clade I, nine known species [*A. auriporus* (Peck) Pouza, *A. duplicatoporus* (M. Zang) G. Wu & Zhu L. Yang, *A. formosus* Ming Zhang & T.H. Li, *A. gentilis* (Quél.) Pouzar, *A. novoguineensis* Hongo, *A. quercus-spinosae* Ming Zhang & T.H. Li, *A. venustus* Fang Li, Kuan Zhao & Qing Li Deng, *A. viridiflavus* Coker & Beers ex Klofac and *A. zangii* X.F. Shi & P.G. Liu] were presented, including the type species *A. gentilis* and a new lineage (lineage I) discovered in this study. Lineage I is presented as a sister group to *A. novoguineensis* with significant statistical support (BS = 100, PP = 1). Clade II comprised five known species [*A. catenarius* G. Wu & Zhu L. Yang, *A. citriniporus* (Halling) Klofac, *A. moravicus* (Vaček) Klofac, *A. roxanae* (Frost) Klofac and *A. yunnanensis* G. Wu & Zhu L. Yang], a new lineage (lineage II) and three unnamed sequences. Lineage II is closely related to an unnamed sample (GDGM71707) from southern China. Clade III is composed of six species, [*A. longicollis* (Ces.) N.K. Zeng & Ming Zhang, *A. marroninus* T.H. Li & Ming Zhang, *A. tenuis* T.H. Li & Ming Zhang, *A. thibetanus* (Pat.) Hongo & Nagas., *A. viscidipes*

(Hongo) G. Wu & Zhu L. Yang] and a new lineage (lineage III), all of which are from Asia. Clade IV was comprised of the North American species *A. auriflammeus* (Berk. & M.A. Curtis) G. Wu & Zhu L. Yang and a new species combination from China. Clade V included five strongly supported species level groups [*A. innixus* (Frost) Halling, A.R. Bessette & Bessette, *A. nephrosporus* G. Wu & Zhu L. Yang, *A. rubellus* Kuan Zhao & G. Wu] and two new lineages (lineage IV and lineage V). Clade VI included four known species [*A. mirabilis* (Murrill) Halling, *A. projectellus* (Murrill) Halling, *A. russellii* (Frost) G. Wu & Zhu L. Yang from North America and *A. shichianus* (Teng & L. Ling) G. Wu & Zhu L. Yang from China]. Clade VII had a single species, *A. clavatus* N.K. Zeng & Ming Zhang, which was recently reported in southern China. Clade VIII represents a single new lineage (lineage VI), which is the basal group of the genus *Aureoboletus*.

Taxonomy

Aureoboletus Pouzar, Česká Mykol. 11: 48, 1957.

Type species. *Aureoboletus gentilis* (Quél.) Pouzar.

Description. Basidiomata small to large. Pileus viscid, dry or sticky when wet, even or smooth to wrinkled, usually subtomentose, rarely glabrous, with or without veil or velar residues hanging at margin. Context white to yellowish-white, usually pinkish to reddish-brown beneath pileipellis, unchanging or changing blue or greenish or pastel red when exposed. Tubes coloured with all kinds of yellows, pale yellow, golden yellow to bright yellow, unchanging or slightly changing to blue when bruised, pores circular to angular, smaller to larger, somewhat relatively larger and shallowly depressed around the stipe, concolorous with tubes. Stipe central, cylindrical or clavate, surface glabrous to striate fibrillose, never or rare forming reticulation or *Leccinum*-like scabrous, dry to viscid, with white basal mycelium. Basidiospores smooth to verrucose or longitudinally striate, subfusiform, oblong ovoid to subglobose, yellowish to yellowish-brown in KOH. Hymenophoral trama boletoid, composed of subcylindrical to cylindrical hyphae, colourless. Pleurocystidia fusiform to subclavate, thin- or thick-walled, sometimes containing golden-yellow contents at first, then gradually changing to yellowish-white to hyaline in 5% KOH. Cheilocystidia present, infrequent or absent, usually similar to pleurocystidia in shape and size, if present. Pileipellis as an interwoven trichoderm, trichoderm or ixotrichoderm, consisting of erect hyphae which are occasionally branched, cylindrical to clavate, thin- to slightly thick-walled, usually less than 1 μm. Stipitipellis hymeniform, as an ixotrichoderm to intricated ixotrichoderm. Caulocystidia clavate, fusoid or ventricose-fusoid. Stipe trama composed of parallel hyphae. Clamp connections absent.

Distribution and ecology. World-wide distribution, mainly known from subtropical Asia and temperate zones of the Northern hemisphere, growing on the ground associated with Fagaceae and other broadleaf trees.

Descriptions of six new species and one new combination of *Aureoboletus*

***Aureoboletus glutinosus* Ming Zhang & T.H. Li, sp. nov.**
MycoBank No: 827103
Figs 2A, B, 3A, 4A–E

Diagnosis. This species is distinguished from other *Aureoboletus* taxa by its smaller and glutinous basidiomata, reddish-brown to ruby pileus usually with irregular reticulation and darker folds, gelatinised veil remnants and smooth basidiospores 10–13.5 × 4.5–5 μm in size.

Etymology. "*glutinosus*" refers to the glutinous basidiomata.

Type. China, Hunan Province, Rucheng Town, Jiulongjiang National Forest Park, on soil and usually growing amongst the mosses under the broadleaf forest, at 25°38'N, 113°77'E, alt. 300 m, 8 May 2014, M. Zhang (holotype: GDGM44477).

Description. Basidiomata small-sized. Pileus 1–2 cm wide, obtuse to convex, becoming broadly convex to plane, fleshy, viscid, especially when young and wet, reddish-brown, violet brown to greyish-ruby (9E6–12E6, 9E7–12E7), slightly fading to pale yellow (2A3–4A3) towards margin, usually forming a pale yellow to even nearly white zone at margin, distinctly wrinkled and often reticulate irregularly with somewhat darker folds at centre, strongly glutinous or mucilaginous when fresh; margin somewhat involute to nearly flat, often attached with yellowish-white to subhyaline and strongly gelatinised veil remnants. Context 2–5 mm thick at stipe, firm and tough in youth, soft when matured, white on the whole, greyish-red (10B5–11B5) beneath pileipellis, practically unchanging to becoming slightly greyish-pinkish or greyish-red (10B5–11B5) when exposed. Tubes 7–10 mm deep, distinctly depressed around stipe, yellowish-white (2A2–4A2) when young, becoming pale yellow, greyish-yellow, pastel yellow to olive yellow (2A3–4A3, 1B3–2B3, 2A4–3A4, 2C6–3C6) with age, often with an olive tint, unchanging when bruised. Pores 0.3–0.5 mm in diam., mostly subangular, slightly radially elongated around stipe at maturity, smaller near pileus margin, concolorous with tubes. Stipe 15–40 × 2–4 mm, central, cylindrical or narrowly clavate, solid, equal to slightly tender downwards, greyish-orange (6B4), greyish-red (7B4) to brownish-orange (6C4–7C4), without reticulation, smooth to faintly longitudinally striate, gelatinous or strongly viscid when young and wet, usually covered with a mucilaginous layer, with white basal mycelium. Odour not distinct. Taste mild.

Basidiospores [150/4/4] (9.5–)10–13.5 × (4–)4.5–5 μm, Q = (2.2–)2.3–2.5(–2.7), Q_m = 2.48 ± 0.18, subfusiform and inequilateral in side view, oblong in ventral view, smooth, yellowish to yellowish-brown in 5% KOH and yellow brown to dark brown in Melzer's reagent, thin-walled. Basidia 20–30 × 7–10 μm, clavate, 4-spored, sterigmata 2–4.5 μm long, yellowish-white to hyaline in 5% KOH, without basal clamps. Pleurocystidia 35–60 × 8–13 μm, fusiform, thin-walled. Cheilocystidia frequent, similar to pleurocystidia in shape and size. Hymenophoral trama composed of subparallel hyphae 4–10 μm broad, yellowish-white to hyaline in 5% KOH. Pileipellis an ixotrichodermium of erect hyphae 5–12 μm in diameter, branched, yellowish-white to hyaline

Figure 2. Basidiomata of six new species and one new combination of *Aureoboletus* from China. **A, B** *A. glutinosus* (**A** GDGM44476 **B** GDGM44477, holotype) **C** *A. griseorufescens* (GDGM28490, holotype) **D, E** *A. miniatoaurantiacus* (**D** GDGM43439 **E** GDGM43282) **F, G** *A. raphanaceus* (**F** GDGM45911, holotype **G** GDGM52890) **H, I** *A. sinobadius* (**H** GDGM44732 **I** GDGM 71932, holotype) **J, K** *A. solus* (GDGM44759, holotype) **L** *A. velutipes* (**L** GDGM44713, holotype). Scale bars: 2 cm.

in 5% KOH, dextrinoid in Melzer's reagent; terminal cells 27–50 × 7–12 µm, cylindrical, clavate or nearly fusoid. Stipitipellis a layer of repent to suberect branching hyphae 3–6 µm in diam., hyaline in 5% KOH. Clamp connections absent in all tissues.

Ecology and distribution. Solitary or scattered on ground with humus and debris, usually growing amongst the mosses (*Fissidens* sp. and *Pottiaceae* sp.) under Fagaceae, mixed with other broadleaf trees, alt. 300–500 m; May to July, known from Guangdong and Anhui Province.

Additional specimens examined. China, Hunan Province, Chenzhou City, Rucheng Town, Jiulongjian National Forest Park, 8 May 2014, H. Huang (GDGM44476); Same location, 12 June 2015, M. Zhang (GDGM44733); Anhui Province, Huangshan City, Huangshan National Forest Park, 27 July 2015, C.H. Li (GDGM44821).

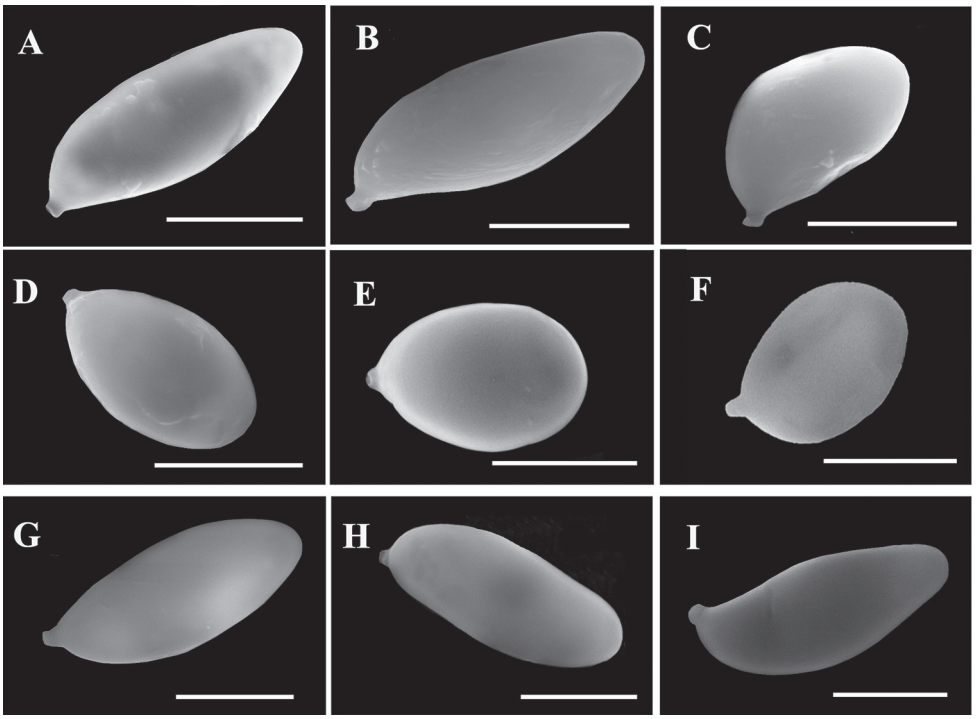

Figure 3. Scanning electron micrograph of basidiospores of six new species and one new combination of *Aureoboletus* from China. **A** *A. glutinosus* (GDGM44477, holotype) **B** *A. griseorufescens* (GDGM28490, holotype) **C, D** *A. miniatoaurantiacus* (**C** GDGM43439 **D** GDGM4855) **E, F** *A. raphanaceus* (GDGM45911, holotype) **G** *A. sinobadius* (GDGM71932, holotype) **H** *A. solus* (GDGM44759, holotype) **I** *A. velutipes* (GDGM44713, holotype). Scale bars: 5 μm.

Notes. Phylogenetic analyses showed that *A. glutinosus* is closely related to *A. marroninus*, *A. tenuis*, *A. thibetanus* and *A. viscidipes*; however, the independent phylogenetic position and different morphological characters can distinguish *A. glutinosus* from these similar species. *Aureoboletus marroninus* differs in having a more wrinkled and darker (violet brown or maroon) pileus, white context and smaller basidiospores 8.5–10 × 4–4.5 μm (Zhang et al. 2014). *Aureoboletus tenuis* has relatively larger basidiomata (pileus up to 3.5 cm broad) usually lacking well-developed veil remnants on pileus margin, smaller basidiospores 11–12 × 4–5 μm and ixotrichodermial stipitipellis composed of terminal hyphae with swollen tips (Zhang et al. 2014). *Aureoboletus thibetanus* is readily separated by its more robust basidiomata (pileus up to 5 cm broad), white ridged reticulation on pileus surface, white stipe and yellowish granular encrustation on cystidia and only known from the temperate zone in southwest China (Patouillard 1895; Yang et al.2003; Klofac 2010). *Aureoboletus viscidipes* differs in having a brownish to brown pileus tinged with yellowish-white, a longer (up to 4 cm long) and nearly white stipe and a thick layer of a reflective pale-yellow substance on the surface of cheilocystidia and pleurocystidia (Wu et al. 2016).

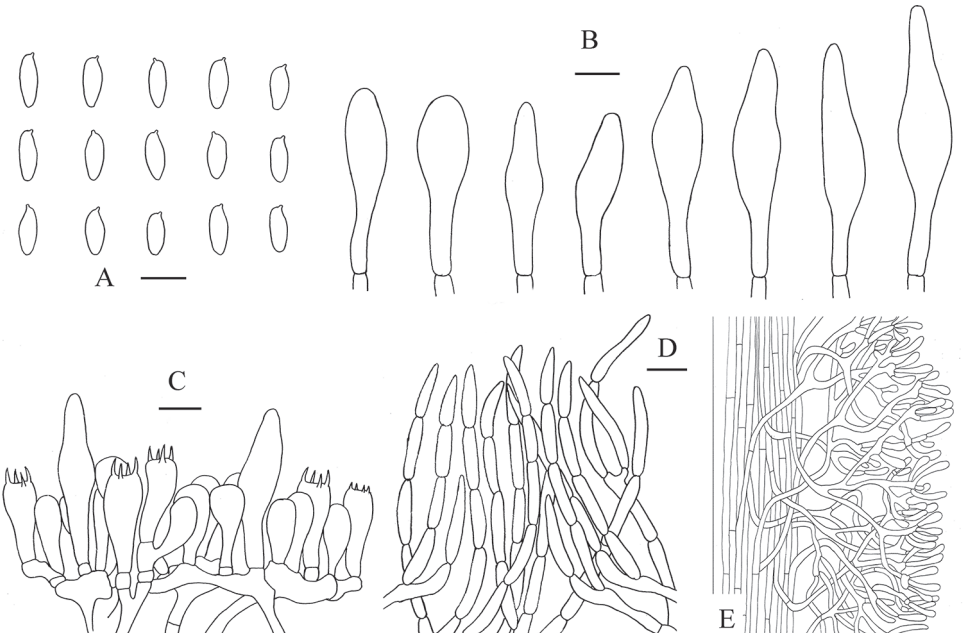

Figure 4. *Aureoboletus glutinosus*. **A** Basidiospores **B** Cheilocystidia and pleurocystidia **C** Basidia and pleurocystidia **D** Pileipellis **E** Stipitipellis. Scale bars: 10 μm (**A–C**); 20 μm (**D, E**).

***Aureoboletus griseorufescens* Ming Zhang & T.H. Li, sp. nov.**
MycoBank No: 827104
Figs 2C, 3B, 5A–E

Diagnosis. This taxon can be distinguished from other *Aureoboletus* species by its brownish-orange to ruby pileus colour, white to yellowish-white context changing to greyish-red or greyish-rose when exposed, light yellow tubes and comparatively small basidiospores 9–10.5 × 4.5–5 μm.

Etymology. "*griseorufescens*" refers to the greyish-red discolouration of context when exposed or bruised.

Type. China, Guangdong Province, Shaoguan City, Chebaling National Natural Reserve, on soil under the broadleaf forest dominated by Fagaceae trees, alt. 300 m, 23°22'N, 113°42'E, 15 July 2008, C.Y. Deng (holotype: GDGM28490) .

Description. Basidiomata small to medium-sized. Pileus 2–5 cm wide, hemispheric when young, becoming convex to nearly plane in age, fleshy, subviscid or slightly viscid when wet, glabrous to minutely velvet-subtomentose, slightly wrinkled to rugulose, even or nearly so at margin, brownish-orange, brownish-red, dark red to greyish-ruby (6C6–7 to 11C6–7). Context 3–6 mm thick at centre, firm and tough, white to yellowish-white (2A1–2 to 3A1–2), more or less greyish-red (9C4–11C4) beneath the pileipellis and browner at the border line adjacent to tubes, gradually changing to greyish-red (9C4–11C4) to greyish-rose (12B5) when exposed. Tubes 2–4 mm deep, light yellow, yellow, pastel yellow

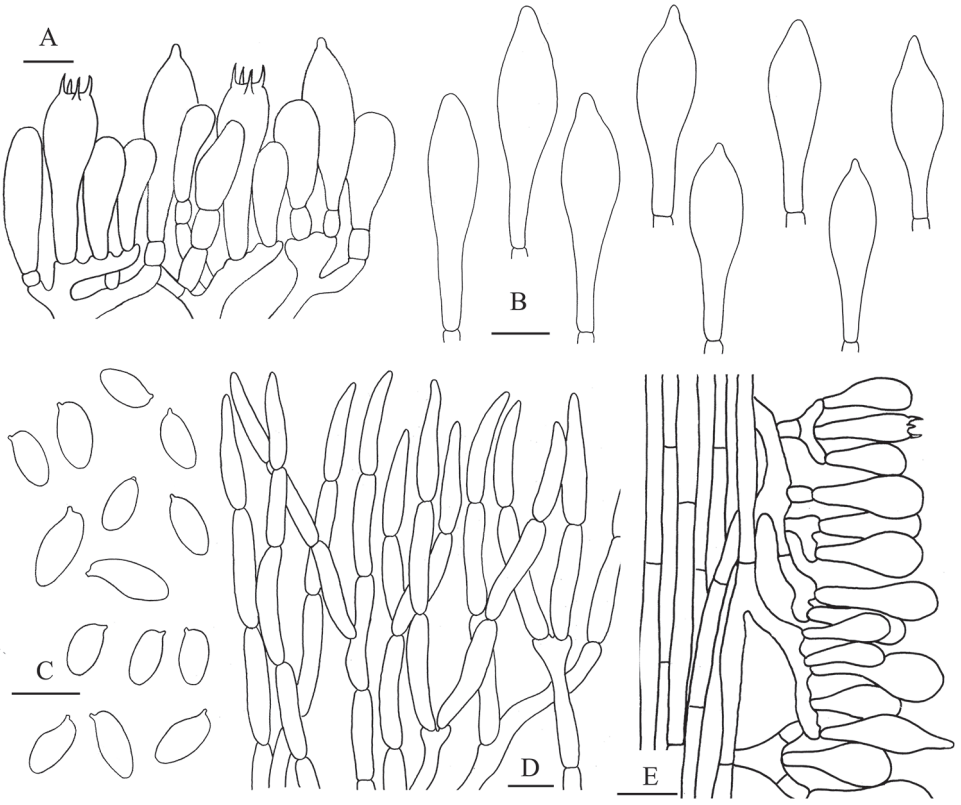

Figure 5. *Aureoboletus griseorufescens*. **A** Basidia and pleurocystidia **B** Cheilocystidia and pleurocystidia **C** Basidiospores **D** Pileipellis **E** Stipitipellis. Scale bars: 10 μm (**A–C**); 20 μm (**D, E**).

to greenish-yellow (2A5, 3A4–6), unchanging when bruised. Pores small, 1–2 per mm, circular to angular, somewhat relatively larger and shallowly depressed around the stipe at maturity, concolorous with tubes, unchanging when bruised. Stipe 35–60 × 4–10 mm, central, cylindrical or clavate, equal to slightly enlarged downwards, smooth, viscid in wet condition, concolorous with pileus, pale in the apex. Stipe context white to reddish-white (9A2–11A2), gradually changing to greyish-red (9C4–11D5) to greyish-rose (12B5) when exposed, especially in the lower part. Basal mycelium white. Odour none. Taste mild.

Basidiospores [50/2/2] (8–)9–10.5(–11) × (4–)4.5–5(–5.5) μm, Q = (1.8–)2–2.2(2.6), Q_m = 2.19 ± 0.18, subfusiform and inequilateral in side view, oblong in ventral view, smooth, yellowish to yellowish-brown in 5% KOH and yellow brown to dark brown in Melzer's reagent, thin-walled. Basidia 4-spored 25–30 × 7–11 μm, clavate, yellowish-white to hyaline in 5% KOH, sterigmata 2–3 μm. Cheilocystidia infrequent. Pleurocystidia 43–70 × 8–13 μm, fusiform, thin-walled, yellowish-white to hyaline in 5% KOH. Hymenophoral trama composed of subparallel hyphae 5–8 μm broad, yellowish-white to hyaline in 5% KOH. Pileipellis an entangled trichodermium of erect hyphae 12–19 μm in diameter, branched, yellowish-white to

hyaline in 5% KOH, yellow brown to dark brown in Melzer's reagent, terminal cells 20–50 × 6–10 μm, cylindrical, clavate or nearly fusoid. Stipitipellis a tangled layer of repent to suberect branching hyphae 7–10 μm in diam., hyaline in 5% KOH, with terminal cells 22–30 × 7–18 μm. Caulocystidia 43–58 × 12–18 μm, numerous, in clusters, clavate, fusoid or fusoid ventricose, mostly clavate, swollen at apex and usually contain yellow to yellowish-brown substance at an early stage in 5% KOH. Clamp connections absent in all tissues.

Ecology and distribution. Solitary or scattered on ground with humus and debris under Fagaceae trees, mixed with other broadleaf trees, alt. 200–400 m; June to September; currently only known from southern China.

Additional specimens examined. China, Hainan Province, Changjiang County, Bawangling National Forest Park, 7 July 2013, M. Zhang (ZhangM131).

Notes. *Aureoboletus griseorufescens* is somewhat similar to the recently reported species *A. venustus* from southern China; however, the latter taxon differs in having relatively larger (pileus up to 8 cm) and more viscous basidiomata, a reddish-orange pileus and broader basidiospores 7.5–10.5 × 5–6 μm (Li et al. 2016). In addition, *A. griseorufescens* formed a separate species level branch at the base of the phylogenetic tree (Fig. 1), indicating that it is in an independent phylogenetic position.

Aureoboletus raphanaceus Ming Zhang & T.H. Li, sp. nov.

MycoBank No: 827106
Figs 2F, G, 3E, F, 6A–E

Diagnosis. This species can be easily distinguished from other *Aureoboletus* taxa by its dry and yellowish-white to pinkish-white pileus covered with fibrillose to tomentose squamules, radish smell and ovoid basidiospores 7.5–9 × 5–6 μm.

Etymology. "*raphanaceus*" refers to the radish smell of the new species.

Type. China, Jiangxi Province, Chongyi Town, Yangling National Forest Park, on soil under the broadleaf forest dominated by Fagaceae trees, at 25°28'N, 114°19'E, alt. 300 m, 1 September 2016, H. Huang (holotype: GDGM45911).

Description. Basidiomata small to medium-sized. Pileus 3–8 cm wide, hemispheric when young, becoming convex to nearly plane in age, fleshy, dry or slightly viscid when wet, covered with greenish-grey, yellowish-grey to brownish-grey (1D2–10D2) fibrillose to tomentose squamules on yellowish-white (1A2–4A2) to pinkish-white background, slightly wrinkled at disc; margin thin, slightly incurved at first, then extending. Context 8–12 mm thick at centre, firm and tough in youth, becoming soft, white, more or less pinkish, brownish-orange (5C4–7C4), greyish-red (8C4–10C4) to light brown (5D4–7D4) beneath the pileipellis, unchanging or slightly changing blue near the hymenophore when exposed. Tubes 4–7 mm deep, greyish-yellow (1B5–3B5), light yellow (1A5–3A5) to yellow (2A7–3A7), unchanging when bruised. Pores small, 0.5–1 per mm, circular to angular, somewhat relatively larger and shallowly depressed around the stipe at maturity; pore-surface concolorous with tubes, unchanging when

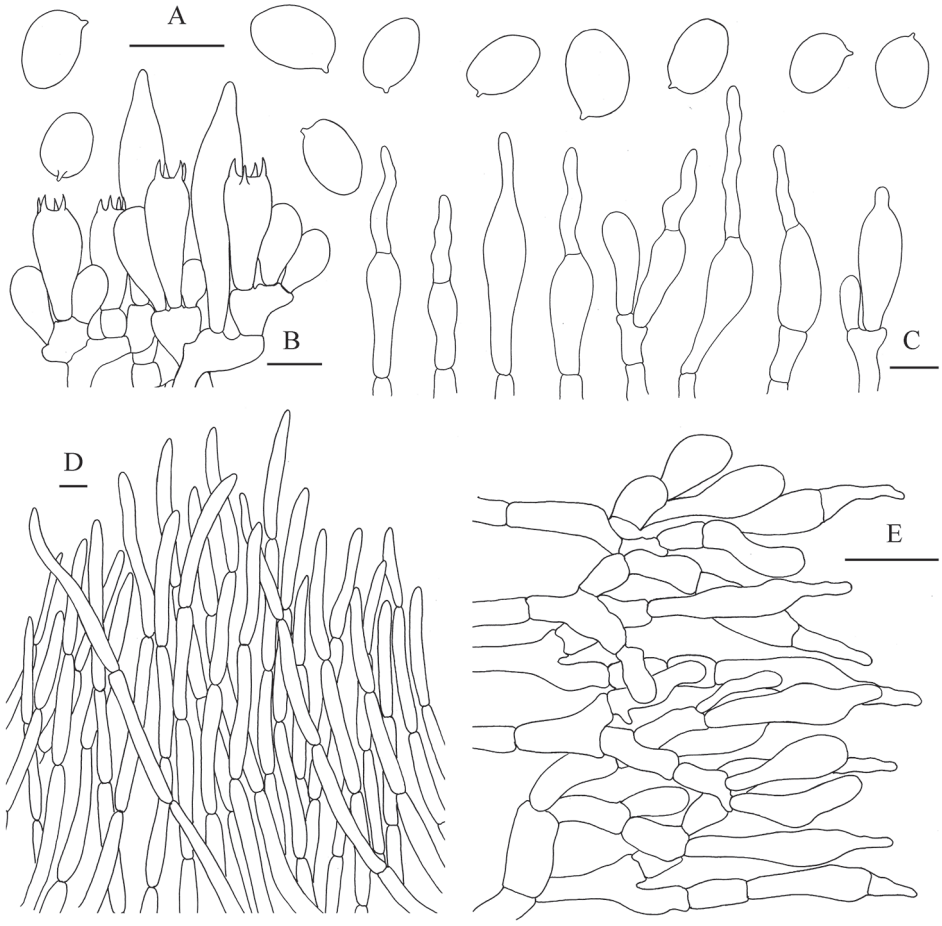

Figure 6. *Aureoboletus raphanaceus*. **A** Basidiospores **B** Basidia and pleurocystidia **C** pleurocystidia **D** Pileipellis **E** Stipitipellis. Scale bars: 10 μm (**A–C**), 20 μm (**D, E**).

hurt. Stipe 20–40 × 8–15 mm, central, cylindrical or clavate, equal to slightly enlarged downwards, dry, concolorous with pileus, longitudinally streaked and faintly pruinose or tomentose, with a very pale flush of pastel red (8A5–10A5) zone at apex. Stipe context white to yellowish-white, slightly changing pale yellow (2A3–4A3) when exposed, especially in the lower part. Basal mycelium white. Odour as radish. Taste mild.

Basidiospores [80/3/3] (7–)7.5–9(–10) × 5–6 μm, Q= (1.27–)1.45–1.6(–1.7), Q_m = 1.51 ± 0.08, ovoid and inequilateral in side view, ovoid in ventral view, smooth, yellowish to pale brown in 5% KOH and yellowish-brown in Melzer's reagent, thin-walled. Basidia 20–30 × 8–11 μm, clavate, 4-spored, rarely 1-, 2-, 3-spored, yellowish-white to hyaline in 5% KOH, without basal clamps, sterigmata 2–3.5 μm long. Pleurocystidia 30–60 × 8–13 μm, fusiform, thin-walled, usually containing golden-yellow contents at first, gradually changing yellowish-white to hyaline in 5% KOH. Cheilocystidia infrequent, similar to pleurocystidia in shape and size. Hymenophoral trama

composed of subparallel hyphae 5–23 μm broad, yellowish-white to hyaline in 5% KOH. Pileipellis an ixotrichodermium to trichodermium of erect hyphae 4–12 μm in diameter, usually covered with yellow to brownish-yellow pigment slightly dissolving in 5% KOH, branched, yellowish-white to hyaline in 5% KOH, dextrinoid in Melzer's reagent; terminal cells cylindrical, clavate or nearly fusoid. Stipitipellis a layer of suberect branching hyphae 4–15 μm in diameter, hyaline in 5% KOH. Caulocystidia 30–60 × 8–12 μm, numerous, in clusters, fusiform to lageniform and usually contain yellow to yellowish-brown substance in an early stage in 5% KOH. Clamp connections absent in all tissues.

Ecology and distribution. Solitary or scattered on ground with humus and debris under Fagaceae trees mixed with other broadleaf trees, alt. 300–1300 m; June to September; Currently known from Jiangxi and Hunan Province.

Additional specimens examined. China, Jiangxi Province, Chongyi County, Yangling National Forest Park, alt. 550 m, 1 September 2016, M. Zhang (GDGM52908); Same locality and date B. Song (GDGM53127), M. Zhang (GDGM52266 and GDGM50266), H Huang (GDGM52890); Hunan Province, Guidong Town, Bamianshan National Nature Reserve, alt. 1250 m, 18 June 2016, Z.P. Song (GDGM52543 and GDGM46333).

Notes. The yellowish-white basidioma colour makes it easy to distinguish *A. raphanaceus* from the other species. *Boletus orientialbus* N.K. Zeng & Zhu L. Yang recently described from China is somewhat similar to *A. raphanaceus* in colour; however, *B. orientialbus* differs in having more robust basidiomata, smooth pileus, reticulate stipe and smaller basidiospores 7–10 × 4.5– 5 μm (Zeng et al. 2013).

Aureoboletus sinobadius Ming Zhang & T.H. Li, sp. nov.

MycoBank No: 827101
Figs 2H, I, 3G, 7A–F

Diagnosis. This species is distinguished from other *Aureoboletus* species by its pastel red to reddish-brown pileus, light yellow hymenophore unchanging when bruised, salty taste and two different shapes of basidiospores.

Etymology. "*sino-*" refers China, the holotype's location of the species; "*badius*" means the brownish-red or chestnut pileus colour.

Type. China, Guangdong Province, Guangzhou City, Baiyun Mountain Scenic Area, on soil and usually growing amongst moss under broadleaf forest, dominated by Fagaceae trees, alt. 280 m, 18 May 2018, M. Zhang (holotype: GDGM71932).

Description. Basidiomata medium to large-sized. Pileus 5–10 cm wide, hemispheric when young, becoming convex to nearly plane in age, fleshy, viscid, especially when young and wet, glabrous to minutely velvet-subtomentose, slightly wrinkled, usually violet brown (10E5–8 to 12E5–8) when young, gradually fading to pastel red (8A5–10A5), brownish-red (9C7–10C7), reddish-brown to brownish-violet (9D6–11D6, 9D7–11D7) at maturity, with a thin and slightly incurved margin. Context

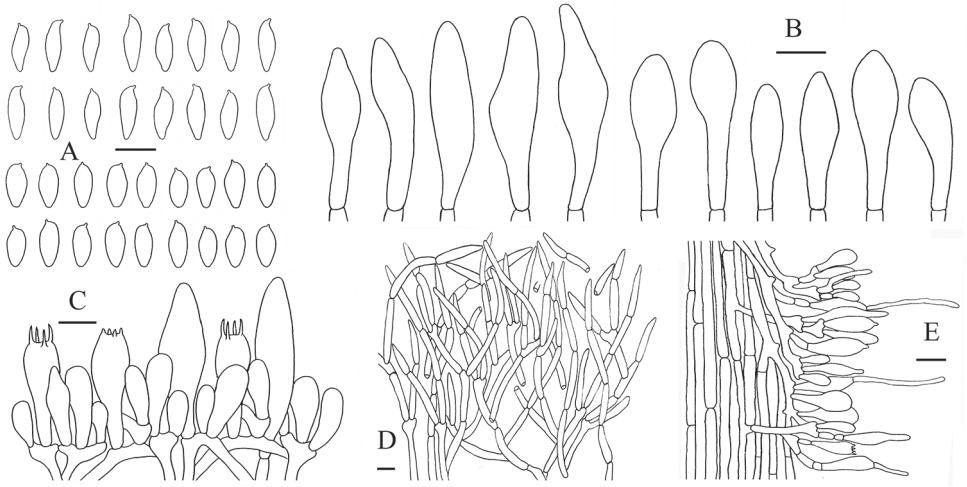

Figure 7. *Aureoboletus sinobadius*. **A** Basidiospores **B** Cheilocystidia and pleurocystidia **C** Basidia and pleurocystidia **D** Pileipellis **E** Stipitipellis. Scale bars: 10 μm (**A–C**); 20 μm (**D, E**).

7–10 mm thick at centre, firm and tough in youth and later soft, white to yellowish-white, and more or less greyish-red (9C4–10C4) beneath the pileipellis, slightly changing to greyish-red (9C4–10D5) when exposed. Tubes 8–15 mm deep, light yellow to greenish-yellow (2A5, 2B5), unchanging when bruised. Pores small, 1–1.5 per mm, circular to angular, somewhat relatively larger and shallowly depressed around the stipe at maturity, unchanging when bruised; pore-surface concolorous with tubes. Stipe 40–80 × 5–9 mm, central, cylindrical or clavate, equal to slightly enlarged downwards, smooth, viscid when wet, pastel red (8A5–10A5), with a very pale flush of pale orange (5A3–6A3) fibrous stripe. Stipe context white to yellowish-white, slightly changing to greyish-red (9C4–10D5) when bruised. Basal mycelium white. Odour mild. Taste salty.

Basidiospores [150/8/5] 10–13(–14) × (4–) 4.5–5 (–5.5) μm, average 11.5–12.5 × 4.5–5, Q = (–2) 2.3–2.67 (–2.88), Q_m = 2.44 ± 0.22, subfusiform and inequilateral in side view with an obtuse apex, oblong to ovoid in ventral view, smooth, yellowish to yellowish-brown in 5% KOH, yellow brown to dark brown in Melzer's reagent, occasionally two different shapes in some specimens. Basidia 22–33 × 8–11 μm, clavate, predominantly 4-spored, partially 2-spored, with sterigmata 2–4 μm long, yellowish-white to hyaline in 5% KOH, without basal clamp. Pleurocystidia 27–50 × 7–13 μm, fusiform, thin-walled, usually containing golden-yellow contents at first, gradually changing from yellowish-white to hyaline in 5% KOH. Cheilocystidia frequent, 23–48 × 9–15 μm, clavate to subfusiform, thin-walled, containing golden-yellow contents at first, gradually changing yellowish-white to hyaline in 5% KOH. Hymenophoral trama composed of subparallel hyphae 4–10 μm broad, yellowish-white to hyaline in 5% KOH. Pileipellis an ixotrichodermium of erect and branched hyphae 6–12 μm in diameter, yellowish-white to hyaline in 5% KOH, dextrinoid in Melzer's reagent; terminal cells 35–60 × 5–10 μm, cylindrical, clavate or nearly

fusoid. Stipitipellis a layer of repent to suberect branched hyphae 3–10 μm in diam., hyaline in 5% KOH. Caulocystidia 30–45 × 9–18 μm, mostly swollen clavate, usually containing yellow to yellowish-brown substance at an early stage in 5% KOH. Clamp connections absent in all tissues.

Ecology and distribution. Solitary or scattered on ground with humus and debris under *Castanopsis fissa* Rehder E.H. Wilson mixed with other broadleaf trees, alt. 200–300 m; known from south China.

Additional specimens examined. China, Guangdong Province, Guangzhou City, Baiyun Mountain Scenic Area, alt. 300 m, 4 June 2015, M. Zhang (GDGM44736 and GDGM44732); Same location, alt. 300 m, 30 May 2013, M. Zhang (GDGM43275); Same location, alt. 300 m, 4 June 2013, M. Zhang (ZhangM55); Same location, alt. 280 m, 14 May 2015, M. Zhang (GDGM45920); Guangdong Province, Huizhou City, Xiangtoushan National Nature Reserve, alt. 300 m, 2 April 2015, M. Zhang (GDGM44473); Hunan Province, Chenzhou City, Jiulongjiang National Forest Park, alt. 280 m, 13 June 2015, M. Zhang (GDGM44730); Guangzhou City, Research Institute of Tropical Forestry, alt. 200 m, 4 May 2018, J. Xu (GDGM72253).

Notes. *Aureoboletus sinobadius* is morphologically similar to *A. auriporus*, *A. flaviporus* (Earle) Klofac, *A. gentilis*, *A. novoguineensis* and *A. venustus*. However, *A. auriporus* differs from *A. sinobadius* in the pinkish cinnamon, vinaceous to vinaceous brown pileus, longer and more robust stipe covered with yellow pruina or floccosity at apex, slight acid taste and broader basidiospores 11–16 × 4–6 μm (Pouzar 1957; Smith and Thiers 1971; Halling 1989; Both 1993; Bessette et al. 2000; Klofac 2010); *A. flaviporus* differs in the pale cinnamon to dark reddish-brown pileus, reddish-brown stipe usually with reticulation at the apex, acidic taste, broader basidiospores 11–15 × 4–6 μm and the known distribution in North America (Bessette et al. 2000); *A. gentilis*, originally described from Europe, differs in having pinkish-brown to flesh-coloured pileus, whitish context unchanging when exposed and longer and broader basidiospores 12–15 × 5–6.5 μm (Singer 1945; Pouzar 1957; Klofac 2010); *A. novoguineensis*, originally described from New Guinea, has pale pink brown or pale red context, shorter (3–4 mm deep) and sometimes compound hymenophore, acid taste and larger basidiospores (11.5–15.5 × 4.5–5.5 μm) and pleurocystidia (36–66 × 13–18 μm) (Hongo 1973); *A. venustus* recently described from southern China differs by its shorter and broader basidiospores 7.5–10.5 × 5–6 μm (Li et al. 2016).

Aureoboletus solus Ming Zhang & T.H. Li, sp. nov.

MycoBank No: 827105
Figs 2, K, 3H, 8A–D

Diagnosis. This species can be easily distinguished from other *Aureoboletus* taxa by its dry and small basidiomata, brownish-yellow to greyish-red pileus, glabrous stipe and smaller basidiospores (7–)8–10.5(–11) × (4–)4.5–5 μm.

Etymology. "*solus*" refers to the solitary habit.

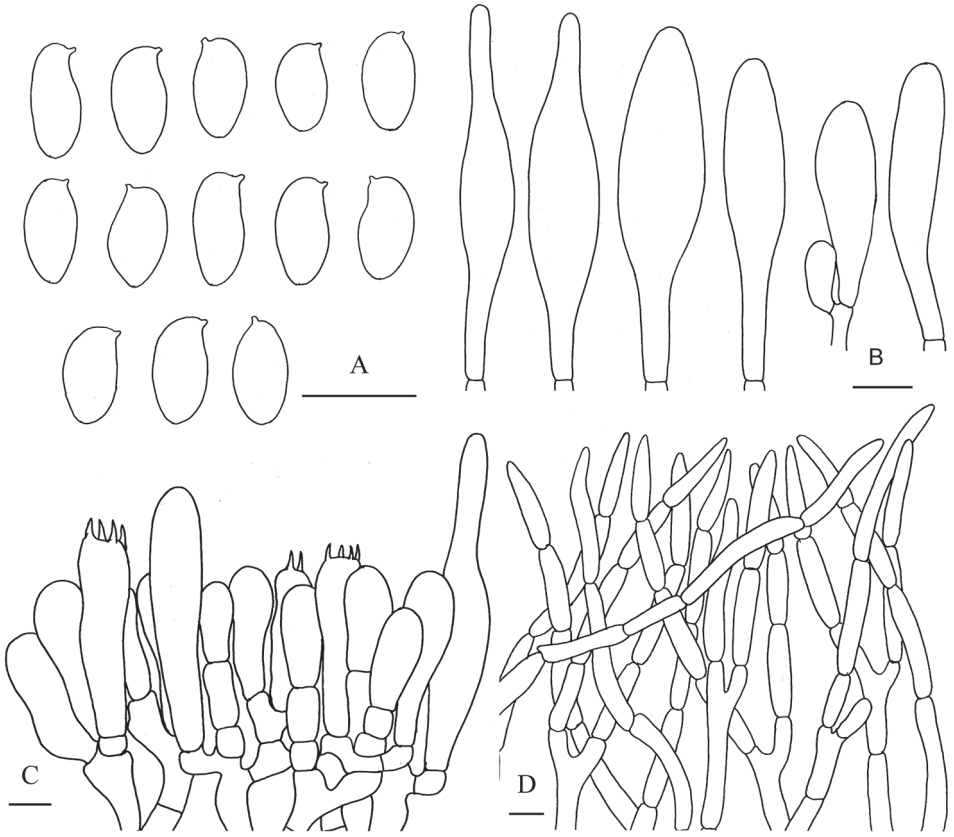

Figure 8. *Aureoboletus solus*. **A** Basidiospores **B** Cheilocystidia and pleurocystidia **C** Basidia and pleurocystidia **D** Pileipellis. Scale bars: 10 μm (**A–D**).

Type. China, Guangdong Province, Shaoguan City, Nanling National Nature Reserve, on soil under the broadleaf forest, dominated by Fagaceae trees, 16 June 2015, M. Zhang (holotype: GDGM44759).

Description. Basidiomata small-sized. Pileus 1.5–2.5 cm wide, hemispheric when young, becoming convex to nearly plane in age, fleshy, dry or slightly viscid when wet, minutely velvet subtomentose, slightly wrinkled, brownish-yellow, brownish-orange, brownish-red to greyish-red (5C7–8C7, 5C5–9C5); margin thin, slightly incurved at first, becoming nearly straight, often appendiculate with small membranous remains of the veil. Context 2–6 mm thick at centre, firm and tough in youth, becoming soft, white, more or less greyish-red (9C5–11C5) to brownish-red (9C7–11C7) beneath the pileipellis, unchanging when exposed. Tubes 2–3 mm deep, gr-yish-yellow (1B5–3B5), light yellow (1A5–3A5) to vivid yellow (1A8–3A8), gradually changing to greenish-yellow when mature, unchanging when bruised, shallowly depressed around the stipe at maturity. Pores small, 1–2 per mm, somewhat larger around the stipe, circular to angular; pore-surface concolorous with tubes. Stipe 20–45 × 2–6 mm, central, cylindrical or clavate, equal to

slightly enlarged downwards, glabrous, dry or slightly viscid when wet, pale orange to pale red (5A3–7A3), pastel red (8A5–10A5), with very pale flush of pastel red (8A5–10A5) fibrous stripes. Stipe context white to pastel red (8A4–10A4), slightly darker when bruised, especially in the lower part. Basal mycelium white. Odour none. Taste mild.

Basidiospores [80/3/3] (7–)8–10.5(–11) ×(4–)4.5–5 μm, Q = (1.5–)1.8–2.2(–2.6), Q_m = 2.0 ± 0.21, subfusiform and inequilateral in side view, oblong to ovoid in ventral view, smooth, yellowish to yellowish-brown in 5% KOH and yellow brown to dark brown in Melzer's reagent, thin-walled. Basidia 1, 2, 4-spored 25–46 × 9–16 μm, clavate, yellowish-white to hyaline in 5% KOH; sterigmata 2–4.5 μm long. Pleurocystidia frequent, 38–66 × 11–15 μm, fusiform, thin-walled, yellowish-white to hyaline in 5% KOH. Cheilocystidia similar to pleurocystidia in shape and size. Hymenophoral trama composed of subparallel hyphae 5–11 μm broad, yellowish-white to hyaline in 5% KOH. Pileipellis an entangled trichodermium of erect hyphae 5–17 μm in diameter, branched, yellowish-white to hyaline in 5% KOH, dextrinoid in Melzer's reagent; terminal cells cylindrical, clavate or nearly fusoid. Stipitipellis a layer of repent hyphae 4–23 μm in diameter, hyaline in 5% KOH. Caulocystidia infrequent. Clamp connections absent in all tissues.

Ecology and distribution. Solitary or gregarious on soil under broadleaf forests dominated by *Castanopsis* spp. and *Cyclobalanopsis* spp. and mixed with other broadleaf trees, alt. 300–1200 m; May to July, currently only known from Guangdong Province.

Additional specimens examined. China, Guangdong Province, Shaoguan City, Nangling National Nature Reserve, alt. 1200 m, 29 July 2017, M. Zhang (GDGM70342); Guangdong Province, Huizhou County, Xiangtoushan National Nature Reserve, alt. 400 m, 16 June 2016, J.P. Zou (GDGM46222); Guangdong Province, Huizhou City, Nankunshan Provincial Nature Reserve, alt. 700 m, 15 May 2013, M. Zhang (GDGM42822); Guangdong Province, Shaoguan City, Danxianshan National Nature Reserve, alt. 300 m, 3 June 2017, M. Zhang (GDGM46807), Same locality, 2 June 2017, M. Zhang (GDGM49404).

Notes. *Aureoboletus solus* looks like *A. tenuis*; however, the latter differs from the former in its viscid basidiomata, ixotrichodermial stipitipellis, composed of terminal hyphae with slightly swollen tips and larger basidiospores (10–)11–12 × 4–5 μm (Zhang et al. 2014). Phylogenetic analyses indicated that *A. solus* is closely related to *A. nephrosporus*, but *A. nephrosporus* differs in having larger basidiomata with a red to brownish-red pileus, ovoid to nephroid basidiospores 8–10.5 × 5–6 μm and cheilocystidia and pleurocystidia covered with a thick layer of a strongly refractive pale yellow substance (Wu et al. 2016).

Aureoboletus velutipes Ming Zhang & T.H. Li, sp. nov.

MycoBank No: 827108
Figs 2L, 3I, 9A–E

Diagnosis. This species can be easily distinguished from others in *Aureoboletus* by its dry and small basidiomata, brown orange to reddish-brown pileus, light yellow to pastel yellow stipe, covered with fibrillose to tomentose squamules and smooth basidiospores 10–13 × 4–6.5 μm.

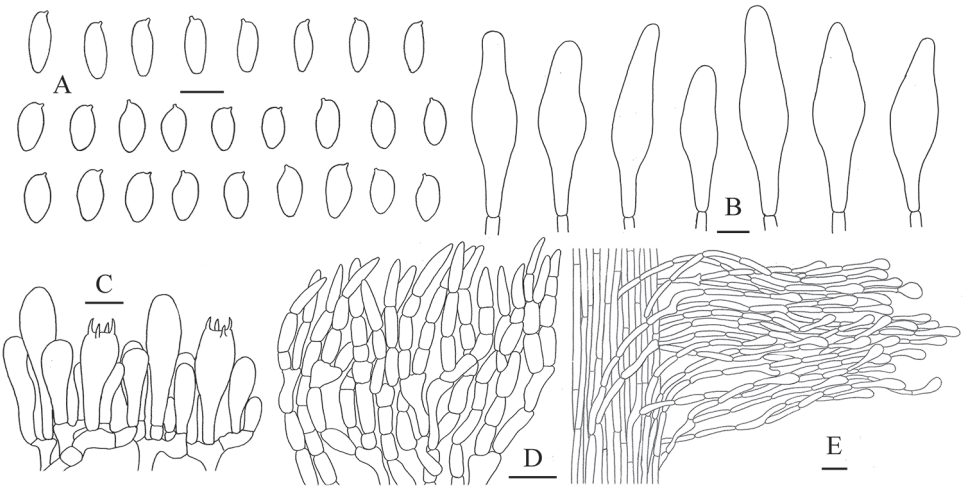

Figure 9. *Aureoboletus velutipes*. **A** Basidiospores **B** Pleurocystidia **C** Basidia and pleurocystidia **D** Pileipellis **E** Stipitipellis. Scale bars: 10 μm (**A–C**), 40 μm (**D, E**).

Etymology. "*velutipes*" refers to the stipe, covered with fibrillose to tomentose squamules.

Type. China, Guangdong Province, Huizhou City, Xiangtoushan National Nature Reserve, on soil under the broadleaf forest, dominated by Fagaceae trees, alt. 350 m, 2 April 2015, M. Zhang (holotype: GDGM44713).

Basidiomata small-sized. Pileus 2–4 cm wide, obtuse to convex when young, becoming broadly convex to plane at mature, fleshy, dry, covered with fibrillose to tomentose squamules, light yellow, light orange (4A4–6A4), brownish-orange (6C7–7C7), brown to reddish-brown (6D7–9D7), slightly fading to light orange to brownish-orange towards margin. Context 3–5 mm thick at stipe, firm and tough in youth, soft when matured, yellowish to white on the whole, more or less reddish-brown beneath the pileipellis, slightly changing to pastel red (7A4–9A4) when exposed. Tubes 3–5 mm deep, distinctly depressed around stipe, yellowish-white (2A2–4A2) when young, becoming pale yellow, greyish-yellow, pastel yellow to olive yellow (2A3–4A3, 1B3–2B3, 2A4–3A4, 2C6–3C6) in age, often with an olive tint, unchanging when bruised. Pores 0.5–0.8 mm in diam., mostly subangular, slightly elongated around stipe at maturity, smaller near pileus margin, concolorous with tubes. Stipe 30–60 × 5–10 mm, central, cylindrical or narrowly clavate, solid, equal to slightly enlarged downwards, covered with white, yellowish-white to yellowish-brown fibrillose to tomentose squamules, usually forming reticulation or longitudinally striate, light yellow to pastel yellow (2A4–4A4, 2A5–4A5), with white basal mycelium. Odour none. Taste mild.

Basidiospores [90/3/3] 10–13 × (4–)5–6(–6.5) μm, Q = (1.75–)1.8–2.2(–2.4), Q_m = 2.08 ± 0.35, subfusiform and inequilateral in side view, oblong to ovoid in ventral view, smooth, yellowish to yellowish-brown in 5% KOH and yellow brown to dark brown in Melzer's reagent, thin-walled. Basidia 25–30 × 9–13 μm, clavate, predominantly 4-spored

but frequently also 2-spored, with sterigmata 2–3 μm long, yellowish-white to hyaline in 5% KOH, without basal clamps. Pleurocystidia 35–65 × 10–18 μm, fusiform, thin-walled. Cheilocystidia frequent, similar to pleurocystidia in shape and size. Hymenophoral trama composed of subparallel hyphae 6–10 μm broad, yellowish-white to hyaline in 5% KOH. Pileipellis a trichodermium of erect and often branched hyphae 4–17 μm in diameter, yellowish-white to hyaline in 5% KOH, dextrinoid in Melzer's reagent; terminal cells 30–60 × 4–17 μm, cylindrical, clavate or nearly fusoid. Stipitipellis a layer of repent to suberect branching hyphae 3–15 μm in diameter, with swollen tips, terminal cells 30–70 × 11–21 μm, hyaline in 5% KOH. Clamp connections absent in all tissues.

Ecology and distribution. Scattered on soil in subtropical forests, dominated by Fagaceae (*Castanopsis* spp., *Lithocarpus* spp. and *Quercus* spp., etc). Currently known from southern China.

Additional specimens examined. China, Guangxi Province, Guilin City, Maoershan National Nature Reserve, alt. 1380 m, 1 July 2012, M. Zhang (GDGM42608); Jiangxi Province, Jinggangshan City, Jingganshan National Nature Reserve, alt. 1000 m, 21 June 2016, H. Huang (GDGM52409).

Notes. The obviously villose or fibrous squamulose stipe can distinguish it from other species in *Aureoboletus*. *Aureoboletus catenarius*, recently described from southwest China, is somewhat similar to *A. velutipes* with a dry and tomentose pileus, but *A. catenarius* has a cracked and light brown to reddish-brown pileus, faintly or finely fibrillose stipe and smaller basidiospores 7–9 × 3.5–5 μm (Wu et al. 2016).

***Aureoboletus miniatoaurantiacus* (Bi & Loh) Ming Zhang, N.K. Zeng & T.H. Li, comb. nov.**

MycoBank No: 827109

Figs 2D, E, 3C, D, 10A–D

Basionym. *Boletus miniatoaurantiacus* C.S. Bi & Loh, in Bi, Loh & Zheng, Acta Bot. Yunn. 4(1): 60, 1982

Synonym. *Aureoboletus tomentosus* G. Wu & Zhu L. Yang, in Wu, Li, Zhu, Zhao, Han, Cui, Li, Xu & Yang, Fungal Diversity 81: 51, 2016

Diagnosis. In Bi et al. (1982): Pileus 1–1.6 cm latus, siccus, obtuse hemisphaerius, aurantiacus, confertim et minute villoso-tomentosus. Contexto flava, immutibili, ad stipitem 2–3 cm crasso, sapor mitis et odor nullus. Stipes centralis, 3–3.3 cm longus, 3–6 mm crassus, albidus, in parte in feriore flavus, subcylindraceus, solidus, velutinus. Tubuli albidi, immutabiles, ad stipitem breviter decurrentes, 3 mm longi, facile denudati; pori ovati, majuscules, 3 mm diam. Sporae ellipsoideae, laeves, pallido-flavae, 7–10 × 3.3–4 μm, 1 guttatae. Pleurocystidiis 35 × 6.5 μm, paucis.

Basidiomata small to medium-sized. Pileus 1.5–8 cm wide, hemispheric when young, becoming convex to nearly plane in age, fleshy, dry or viscid when wet, surface minutely tomentose or pulverous, slightly wrinkled, orange yellow, reddish-yellow, orange to reddish-orange (4A6–7A6, 4A7–7A7), commonly with a thin and slightly extended margin.

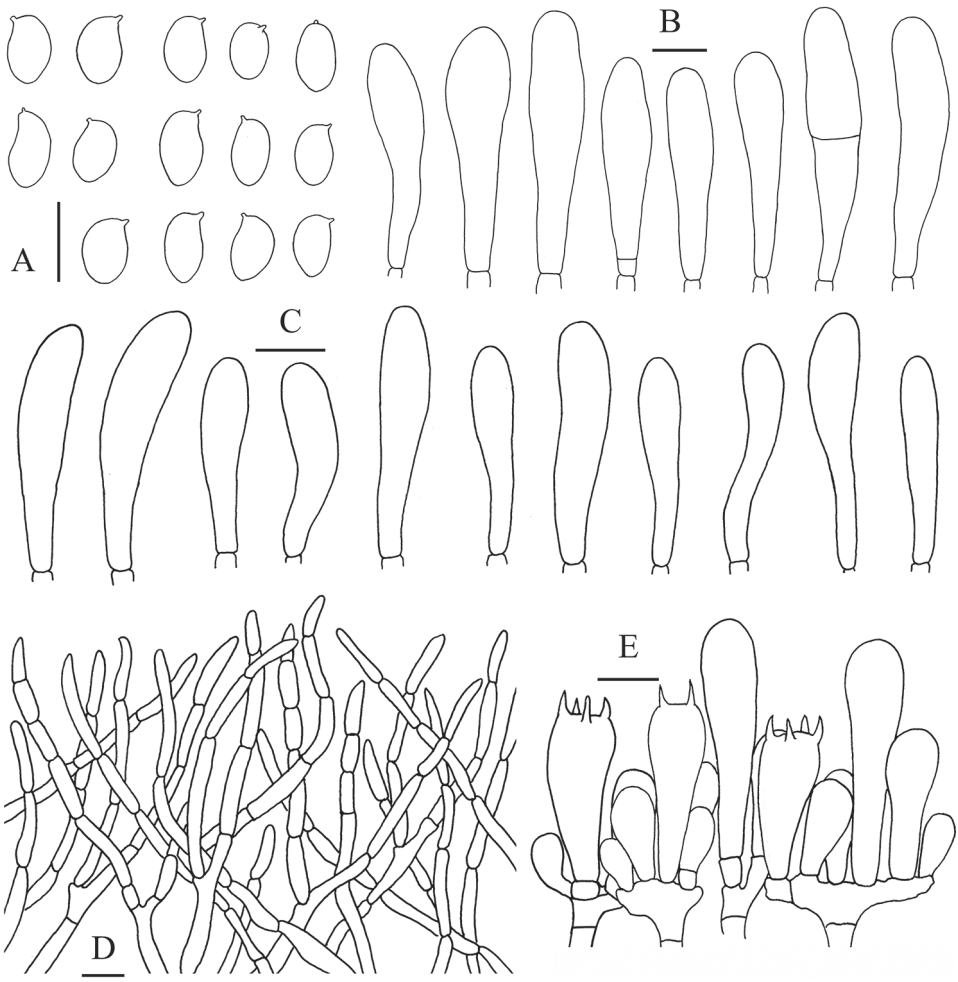

Figure 10. *Aureoboletus miniatoaurantiacus*. **A** Basidiospores **B** Cheilocystidia **C** Pleurocystidia **D** Basidia and pleurocystidia **E** Pileipellis. Scale bars: 10 μm (**A–D**), 20 μm (**E**).

Context 5–10 mm thick at centre, firm and tough in youth and, later, soft, white to yellowish-white, with more or less green tint at border contacting tubes, unchanging when exposed. Tube 3–10 mm deep, light orange to orange unchanging when bruised. Pores polygonal, 0.5–1.5 per mm, somewhat relatively larger and shallowly depressed around the stipe, orange to pale orange unchanging when bruised. Stipe 30–80 × 4–10 mm, central, solid, cylindrical or clavate, equal to slightly enlarged downwards, smooth to distinctly longitudinally streaks or broad reticulations, viscid in wet condition, concolorous with pileus. Stipe context concolorous with that of pileus, unchanging when exposed. Basal mycelium white to yellowish-white. Odour strong. Taste mild.

Basidiospores [90/3/3] (6.5–)7–10.5(–11) × (4–)4.5–5.5(–6) μm, Q = (1.42–)1.6–2.0(–2.3), Q_m = 1.79 ± 0.18, ovoid and inequilateral in side view with an obtuse apex,

ovoid in ventral view, smooth, yellowish to yellowish-brown in 5% KOH and yellow brown to dark brown in Melzer's reagent, thin-walled. Basidia 18–35 (45) × 7–14 μm, 4-spored, rarely 1-, 2-, 3-spored, clavate, yellowish-white to hyaline in 5% KOH, sterigmata 2–3 μm. Cheilocystidia (21) 26–55 (61) × (6) 8–12 μm, fusiform to subclavate, thin-walled, contained with bright yellow pigments. Pleurocystidia similar to cheilocystidia in shape and size, thin-walled, yellowish-white to hyaline in 5% KOH. Hymenophoral trama composed of interwoven branched hyphae 6–15 μm wide, yellowish-white to hyaline in 5% KOH. Pileipellis an entangled trichodermium to ixotrichodermium of erect hyphae 4–18 μm in diameter, composed of yellow to bright yellow vacuolar pigmented filamentous hyphae, terminal cells cylindrical, clavate or nearly fusoid. Stipitipellis a tangled layer of repent to suberect branching hyphae 7–12 μm in diameter, hyaline in 5% KOH. Caulocystidia 25–75 × 12–18 μm, common, clavate, fusoid or fusoid ventricose and usually contain yellow to yellowish-brown substance in an early stage in 5% KOH. Stipe trama composed of parallel hyphae 4–18 μm wide. Clamp connections absent in all tissues.

Ecology and distribution. Scattered on soil in tropical to subtropical forests dominated by Fagaceae (*Castanopsis chinensis*, *C. fissa*, *Lithocarpus* spp. and *Quercus* spp.). Currently known from southern and southwest China

Additional specimens examined. China, Guangdong Province, Zhaoqing City, Dinghu Mountain, 6 September 1980, C.S. Bi et al. 677 (GDGM4677, holotype of *B. miniatoaurantiacus*); Same locality, 14 April 1981, C. Li (GDGM5071); 11 August 1981, C.S. Bi et al. 855 (GDGM4855); Fujian Province, Zhangping City, alt. 350 m, 2 September 2009, N.K. Zeng 664, 669 (FHMU424, 429); same locality, 27 July 2013, N.K. Zeng 1294 (FHMU848); 29 July 2013, N.K. Zeng 1323 (FHMU876); 1 August 2013, N.K. Zeng 1339 (FHMU891); Guangdong Province, Guangzhou City, Tianluhu Forest Park, alt. 200 m, 29 May 2015, M. Zhang (GDGM42855); Guangdong Province, Shaoguan City, Chebaling National Nature Reserve, alt. 300 m, 3 September 2013, M. Zhang & C.Q. Wang (GDGM43282); Guangdong Province, Huizhou City, Xiangtoushan National Nature Reserve, alt. 300 m, 7 July 2015, M. Zhang (GDGM44727); Jiangxi Province, Chongyi County, Yangling National Forest Park, alt. 280 m, 14 August 2015, M. Zhang (GDGM51694 and GDGM43439); same locality, 31 August 2016, H. Huang (GDGM52888); Same locality, 1 September 2016, M. Zhang (GDGM53350); Same locality, 2 September 2016, M. Zhang (GDGM53274); Same locality, 3 September 2016, M. Zhang (GDGM53501).

Notes. *Aureoboletus miniatoaurantiacus*, originally described as *B. miniatoaurantiacus*, is a rather common species in southern China and can be easily distinguished by its bright orange-yellow basidiomata, tomentose or pulverulent pileus surface, light orange to orange hymenophore unchanging when bruised and ovoid basidiospores. Based on a re-study of the type specimen and other collections quoted by Bi et al. in 1994, we found that the type specimen is composed of two small immature basidiomata, which are in a poor condition for morphological observation, but other voucher specimens fit well with the description of *A. tomentosus*. Thus, the newly described species *A. tomentosus* is, in fact, a synonym of *A. miniatoaurantiacus*, this conclusion also being supported by molecular data in this study (Bi et al. 1982; Bi et al. 1994; Wu et al.

2016). *Aureoboletus auriflammeus*, originally described from North America, is similar to *A. miniatoaurantiacus*; however, the former differs in having a distinctly reticulate stipe and narrower basidiospores (8–12 × 3–5 μm) (Murrill 1908; Bessette et al. 2000).

Key to the species of *Aureoboletus* known in China

1 Pileus dry or slightly viscid when wet **2**
– Pileus viscid **13**
2 Basidiomata medium to larger (≥ 6 cm in diam.) **3**
– Basidiomata smaller (< 6 cm in diam.) **4**
3 Pileus 6–10 cm in diameter, greyish-orange to brownish-orange; stipe glabrous, greyish-yellow on the upper part to blond on the lower part; context unchanging when cut; basidiospores 9–11 × 4–5.5 μm ..... ***A. yunnanensis***
– Pileus 6–15 cm in diameter, brownish-red to reddish-brown; context yellowish-white changing to yellowish-olivaceous when injured; hymenophore pale yellow to olivaceous yellow; stipe surface with longitudinal stripe, brownish-red to reddish-brown; basidiospores subglobose, 7–8 × 5.5–6 μm ..... ***A. clavatus***
4 Stipe surface smooth or with small dots or splotches **5**
– Stipe surface non-smooth, with reticula, longitudinal stripe, flocci or others **11**
5 Basidiospores nodulose to verrucose, 12–15 × 8–11 μm; basidiomata small, golden brown to umber; stipe up to 7 cm long ..... ***A. shichianus***
– Basidiospores surface smooth; other characters not as above **6**
6 Hymenophore bright yellow to vivid yellow, unchanging when old 7
– Hymenophore pale yellow, light yellow, greenish-yellow to olive brown **8**
7 Pileus greyish-rose to brownish-red, glabrous to slightly subtomentose; context pale yellow to light yellow unchanging when cut; stipe dark orange to yellow ochre, with distinct longitudinal streaks and furfuraceous scales; basidiospores 8–10.5 × 5–6 μm ..... ***A. nephrosporus***
– Pileus reddish-brown to greyish-ruby, smooth to minutely velvet-subtomentose; context white to yellowish-white changing to greyish-red to greyish-rose when exposed; stipe smooth, concolorous with pileus; stipe context white to reddish-white gradually changing to greyish-red to greyish-rose when bruised; basidiospores 9–10.5 × 4.5–5 μm ..... ***A. griseorufescens***
8 Pileus yellowish-white to reddish-white; context white, unchanging or slightly changing blue near the hymenium when exposed; tubes greyish-yellow to light yellow, unchanging when bruised; stipe context white to yellowish-white, slightly changing pale yellow when exposed; odour with radish scent; basidiospores 5–9 × 5–6 μm ..... ***A. raphanaceus***
– Pileus coloured with brownish-red to reddish-brown tonalities **9**
9 Pileipellis epithelium; basidiospores subfusoid, 7–9 × 3.5–5 μm ..... ***A. catenarius***
– Pileipellis trichoderm **10**
10 Basidiospores fusiform to ovoid, 8–10.5 × 4.5–5 μm ..... ***A. solus***
– Basidiospores oblong to ovoid, 8.5–10.5 × 5–5.5 μm ..... ***A. rubellus***

11 Stipe surface ornamented with distinctly reticulation, pileus surface covered with coarse tomentose, basidiospores (20–)22–27(–28) × 9–13 μm ..... ***A. mirabilis***
– Stipe surface without reticulation or the reticulation inconspicuous **12**
12 Stipe surface ornamented with distinctly longitudinally streaks or dotted scales; pileus surface orange yellow, reddish-yellow to reddish-orange, covered with tomentose; hymenophore light orange to orange; basidiospores 7–11 × 4.5–6 μm ..... ***A. miniatoaurantiacus***
– Stipe surface covered with distinctly fibrillose to tomentose squamules; pileus surface brownish-orange to reddish-brown, covered with fibrillose to tomentose squamules; context yellowish-white changing to pastel red when exposed; basidiospores 10–13 × 4–6.5 μm ..... ***A. velutipes***
13 Pileus margin with a gelatinised membranous veil **14**
– Pileus margin without any membranous veil **19**
14 Pileus surface distinctly reticulate, coarsely rugose, chestnut-brown to pale brown; stipe whitish; pleurocystidia covered with yellow substance on surface; basidiospores 9.5–13 × 4.5–5 μm ..... ***A. thibetanus***
– Pileus glabrous or slightly rugose in central **15**
15 Basidiospores smooth **16**
– Basidiospores longitudinally costate, 12–16 × 9–12 μm ..... ***A. longicollis***
16 Pileus brownish to brown; basidiospores 10–12.5 × 4.5–5 μm ..... ***A. viscidipes***
– Pileus reddish-brown to violet brown **17**
17 Basidiomata usually ≥ 2.5 cm; basidiospores 11–13.5 × 4.5–5.5 μm ..... ***A. tenuis***
– Basidiomata usually < 2.5 cm **18**
18 Basidiospores 8.5–10 × 4–4.5 μm ..... ***A. marroninus***
– Basidiospores 10–13.5 × 4.5–5 μm ..... ***A. glutinosus***
19 Pileus wrinkled, greyish-yellow to brownish-orange; taste salty; distribution in subalpine zone, ectomycorrhizal with *Quercus spinose*; basidiospores 15–21 × 5–6.5 μm ..... ***A. squercus-spinosae***
– Pileus smooth, fibrillose to tomentose; the rest of the characters usually not as above **20**
20 Basidiospores relatively broader, 7.5–10.5 × 5–6 μm, Q_m < 2 ..... ***A. venustus***
– Basidiospores relatively narrower, usually Q_m ≥ 2 ..... **21**
21 Basidiospores comparatively larger, 15–16.5 × 4.5–5 μm ..... ***A. formosus***
– Basidiospores comparatively smaller, commonly < 15 μm long **22**
22 Basidiomata small to medium-sized (pileus usually < 5 cm). Pileus yellowish-brown or reddish-golden, subtomentose; stipe light brown to brownish-orange; basidiospores 9–11 × 4–5 μm ..... ***A. zangii***
– Basidiomata medium to large (pileus usually > 5 cm) **23**
23 Pileus violet brown to brownish-violet, glabrous to minutely velvet-subtomentose; stipe pastel red with a pale flush fibrous stripe; taste salty; basidiospores 10–14 × 4.5–5.5 μm ..... ***A. sinobadius***
– Pileus reddish-brown to brownish-red, nearly glabrous; stipe reddish-orange to garnet brown with faintly longitudinal streaks; taste unknown, basidiospores 8.5–13 × 4.5–5.5 μm ..... ***A. duplicatoporus***

Discussion

Species delimitation, species diversity and new taxa in China

In the taxonomic circumscription of the genus *Aureoboletus* proposed by Pouzar (1957), 35 species were identified prior to this study, of which 20 species were recorded from China (i.e. *A. auriporus*, *A. catenarius*, *A. clavatus*, *A. duplicatoporus*, *A. formosus*, *A. longicollis*, *A. marroninus*, *A. mirabilis*, *A. nephrosporus*, *A. quercus-spinosae*, *A. rubellus*, *A. shichianus*, *A. tenuis*, *A. thibetanus*, *A. tomentosus*, *A. venustus*, *A. viscidipes*, *A. viscosus*, *A. yunnanensis* and *A. zangii*). However, the report of the North American species *A. auriporus* was excluded from China in this study due to a misidentification, as its correct name is *A. sinobadius*. The previously described species, *A. tomentosus*, was proven to be *A. miniatoaurantiacus* and so, a new combination is proposed here. Six species, *A. glutinosus*, *A. griseorufescens*, *A. sinobadius*, *A. solus*, *A. raphanaceus* and *A. velutipes*, obtained from China, are newly described in this study.

The present study demonstrates that species of *Aureoboletus* are very diverse in China, especially in its southern areas. Common morphological characteristics and molecular data make *Aureoboletus* easily distinguishable from other existing genera in Boletaceae, but some variable morphological features make it difficult to recognise some species. Careful examination showed that several morphological characteristics are available to delimit these species in China. For example, the colour of the hymenophore and pattern of the pileus are important characteristics: *A. glutinosus* has a light yellow to olive yellow hymenophore and a coarse pileus with irregular reticulation; *A. sinobadius* has a vivid yellow hymenophore and a subtomentose to glabrous and viscid pileus; *A. miniatoaurantiacus* has a light orange to orange hymenophore and a tomentose to pulverous pileus; regarding the size of basidiomata, *A. clavatus* and *A. yunnanensis* have relatively larger basidiomata up to 10 cm in diameter, whereas *A. glutinosus* and *A. marroninus* have smaller basidiomata usually less than 2.5 cm in diameter. The colour of the pileus and the colour and odour of the context also help to identify species in the field. In contrast to macro-morphology, several micro-morphological features can also be used to discriminate species of *Aureoboletus*, such as the size and shape of basidiospores and the shape and inclusion of cystidia, pileipellis and stipitipellis seem to be rather constant amongst the different species.

Phylogenetic analyses supported the presence of eight clades in *Aureoboletus*

In the present study, all selected samples of *Aureoboletus* formed a well-supported monophyletic group and eight major clades are proposed here, based on morphological characteristics and phylogenetic inference.

Clade I is characterised by the presence of a viscid pileus, a vivid yellow to greyish-yellow hymenophore that is unchanging when bruised, smooth basidiospores and

ixotrichodermium pileipellis. In the present study, this group contains ten species, including the type species *A. gentilis* and the new species *A. sinobadius*. This clade is a rather homogeneous group in terms of morphology, which is consistent with the definition of *Aureoboletus* given by Pouzar (1957). Species in this clade can be separated from each other by pileus colour and the size of basidiospores. In addition, two unsequenced species, *A. flavimarginatus* and *A. flaviporus*, should belong to this clade, based on their morphological characteristics (viscid pileus and vivid yellow hymenophore).

Clade II is characterised by the presence of a dry (or slightly sticky when wet) pileus, a vivid yellow to olive yellow hymenophore that is unchanging when bruised, smooth basidiospores and trichodermium pileipellis. This clade includes six species, of which *A. velutipes* has distinctive morphological characteristics, such as a villous pileus and stipe, pale yellow to olive yellow hymenophore and swollen tips in terminal cells of the stipitipellis.

Clade III is well-characterised by the presence of a viscid pileus with well-developed yellowish to subhyaline veil remnant at the margin, greyish-yellow to olive yellow hymenophore, smooth to longitudinally costate basidiospores and ixotrichodermium pileipellis. *Aureoboletus longicollis*, originally described from Malaysia, is a well-defined species in this clade and is readily distinguished by its more viscid and larger basidioma, longer stipe and longitudinally costate basidiospores. A Chinese species, *A. viscosus*, shares similar traits with *A. longicollis* and the two species cannot be separated from each other in morphology. In this study, we did not have access to specimens of *A. longicollis* from Malaysia for morphological and phylogenetical study and it is not possible to make a taxonomic decision on whether *A. viscosus* is the same or a different species to *A. longicollis* without phylogenetic data. Thus, the name *A. longicollis* is temporarily used in this study and further studies with more materials are needed. The other species in this clade are characterised by smooth basidiospores and they can be distinguished from each other by their pileus colour and the size of basidiospores.

Clade IV contains the species *A. auriflammeus* and *A. miniatoaurantiacus*, which are mainly characterised by their bright orange yellow basidiomata, tomentose pileus surface and ovoid basidiospores. Species in this clade can be easily distinguished from others in this genus.

Clade V is characterised by the presence of a dry or somewhat tacky pileus, greyish-yellow to vivid yellow hymenophore changing to olive yellow when mature and oblong, ovoid to nephroid basidiospores. This clade contains five species, including the two species *A. solus* and *A. raphanaceus* described above.

Clade VI is composed of four distinct species, which have all been recently added to *Aureoboletus*, based on phylogenetic analyses (Halling et al. 2015, Wu et al. 2014, 2016). *Aureoboletus projectellus*, *A. mirabilis* and *A. russellii* were originally described from North America and have a dry or coarsely tomentose pileus, distinct coarse reticulations on the stipe and larger basidiospores (up to 20 μm); however, the basidiospores of *A. projectellus* and *A. mirabilis* are smooth, while *A. russellii* has longitudinally costate basidiospores (Murrill 1938; Singer 1945; Smith and Thiers 1971; Pegler and Young 1981; Bessette et al. 2000). *A. shichianus*, originally described from southwest China, is a remarkable species in this clade and differs from the others by its small basidiomata,

tomentose pileus, radially arranged pores, comparatively long and glabrous stipe and scabrous basidiospores with nodules. Species in this clade are quite diverse, though the coarsely reticulated stipe and ornamented basidiospores are unique in the genus.

Clade VII is currently formed by a single species, *A. clavatus*. The most striking characteristics are the large basidiomata with slightly viscid pileus, yellowish-white context staining yellowish-olivaceous when exposed, pale yellow to olivaceous-yellow hymenophore, subglobose basidiospores and the pileipellis composed of a turf of clavate hyphae. Besides the slightly viscid pileus, this species shares nearly none of the basic morphological traits of the genus *Aureoboletus*. However, phylogenetic analyses showed that it belongs to *Aureoboletus* and formed a separate branch.

Clade VIII is formed by a single species *A. griseorufescens*. Morphologically, *A. griseorufescens* is similar to those species in Clade I with a vivid yellow hymenophore and subviscid pileus; however, the most striking characteristic of *A. griseorufescens* is its white to yellowish-white context changing to greyish-red or greyish-rose when exposed. In the phylogenetic tree, *A. griseorufescens* formed the basal branch of *Aureoboletus* with highly-supported values, which showed that it might be an early divergent species from *Aureoboletus*.

Geographical distribution and species evolution

Aureoboletus is a cosmopolitan genus, but most known species have relatively distinct habitats or regional locations. Currently, most of known *Aureoboletus* species are distributed in East Asia (mainly in China) and North America and intercontinentally-distributed species are infrequent. Two species *A. projectellus* and *A. mirabilis*, originally reported from North America, were examined in several studies and found to have disjunctive distributions in the North Temperate region from North America to Asia (China, Japan) and Europe (Hongo 1973, Chen et al. 1988, Motiejūnaitė et al. 2013, Halling et al. 2015, Wu et al. 2016). In Asia and North America, some morphologically similar and phylogenetically related species also exist. For example, *A. auriporus* and *A. viridiflavus* are similar to *A. sinobadius* and *A. formosus* and *A. auriflammeus* is similar to *A. miniatoaurantiacus*. However, they can be clearly separated from each other by molecular data. In Europe, only *A. gentilis* was originally described and not found in other continents; this represents a separate geographical region of *Aureoboletus*.

Phylogenetic analyses based on 144 collections uncovered some useful information regarding the geography of *Aureoboletus*. Species in Clades III, V and VIII are found in Asia (China-Japan-Malaysia-Vietnam), representing subtropical-tropical Asia distributions. Compared with North America and Europe, China has the greatest number of *Aureoboletus* species and endemic species, especially in the subtropical-tropical region. Furthermore, many regions in China are under-sampled and more under-described indigenous *Aureoboletus* species will undoubtedly be discovered in the future. The high diversity of *Aureoboletus* species in China indicates that the subtropical-tropical region of China (or Asia) is the current species diversity centre of *Aureoboletus*.

In this study, some evolutionary patterns of morphological characteristics were also discovered. The traits of dry or viscid pileus surface and hymenophore colour appear to be relatively stable evolutionary characteristics and were wellsupported by monophyletic clades on the phylogenetic tree. The shape and surface ornamentation of basidiospores are not reliable characteristics for delimiting *Aureoboletus*, but are useful for species identification. Basidiospores ornamentation may have evolutionarily originated several times within *Aureoboletus* history. More morphological and molecular data are needed to understand this trait.

Acknowledgements

The authors are grateful to the editors and anonymous reviewers for their constructive comments and suggestions. Thanks are given to Mr. Hao Huang, Ting Li, Jun-Ping Zou, Zong-Ping Song (Guangdong Institute of Microbiology) and Yu Chen (Guangdong Xiangtoushan National Nature Reserve Administration) for their kind help in the fieldwork; to Dr. Chun-Ying Deng (Guizhou Academy of Sciences) and Dr. Chuan-Hua Li (Institute of Edible Fungi, Shanghai Academy of Agricultural Sciences) for providing collections. This study was supported by the National Natural Science Foundation of China (Nos. 31700021, 31770014, 31670029), the Ministry of Science and Technology of the People's Republic of China (2013FY111500), the Ministry of Ecology and Environment (2019HB2096001006) and the GDAS' Special Project of Science and Technology Development (2019GDASYL-0104009).

References

Bessette AE, Roody WC, Bessette AR (2000) North American Boletes: a color guide to the fleshy pored mushrooms. Syracuse University Press, New York.

Bi CS, Loh TC, Zheng GY (1982) Basidiomycetes from Dinghu Mountain of China II, Some new species of Boletaceae (1). Acta Botanica Yunnanica 4(1) : 55–64.

Bi CS, Zheng GY, Li TH (1994) Macrofungus Flora of Guangdong Province. Guangdong Science and Technology Press, Guangzhou.

Binder M (1999) Zur molekularen Systematik der Boletales: Boletineae und Sclerodermatineae subordo nov. PhD Thesis, University of Regensburg, Regensburg.

Binder M, Fischer M (1997) Molekularbiologische Charakterisierung der Gattungen *Boletellus* und *Xerocomus*: *Xerocomus pruinatus* und verwandte Arten. Bollettino Del Gruppo Micologico G. Bresadola 152: 79–90.

Binder M, Hibbett DS (2007) Molecular systematics and biological diversification of Boletales. Mycologia 98: 971–981. https://doi.org/10.1080/15572536.2006.11832626

Both EE (1993) The boletes of North America: a compendium. Buffalo Museum of Science, Buffalo.

Castresana J (2000) Selection of conserved blocks from multiple alignments for their use in phylogenetic analysis. Molecular Biology and Evolution 17: 540–552. https://doi.org/10.1093/oxfordjournals.molbev.a026334

Chen CM, Yeh KW, Hsu HK (1998) The boletes of Taiwan (X). Taiwania 43: 140–149.

Corner EJH (1972) *Boletus* in Malaysia. Government Printer, Singapore.

Dentinger BT, Ammirati JF, Both EE, Desjardin DE, Halling RE, Henkel TW, Moreau PA, Nagasawa E, Soytong K, Taylor AF, Watling R, Moncalvo JM, McLaughlin DJ (2010) Molecular phylogenetics of porcini mushrooms (*Boletus* section *Boletus*). Molecular Phylogenet Evolution 57: 1276–1292. https://doi.org/10.1016/j.ympev.2010.10.004

Fang JY, Wu G, Zhao K (2019) *Aureoboletus rubellus*, a new species of bolete from Jiangxi Province, China. Phytotaxa 420: 72–78. https://doi.org/10.11646/phytotaxa.420.1.5

Hall TA (1999) BioEdit: a user-friendly biological sequence alignment editor and analysis program for Windows 95/98/NT. Nucleic Acids Symposium Series 41: 95–98.

Halling R, Fechner N, Nuhn M, Osmundson T, Soytong K, Arora D, Binder M, Hibbett D (2015) Evolutionary relationships of *Heimioporus* and *Boletellus* (Boletales) with an emphasis on Australian taxa including new species and new combinations in *Aureoboletus*, *Hemileccinum*, and *Xerocomus*. Australian Systematic Botany 28: 1–22. https://doi.org/10.1071/SB14049

Halling RE (1989) A synopsis of Colombian Boletes. Mycotaxon 34: 93–114.

Hongo T (1973) Enumeration of the Hygrophoraceae, Boletaceae and Strobilomycetaceae. Bulletin. National Science Museum (Tokyo) 16: 537–557.

Klofac W (2010) The genus *Aureoboletus*, a world-wide survey. A contribution to a monographic treatment. Österreichische Zeitschrift für Pilzkunde 19: 133–174.

Kornerup A, Wanscher JH (1978) Methuen handbook of colour. Eyre Methuen, London.

Li F, Zhao K, Deng QL, Zhang M, Staehelin C, Chen XX, Chen HY, Wang GS, Li BS (2016) Three new species of Boletaceae from the Heishiding Nature Reserve in Guangdong Province, China. Mycological Progress 15: 1269–1283. https://doi.org/10.1007/s11557-016-1233-5

Motiejūnaitė J, Kasparavičius J, Kačergius A (2011) *Boletellus projectellus* – An alien mycorrhizal bolete new to Europe. Sydowia 63(2): 203–213.

Murrill WA (1908) Boleti from Western North Carolina. Torreya 8: 209–217.

Murrill WA (1938) New boletes. Mycologia 30: 520–525. https://doi.org/10.1080/00275514.1938.12017294

Neves MA, Binder M, Halling RE, Hibbett D, Soytong K (2012) The phylogeny of selected *Phylloporus* species, inferred from NUC-LSU and ITS sequences, and descriptions of new species from the Old World. Fungal Diversity 55: 109–123. https://doi.org/10.1007/s13225-012-0154-0

Nuhn ME, Binder M, Taylor AFS, Halling RE, Hibbett DS (2013) Phylogenetic overview of the Boletineae. Fungal Biology 117: 479–511. https://doi.org/10.1016/j.funbio.2013.04.008

Nylander JAA (2004) MrModeltest v2. Program distributed by the author. Evolutionary Biology Centre, Uppsala University, Uppsala.

Patouillard N (1895) Enumération des champignons récoltés par les RR. PP. Farges et Soulié, dans le Thibet oriental et Su-tchuen. Bulletin de la Société Botanique de France 11: 196–199.

Pegler D, Young T (1981) A natural arrangement of the Boletales, with reference to spore morphology. Transactions of the British Mycological Society 76: 103–146. https://doi.org/10.1016/S0007-1536(81)80013-7

Pouzar Z (1957) Nova genera macromycetum I. Ceská Mykologie 11: 48–50.

Quélet L (1884) Quelques especes critiques ou nouvelles de la Flore Mycologique de France. Comptes Rendus de l´Association Française pour l´Avancement des Sciences 12: 498–512.

Ronquist F, Huelsenbeck JP (2003) MrBayes 3: Bayesian phylogenetic inference under mixed models. Bioinformatics 19: 1572–1574. https://doi.org/10.1093/bioinformatics/btg180

Saccardo PA (1888) Sylloge Hymenomycetum, Vol. II. Polyporeae, Hydneae, Thelephoreae, Clavarieae, Tremellineae. Sylloge Fungorum 6: 1–928.

Shi XF, Liu PG (2013) *Aureoboletus zangii* (Boletaceae), a new species from China. Mycotaxon 123: 451–456. https://doi.org/10.5248/123.451

Singer R (1942) Das System der Agaricales 2. Annales Mycologic 40: 1–132.

Singer R (1945) The Boletineae of Florida with notes on extralimital species. II. The Boletaceae (Gyroporoideae). Farlowia 2: 223–303.

Singer R (1947) The Boletoideae of Florida with notes on extralimital species. III. American Midland Naturalist 37: 1–135. https://doi.org/10.2307/2421647

Singer R (1986) The Agaricales in modern taxonomy (4th edn). Koeltz Scientific Books, Koenigstein.

Smith AH, Thiers HD (1971) The boletes of Michigan. Ann Arbor, University of Michigan Press, Michigan.

Smith SA, Dunn CW (2008) Phyutility: a phyloinformatics tool for trees, alignments and molecular data. Bioinformatics 24: 715–716. https://doi.org/10.1093/bioinformatics/btm619

Stamatakis A (2006) RAxML-VI-HPC: maximum likelihood-based phylogenetic analyses with thousands of taxa and mixed models. Bioinformatics 22: 2688–2690. https://doi.org/10.1093/bioinformatics/btl446

Šutara J (2005) Central European genera of the Boletaceae and Suillaceae, with notes on their anatomical characters. Česká Mycology 57: 1–50.

Šutara J (2008) *Xerocomus* s. l. in the light of the present state of knowledge. Czech Mycological 60(1): 29–62. https://doi.org/10.33585/cmy.60104

Terashima Y, Takahashi H, Taneyama Y (2016) The fungal flora in southwestern Japan: agarics and boletes. Tokai University Press, Tokyo.

Vilgalys R, Hester M (1990) Rapid genetic identification and mapping of enzymatically amplified ribosomal DNA from several Cryptococcus species. Journal of Bacteriology 172: 4238–4246. https://doi.org/10.1128/jb.172.8.4238-4246.1990

Watling R (1965) Notes on British Boleti: IV. Transactions of the Botanical Society of Edinburgh 40(1): 100–120. https://doi.org/10.1080/03746606508685128

Watling R (2008) A manual and source book on the Boletes and their allies. Synopsis Fungorum 24: 1–248.

Wu G, Feng B, Xu J, Zhu XT, Li YC, Zeng NK, Hosen MI, Yang ZL (2014) Molecular phylogenetic analyses redefine seven major clades and reveal 22 new generic clades in the

fungal family Boletaceae. Fungal Diversity 69: 93–115. https://doi.org/10.1007/s13225-014-0283-8

Wu G, Li YC, Zhu XT, Zhao K, Han LH, Cui YY, Li F, Xu JP, Yang ZL (2016) One hundred noteworthy boletes from China. Fungal Diversity 81: 25–188. https://doi.org/10.1007/s13225-016-0375-8

Yang ZL, Wang XH, Binder M (2003) A study of the type and additional materials of *Boletus thibetanus*. Mycotaxon 86: 283–290.

Zang M (1992) *Sinoboletus*, a new genus of Boletaceae from China. Mycotaxon 45: 223–227.

Zang M, Yuan MS, Gong MQ (1993) Notes on and additions to Chinese members of the Boletales. Acta Phytophysiologica Sinica 12: 275–282.

Zang M (2006) Flora fungorum sinicorum. Vol. 22. Boletaceae I. Science Press, Beijing.

Zeng NK, Liang ZQ, Yang ZL (2013) *Boletus orientialbus*, a new species with white basidioma from subtropical China. Mycoscience 55: 159–163. https://doi.org/10.1016/j.myc.2013.07.004

Zeng NK, Zhang M, Liang ZQ (2015) A new species and a new combination in the genus *Aureoboletus* (Boletales, Boletaceae) from southern China. Phytotaxa 222: 129–137. https://doi.org/10.11646/phytotaxa.222.2.5

Zhang M, Li TH, Nuhn EM, Tsering T, Song Bin (2017) *Aureoboletus quercus-spinosae*, a new species from Tibet of China. Mycoscience 58: 192–196. https://doi.org/10.1016/j.myc.2017.01.007

Zhang M, Li TH, Song B (2014) A new slender species of *Aureoboletus* from southern China. Mycotaxon 128: 195–202. https://doi.org/10.5248/128.195

Zhang M, Li TH, Wang CQ, Song B, Xu J (2015a) *Aureoboletus formosus*, a new bolete species from Hunan Province of China. Mycological Progress 14: 118. https://doi.org/10.1007/s11557-015-1142-z

Zhang M, Li TH, Xu J, Song B (2015b) A new violet brown *Aureoboletus* (Boletaceae) from Guangdong of China. Mycoscience 56: 481–485. https://doi.org/10.1016/j.myc.2015.02.002